



Research article

Remote sensing search for cross border foci of onchocerciasis; A case study in the Democratic Republic of Congo bordering Uganda

Ben jamin G. Jacob¹, Samuel S. Alao¹, Thomas Lakwo², Thomas Unnasch¹

1- Department of Global Health, College of Public Health, University of South Florida, Tampa, FL.
2- Vector Control Division, Ministry of Health, Kampala, Uganda
E-mail: bjacob1@health.usf.edu

RUNNING HEAD: Satellite models for identifying cross-border, breeding foci of *S.damnosum* s.l.,



OPEN ACCESS

This work is licensed under a [Creative Commons Attribution 4.0 International License](https://creativecommons.org/licenses/by/4.0/).

Abstract: The use of remote sensing has found its way into the field of vector, arthropod, breeding foci identification within the last decade. This technology has been adapted to identifying habitats of *Simulium damnosum* s.l., a black fly vector of onchocerciasis (“river blindness”) in African countries where the disease is endemic. One potential use of this technology is to identify potential breeding sites in cross border areas where political instability prevents ground based investigations of the presence of onchocerciasis and its vector in a neighboring country. The presence of breeding sites close to a border may represent a threat of invasion of parasites carried by flies breeding in areas with little or no effective control, slowing the progress of onchocerciasis elimination in the more stable country. Here, we report the application of this technology to a such a cross border area, that of Uganda and the Democratic Republic of the Congo (DRC).

Methods: Two RapidEye™ 5 meter (m) spatial resolution polygons were obtained along the border of the DRC and Uganda during the rainy season of 2016. A 0.5 km² grid-stratified algorithmic matrix was overlaid onto the polygons. The matrix was employed to calculate precise land use land cover (LULC) feature indices (e.g., partially shaded, discontinuously canopied trailing vegetation) for identifying *S. damnosum* s.l. breeding foci. Besides the widely employed proxy biophysical signals from Normalized Difference Vegetation Index (NDVI) and Soil Adjusted Vegetation Index (SAVI) other geometric endmember habitat signatures [e.g., collections of three-dimensional [3-D), digital elevation model (DEM), wavelength, altitude parameters] were interpolated for identifying habitats of *S. damnosum* s.l. on the DRC side of the border. The models were also constructed employing multiple, microtopographic, canopied and non-canopied, landscape determinants. The interpolated outputs were inspected and field validated for LULC breeding appropriateness along multiple cross-border, riverine tributaries in the DRC study site polygons. All LULC, endmember, data conversion, data management, and map automation for the endmember landscape analyses was geoprocessed within ArcPy, a Python site package.

Results: ArcPy functions resolved multiple differential diagnostic equations and provided functions for the vegetation, proxy, 5m, endmember, LULC signatures for optimally displaying vegetational and non-vegetational, partially shaded, geoclassified, diagnostic covariates. The functions and classes provided additional functionality



to support Python-based workflows in the orthogonal, grid-stratified, entomological, bare soil and trailing uncanopied, sub-pixel datasets. The models did not identify any habitat suitable for *S. damnosum* s.l. breeding in the DRC border region examined

Conclusions

An uncoalesced dataset of interpolated, 5m, wavelength, frequency explainers, including VI model, reference signature, LULC estimators could not identify any cross-border, *S. damnosum* s.l. habitats within two DRC, grid-stratified, study site, riverine, tributary, 5m, geoclassified polygons. Regardless, the modeling approach and the ArcGIS scripting module presented here is potentially useful for optimally, remotely, identifying, geoclassifiable landscapes in cross-border, African riverine tributaries particularly in politically unstable regions where the vector foci could exist using moderate resolution data. Query optimization of Rapid Eye™ 5m, Red Edge inflection point landscape metadata employing asymptotic variance of the weighted kappa coefficient can aid in rewriting existing ArcMap toolbox and Python scripts for robustly interpolating a 5m, LULC, target, discontinuous canopied, capture point, wavelength signal. Continued compiling of moderate resolution, geoclassifiable, LULC datasets employing *S. damnosum* s.l., breeding foci, geometric endmember signatures in conflict-ridden, African, riverine tributary environments using Rapid Eye™ data and ArcGIS scripting languages (e.g., Java, PowerShell, Ruby, Scala, Perl,) may reveal specific landscape features such as meandering, seasonal, water, body reformations or specific plant fauna for implementing, targeted, larval, control strategies in these cross-border ecosystems.

Keywords: Remote sensing onchocerciasis cross-border, *Simulium damnosum*, riverine Uganda

1.0 Introduction

Landscape heterogeneity in riverine pathways can play a role in the development of breeding habitats of Onchocerciasis vector, *Simulium* (Edwardsellum) *damnosum sensulato* (s.l.) (Diptera: Simuliidae). Onchocerciasis, is a filarial infection caused by the nematode *Onchocerca volvulus* that can lead to visual morbidity via multiple mechanisms including chorioretinitis, uveitis, and sclerosing keratitis [www.who.int/blindness/partnerships/onchocerciasis_Onchocerciasis Control Programme (OCP)]. The disease manifests systemically but is best known for its cutaneous and ocular pathologies which has been shown to lead to a four-fold increase in mortality (Post 1986). *Simulium* larvae are limited to well-aerated fluvial ecosystems and its ecology has been recorded in water courses which run through various quaternary, sedimentary, land use land cover (LULC) and geospatial object formations including, stones, rocks, large pebbles and coarse, sharp, sand bed with earth stones or from bedrocks, tertiary volcanic of Precambrian origin (Review of the works of the Volta river basin area from 1974-1984. 1985). The breeding sites of *Simulium* spp. can also be attached to a variety of LULCs associated to water plants, trailing roots and branches. For example, Jacob et al. [1] found that LULCs associated with *S. damnosum* s.l. larval breeding attachments included partially canopied *Oryzabarthii*, *Pterocarpus santalinoides*, *Andropogon gayanus* and *Lawsonia inermis* along the Sirb tributary of the Niger river in Burkina Faso in West Africa.

In Jacob et al. [2], larvae were collected along the trailing roots of *P. santalinoides* in the heavily canopied shaded parts of the Sarakaw tributary ecosystem of the Oti river in Togo, near the border with Burkina Faso. This cross-border tributary is endemic for the savanna dwelling sibling species of *S. damnosum* s.l. (*S. damnosum sensu strictu* and *S. sirbanum*) which together represent the most important *Onchocerca volvulus* vectors in the savanna regions of sub-Saharan Africa. Subsequently, larvae were collected on the leaves and hollow openings in the plant *Oryzabartii* which were growing in the un-shaded areas of the tributary. Female *Simuliids* are hematophagous while male feeds on plant juices [3]. In South-West Nigeria, human activities along the Osun river are gradually diminishing the rain forest, altering the eco-geographical, LULC distribution of various plant species faunas [4]. These activities include burning, cultivation, tree falling and cattle grazing. Incidence of vector-borne disease in host populations is rarely, if ever, evenly distributed across any landscape [5].

The persistence and quality of *S. damnosum* s.l. breeding foci on riverine landscapes may vary significantly across political boundaries especially in areas of cross-border civil unrest (e.g., Niger and Nigeria), which may influence vector habitat, species composition and location. Remotely identifying *S. damnosum* s.l.,



larval habitats may allow onchocerciasis researchers, epidemiologists and others to use ArcGIS to generate distinct overhead cross-border gradients of transmission potential across geoclassifiable, moderate resolution, LULC employing imaged grid-stratified neighbourhoods of African riverine ecosystems.

Since its discovery in 1937, West Nile virus (WNV) has spread beyond its original known geographic range and caused human disease in DRC. Infectious diseases may constitute public health emergencies of international concern when a pathogen arises, acquires new characteristics, or is cross-bordered, leading to the potential for loss of human lives as well as societal disruption. Serological evidence of human exposure to WNV has been reported in the Central African Republic and the Democratic Republic of Congo (www.who.gov). Where multiple cross-border, risk drivers interact, the potential impact of a disease outbreak may be amplified. The varying temporal and geographic frequency with which cross-border, infectious disease events such as WNV occur adds yet another layer of complexity to the issue of larval control of immature vector habitats. Mitigating the emergence and spread of infectious disease necessitates mapping such vector arthropod disease such as WNV and prioritizing the interdependencies between public health and other sectors.

Eigendecomposed, autoregressive quantitative optimization of grid-stratified, moderate resolution, orthogonal, spatial filter, synthetic, endmember (i.e., sub-pixel), geoclassifiable, LULC, explanatory uncoalesced datasets of dependent (i.e., response), and independent oviposition, covariance weightages employed in an ArcGIS-derived, eco-cartographic, biogeophysical, capture point, immature habitat, identification model may reveal corridors of unknown, breeding foci, whilst optimally estimating clustering tendencies and their propagational uncertainties [i.e., spatial heteroskedascity (i.e., uncommon variance)]. In linear algebra, eigendecomposition (i.e., spectral decomposition) is the factorization of a matrix into a canonical form, whereby the matrix is represented in terms of its eigenvalues and eigenvectors [6]. In linear algebra, an eigenvector or characteristic vector of a linear transformation is a non-zero vector whose direction does not change when that linear transformation is applied to it [7].

More formally, if T is a linear transformation from a vector space V over a field F into itself and v is a vector in V that is not the zero vector, then v is an eigenvector of T , if $T(v)$ is a scalar multiple of v when $T(v) = \lambda(v)$ (Eqn 1.1) [6]. If the vector space V is finite-dimensional in a cross-border, eco-georeferenceable, African, riverine, tributary, geoclassifiable, *S. damnosum* s.l., breeding foci, seasonal, hyperproductive, biogeophysical, eco-epidemiological, capture point, ArcGIS, identification model, then the linear transformation T may be illustratable as a square matrix A , and the vector v by a column vector. In so doing, the algorithm would optimally render an eco-epidemiological, explanatorial, eco-georeferenceable, forecast, vulnerability, immature habitat, eigenvector map in Spatial Analyst™ based on matrix multiplication for scaling of the column vector on the right hand side in Equation 1.1. In mathematics, matrix multiplication or the matrix product is a binary operation that produces a matrix from two matrices [7].

Signature authentication of eco-georeferenceable, explanatory LULC systems that make usage of statistical verification methods often render optimum performance but only under limited and restricted, geoclassifiable, conditions in uncoalesced, gemetric, endmember, vector arthropod, remotely sensed, eco-epidemiological, entomological, immature habitat, forecast, vulnerability, eco-georeferenceable, identification model parameter estimator datasets. Moreover, several constraints are impossible in ArcGIS on the end-user so that the remotely sensed model may work optimally, and as expected for remotely identifying, cross-border, African, riverine, tributary, capture point, seasonal, hyperproductive, *S. damnosum* s.l., breeding foci. For example, an onchocerciasis researcher or epidemiologist may sign within a small delimited text box in Spatial Analyst™ in order to limit a cross-border, endmember, moderate resolution, canopied, endmember, *S. damnosum* s.l., LULC, specified, spectral signature to a predefined set of unmixed frequency, wavelength dimensions. In so doing, the necessity for scaling the data would be eliminated. Moreover, the angular rotation with respect to the referenced, black fly, cross-border, African, riverine, tributary, breeding foci, microtopographic, geo-spectrally classified LULC irradiance may inadvertently introduce bias (negative autocorrelation) rendering systematic and random errors and endmember noise into the eigenfunction decomposition simulation exercise. Imprecise separation of signals can hamper performance of wavelength, frequency interpolation and unmixed signature spectroradiometric verification systems [5].

Linear spectral unmixing can determine the relative abundance of biogeophysical materials that are depicted in multispectral or hyperspectral imagery based on the materials' spectral characteristics [8]. The



reflectance at each pixel of the image is assumed to be a linear combination of the reflectance of each material (or endmember) present within the pixel. For example, if 25% of a cross-border, *S. damnosum* s.l., LULC pixel contains partially canopy-shaded, immature, capture point, grid-stratified, habitat material A, 25% of the pixel contains material B (partially unshaded Precambrian rock), and 50% of the pixel contains material trailing discontinuous vegetation, the wavelength spectrum for that vector arthropod habitat pixel would be a weighted average of 0.25 times the spectrum of material A, plus 0.25 times the spectrum of material B, plus 0.5 times the spectrum of material C. The incidence of onchocerciasis is not distributed uniformly across a riverine tributary ecosystem, but there is a clear correlation with basic geology because the riverine conditions which create suitable breeding sites for the vector, *S. damnosum* s.l., are most common where the Precambrian basement rock is exposed to break the flow of the water and create rapids[3].

So, given the resulting spectrum (i.e., the input vector arthropod, uncoalesced, LULC moderate resolution, geoclassified, data) and the endmember, biogeophysical spectra, linear spectral unmixing would solve for the abundance values of each pure pixel endmember, for every cross-border, black fly, eco-epidemiological, hyperproductive, seasonal, capture point. The number of endmembers must be less than the number of spectral bands, and all the endmembers in the image must be used (www.esri.com). Spectral unmixing results are highly dependent on the input, spectral LULC endmembers; changing the endmembers changes the results[8].

Spectral unmixing has two constraint options: unconstrained or a partially constrained unmixing. In the unconstrained method, abundances may assume negative values and are not constrained to sum-to-unity (one). ArcGIS also supports an optional, variable-weight, unit-sum constraint in the linear-mixing algorithm. Hence, an onchocerciasis researcher or an epidemiologist can apply a non-linear, weighted, matrix to tease out noisy disturbances in an endmember LULC moderate resolution dataset since unquantified outliers can propagate in an empirical, uncoalesced, geosampled dataset of African, riverine tributary, agro-village, immature habitat, seasonal, hyperproductive foci rendering erroneous coefficients in an eco-epidemiological, forecast, vulnerability, malaria, mosquito, oviposition, immature habitat, biogeophysical, capture point, identification model. This would allow defining critical components for optimal quantification, for example, the weight of a sum-to-unity constraint on the abundance fraction from a capture point, cross-border, *S. damnosum* s.l., hyperproductive, eco-georeferenceable, eco-epidemiological, breeding foci. It also may permit proper unmixing of the transformed data, with zero-mean bands.

The Minimum Noise Fraction (MNF) transform as modified from Green et al. [9] is implementable for optimally quantifying geometric endmember noise from an empirical uncoalesced dataset of cross-border, *S. damnosum* s.l., immature habitat, moderate resolution, spectral, LULC wavelength frequencies in ArcGIS. The unmixing algorithm is based on a linear transformation that consists of realizations rendered from separate principal components analysis. Principal component analysis (PCA) is a statistical procedure that uses an orthogonal transformation to convert a set of geospectrally parameterizable observations of possibly correlated variables (e.g.,) into a set of values of linear uncorrelated variables (i.e., principal components or sometimes, principal modes of variation)[8]. The number of principal components is less than or equal to the smaller of the number of original variables or the number of observations[10]. This transformation is definable in such a way that the first principal component has the largest possible variance (that is, accounts for as much of the endmember variability in the LULC data as possible), and each succeeding component in turn has the highest variance possible under the constraint that it is orthogonal to the preceding components. The resulting vectors for example, rendered from PCA of an uncoalesced sub-pixel, geoclassified, eco-georeferenceable, empirical dataset of moderate resolution, cross-border, eco-epidemiological, black fly capture point, wavelength frequencies), would be an uncorrelated orthogonal basis set. PCA is sensitive to the relative scaling of the original variables[5].

A PCA can be conducted by eigenvalue decomposition of a data covariance (or correlation) matrix or singular value decomposition of a data matrix, usually after mean centering and normalizing the data matrix in ArcGIS for each attribute feature, grid-stratified, geoclassifiable, LULC (e.g., uncanopied, partially canopied, cross-border, *S. damnosum* s.l., agro-village, tributary, capture point). The results of a PCA are usually discussed in terms of component scores, sometimes called factor scores (i.e., the transformed moderate resolution, uncoalesced, geometric, endmember geoclassified, unshaded, LULC variable values corresponding to a particular seasonal, black fly, oviposition, eco-georeferenceable, hyperproductive, capture point), and loadings (the weight by which each standardized original variable should be multiplied to get the component score). PCA is the simplest of the true eigenvector-based multivariate analyses[6]. Often, its operation can be



thought of as revealing the internal structure of the data in a way that best explains the variance in the data. If a multivariate uncoalesced, eco-georeferenceable, explanatory, optimally fractionalized, geometric endmember dataset of cross-border, *S. damnosum* s.l. African, riverine tributary eco-epidemiological, capture points is geovisualized as a set of coordinates in a high-dimensional data space (e.g., 1 axis per LULC variable), PCA can supply the user (onchocerciasis researcher or epidemiologist) with a lower-dimensional projection of this object when viewed from its most informative remote viewpoint. This may be conducted by employing only the first few principal components so that the LULC dimensionality of the transformed, black fly data is reduced. CA is closely related to factor analysis[7]. Factor analysis typically incorporates more domain specific assumptions about the underlying structure and solves eigenvectors of a slightly different matrix [6]. PCA is also related to canonical correlation analysis (CCA). CCA defines coordinate systems that optimally describe the cross-covariance between two datasets (a cross-border moderate resolution, uncanopied, immersed trailing vegetation, endmembers and a eco-georeferenced, black, fly, hyperproductive breeding foci) while PCA defines a new orthogonal coordinate system that optimally describes variance in a single dataset. In probability and statistics, given two stochastic processes and, the cross-covariance is a function that gives the covariance of the one process with the other at pairs of time points[7]. Cross-covariance is related to the more commonly used cross-correlation of the processes in question in entomological, eco-epidemiological, vector habitat predictive risk mapping[8].

In SAS/GIS after first rotation uses the principal components of the covariance matrix to decorrelate and rescale the noise in an uncoalesced, cross-border, *S. damnosum* s.l., eco-epidemiological, immature habitat, breeding foci, empirical, geometric, endmember dataset of uncanopied, trailing vegetation, cross-border, African, riverine, tributary, moderate resolution, data (i.e., noise whitening), the transformed endmember will reveal optimal unit variance and no band-to-band correlations. The second rotation would employ the principal components derived from the original black fly oviposition, LULC eigen-image data after they have been noise-whitened by the first rotation and rescaled by the noise standard deviation in SAS/GIS. Since further spectral processing will occur, the inherent dimensionality of the African, riverine tributary, vector arthropod, geoclassified, eco-epidemiological, LULC data would be determined in Statistical Analyst™ by examining the final eigenvalues and the associated images.

Conversely an onchocerciasis researcher or epidemiologist may divide the data space of a moderate resolution, cross-border, *S. damnosum* s.l., eco-georeferenced, uncoalesced, capture point, seasonal, hyperproductive, immature habitat into two parts: one part associated with large tabulated LULC breeding foci eigenvalues with coherent eigenimages, and a complementary part with near-unity eigenvalues and noise-dominated images, in Statistical Analyst™. Employing only the coherent portions in a moderate resolution, remotely geoclassified, cross-border, African riverine tributary, *S. damnosum* s.l., uncoalesced, eco-epidemiological, wavelength, frequency, immature habitat, biogeophysical, identification model would separate the endmember noise from the geoclassified, LULC data, thus improving spectral processing results in Statistical Analyst™. An onchocerciasis researcher or epidemiologist may also use the MNF transform to remove noise from the endmember, capture point, eco-georeferenceable, breeding foci, immature habitat, LULC data by performing a forward transform for determining which bands contain the coherent images. By examining the images and eigenvalues extracted from the immature habitat, eco-epidemiological, model explanatory forecasts in Spatial Analyst™ and running an inverse transform employing a spectral subset to include only the good wavebands, only optimally remotely identifiable eco-epidemiological, African, riverine, tributary, capture point, cross-border, black fly, uncoalesced, wavelength frequencies will be selected for smoothing the noisy bands before the simulation procedure. Furthermore, an onchocerciasis researcher or epidemiologist may have the option to subset the output of the MNF rotation in Spatial Analyst™ based on geoclassifiable, cross-border, grid-stratified, *S. damnosum* s.l., moderate resolution, LULC eigenvalues, which in actuality could signify that the unmixing algorithm may generate an output cube of hundreds of frequency bands (e.g., floating-point, black fly, geoclassified, uncanopied, trailing vegetation, African, riverine tributary, unmixed, geometric endmembers).

Alternatively, a robust system may be proposed in Statistical Analyst™ that optimizes an uncoalesced, moderate resolution, geoclassifiable, iteratively qualitatively interpolative, endmember, LULC, cross-border, spectral *S. damnosum* s.l., immature habitat, iteratively interpolatable, endmember wavelength, signature by generating a large range of algorithmic, non-frequentistic, quantitation processes. By deducing variation in Rotation-Scaling-Translation (RST) in the module breeding foci of the African, riverine, tributary, vector, arthropod geoclassified, LULCSs may be optimally remotely identified and their errorneous, irradiance parameters (non-homoscedastic, autocorrelated, endmember, spectral wavelengths) resolved employing the user signature per the reference signature stored in Spatial Analyst™.



Eigenvector spatial filtering (ESF) furnished in Spatial Analyst™ can account for dependency in ecogeoreferenceable, entomological, geoclassifiable, vector arthropod, breeding foci, time series, fractionalized, moderate resolution, endmember, uncoalesced, LULC, signature datasets employing weighted grid-stratified matrices [11-13], which to date, has been the domain of spatial autoregressive (SAR) models [6]. Its fundamental idea can exploit the eigen-function decomposition of an eco-georeferenceable, biogeophysical, eco-epidemiological, capture point, seasonal, hyperproductive, *S. damnosum* s.l., geoclassifiable, moderate resolution, cross-border, breeding foci and their unmixed, geoclassified, endmember, spectral, wavelength, frequencies into the following three components: trend, spatially structured random component (i.e., stochastic signal), and random noise.

The aim of the endmember spectral wavelength, paradigms in ArcGIS could be to separate geospatially structured, random, frequency components from both trend and random noise, and, consequently, furnish a sounder statistical inferential for optimal visualization of a microtopographic, uncanopied, moderate resolution, trailing vegetation, geoclassified LULC associated to a hyperproductive, seasonal, eco-georeferenceable, eco-epidemiological, capture point, cross-border, African, riverine, tributary, black fly, seasonal, breeding foci. In other words, ESF could employ a set of synthetic, moderate resolution, proxy, microtopographic, geoclassified, uncoalesced, endmember, specified, LULC, wavelength, covariates (e.g., moderate resolution, empirical partially canopied, immersed vegetation, spectral, irradiance values) in Spatial Analyst™, which may optimally extractable as orthogonalizable spatial filter, LULC eigenvectors from a connectivity matrix that ties the sub-pixel, target signature explanative objects with cross-border, *S. damnosum* s.l., capture points together in space. By adding these iteratively interpolatable, vectors in geographic space in Statistical Analyst™ as control variables in an eco-epidemiological, identification, forecast-oriented, LULC vulnerability model specification, these control variables may identify and isolate the stochastic spatial dependencies amongst the referenced signature, geometric, endmember, geoclassified, LULC, wavelength, immature, habitat frequencies. In so doing, the entomological, eco-epidemiological, forecast, remote, sensing, vulnerability model construction would proceed as if the eco-georeferenced, iteratively interpolatable, eco-epidemiological, endmember observations are independent.

Because ESF model specifications in Statistical Analyst™ are flexible, it can be utilized to optimally describe uncoalesced, geometric, endmember, LULC, moderate resolution, cross-border, eco-epidemiological, capture point, *S. damnosum* s.l. African, riverine, tributary, breeding foci, unbiased estimator employing orthogonal, endmember, eigen-decomposable, moderate resolution, LULC, spectral wavelength, explanatory, frequency variables following various types of distributions including the Gaussian, Poisson, and binomial [2, 14]. Different, ESF, geo-spectrotemporal and or geo-spatiotemporal, uncoalesced, moderate resolution, endmember, LULC, wavelength frequency specifications may then be compared with other specifications, such as the SAR, auto-Poissonian and auto-logistic for optimally remotely identifying cross-border, eco-epidemiological, seasonal, hyperproductive, capture point, eco-georeferenceable, *S. damnosum* s.l., riverine, cross-border, immature habitats on moderate resolution, African tributary, agro-village, geoclassified, LULCs in Statistical Analyst™.

Unfortunately, the ESF method potentially is plagued by common problems associated with stepwise regression techniques which is commonly employed for validating remotely sensed, entomological, vector, arthropod, moderate resolution, endmember, LULC, geo-specified, breeding foci, simulation models. There are four principal assumptions which justify the usage of linear regression for vulnerability, entomological, vector arthropod, remotely sensed, immature habitat, eco-epidemiological, breeding foci, identification, models for, purposes of inference or prediction: (i) linearity and additivity of the relationship between dependent (i.e., unmixed, spectral, frequency, immature habitat, capture point, endmember, LULC signature) and independent variables [eco-georeferenceable, cross-border, African, riverine, tributary, *S. damnosum* s.l., habitat seasonal, mean sample discontinuous canopy “gap” counts]. The expected value of an endmember, LULC-related, explanatory, frequency, dependent variable would be then optimally remotely illustratable as a straight-line function of each explicative, endogenous independent variable in Statistical Analyst™, holding the others fixed in the remotely sensed, eco-epidemiological, forecast, vulnerability, endemic model [1]. The slope of that line would not depend on the endmember, values of the other LULC variables. The effects of different moderate resolution geoclassifiable, entomological, vector arthropod, explanatory, independent variables on the expected value of the dependent variable would be additive.

Other regression assumptions that should not be violated in a moderate resolution, endmember, geoclassifiable, endmember, LULC, cross-border, immature, *S. damnosum* s.l., African, riverine, tributary, capture point, ArcGIS habitat, eigenvector, identification, model would be statistical independence of the



frequency, wavelength, unquantiated, propagational, spectral errors (in particular, no correlation between consecutive errors especially in the case of fractionalized, breeding foci, geoclassifiable, empirical datasets. Additionally homoscedasticity (i.e., constant variance) of the endmember model residual errors would be necessitated. Next, parameterized geoclassified data must be evaluated against: (a) time (e.g., in the case of cross-border, riverine tributary, agro-village, geoclassified, moderate LULC change data)(b) versus the eco-epidemiological explanatory diagnostic forecast, (e.g., targeted, seasonal, hyperproductive, black fly, eco-georeferenceable, capture points) (c) versus any independent geosampled, uncoalesced, sub-pixel, eco-epidemiological, specified, explanatory, predictor variable. Importantly the assumption of normality of the error distribution must be imposed to obtain a viable, cross-border, *S. damnosum* s.l. breeding foci, risk-related, frequency wavelength, sub-model prognostication (e.g., a remotely identified and field verified (“ground truthed”) hyperproductive, *S. damnosum* s.l., seasonal immature habitat, capture point, breeding foci) on a moderate resolution, African riverine tributary, geoclassified LULC. If any of these assumptions is violated (i.e., if there are nonlinear relationships between explanatory dependent (i.e., response) and independent, microtopographic, geoclassified, or non-geoclassified, frequency, endmember, LULC variables or the wavelength geospectral errors exhibit correlation, heteroscedasticity, or non-normality) in Statistical Analyst™, then the eco-georeferenceable, eco-epidemiological, diagnostic forecasts, confidence intervals, and scientific insights yielded by the cross-border, African, riverine tributary, immature habitat, endmember, forecast, vulnerability, signature, identification, regression model may be (at best) inefficient or (at worst) seriously biased or misleading.

Ideally statistical software could be utilized to automatically provide charts and statistics that test whether regression assumptions are satisfied for any given endmember, cross-border, moderate resolution, capture point, eco-georeferenceable, seasonal, hyperproductive, entomological, vector arthropod, eco-epidemiological, forecast, vulnerability, immature habitat, remote, identification model. Unfortunately, many software packages do not provide such output by default (e.g., additional menu commands must be executed or code must be written) and some (such as Excel’s built-in regression add-in) offer only limited options. RegressIt does provide such output and in graphic detail. Although geometric endmember outputs from a remotely sensed, uncoalesced, seasonal, black fly, African, riverine tributary, moderate resolution, geoclassifiable, LULC immature habitat, identification model may violate all the assumptions, it may be still likely to be accepted by a naïve user based on a large value of R-squared.

In statistics, the coefficient of determination, denoted R^2 or r^2 is a number that indicates the proportion of the variance in the dependent variable that is optimally forecastable from the independent variable(s) [15]. It is a statistic employed in the context of entomological, endemic, spectral frequency, wavelength, vector arthropod, statistical, geometric, endmember, LULC, signature, breeding foci, vulnerability models whose main purpose is either the prediction of future outcomes or the testing of hypotheses, on the basis of other related information. Such models could provide a measure of how well observed endmember, LULC habitat seasonal outcomes (e.g., larval density counts) are replicated by the moderate resolution model, based on the proportion of total variation of potential outcomes explained by across-border, African, riverine tributary, regression, immature habitat, identification, spectral wavelength, frequency, uncoalesced, endemic model. If additional, diagnostic, time series, uncoalesced, black fly, moderate resolution, geoclassifiable, endmember, wavelength, LULC explanatory, regressors are included, R^2 would be the square of the coefficient of multiple correlation. In both such cases, the coefficient of determination would range from 0 to 1.

Important cases where the computational definition of R^2 in an endmember, cross-border, African, riverine tributary, moderate resolution, geoclassified, spectral, endmember, wavelength, *S. damnosum* s.l., immature habitat, signature, identification model in ArcGIS can yield negative values (e.g., finding repeating LULC, patterns such as the presence of a periodic, eco-epidemiological, eco-georeferenceable, biogeophysical, explanative, capture point, discontinuous, canopy signal obscured by noise. Identifying the missing fundamental frequency in a partially shaded, immersed, trailing vegetation, breeding foci, Precambrian rock signal for example, may be implied by its harmonic frequencies used in signal processing when analyzing geometric, endmember, orthogonal eigenfunctions or series of spectral eigendecomposable values, such as time domain signals.

Additionally, negative values of R^2 may occur when fitting non-linear, ArcGIS, optimizable functions to uncoalesced, endmember, LULC, moderate resolution, geoclassifiable, *S. damnosum* s.l. cross-border, immature, habitat data. In cases where negative values arise, the mean of the sub-pixel capture point, data may provide a better fit to the outcomes (e.g., remotely identified, seasonal, moderate resolution, geoclassified



LULC, eco-epidemiological, hyperproductive, seasonal, *S. damnosum*s.l., immature habitat) than do the fitted function values, per this criterion in ArcGIS.

Thus, many questions would arise when applying geoprocessing ArcGIS tools for constructing a feasible, moderate resolution, probabilistic, immature habitat, unmixed, wavelength, interpolation, signature paradigm for revealing eco-georeferenceable, African, riverine tributary, cross-border, eco-epidemiological, *S. damnosum* s.l. immatures employing an ESF such as: Is the correct set of fractionalized, eigenvectors selected for the geoclassified microtopographic LULCs? Are superfluous, black fly, orthogonal spatial filters selected? Is moderate resolution, geoclassifiable, uncoalesced, signature eigenvalues not selected that should be selected? Are results biased? How does ESF relate to the multiple testing problems in a remotely sensed, immature habitat, identification, forecast, vulnerability, endemic, entomological, risk model? Fortunately, ESF avoids complications affiliated with multicollinearity as synthetic, orthogonal, spatial filter, eigenvectors are mutually orthogonal and uncorrelated [6]. Regardless, propagational, erroneous coefficients (i.e., negative autocorrelation, sub-pixel, LULC estimators) may be inconspicuously embedded in an eco-epidemiological, vulnerability, cross-border, African, tributary, eco-georeferenceable, spectral wavelength, moderate resolution, *S. damnosum* s.l., capture point, seasonal, riverine, geoclassified, remotely sensed, immature, habitat, identification, vulnerability model which can lead to misspecifications in residual forecasts of targeted hyperproductive, breeding foci on grid-stratified, LULC data.

When autoregressively eigen-decomposed, geoclassified, LULC data are incomplete or subject to disturbances (e.g., propagational Gaussian white noise), Spatial Analyst™ provides a framework for robustifying spatial filter, propagational, orthogonal, geoclassified, LULC, synthetic variables [16] for differentiating non-homoscedasticity and geospatially extreme outliers. This is vital in situations where the deviation of the probabilistic, geosampled, geometric, endmember, LULC, orthogonal, frequency, decomposed, eigenvector values rendered from the unobservable, true value of an eco-georeferenceable, capture point, immature habitat quantity (e.g., percent of immersed vegetation at a seasonal, cross-border, hyperproductive, *S. damnosum* s.l., seasonal, eco-epidemiological, capture point) is related to hyperendemic, regression residual, field-operationalizable, optimally parameterizable covariate (e.g., a larval, seasonal, population, mean count). In such circumstances, the residual of an observed, immature, black fly, breeding foci, ESF, sample value would be based on the quantitated difference between the observed, endmember, LULC value and the estimated value of the quantity of interest [e.g., near infra-red (NIR) wavelength, unmixed, radiance from unshaded floating canopy leaves surrounding a hyperproductive, cross-border, seasonal African, riverine, tributary, capture point, *S. damnosum* s.l., discontinuous canopy gap].

In statistics and optimization, propagational errors and residuals are two closely related and easily confused measures of the deviation of an observed value of an element of a statistical sample from its "theoretical value" [10]. The distinction is most important in eco-epidemiological, capture point, spectral, wavelength, frequency, uncoalesced, ESF-specified, prognosticative, endmember, LULC, moderate resolution, signature-related, temporal, regression analysis, where the iterable, interpolative residuals may lead to the erroneous, commutated, uncoalesced, wavelength, frequency weights. A studentized residual is the quotient resulting from the division of a residual by an estimate of its standard deviation [17].

Typically the standard deviations of optimally autoregressive, eigen-function, decomposable, moderate resolution, uncoalesced, LULC endmember, reference wavelength, frequency, signature, regression residual, eco-cartographically illustrating targeted, seasonal, hyperproductive, agro-village, *S. damnosum* s.l., African, riverine, narrow or wide, tributary breeding foci, in a sample frame vary greatly from one sample capture point to another [2]. Hence, it may not make sense to compare seasonal, cross-border, black fly, eco-epidemiological, seasonal, hyperproductive, eco-georeferenceable, capture point, cross-border, immature habitat, capture point, optimizable endmember geospatially filtered, moderate resolution, geo-spectrotemporal, uncoalesced, wavelength regression frequency residuals at different immature, seasonal, LULC, explanatory, data points without first studentizing in ArcGIS Desktop. Unlike query functions which can render sub-pixel, LULC irradiance information about individual, vector arthropod, breeding foci, "hot spot" clustering (e.g., percent of unshaded, canopy, trailing vegetation) — Statistical Analysis™ in ArcGIS can reveal the landscape characteristics of an empirical set of geoclassifiable, orthogonal, grid-stratified, time series, eigen-decomposed, immature habitat, eco-georeferenceable, attribute features. The quantitated endmember, moderate resolution, entomological, LULC signatures may be most well-suited for interactive applications, such as in ArcMap, thus allow selecting and geovisualization of optimizable, eco-epidemiological, uncoalesced, geoclassifiable eco-epidemiological, iteratively qualitatively interpolatable, LULC data in an ad-hoc and fluid environment. Although ArcMap's menus and toolbars do not currently have a geoprocessing tool, other tools exist in



StatisticalAnalyst™ for optimallyremotely quantitating non-normality,in seasonal empirical datasets of, calculable,discrete, probability distributions (e.g., leptokurtotic, cross-border, *S. damnosum*.s.l., moderate resolution, endmember, eigendecomposed, discontinuouslycanopied, LULC emissivityskews), forrobust surface constituent identification for land use mapping.

If negative exponential attenuation of light within individual, remotely identifiable moderate resolution, eco-epidemiological, geoclassifiable, cross-border, eco-georeferenceable, *S. damnosum* s.l. capture point, breeding foci, LULC canopies is assumed, the problem of immature habitat, modeling the gap probability then becomes the problem of estimating the distribution of distances within canopies in ArcGIS through which a photon emitted by the source of illumination will pass. This, in turn, is not difficult if the distribution of individual canopy sizes and shapes is known in ArcGIS and individual black fly oviposition habitat canopies are randomly distributed but do not overlap.

Canopy gaps are small-scale openings in forest canopies which offer suitable micro-climatic conditions for tree regeneration[8]. Several studies have used Canopy Height Models (CHM) derived from airborne laser scanning (ALS) to delineate gaps but limited field accuracy assessment has been carried out, especially regarding the discontinuous gap geometry. Jacob et al.[11] investigated mapping methods based on raster layers in ArcGIS produced from per-pixel and per-object supervised classifications for optimally identifying, eco-epidemiological, capture point, eco-georeferenceable, *S. damnosum* s.l., immature habitat remotely. In addition to the CHM, other metrics related to the canopy porosity were examined. The gap detection performed well with a global accuracy up to 85% and consumer's accuracy often exceeding 92%. The Geometric Accuracy (GAc) was analyzed with the quantitated gap area tabulations, main orientation, gap shape-complexity index and a quantitative assessment index in ArcGIS of the geoclassified, LULC endmember polygons. The performance of CHM-based thresholding was exceeded by that of other methods, especially thresholding of canopy porosity rasters and the per-pixel supervised classification in ArcGIS. Beyond assessing the methods performance, the authors of Jacob et al. [11] argue the critical need for future gap studies to consider the geometric accuracy of results for optimally remotely identifying African riverine, tributary, eco-georeferenceable, eco-epidemiological,*S. damnosum*s.l.,African, riverine, tributary, seasonal, hyperproductive, capture point, breeding foci.

If the canopies do intersect and/ or overlap such that foliage density remains constant within the overlap area, in an cross-border, African, riverine tributary, eco-georeferenceable, *S. damnosum* s.l., forecast, vulnerability, eco-epidemiological immature habitat, remotely sensed, moderate resolution, identification model the problem maybe more difficult to resolve, It may be approached with an exact solution as well as alternative approximations in ArcGIS.Forest canopy density and height may be optimally employable as regressors in a number of cross-border, *S. damnosum* s.l., African riverine, tributary, capture point, geometric endmember, geoclassifiable, LULC, forecast vulnerability, immature habitat, modeling applications, such as biomass estimation, vegetation coverage, and biodiversity determination. Canopy density, or canopy cover, is the ratio of vegetation to ground as seen from the air while canopy height measures how far above the ground the top of the canopy is. [8]. Moderate resolution, geoclassifiable, microtopographic LULCs may be employable to qualitatively quantitate these geoclassifiable, larval habitat oviposition, vector arthropod, eco-epidemiological, moderate resolution,geoclassifiable, LULC, siagmenture, capture point, uncoalesced, predictor variables. The most effective way to determine the canopy density is to divide the study area into many small equal-sized units through rasterization in ArcGIS (www.esri.com).In each raster cell, an onchocerciasis researcher or epidemiologist may optimally compare the number of above seasonal, hyperproductive, cross-border, capture point,African, riverine tributary, *S. damnosum* s.l., immature habitats, to the total number of discontinuous canopied, trailing vegetated,eco-georeferenceable, breeding foci,capture points based on appropriate stratified, grid cell size algorithmic, endmember, spectral wavelength, frequency, LULC determination in Statistical Analyst™ for determining canopy height,

In probability and statistics, Student's *t*-distribution (or simply the *t*-distribution) is any member of a family of continuous probability distributions that arises when estimating the mean of a normally distributedpopulation (e.g., uncoalesced, empirical dataset of eco-georeferenced, moderate resolution, geoclassified, LULC, cross-border, African, riverine tributary, *S. damnsoum* s.l.,breeding foci, endmember, capture points) in situations where the sample size is small and population standard deviation is unknown[10]. Whereas a normal distribution describes a full population(e.g., unmixed, spectral endmember, wavelength,frequency datasetsof eco-georeferenceable,moderate resolution, immersed, vegetation,cross-border, discontinuously canopied, oviposition, black fly capture point, LULC, sub-pixel, immature, habitat, microtopographic components),*t*-distributions would describe samples drawn from theseasonal,eco-



epidemiological, field-operationizable dataset accordingly : the t -distribution for each sample size would be symmetrically quantitated in Statistical Analyst™. Optimally the probability density function must resemble the bell shape of a normally distributed endmember variable with mean 0 and variance 1[19]. The larger the sample, the more the distribution resembles a normal distribution[20].

In Statistical Analyst™, there are four approximation methods precisely usable for qualitative, iterative interpolation of a geoclassified, temporal, endmember, moderate resolution, iteratively interpolative, eigen-decomposed, cross-border, African, riverine tributary, *S. damnosum* s.l., immature habitat, endmember, LULC signature: direct, linear, Gaussian kernels, and multiplicative skewing. The direct method would employ the observed cumulative distribution in the linear method fits lines between each step of the cumulative distribution, and the Gaussian kernels method would approximate the cumulative distribution by fitting a linear combination of component cumulative normalized distributions (e.g., , moderate resolution, endmember, black fly, uncoalesced geoclassified, wavelength, LULC, radiance frequencies sampled at a cross-border, eco-georeferenceable, eco-epidemiological, African, riverine, tributary, seasonal, breeding foci).

Multiplicative skewing may approximate the cumulative distribution in the entomological, vector, arthropod, immature habitat, eco-epidemiological, identification, model by fitting a base distribution [e.g., Student's t , lognormal, gamma, empirical, and log empirical) that may then be skewed by a fitted linear combination of beta distributions (e.g., the skewing is conducted with the inverse, probability, integral, spectral, wavelength, frequency transformation). Lognormal, gamma, and log empirical base, moderate resolution, endmember LULC, uncoalesced, spectral, wavelength, frequency, decomposed, endmember distributions may only be employable for optimally remotely securitizing a cross-border, African, riverine tributary, geoclassified, capture point, *S. damnosum* s.l., breeding foci, in an uncoalesced, moderate resolution, endmember, LULC dataset and the immature habitat eco-epidemiological, model, predictions (e.g., seasonal, hyperproductive, eco-georeferenceable, capture points),

Akaike's Information Criterion (AIC) in ArcGIS may provide a method to judge the quality of the fitted model. The AIC is a measure of the relative quality of statistical models for a given set of data (e.g., uncoalesced, empirical, geoclassified, moderate resolution, cross-border, *S. damnosum* s.l., endmember, uncoalesced, wavelength, capture point, eco-epidemiological, spectral wavelength, LULC, signature foci frequency explainers). Given an empirical dataset collection of optimally regressively parameterizable, geoclassifiable, endmember, LULC covariates for optimally, remotely, identifying, cross-border, *S. damnosum* s.l., immature habitat, eco-epidemiological, capture points on geoclassifiable, moderate resolution, grid-stratified data, AIC will estimate the quality of each model regressor relative to each of the other. In so doing, AIC can provide a means for statistical model selection for aiding in identifying immature, black fly, capture points in politically unstable, African, riverine, tributary ecosystems.

AIC is founded on information theory: it offers a relative estimate of the information lost when a given model is used to represent the process that generates the data[7]. Thus, the trade-off between the goodness of fit of a cross-border, remotely sensed, moderate resolution, eco-epidemiological, forecast, vulnerability, eco-georeferenceable, capture point, LULC, *S. damnosum* s.l., immature habitat, identification model and the complexity of the model could be optimally quantitated in ArcGIS.

According to the literature[21], when using AIC with least-squares regression in PROC REG, the number of optimally parameterizable covariate, geometric endmember, moderate resolution, LULC estimators (e.g., the density of moderate resolution geoclassifiable, African, riverine, tributary, partially canopied, *S. damnosum* s.l., agro-village, capture point, wavelength frequency covariates) would be equal to the number of dependent variables (e.g., total number of remotely, identified seasonal, hyperproductive, breeding foci) in the moderate resolution, black fly, model employing the intercept and the error term. When employing the MIXED procedure and estimation via maximum likelihood, $AIC = -2LL + 2*(q + p)$ may be optimally determined for a moderate resolution, eco-epidemiological, unmixed dataset of African, riverine, tributary, geoclassified, moderate resolution, LULC endmembers where q would be the number of geovisualizable, cross-border, eco-georeferenceable, eco-epidemiological, capture point, *S. damnosum* s.l., immature habitat, breeding foci in the covariance matrix in MIXED where p would be the number of parameters that are estimated as part of the model fixed effects.

Note, though, that if an onchocerciasis researcher or epidemiologist employs the MIXED procedure, the restricted (or residual, or reduced) maximum likelihood REML estimation, the AIC formula for the cross-border, *S. damnosum* s.l., eco-epidemiological, immature habitat identification, moderate resolution, endmember, forecast, vulnerability model would be quantitated by $AIC = -2LL + 2q$. In statistics, REML



approach is a particular form of maximum likelihood estimation which does not base estimates on a maximum likelihood fit of all the information, but instead uses a likelihood function calculated from a transformed set of data, so that nuisance parameters have no effect [22]. It should be observed that when quantitatively estimating sub-pixel, entomological, vector, arthropod, endemic, capture point, eco-epidemiological, moderate resolution, black fly, African, tributary, forecast, vulnerability, explanatory, focimodels employing REML, it would not be appropriate to use likelihood-based statistics to select microtopographic, declassifiable, frequency wavelength, geoclassifiable, LULC parameters which are amongst the model fixed effects [18].

After the Geostatistical Wizard makes an eco-epidemiological eco-georeferenceable, optimizable frequency LULC moderate resolution, eco-epidemiological, optimizable dataset of cross-border, moderate resolution, *S. damnosum* s.l., immature habitat, predictions based on a transformed scale of geoclassified moderate resolution data (e.g., uncanopied, trailing immersed vegetation), it automatically would transform the data then back to the original scale. The choice of approximation method for identifying the African, riverine, tributary, immature habitats robustly would depend on the assumptions an onchocerciasis researcher or epidemiologist is willing to make and the smoothness of the approximation in Geostatistical Wizard. The direct method would be the least smooth method for optimally remotely identifying cross-border, *S. damnosum* s.l. breeding foci capture points, in cross-border, vectored African riverine tributaries which would also have the fewest assumptions, especially when the linear method is intermediate. The Gaussian kernels and multiplicative skewing methods have smooth reverse transformations but assume that the data distribution can be approximated by a finite combination of known spatial and non-spatial distributions [6].

Statistical analysis functions in ArcGIS for Desktop are either nonspatial (tabular) or spatial (containing location). Nonspatial statistics (e.g., Sum, Mean, Maximum, Minimum, Range, Standard Deviation,) may be parsimoniously employable to analyze eigenfunction decomposed, geoclassified, moderate resolution, geometric endmember, LULC, uncoalesced, feature, attribute values associated with remotely identified, hyperproductive, seasonal, cross-border, African, riverine, tributary, breeding foci (porosity of discontinuous remotely identified canopy gaps). The values may be accessed directly from a layer's feature attribute table. The Summary Statistics tool may be employable subsequently to calculate the number of vacant parcels for a set of eco-georeferenceable, seasonal, hyperproductive, geoclassifiable, moderate resolution, black fly, capture points including the total, the mean, and the standard deviation. The Output Table may consist of fields containing the result of the statistical operation in Statistical Analyst™. For example, an eco-epidemiological, hyperproductive, cross-border, seasonal, African, riverine, tributary, eco-georeferenceable, capture point, cross-border, *S. damnosum* s.l., breeding foci on a moderate resolution eigen-geoclassified, explanatory LULC field in Statistical Analyst™ may be created for each orthogonal, decomposed, statistic type employing the following naming convention: SUM_<field>, MAX_<field>, MIN_<field>, RANGE_<field>, STD_<field>, FIRST_<field>, LAST_<field>, COUNT_<field> (where <field> which would be the name of the input field (e.g., immature, black fly, eco-epidemiological, remotely sensed, immature, habitat identification model) for which the statistic may be computed in ArcGIS. The field name may truncated to 10 characters when the output table is a dBASE table.

Studentized, African, riverine tributary, cross-border, endmember, *S. damnosum* s.l., immature, capture points on moderate resolution, geoclassified LULCs in ArcGIS may reveal outliers ("extreme observation"). In spatial statistics, an outlier is a georeferenced observation point that is distant from other observations [8]. An outlier in an eco-epidemiological, African, riverine, tributary, cross-border, *S. damnosum* s.l., capture point, eco-georeferenceable, forecast, vulnerability, immature habitat, identification model may be due to variability in the focal measurement or it may indicate experimental error; the latter are sometimes excluded from the sample remote sensed database. Given a set of unmixed, eco-epidemiological, capture point, moderate resolution, geoclassified, endmember, LULC *S. damnosum* s.l., diagnostic, input diagnostic features (e.g., geoclassifiable, moderate resolution, uncoalesced, frequency, LULC, wavelength, irradiance measurements) and an input identification field, the Cluster and Outlier Analysis tool in Geospatial Analyst™ may optimally visualize, individual, cross-border, breeding foci, or grid-stratified, clustering outliers of eco-georeferenceable, African, riverine, vector arthropod, hyperproductive, immature habitats. These observations can have a disproportionate effect on statistical analysis, such as the mean, which can lead to misleading results (falsely prognosticated, cross-border, LULC, *S. damnosum* s.l., hyperproductive, riverine, tributary, breeding foci).

Ironically outliers can provide useful information about data or process, so it's important to investigate them [10]. Jacob et al. [23] calculated terrain curvature from a 3-dimensional (D), Digital Elevation Model (DEM) for remotely investigating an eco-georeferenced, capture point, seasonal, hyperproductive, *S. damnosum* s.l.,



immature, habitat, eco-epidemiological foci in an African, riverine, tributary neighbourhood (Chutes Dienkoa) in Burkina Faso. A DEM is a raster representation of a continuous surface, usually referencing the surface of the earth [8]. The accuracy of this geoclassified LULC data was determined primarily by the resolution (e.g., the Euclidean distance measurement between sample, African, riverine, tributary, eco-georeferenceable, geoclassifiable, LULC, *S. damnosum* s.l., seasonal, capture points), whilst other co-factors affecting accuracy were data type (e.g., integer or floating point) and the actual sampling of the surface. The authors reasoned that the topographic LULC changes may have occurred when creating the original DEM. The point, elevation data from the 3-D DEM was overlaid with an iteratively interpolated, endmember, LULC, black fly, geoclassified, breeding foci, iteratively interpolated, reference signature map in Spatial Analyst™.

Generally, the 3-D, orthogonal, grid-stratified, DEM performed well for remotely identifying, capture point, *S. damnosum* s.l., immature habitats, but some artifacts from the interpolation existed in the vulnerability endemic explanatory forecasts. Those artifacts caused extreme LULC values (i.e., outliers) for curvature. Around 90% of the curvature values were between -25 and 25, but the other 10% were between -500 and 500. The authors of Jacob et al [11] then employed a histogram in ArcGIS to equalize the LULC data so as to properly geovisualize the curvature raster. The question was: How to exclude the extreme values from the raster so as to optimally identify the capture point, *S. damnosum* s.l. immature habitat breeding foci? The authors assumed initially a pseudo-code would rectify the LULC parameter misspecification by employing:

```
m = median("curvature")
```

```
IF ("curvature. Value") > m * 10 THEN ("curvature. Value") = m * 10("curvature. Value") = m * 10
```

Unfortunately, the LULC elevation parameters could not optimally quantitate the 3-D values, as suggested by the pseudocode in the *S. damnosum* s.l., remote, eco-epidemiological, forecast, vulnerability, immature, habitat, identification model as the curvature artifacts did not necessarily correspond to high-[8] curvature areas.

The authors in Jacob et al. [11] then considered smoothing the DEM before computing the curvature for optimally identifying microtopographic, biogeophysical, geoclassified LULCs where hypereproductive, seasonal, eco-georeferenceable, black fly immature habitat, capture points existed. Smoothing is a statistical technique that helps spot trends in noisy data, which may be usable to compare trends between two or more fluctuating time series [7]. In so doing, the authors assumed that could slightly reduce the curvatures for rendering, reasonable, eco-epidemiologically quantitative microtopographic LULC values (e.g., 3-D slope coefficients). To optimally regressively quantiate canopy height, the authors subtracted the bare earth surface (DEM) from a Digital Surface Model (DSM) surface generated in Spatial Analyst™) for geovisualizing the eco-georeferenceable, cross-border, African riverine, tributary, *S. damnosum* s.l. immature habitat, 3-D, capture point geolocations. Smoothing the DEM can be done with local medians or means [8].

Unfortunately a robust way to estimate curvature is not currently available in any Arc* software, so the authors of Jacob et al. [11] employed smoothing techniques in R. Smoothing splines, like kernel regression and k -nearest-neighbors regression, provide a way of optimally estimating the underlying regression function: $r(x) = E(Y | X = x)$ [7]. Splines have been used traditionally as mathematical analogues to the thin flexible strips used in drafting for iteratively qualitatively interpolating new values between adjacent endmember, fractionalized eco-georeferenceable LULC measurements [6]. In pattern recognition, the k -nearest neighbors algorithm (k -NN) is a non-parametric method used for classification and regression [19]. In both cases, the input consists of the k closest training examples in the feature space. Kernel regression is a non-parametric technique in statistics to estimate the conditional expectation of a random variable [24]. The objective is to find a non-linear relation between a pair of random sub-pixel, geoclassified, LULC variables X and Y . [11] employed the following statements in R

```
smooth. Spline (x, y = NULL, w = NULL, do, spar = NULL,
```

```
cv = FALSE, all. Knots = FALSE, nknots = NULL,
```

```
keep.data = TRUE, df.offset = 0, penalty = 1,
```

```
control.spar = list(), tol = 1e-6 * IQR(x))
```




Subsequently, the authors of Jacob et al. [11] obtained the equation of the fitted smooth spline function for optimally interpreting the geoclassified, endmember, LULC, moderate resolution, *S. damnosum* s.l. immature habitat, regression coefficient endmember outputs whilst optimally computing the R^2 of the fitted function. They then computed the analytical first derivative of the fitted tabulated function, and obtained its equation with actual geosampled, eco-georeferenced, black fly, breeding foci, geoclassified, LULC coefficients.

The immature, spectral frequency, moderate resolution, LULC, wavelength, endmember, larval habitat, optimizable, eco-epidemiological, eco-georeferenceable, capture point dataset was computed as

```
library(stats)

x <- 1:11

y <- c(0.2, 0.40, 0.6, 0.75, 0.88, 0.99, 1.1, 1.15, 1.16, 1.16, 1.16)

plot(x, y)

spline <- smooth.Spline(x, y)

lines(spline)
```

The immature, *S. damnosum* s.l., endmember, habitat, uncoalesced, LULC data fit a natural spline (linear tail restricted) employing truncated power. Truncated power functions can be employable for construction of B-splines. In the mathematical subfield of numerical analysis, a B-spline, or basis spline, is a spline function that has minimal support with respect to a given degree, smoothness, and domain partition [6]. Any spline function of given degree can be expressed as a linear combination of B-splines in ArcGIS for quantitating degrees in an eco-georeferenceable, eco-epidemiological, cross-border, African riverine tributary, *S. damnosum* s.l., capture point, breeding foci. Cardinal B-splines have knots that are equidistant from each other. B-splines can be employed for curve-fitting and numerical differentiation of experimental data.

The Spline tool in ArcGIS pro uses an interpolation method that estimates values using a mathematical function that minimizes overall surface curvature, resulting in a smooth surface that passes exactly through the input points (www.esri.com).

In Jacob et al. [11] the uncoalesced, endmember, cross-border, *S. damnosum* s.l. eco-epidemiological, forecast, vulnerability immature habitat, identification model, default knots based on quantiles of the vector, arthropod, immature habitat, explanatory predictors were not used; instead the authors specified 4 knots. The abscissa or X-axis values of the join points are called knots [7]. The only way to get a test of goodness of fit is to postulate a richer model than this and see if it improves the model fitted [6]. An ANOVA tested the goodness of fit of a linear relationship by pooling the nonlinear, unmixed, riverine, tributary, immature habitat terms into a composite ("chunk") test ($F=176.49$). The immature habitat explanatory functions re-expressed the restricted cubic spline in the cross-border, *S. damnosum* s.l. model's uncoalesced, spectral, wavelength frequency, LULC estimators simplest form without the outliers. A cubic spline is a spline constructed of piecewise third-order polynomials which pass through a set of control points [7]. The first derivative in the immature, habitat, eco-epidemiological, LULC, identification model was then remotely quantitated in ArcGIS Pro by:

```
function(x) 0.174 - 3 * 0.00279 * pmax(x - 3, 0) ^ 2 + 3 * 0.0015 * pmax(x - 5, 0) ^ 2 + ..
```

In general, curvature may be estimated by fitting a quadratic and specialized low-order polynomial in a cross-border, African, riverine, tributary neighborhood in ArcGIS Pro. The authors of Jacob et al. [11] performed a usual fitting method (i.e., least-squares), which was sensitive to slight local spectral wavelength LULC endmember variations in the 3-D, black fly, eco-epidemiological, immature habitat identification, forecast, vulnerability, eco-epidemiological model. The OLS tool also produces an output feature class and optional tables with coefficient information and diagnostics. (www.esri.com). Hence, by expanding a African, riverine, tributary, cross-border neighborhood and using a fitting method in ArcGIS, the outlying, cross-border, *S. damnosum* s.l. breeding foci, capture point, regression residuals may be downweighted so as representative and accurate curvature estimates may be parsimoniously rendered from the immature habitat identification model. The authors in Jacob et al. [11] replaced the extreme curvature values with NoData. This was a draconian measure, but it was appropriate since the extreme, immature, capture point, habitat,



explanatory, microtopographic, remotely quantitated, uncoalesced, explanatory, eco-georeferenceable microtopographic LULC values were artifacts of the interpolation and therefore, did not reflect truly high curvatures in the elevation endmember model for optimally identifying, eco-epidemiological, seasonal, hyperproductive, *S. damnosum* s.l., breeding foci. Subsequently, an onchocerciasis researcher or epidemiologist may choose an iterative interpolation method in Spatial Analyst™ that produces smoother surfaces. For example, the 'map algebra' syntax for replacing values with NoData uses the SetNull command, as in

```
SetNull(Abs([Curvature grid]) > 10*Abs(m), [Curvature grid])
```

Map Algebra is a simple and powerful algebra in Spatial Analyst™ which can execute tools, operators, and functions to perform eco-geographic, time series, robust LULC analysis for identifying a moderate resolution, geoclassified, endmember, cross-border, African, riverine tributary, seasonal, hyperproductive, *S. damnosum* s.l. breeding foci. Map Algebra is available through the Spatial Analyst module; an extension of the ArcPy Python site package. As Map Algebra, has been integrated in Python, all the functionality of Python and ArcPy and its extensions (modules, classes, functions, and properties) are available for optimizing, cross-border, seasonal, capture point, African, riverine, tributary, moderate resolution, endmember, LULC, *S. damnosum* s.l., immature, habitat, endmember mapping. Spatial Analyst tools are accessed through an algebraic format. That is, an object (e.g., eco-georeferenceable, trailing vegetation, hyperproductive, capture point, black fly, breeding foci) whose name is identified to the left of an equal sign may be created based on a tool or operator stated to the right of the equal sign which may be written in ArcPy as:

```
from arcpy.sa import *  
outRas = Slope("indem")
```

The above statement may calculate the slope for each cell in the indem dataset and create a Raster object called outRas to store the vector arthropod breeding foci, microtopographic, spectral, wavelength, frequency, LULC results for optimally identifying the African riverine, tributary, cross-border, capture point, vector, arthropod foci.

Importantly, in a remotely sensed, cross-border, 3-D, *S. damnosum* s.l. immature habitat, African riverine tributary, ecosystem, forecast, vulnerability, eco-epidemiological, remotely sensed, endmember, identification model, the median curvature should not be employed when geovisualizing eco-georeferenceable breeding foci: the median often will be close to zero and therefore will not reflect typical large curvatures (positive or negative) [8]. In Jacob et al. [11] large multiples of the median absolute curvature was a reasonable choice for smoothing the endmember, vector arthropod, entomological, LULC data. The histogram of curvatures found the threshold LULC values.

Furthermore, if the SetNull approach pokes too many NoData holes in a moderate resolution, grid-stratified, remote sensing, moderate resolution, cross-border, African, riverine tributary, geoclassifiable, LULC, immature habitat, identification eco-epidemiological, endmember model, an onchocerciasis researcher or epidemiologist could consider determining whether the curvature grid could be smoothly varying in ArcGIS. If so, and if those "holes" tend to be isolated (or in narrow stripes--which would be a strong indicator that a poor interpolator was used) in the cross-border, African riverine, tributary, immature, habitat identification model, an onchocerciasis researcher or epidemiologist could fill them by computing a focal mean and pasting the mean values over the holes in Spatial Analyst™. The pasting is done with the conditional operator, as in

```
Con(IsNull([Modified curvature grid]), [Focal mean grid], [Modified curvature grid])
```

Note the use of IsNull can detect the NoData cells (www.esri.com)

Alternatively, ArcPy may identify which cells in the input raster are NoData, and outputs the result as an IMG raster in a cross-border, endmember, *S. damnosum* s.l. African, riverine, tributary, breeding foci on anecogeoreferenced, geoclassifiable, moderate resolution, LULC. employing:

```
import arcpy
```



```
from arcpy import env
```

```
from arcpy.sa import *
```

```
env.workspace = "C:/sapyexamples/data"
```

```
outIsNull = IsNull("degs")
```

```
outIsNull.save("C:/sapyexamples/output/outisnull.img")
```

IsNull example 2 (stand-alone script)

For remotely identifying which geoclassified, moderate resolution, LULC cells in the input raster in the, cross-border, spectral eigen-function decomposed, wavelength, endmember, *S. damnosum*, breeding foci, capture point, immature habitat, identification, frequency model are NoData, and outputting the results as a grid raster in ArcGIS, an onchocerciasis researcher or epidemiologist may use:

```
# Name: IsNull_Ex_02.py
```

```
# Description: Find which cell values of the input raster are NoData
```

```
# Requirements: Spatial Analyst Extension
```

```
# Import system modules
```

```
import arcpy
```

```
from arcpy import env
```

```
from arcpy.sa import *
```

```
# Set environment settings
```

```
env.workspace = "C:/sapyexamples/data"
```

```
# Set local variables
```

```
inRaster = "degs"
```

```
# Check out the ArcGIS Spatial Analyst extension license
```

```
arcpy.CheckOutExtension("Spatial")
```

```
# Execute IsNull
```



```
outIsNull = IsNull(inRaster)
```

```
# Save the output
```

```
outIsNull.save("C:/sapyexamples/output/outisnull")
```

High or low, unmixed, explicative, grid-stratifiable, formally optimizable, uncoalesced, eigen-decomposed, moderate resolution, LULC, spectral uncoalesced, endmember, wavelength, frequency values in Statistical Analyst™ may also simultaneously quantitate, outliers in prognosticated, remotely targeted, hyperproductive, seasonal, entomological, vector arthropod, immature habitat, geoclassified, capture point, endmember datasets. To do this, the tool would calculate a local Moran's *I* value [6]. The Spatial Autocorrelation (Global Moran's *I*) tool in Statistical Analyst™ measures spatial autocorrelation based on both LULC sub-pixel, feature locations and feature values simultaneously (www.esri.com). Given a set of unmixed, moderate resolution, geoclassified, spectral, LULC wavelength frequency feature attributes and an associated geoclassifiable, cross-border, African, riverine, tributary, *S. damnosum* s.l., eco-epidemiological, capture point, feature attribute, the Arc tool could evaluate whether the eco-cartographically, forecasted LULC pattern expressed is clustered, dispersed, or random. The tool will calculate the Moran's *I* Index value and both a z-score and p-value to evaluate the significance of that LULC index for optimally remotely identifying a cross-border, black fly, breeding foci. P-values are numerical approximations of the area under the curve for a known distribution, limited by the test statistic [10].

Z-scores are simply standard deviations especially in a moderate resolution, remotely sensed, oviposition, LULC, geoclassifiable, vector, arthropod-related, eco-epidemiological, immature habitat, identification eco-georeferenceable forecast, vulnerability model. If for example, a tool in ArcGIS returns a z-score of +2.5 in an immature, habitat identification, LULC eco-georeferenceable, *S. damnosum* s.l., endmember model, an onchocerciasis researcher or an epidemiologist could say that the result is 2.5 standard deviations. Both z-scores and p-values in these vulnerability models would henceforth be associated with the standard normal distribution generated by a geospatial, geoclassifiable, moderate resolution, seasonally imaged, *S. damnosum* s.l., cross-border, capture point, explanative, LULC, stochastic or deterministic, endmember iterative interpolator [2]. The z-scores and p-values returned by the spatial, LULC pattern analysis tools in Statistical Analyst™ may tell an onchocerciasis researcher or an epidemiologist whether he or she should reject the null hypothesis or not (e.g., an interpolated, endmember, cross-border, LULC, target signature of a capture point, hyper productive, seasonal, cross-border, *S. damnosum* s.l., breeding foci can identify endmember, geolocations of other unknown, un-sampled, black fly foci in an African, riverine, tributary).

The Spatial Autocorrelation tool returns five values: the Moran's *I* Index, Expected Index, Variance, z-score, and p-value. These values are written as messages at the bottom of the Geoprocessing pane during tool execution and passed as derived output values for potential use in cross-border, African, riverine tributary, *S. damnosum* s.l. eco-epidemiological, habitat models or scripts. The messages may be accessed by hovering over the progress bar, clicking on the pop-out button, or expanding the messages section in the Geoprocessing pane. The messages may be also accessed for a previously run tool via the Geoprocessing History. Optionally, this tool will create an HTML report file with a graphical summary of the moderate resolution, grid-stratified, LULC immature, black fly, eco-epidemiological, capture point, habitat, identification endmember, model results. The path to the report will be included with the messages summarizing the tool execution parameters. Clicking on that path will pop open the report file.

A positive value for Moran's *I* in Statistical Analyst™ would indicate that a cross-border, African, riverine, tributary, *S. damnosum* s.l., clustering, immature habitat, moderate resolution, extrapolated, LULC attribute feature has neighboring topographies with similarly high or low attribute values; this feature would be a part of an breeding foci cluster

A negative value for the product moment correlation coefficient would indicate that the feature has neighboring uncoalesced, endmember LULC features with dissimilar values (i.e. a negatively autocorrelated, quantized, geospatial, African, riverine, tributary, cross-border, *S. damnosum* s.l., immature habitat clustering propensity); this feature is an outlier. In either instance, the p-value for the explanatory, LULC feature must be small enough for the cluster or outlier to be considered statistically significant in the remotely sensed, LULC, immature habitat, endmember, identification model, summary statement.



The output field, cluster/outlier type (COType) in ArcGIS will distinguish between a statistically significant (0.05 level) cross-border, African riverine tributary, *S. damnosum* s.l., endmember, immature, habitat cluster of high values (HH), cluster of low values (LL), outlier in which a capture point, high value is surrounded primarily by low values (HL), and outlier in which a low value is surrounded primarily by high values (LH). This ArcGIS tool can create a new output robustifiable, cross-border, endmember, *S. damnosum* s.l., immature habitat, feature class with the following attributes for each feature in the input LULC class: local Moran's *I* index, and COType. The field names of uncoalesced, spectral, wavelength, frequency, feature attributes can also be returned as derived tool string outputs in ArcGIS for potential use in custom models or scripts.

When a clustering tool runs in ArcMap, the output explanatory, uncoalesced, endmember, spectral, wavelength LULC feature class will be automatically added to the table of contents (TOC) with default rendering applied to the COType field. The rendering applied to an eco-epidemiological, crossborder, *S. damnosum* s.l. African, riverine, tributary, geoclassifiable, eco-georeferenceable, LULC capture point, breeding foci would be eco-cartographically optimally definable by a layer file in ArcToolbox, TemplateLayers. The Cluster and Outlier Analysis (Anselin Local Moran's *I*) tool can identify these foci geolocations in an agro-village study area where anomalous, endemic, immature habitat, eco-epidemiological, spatial patterns may be associated with an unexpectedly high rate of onchocerciasis.

There are three main components of Geostatistical Analyst™ that may be usable for constructing an eco-georeferenceable, robust, geoclassifiable, moderate resolution, eco-epidemiological, cross-border, African, riverine tributary, *S. damnosum* s.l., breeding foci, remote, immature, capture point, immature habitat, identification, spatial trend, eco-georeferenceable model parsimoniously: 1) A set of exploratory uncoalesced endmember, spatial data analysis (ESDA) graphs, 2) The Geostatistical Wizard; and, 3) The Geostatistical Analyst toolbox, which houses geoprocessing tools specifically designed to extend the capabilities of the Geostatistical Wizard and allow further microtopographic analysis of the LULC surfaces it generates. Non-linearly, exploratorily, autoregressively, eigen-orthogonal, unmixed datasets of, hyperproductive, eco-georeferenceable, trailing vegetation, partially canopied, geo-spectrotemporal, geosampled, cross-border, *S. damnosum* s.l., immature habitat, endmember wavelength, geoclassifiable, LULC data for example, can produce a variety of output surfaces, which may be transformable into geostatistical layers in Spatial Analyst™ for performing simulation and sensitivity analysis. Such a model may aid in designing field-sampling cyber-networks for optimizing *S. damnosum* s.l., breeding foci in African riverine environments [23]. An iterative autoregressive diagnostic indecomposable process in an entomological, moderate resolution, geo-spectrotemporal or geo-spatiotemporal, geoclassifiable, black fly vulnerability, immature LULC, habitat eco-epidemiological, forecast vulnerability, time series model may operate under the premise that past seasonal, sampled, immature, density, count values influence current immature habitat values based on quantitatively, tabulated seasonal, land cover, transitional probabilities. Hence, prognosticative, remotely identifying cross-border, *S. damnosum* s.l., breeding foci on moderate resolution, imaged, African, riverine tributary, LULCs in Statistical Analyst™ would allow optimal unbiased forecasting of eco-epidemiological, eco-georeferenceable, capture point, geosampled, geoclassifiable data.

Subsequently, techniques in Statistical Analyst™ may be optimally employable to describe geoclassifiable, moderate resolution, seasonal, uncoalesced, empirical datasets of LULCs and their geospatial, endmember, wavelength, frequency emissivity, geospatial patterns (e.g., variography), while optimally iteratively qualitatively interpolating, endemically summarized values at unmeasured, remotely identified, African, riverine, cross-border, tributary, eco-geographical, *S. damnosum* s.l. immature, habitat, geolocations (co-kriging), based on, eco-georeferenceable, uncoalesced, microtopographic, landscape, endmember, wavelength, uncoalesced, signature, feature attributes. In applied statistics, regression-kriging (RK) is a spatial prediction technique that combines a regression of the dependent variable on auxiliary variables (e.g., seasonal, black fly, geoclassifiable, parsimoniously parameterizable, moderate resolution uncoalesced, spectral wavelength, LULC estimators retrieved from digital elevation modelling, remote sensing/imagery, and thematic maps) with kriging of the regression residuals [8]. It is mathematically equivalent to the method variously called universal kriging and kriging with external drift, where auxiliary predictors are employed directly to solve signature interpolation. Furthermore, the error, innovation and noise term contribution on geo-Spectrotemporally and or geo-spatiotemporally associated with microtopographic, geoclassified, moderate resolution, LULC endmember, optimally forecasted, *S. damnosum* s.l., cross-border, vector arthropod, immature habitat, remotely sensed, moderate resolution, eco-epidemiological, identification model unbiased estimator would be assessable in Spatial Analyst™. Under suitable assumptions on the priors, kriging gives the best linear unbiased prediction of the intermediate values [7].



A prior can be elicited from the purely subjective assessment of an experienced expert. An uninformative prior can be created in Spatial Analyst™ to reflect a balance among outcomes when no information is available. Priors can also be chosen according to some principle, such as symmetry or maximizing entropy given constraints; examples are the Jeffrey's prior or Bernardo's reference prior. When a family of conjugate priors exists, choosing a prior from that family simplifies calculation of the posterior distribution. In Bayesian statistical inference, a prior probability distribution, often simply called the prior, of an uncertain quantity is the probability distribution that would express one's beliefs about this quantity before some evidence is taken into account[7].

The lack of a complete geoclassified, moderate resolution, LULC eco-epidemiological, cross-border, African, riverine tributary, habitat, identification model hinders the choice of the optimum interpolation algorithm for robust signature interpolation for identifying seasonal, eco-georeferenceable, hyperproductive, cross-border, *S. damnosum* s.l., breeding foci, capture points in African riverine tributary environments. A plausible solution to this problem may be found by investigating the performance of alternative interpolation algorithms in Spatial Analyst™ for employing synthetically generated surfaces for various black fly, cross-border, field sampling scenarios. The synthetic LULC data in Spatial Analyst™ could represent the possible trends and variations of seasonal onchocerciasis. The performance of Random Field Priors (RFP) and Kriging interpolation algorithms may be investigated in Spatial Analyst™ over a moderate resolution, geoclassifiable, orthogonal, LULC, parameter estimator, eigenvector dataset of spatially correlated synthetic endmember regressors for optimally tabulating various variance, range and trend options. Synthetic, eigen-decomposed, orthogonal, eigenvector, moderate resolution, geoclassified, LULC data may be sampled with regular and random sampling patterns in Spatial Analyst™ for quantifying a number of moderate resolution samples from sparse to dense samplings. Interpolation scenarios may be optimally generated to investigate the improvement of the interpolation accuracy of the methods for each black fly, eigen-decomposed, moderate resolution, LULC parameter. It may be observable that for the random sampling, orthogonal endmember, orthogonal, synthetic, LULC patterns in Spatial Analyst™ the trend may not be correct. The residual ESF propagational errors of the interpolation algorithm increases when the trend is modeled correctly; the reconstruction errors decrease [6](Griffith 2003). For the regular sampling patterns, the trend model may not affect the accuracy of the methods in an eco-georeferenceable, cross-border, seasonal, hyperproductive, capture point, *S. damnosum* s.l. breeding foci and the identification remotely sensed model reconstruction errors when close to lower bound values in Statistical Analyst™. An example reconstruction may also be provided over differentially corrected GPS-derived, (DGPS) moderate resolution, geoclassified, endmember LULC data points (remotely identified, black fly, cross-border, eco-epidemiological, capture point) and error variances which may be comparable over kriging and random field prior algorithms in Spatial Analyst™. In Spatial Analyst™ kriging or Gaussian process regression is a method of interpolation for which the interpolated values are modeled by a Gaussian process governed by prior covariances, as opposed to a piecewise-polynomial spline chosen to optimize smoothness of the fitted values (www.esri.com).

A variety of endmember signature LULC interpolation applications with a prior distribution on a covariance matrix can be specified in Geospatial Analyst™ for optimally interpolating, endmember, African, riverine, tributary, moderate resolution, geoclassifiable, cross-border, *S. damnosum* s.l., LULC, breeding foci in a Gaussian field once a capture point has been remotely identified. In probability theory and statistics, a covariance matrix (also known as dispersion matrix or variance-covariance matrix) is a matrix whose element in the i, j position is the covariance between the i^{th} and j^{th} elements of a random vector. A random vector is a random variable with multiple dimensions. Each element of the vector is a scalar random variable. Each element has either a finite number of observed empirical values or a finite or infinite number of potential values[19]. The potential values (i.e., forecasted, remotely sensed, African, riverine, tributary, immature *S. damnosum* s.l., cross-border, capture point, breeding foci) may be specified by a theoretical joint probability distribution.

Intuitively, the covariance matrix generalizes the notion of variance to multiple dimensions. As an example, the variation in a collection of cross-border, African, riverine, tributary, immature *S. damnosum* s.l., capture point, breeding foci geoclassifiable, explanatory, eco-epidemiological, LULC random points in two-dimensional space in Spatial Analyst™ cannot be remotely characterized fully by a single number, nor would the variances in the x and y directions contain all of the necessary information; a 2×2 matrix would be necessary to fully characterize the two-dimensional variation.

Because the covariance of the i^{th} random variable with itself is simply that random variable's variance, each element on the principal diagonal of the covariance matrix is the variance of one of the random variables[6]. Hence the covariance of the i^{th} cross-border, moderate resolution, geoclassifiable LULC, African,



riverine, tributary, immature *S. damnosum* s.l., capture point, breeding foci random variable with the j^{th} one would be the same thing as the covariance of the j^{th} random variable with the i^{th} one. Every covariance matrix is symmetric [7]. In addition, every covariance matrix is positive semi-definite.

In linear algebra, a symmetric \times real matrix is said to be positive definite if the scalar is positive for every non-zero column vector of real numbers [17]. Positive definite matrices are closely related to positive-definite symmetric bilinear forms (or sesquilinear forms in the complex case), and to inner products of vector spaces. Some authors use more general definitions of "positive definite" that include some non-symmetric real matrices. Suppose an onchocerciasis researcher or epidemiologist employs a response vector y (e.g., red green blue (RGB), breeding foci, blackfly, moderate resolution, sub-pixel, LULC, signature) in Spatial Analyst™ in a moderate resolution, hierarchical, regression, immature habitat, forecast, vulnerability, eco-epidemiological, identification, model with a positive definite covariance matrix. The regression model may provide a decent fit in Spatial Analyst™. The estimations or predictions may be optimally calculable as weighted averages of known input point values, similar to the Moving Average operation in Spatial Analyst™ based on a remotely identified, eco-epidemiological capture point, cross-border, eco-georeferenceable, African, riverine, tributary, *S. damnosum* s.l., seasonal eco-epidemiological, capture point along with some spatially quantitative explanatory eco-eco-georeferenceable, immature habitat, predictor x (e.g., percent of uncanopied trailing vegetation at a capture point).

In statistics, a moving average (rolling average or running average) is a calculation to analyze data points (e.g., geoclassifiable, moderate resolution LULCs where African, riverine, tributary, cross-border, *S. damnosum* s.l. breeding foci exist) by creating series of averages of different subsets of the full sample dataset. It is also called a moving mean (MM) or rolling mean and is a type of finite impulse response filter. In signal processing, in Geospatial Analyst™ a finite impulse response (FIR) filter is a filter whose impulse response (or response to any finite length input) is of finite duration, because it settles to zero in finite time. [8] which is in contrast to infinite impulse response (IIR) filters, which may have internal feedback and may continue to respond indefinitely (usually decaying).

Assume a moderate resolution, geoclassified, cross-border, *S. damnosum* s.l. hyper productive, seasonal, African, riverine tributary, geoclassified LULC, explanatory, spectral wavelength, endmember predictor variable X defined in a domain of a line segment and observations have been made at some, capture point geolocations along the eco-epidemiological, study site segment with irregular spaces for simplification. These observations create capture point values X_1, X_2, \dots, X_n in Spatial Analyst™ as the realizations of X at some selected, remotely identified, immature habitat, hyperproductive breeding foci geolocations. To robustly create a smooth curve to represent the distribution of X in the entire segment, the values of X at the immature habitat geolocations there must be no observed values that have to be interpolated from the signature values of their neighborhood breeding foci locations, which may be expressed in Spatial Analyst™ as $0 \leq w_i \leq 1$ ($i = -k + 1, \dots, k$) to optimally represent the vector, arthropod, sampled covariance oviposition weights with the following constraint: k is a predetermined searching tolerance or moving window size. Various techniques in Spatial Analyst™, such as moving average, reverse distance weighting and kriging, have been developed based on least square.

When data are incomplete or subject to error, Statistical Analyst™ provides a probabilistic framework for quantifying uncertainties. Statistical Analyst™ creates surfaces from sample data using these interpolation methods: Inverse distance weighted, Radial-based functions, Global and local polynomials, Kriging for exact data and for error-contaminated data, Cokriging (multivariate version of the kriging models) and Isotropical or anisotropical models [8]. The many tools in ArcGIS Statistical Analyst™ allow determination of optimal surface for interpolation of the data. (www.esri.com) Geostatistical simulation produces multiple surfaces that mimic the real phenomenon and provide possible values [7]. This provides a basis for risk analyses, field-decision making, and other estimations involving uncertainty, allowing onchocerciasis researchers and epidemiologists to make more informed decisions about remotely identified, cross-border, African, riverine, tributary, *S. damnosum* s.l., immature habitat, capture point eco-georeferenceable, breeding foci employing moderate resolution, geoclassified data. Within Statistical Analyst™ a discontinuous canopied, cross-border, *S. damnosum* s.l., breeding foci map surface, or, measured sample points stored in a point feature layer or raster layer may reveal grid-stratified, polygon-village centroids in cross border ecosystems.

Whilst deliberate implementation of kriging in control programmes across multiple cross border, African, riverine, LULC tributaries has yet to be trialed on a large scale, several examples of remotely targeted, cross border, breeding foci, *S. damnosum* s.l., immature, forecast, vulnerability, eco-epidemiological, interpolated



models in the literature suggest the potential of such a remote sensing, LULC approach. For example, in Jacob et al. (2016), a smoothness regularization algorithm was employed in Geospatial Analyst™ for parsimoniously constructing a Rapid Eye™, endmember, 5 meter (m), chlorophyll (Chl-*a*), trailing vegetation, near -infra-red (NIR), turbid water, capture point, black fly, vector, endmember, immature habitat, LULC signature, which was used as a response variable in a stochastic, iterative, Gaussian process, interpolator (i.e., Ordinary kriging) for implementing onchocerciasis larval control strategies (i.e., ‘Slash and Clear’) in two agro-village complexes in the Goma district in northern Uganda. Chlorophyll *a* is a specific form of chlorophyll used in oxygenic photosynthesis [25], which absorbs most energy from wavelengths of violet-blue and orange-red light; it also reflects green/yellow light, and as such contributes to the observed green color of most plants [8]. The study sites were located 1 kilometer (km) or less from the river Ayago, and were separated by approximately 15 kilometer (km) from one another. Interventions were conducted in the Gongcoyo and Adibuk villages, whilst *S. damnosum* s.l., larval control monitoring with no interventions were conducted in the Ayago-Nile and Laminlatoo villages.

A line transect delineating a plot of 15 kilometer (km) × 15km was measured onto a 128km x 128km, RapidEye™, 5m resolution, polygon employing four, differentially corrected, cardinal points to calculate the frequency of occurrence of the dominant flora encompassing the oviposition, eco-georeferenceable, LULC, capture points geosampled at the agro-village, tributary study sites. RapidEye's satellites are the first commercial satellites to include the Red-Edge band, which is sensitive to changes in Chl-*a* content (www.geoimage.com). An interpretive, three-band, signature, LULC model was tuned to select the 5m, spectral wavebands for optimal, iterative interpolation employing a Gaussian process governed by prior covariances of the endmember, Chl-*a*, geoclassified, discontinuous, LULC, canopy foliage.

In probability theory and statistics, covariance is a measure of the joint variability of two random explanatory variables whereby the greater values of one variable mainly correspond with the greater values of the other variable, and the same holds for the lesser values, (i.e., the variables tend to show similar behavior, the covariance is positive). (<http://mathworld.wolfram.com/Covariance.html>). The normalized version of the covariance in a forecast, entomological, vector arthropod, vulnerability regression paradigm can render a correlation coefficient (i.e., Pseudo R^2) which can measure how well the model fits the habitat observations by summarizing the discrepancy between observed values and the values expected. In statistics, the coefficient of determination, denoted R^2 or r^2 , is a number that indicates the proportion of the variance in the variable that is predictable from the independent variable(s).¹

In Jacob, et al. [28] the eco-georeferenced, RapidEye™, endmember, 5m, Chl-*a*, -detected oviposition, geoclassified, endmember, LULC site was geospatially and geo-Spectro temporally associated to a proportion of the variance in the decomposed non-randomness in the pixel reflectance spectrum which was optimally eco-cartographically delineated in an object-based classifier (Spectral Angle Mapper) in ENVI. The geospectral object classification algorithm then employed a divergence measure to match the spectral wavelengths and pixel, endmember, unmixed, LULC radiance of the eco-georeferenced, black fly, capture point, breeding foci. Leaf, reference, LULC spectra, eigenvector emittance was measured by the adaxial, sparsely shaded, leaf surfaces specifically where light passed through the leaf into the integrating, wavelength, 5m, sphere in the LULC, eco-epidemiological, vulnerability models. These immature paradigms were optimally constructed employing the differentially corrected GPS (DGPS) coordinates of the intervention, riverine, tributary, agro-village, gridded complexes in the multivariate, stratified, satellite datasets. DGPS sampled points have a positional accuracy of 0.178 m [26]. The residual, prediction deviation (RPD) scores and the root mean squares RMS error of calibration sets, were used to evaluate the eco-epidemiological forecasts (e.g., targeted, seasonal, hyperproductive, cross-border foci). Visible Near-Infra-red (VNIR) calibration obtained accounted for at least 65% of the variance in log Chl-*a* wavelengths employing only VNIR spectra. The high RPD of 2.81 obtained suggested that the remotely sensed, algorithmic, iterative, predictive, risk model derivations was suitable and robust to predict Chl-*a*, canopy concentrations in the eco-georeferenced, capture point, immature habitat, eco-epidemiological, geoclassified, LULC datasets. The uncoalesced, geo-spectral, three-band, remote sensing, immature habitat, wavelength model datasets included 675 and 755 nm (R_{675} - R_{755}) and reflectance of Red Edge center wavelength at 731nm (R_{718}), with the equation $RES = (R_{718} - R_{675}) / (R_{755} - R_{675})$ where R was λ . A differential equation was generated where F was written as a linear combination of the

$$y^{(n)} = \sum_{i=0}^{n-1} a_i(x) y^{(i)} + r(x)$$

spectral derivatives of y : where $a_i(x)$ and $r(x)$ were continuous functions in x . The articulated, proxy, 5m, LULC, endmember, LULC signature, extracted radiance accounted for an average of



83.7% of variation in Chl-*a*, interpolated, LULC, capture point, breeding foci, canopy concentration values with a RMSE of less than 7.14%. The geoclassified, discontinuous, trailing vegetation, quantified emittance rendered from the Chl-*a*, canopy material sample was linked to its optical depth (τ) and to the breeding foci, capture point, LULC decomposed surfaces. By developing a tool in Geostatistical Analyst™ based on simultaneous diagonalization of positive definite kernels, minimax rates of convergence were achieved in a robust, Bayesian, *S. damnosum* s.l., 5m, resolution, diagnostic, autoregressive eco-epidemiological, remotely sensed, LULC model.

Bayesian statistics for optimally regressively, quantitating, remotely identified, entomological, vector arthropod, breeding foci, on moderate resolution, geoclassified, African, riverine tributary, empirical observational LULC datasets, assume that the kernel of a probability mass function (pmf) in which any geoclassified oviposition, LULC factor that are not functions of any geospectral variables in the domain are omitted [18, 27]. In probability theory and statistics, a pmf is a function that renders the probability that a discrete random variable is exactly equal to some value [19]. The pmf in a geo-spectrotemporal, explanatory, forecast, vulnerability, entomological, cross-border, *S. damnosum* s.l. African, riverine, tributary, probabilistic, moderate resolution, LULC paradigm may be the primary means of defining a discrete endmember probability distribution whose functions may exist either as scalar or multivariate random variables where domains may be discrete. Note that such co-factors (e.g., empirically orthogonally eigen-decomposed, moderate resolution, explanatory, endmember dataset of uncoalesced, geoclassifiable, spectral, wavelength, LULC, oviposition, *S. damnosum* s.l., capture point, identification model eco-georeferenceable regressors) may well be functions of the moderate resolution, geoclassified, LULC parameters of the pmf. These factors may form part of the normalization factor of the probability distribution in an optimizable, cross-border, LULC, African riverine tributary, *S. damnosum* s.l., eco-epidemiological, eco-georeferenceable, stochastic and or deterministic, iterative interpolator in Geospatial Analyst™ for optimal immature habitat identification employing moderate resolution, geoclassified, grid-stratified LULC data.

[18] employed Bayes' theorem to describe the probability of sampling event of a, hyperproductive, *S. damnosum* s.l., breeding foci, based on prior knowledge of LULC conditions (e.g., geoclassifiable, African, riverine, tributary moderate resolution, LULCs). In Bayesian probability theory, if the posterior distributions $p(\theta|x)$ are in the same family as the prior probability distribution $p(\theta)$, the prior and posterior are then called conjugate distributions, and the prior is called a conjugate prior for the likelihood function [28].

The authors of [12] employed multiple geo-spatiotemporal, geosampled, empirically unmixed, bio-ecological, eco-geographic datasets of eco-epidemiological, geoclassified endmember, LULC, wavelength, spectral covariates of eco-georeferenced, larval habitats of *S. damnosum* s.l., geosampled at the agro-village level in a riverine tributary, (Chute Dienkoa) in Burkina Faso with their retrospective tabulated prevalence rates. Semi-parametric, orthogonal spatial filter, eigenvectors and iteratively, interpolated, Bayesian, endmember, LULC signatures rendered a robust dataset of ARIMA, risk model, residual, eco-georeferenceable, vulnerability forecasts by reducing latent unobservable, erroneous coefficients (multicollinear variables) in the regressed, geo-spatiotemporal, field-sampled, immature, *S. damnosum* s.l., immature density, count datasets for optimizing the risk mapping of seasonal, onchocerciasis, endemic, transmission zones. In statistics and econometrics, and in particular in time series analysis, an autoregressive integrated moving average (ARIMA) model is a generalization of an autoregressive moving average (ARMA) model. These models are fitted to time series data either to better understand the data or to predict future points in the series (forecasting). The parameterizable, endmember LULC covariate, remotely sensed estimators were thereafter regressed employing the modified sum of squares technique. The model revealed that 5 to 10 km was mesoendemic, 10 to 15 km was hypoendemic and after 15 km there was no transmission.

Introducing a variational inference framework for training the latent, Gaussian processes in an eco-epidemiological, *S. damnosum* s.l. breeding foci, explanatory, endmember, moderate resolution, geoclassified, immature habitat, identification model and performing, nonlinear, Bayesian, dimensionality reduction may reveal immature, vector habitat, capture points in cross-border, African riverine, agro-village tributaries on geoclassified LULCs. This method would allow an onchocerciasis researcher or an epidemiologist to variationally integrate out the input, breeding foci, immature habitat, erroneous, LULC variables of the Gaussian process and compute a lower bound on the exact marginal likelihood of the latent, nonlinear, entomological, black fly, optimizable, LULC, variable model. The maximization of the variational lower bound in ArcGIS may provide a Bayesian training procedure that is robust to overfitting whilst automatically selecting the dimensionality of the nonlinear latent space for conducting the regression simulation exercises. Arc 10.1 includes Bayesian Kriging with the Geostatistical Analyst™. (www.esri.com). The method may iteratively quantitatively



interpolated moderate resolution orthogonal, eigen-decomposed, spatial filter, unmixed, LULC signature, endmember datasets. The algorithm may be applicable for robustly performing a training Gaussian process in a cross-border, *S. damnosum* s.l. breeding foci, immature habitat identification model in the presence of missing or uncertain input spectral values.

Furthermore, a Bayesian, Gaussian, immature, uncoalesced, moderate resolution, LULC endmember dataset of cross-border, African, riverine tributary, *S. damnosum* s.l., capture point, eco-georeferenceable, hyperproductive, geoclassifiable, LULC, seasonal, breeding foci spectral endmember wavelengths may be found to be conjugate to itself (i.e., self-conjugate) with respect to a Gaussian likelihood function: if the likelihood function is truly Gaussian. The Gaussian or normal distribution plays a central role in all of statistics and is the most ubiquitous distribution; measurement errors, and in particular, instrumental errors are generally described by this probability distribution [19]. Gaussian processes offer a nonparametric Bayesian framework for nominal, and ordinal, inferentials of highly, nonlinear, latent functions from observed, geoclassified, moderate resolution, LULC explanatory data in ArcGIS. They have become very popular in machine learning for solving problems such as nonlinear regression and geoclassifications [13, 29] [27, 30]. In cross-border, Gaussian, *S. damnosum* s.l. African, riverine, tributary, seasonal, hyperproductive, immature, eco-epidemiological, time series, capture point, geoclassifiable, moderate resolution, LULC, paradigms choosing a prior over the mean may ensure that the posterior distribution is also Gaussian. As such, the Gaussian, entomological, vector arthropod, breeding foci, capture point, normalized distribution would be a conjugate prior for the likelihood that is also Gaussian.

The Gaussian smoothing operator is a 2-D convolution operator in ArcGIS that is usable to 'blur' images and remove detail and noise. In this sense it is similar to the mean filter, but it uses a different kernel that represents the shape of a Gaussian ('bell-shaped') hump. Convolution provides a way of 'multiplying together' two arrays of numbers, generally of different sizes (e.g., eigenvectors formulated from a geospatially weighted autocorrelation cross-border, African, riverine, tributary, study site, weighted, error coefficient matrix), but of the same dimensionality, to produce a third array of numbers of the same LULC dimensionality (e.g., uncanopied, rocks) which may be employable in image processing in ArcGIS to implement operators whose output pixel values are simple linear combinations of certain input pixel values (hyperproductive seasonal, capture point, black fly discontinuous canopy). Hence, the form of the kernel in the cross-border, *S. damnosum* s.l., moderate resolution LULC, eco-epidemiological, eco-georeferenceable, moderate resolution, forecast, vulnerability model may be examined, and if it matches a known distribution, the normalization factor can be reinstated in ArcGIS, for providing a good approximation of the true governing LULC distribution at the tributary study site. For many iteratively qualitatively, optimally interpolative, uncoalesced, eco-georeferenceable, *S. damnosum* s.l., hyperproductive, breeding foci, capture point, endmember, moderate resolution, LULC signature distributions, the kernel can be written in closed form, but not the normalization constant [12].

In [11], the eco-epidemiological, vulnerability, orthogonal, eigen-decomposed, uncoalesced, wavelength, eco-epidemiological, eco-georeferenceable, LULC forecasts rendered from an iterative stochastic interpolator in Geospatial AnalystTM revealed that the optimal rate of convergence for the regularized estimator (i.e., f_{nX}) was $n^{-2(1-a)}(r+s)^{1/a}(r^s+1)$. The decomposition eigen-function, spatial, filter, orthogonal algorithm revealed that smoothness, regularized, CDOM-specific, remotely sensed, eco-georeferenceable, LULC capture point, 5m resolution, uncoalesced explanators could achieve optimal RMSE (< 11.3 %) with autoregressive rates of convergence for unbiasedly, robustly revealing interpolable, Chl-*a*, endmember, eigenvector ensembles.

Numerical results were formulated in Geostatistical AnalystTM to elucidate the merits of the targeted, immature habitat, removal technique (i.e., "Slash and Clear") in Jacob et al. (2015) based on the geospectrally, geoclassified, Chl-*a*, discontinuous canopied, endmember, breeding foci, capture point, explicatively, interpolated, proxy, uncoalesced, geoclassified, LULC, signature maps in Geospatial AnalystTM of the intervention villages. In Gonycogo, the mean daily collection during the last three days of the 31 day study was 32.66, representing an 89.10% reduction in biting density from the mean collection in the baseline collection of 292.4 adults. In contrast, the mean daily collection in the paired control village of Ayago/Nile was essentially unchanged from the baseline collection during the last three days of the study (352.7 baseline versus 348.6 at the end of the study). Similar results were seen in the other village pair. An 81.21% reduction in biting rate was observed in the intervention village (Adbuk), while the biting rate in the control village (Laminlato) at the end of the study was 98.11% of that seen in the baseline evaluation.

Hence, combining contemporary moderate resolution, geoclassifiable, eco-georeferenceable, capture point, LULC maps constructed in ArcGIS Pro of cross-border, African, riverine, tributary, *S. damnosum* s.l.,



habitats, breeding foci, could enable an onchocerciasis researcher or epidemiologist to optimally ecocartographically delineate and or autoregressively, optimally, quantitate, immature abundance and distribution of multiple, seasonal, vector breeding foci to estimate anthropogenic, populations jointly at risk for the disease in such ecosystems. Such an analysis may reveal that over 80 % of the population lives in a hyperendemic vulnerable, region at risk from the vector-borne disease. Furthermore, eco-georeferenceable, moderate resolution, remotely sensed, eco-epidemiological, geosampled, entomological, forecast, vulnerability models may emphasize the heterogeneity of the black fly, oviposition, immature habitat, unmixed, LULC components based on endmember distribution of immature, geosampled, count data in ArcGIS. In so doing, sub-pixel explanatory spectroradiometric, moderate resolution, uncoalesced, LULC variables that are associated to an eco-georeferenceable, hyperproductive, seasonal, iteratively interpolated, capture point, *S. damnosum* s.l., geoclassified, breeding foci signature geo-spatiotemporally or geo-spectrotemporally extracted from an African, riverine, tributary, eco-epidemiological neighbourhood may be optimally non-linearly geovisually distinguishable in the empirical regression dataset.

Remotely sensed, time series, geoclassifiable, endmember, spectral wavelength, optimizable reference signature, predictors regressively quantitated in Geostatistical Analyst™ may reveal non-homogeneous, black fly, seasonal, geoclassified moderate resolution, LULCs associated to an eco-georeferenced, African, riverine, ecosystem, tributary, eco-epidemiological, capture point, breeding foci in a conflict-ridden, crossborder zone. For example, the OLS tool in Geostatistical Analyst™ may calculate a coefficient for each synthesized, moderate resolution, geo-spectrotemporal or geospatiotemporal, orthogonal, eigen-decomposed, endmember LULC explanatory variable in a cross-border, African, riverine tributary, *S. damnosum* s.l., breeding foci, habitat, identification model whilst optimally performing a statistical test to determine whether that variable is helping the model or not. The statistical test will compute the probability that the coefficient is actually zero. If the coefficient in the regressed, cross-border, eco-epidemiological, uncanopied, trailing vegetation, African, riverine tributary, immature habitat, *S. damnosum* s.l. capture point, breeding foci, for example, is zero (or very near zero), the associated explanatory, endmember, LULC variable may not be helping the model identify a potential eco-georeferenceable, hyperproductive, capture point. When the statistical test returns a small probability (i.e., p-value) for a particular moderate resolution, geoclassified LULC variable, on the other hand, it may indicate that it is unlikely (there is a small probability) that the coefficient is zero in the black fly immature habitat identification model. When the probability is smaller than 0.05, an asterisk next to the probability on the black fly, geoclassified, moderate resolution, habitat identification OLS summary report in ArcGIS would indicate the associated explanatory endmember, LULC variable is important to the forecast, vulnerability, remotely sensed, habitat identification, endemic, model (in other words, its coefficient is statistically significant at the 95 percent confidence level).

Most statistical tests for uncoalesced, immature, vector arthropod, breeding foci, eco-epidemiological, hyperproductive, seasonal, capture point, data analyses in Statistical Analyst™ or any cartographic or statistical package begins by identifying a null hypothesis (see [27, 31]). The null hypothesis for moderate resolution, endmember, LULC, risk pattern analysis tools in ArcGIS (e.g., Analyzing Patterns toolset and Mapping Clusters toolset) can explanatively, optimally quantitate Complete Spatial Randomness (CSR), either of the selected, orthogonalized, operationized, geoclassified, moderate resolution, immature, habitat, uncoalesced, empirical, endmember, LULC, attribute feature geospatiotemporally and or geo-spectrotemporally associated with an eco-georeferenceable, cross-border, capture point, *S. damnosum* s.l., microtopographic geospatial, object (e.g., the number of shaded, canopy leaves that are associated with a African, riverine tributary, trailing vegetation, partially canopied, seasonal, cross-border, breeding foci).

A statistic is sufficient with respect to a statistical model and its associated unknown parameter if no other statistic can be calculated from the same sample nor provide any additional information to the value of the parameter [32]. Roughly, given a dataset of independent identically distributed (i.i.d.), uncoalesced, eco-georeferenceable, satellite-derived, cross-border, African, *S. damnosum* s.l., breeding foci, geoclassified, eco-epidemiological, time series, optimizable, geo-spectrotemporally or geo-spatiotemporally, elucidatively parameterizable, LULC covariates conditioned on an unknown parameter, a maximum likelihood estimate may be optimally definable in SAS/GIS. In so doing, the LULC habitat identification process would be based on distinct, discrete integer thresholds. The onchocerciasis researcher or epidemiologist may enforce model conditions employing lower and upper boundary constraints in SAS/GIS. The three-parameter Weibull estimation can numerically provide good initial estimates in SAS/GIS (www.esri.com). Therefore, the first black fly model estimate σ and C of the Weibull distribution in a robust, cross-border, African, riverine tributary, eco-



georeferenceable, moderate resolution, LULC, eco-epidemiological, forecast vulnerability model would include constant $\theta = 0$. The optimal parameters $\hat{\sigma}$ and \hat{c} may be thereafter parsimoniously employable as starting values for the Weibull habitat estimation paradigm in which may be written in SAS/GIS as.

```
data par1(type=est);
  keep _type_ sig c theta;
  _type_='parms'; sig = .5;
  c = .5; theta = 0; S. damnsoum s.l. habitat output;
  _type_='lb'; sig = 1.0e-6;
  c = 1.0e-6; theta = .; output;
run;
```

In so doing, moderate resolution, LULC regressors may be able to optimally identify, cross-border, African, riverine, tributary, capture point, seasonal, hyperproductive, *S. damnosum* s.l. breeding foci whilst specifying initial values and lower boundary constraints:

SAS/GIS can specify geoclassifiable, uncoalesced, iteratively qualitatively interpolative, moderate resolution, optimally parameterizable, time series, LULC covariates for identifying cross-border, capture point, seasonal, *S. damnosum* s.l., eco-georeferenceable, breeding, foci, hyperproductive habitats. An INEST= data set may be employable in PROC NLP. Optimally the maximization of the log-likelihood function for the Weibull, moderate resolution, LULC, black fly, immature habitat, identification estimation would be quantifiable for the constant $\theta = 0$. PROC NLP call may specify the maximization of the log-likelihood function for a two-parameter Weibull estimation for constant $\theta = 0$ for an eco-epidemiological, African, riverine, tributary eco-georeferenceable, forecast, vulnerability, eco-epidemiological, moderate resolution, geoclassifiable model for identifying immature habitat, cross-border *S. damnosum* s.l. breeding foci.

```
proc nlp data=pike tech=tr inest=par1 outest=opar1
  S. damnosum s.l. habitat model=model cov=2 vardef=n pcov phes;
  max logf;
  parms sig c;
  profile sig c / alpha = .9 to .1 by -.1 .09 to .01 by -.01;

  x_th = days - theta;
  s = - (x_th / sig)**c;
  if cens=0 then s + log(c) - c*log(sig) + (c-1)*log(x_th);
  logf = s;
run;
```

Typically, the sufficient statistic is a simple function of the data, (e.g. the sum of all the remotely identified, cross-border, *S. damnosum* s.l., African, riverine tributaries, eco-georeferenced, LULC data points). More generally, the unknown, geoclassifiable, endmember, LULC parameter may represent a vector of unknown quantities or may represent everything about the model that is unknown or not fully geo-specified in ArcGIS. In such a case, the sufficient statistic may be a set of orthogonal functions (i.e., a jointly sufficient cross-border, *S. damnosum* s.l. immature habitat, moderate resolution, eigen-decomposed, LULC statistic). Typically, there are as many functions as there are parameters. For example, for a Gaussian distribution with unknown mean and variance, the jointly sufficient statistic, from which maximum likelihood estimates of remotely identifiable, optimally parameterizable, moderate resolution, geoclassified, cross-border, African riverine, tributary, *S. damnosum* s.l., explanatory, LULC regressors may be estimated, based on two functions: the sum of all the breeding foci, data points and the sum of all squared foci data points (or equivalently, the sample mean and sample variance). The method would allow choosing values for an eco-epidemiological, eco-georeferenceable, black fly, LULC regression, variable subset which could minimize some expected loss function (e.g., the probability of decision error in an empirical dataset of residually iteratively uncoalesced, qualitatively, optimally, iteratively interpolatable, *S. damnosum* s.l., LULC endmember, signature, immature, forecast targeting an eco-georeferenceable, seasonal, hyperproductive, capture point, *S. damnsoum* s.l. cross-border, African riverine tributary, breeding foci).

Ordinary least-squares regression models the relationship between one or more covariates X and the conditional mean of a response variable Y given $X = x[10]$. In contrast, quantile regression models the



relationship between X and the conditional quantiles of Y given $X = x$, so it is especially useful in applications where extremes are important, such as moderate resolution, African, riverine, cross-border, tributary, immature, capture point, LULC, *S. damnosum* s.l., habitat model identification where upper quantiles of pollution levels are critical from a public health perspective (e.g., choosing variables for a larval habitat map with a 5 km buffer of an eco-georeferenced, agro-village tributary centroid). Quantile regression also provides a more complete picture of the conditional distribution of Y given $X = x$ when both lower and upper or all quantiles are of interest, as in the analysis of body mass index where both lower (underweight) and upper (overweight) quantiles are closely watched standards. This the new QUANTREG procedure in SAS /GIS can compute LULC, estimates and related quantities in a moderate resolution, remotely sensed, cross-border, *S. damnosum* s.l., habitat identification, forecast, vulnerability map.

1.

Joint F-Statistic and Joint Wald Statistic may be usable as measures of overall model statistical significance for assessing, eco-epidemiological, forecast-oriented, cross-border, moderate resolution, African riverine, tributary, capture point, LULC, eco-georeferenceable, *S. damnosum* s.l., model significance. Whenever a relationship within or between data items can be expressed as a statistical model with parameters to be estimated from a sample, the Wald test can be used to test the true value of the parameter based on the sample estimate. An F-test is any statistical test in which the test statistic has an F-distribution under the null hypothesis. The Joint F-Statistic is trustworthy only when the Koenker (BP) statistic is not statistically significant [33].

The Koenker (BP) Statistic (Koenker's studentized Bruesch-Pagan statistic) is an ArcGIS test which can quantify whether explanatory variables in a model have a consistent relationship to the dependent variable both in geographic space and in data space. When the model is consistent in geographic space, the spatial processes represented by the explanatory variables behave the same everywhere in the study area (the processes are stationary) [6]. When an eco-georeferenced, cross-border, capture point, LULC cross-border, African, riverine, wide tributary, *S. damnosum* s.l., moderate resolution, immature habitat identification, endmember, spectral, wavelength, frequency model, for example, is consistent in data space, the variation in the relationship between the remote identified and predicted habitat values for each explanatory geoclassified LULC variable does not change with changes in variable magnitudes (i.e., there is no heteroscedasticity in the model). Suppose an onchocerciasis researcher or epidemiologist desires to eco-epidemiologically forecast impact of one optimally geoclassified uncoalesced, moderate resolution, endmember wavelength ArcGIS-derived, microtopographic, cross-border, geoclassified, black fly, foci, LULC variable (e.g., percent of partially canopied, capture point floating vegetation) regressively quantifiable explanatory variable. The model would have problematic heteroscedasticity if the cross-border, black fly, immature habitat, capture point foci predictions were more accurate for geolocations with small mean habitat larval counts than they were for habitat geolocations with large, seasonal, immature, density counts. The null hypothesis for this test in ArcGIS may be that the immature habitat identification, cross-border, *S. damnosum* s.l. geoclassified, LULC analysis is stationary. For a 95 percent confidence level, a p-value smaller than 0.05 would indicate statistically significant heteroscedasticity and/or nonstationarity in the remotely sensed, moderate resolution, immature habitat, identification, endmember, spectral, wavelength, frequency model. When results from this test are statistically significant, an onchocerciasis researcher or epidemiologist may consult the robust coefficient standard errors and probabilities in the Geostatistical Analyst™ model summary statement to assess the effectiveness of each moderate resolution, geoclassified, LULC explanatory endmember, spectral, wavelength, frequency variable for identifying a eco-epidemiological, cross-border, breeding foci, hyperproductive, eco-georeferenceable, seasonal, *S. damnosum* s.l. capture points in cross-border, African riverine tributary ecosystems. Regression models with statistically significant nonstationarity are often good candidates for Geographically Weighted Regression (GWR) analysis [6].

ArcGIS provides a tool that generates spatially calibrated regression models (known as Geographically Weighted Regression (GWR) (www.esri.com)). This tool can generate a separate regression equation for every moderate resolution, hyperproductive, eco-georeferenceable, eigen-decomposable, endmember, *S. damnosum* s.l. seasonal, breeding foci, uncoalesced, wavelength, geoclassified, capture point explanatory, LULC feature analyzed in a sample generated from an cross-border, African riverine tributary ecosystem, eco-epidemiological geospectral dataset. In so doing, a means to address spatial variation in the remotely sensed, immature habitat, identification model may be established. The GWR tool requires an ArcInfo, ArcGIS Spatial Analyst, or ArcGIS Geostatistical Analyst license to perform Geographically Weighted Regression (GWR) (www.esri.com), a local form of linear regression usable to model spatially varying immature habitat *S. damnosum* s.l. capture point, cross-border relationships. GWR can construct a separate equation for every, geoclassifiable, moderate resolution, explanatory, unmixed, LULC attribute feature in an empirical



entomological, eco-georeferenceable endmember, spectral, wavelength, frequency dataset incorporating the dependent and explanatory oviposition, cross-border, black fly microtopographic, iterative, interpolative, endmember, unmixed LULC, signature, variables for eco-cartographically optimally illustrating each target capture point, feature attribute falling within a specific bandwidth. The shape and extent of the bandwidth may be dependent on the onchocerciasis researcher or epidemiologist's input for the Kernel type, Bandwidth method in Geostatistical Analyst™ employing Distance, and Number of neighboring moderate resolution geoclassifiable explanatory, endmember, diagnostic, spectral, wavelength, frequency LULC parameters with one restriction: when the number of black fly, vector arthropod, breeding foci, neighboring features exceeds 1000, only the closest 1000 are integratable into each local equation. Hence, An onchocerciasis researcher or epidemiologist may optimally evaluate how a moderate resolution, geoclassified, cross-border, LULC, *S. damnosum* s.l., African, riverine tributary, immature habitat identification model by performing the following diagnostics: 1) Cross-validation for checking the model's quality, 2) Validation for checking prediction quality, and, 3) comparing cross-validation results of several LULC models.

If the Koenker test for the cross-border, African riverine, tributary, forecast, vulnerability, capture point, eco-epidemiological immature, habitat identification model is statistically significant, an onchocerciasis researcher or an epidemiologist may employ the robust probabilities to assess the moderate resolution geoclassified LULC explanatory variable's statistical significance. Statistically significant probabilities have an asterisk (*) next to them in Geostatistical Analyst™ summary statements (www.esri.com). An black fly specified, endmember, explanatory variable associated with a geostatistically significant LULC coefficient may be vital for constructing robust, oviposition, immature habitat, eco-epidemiological, identification, endmember, spectral, wavelength, frequency model if theory/common sense supports a valid relationship with the dependent variable (e.g., a discrete integer representing the number of remotely identified larval, *S. damnosum* s.l., cross-border habitats), if the relationship being modeled is primarily linear, and if the variable is not redundant to any other explanatory, endmember, LULC variables in the model. The VIF measures redundancy amongst explanatory variables [10]. As a rule of thumb, in an geo-spatiotemporal or geo-spatiotemporal, elucidatively regressible, remotely sensed, moderate resolution, field-operationizable, geoclassifiable, LULC, explanatory *S. damnosum* s., breeding foci, uncoalesced, endmember dataset of LULC wavelength spectral identifiers associated with VIF values larger than about 7.5 should be removed (one by one) from the forecast, eco-georeferenced, endemic, vulnerability, endmember, spectral, wavelength, frequency model [2].

Under the Wald statistical test, the maximum likelihood estimate of the sampled, moderate resolution geoclassified LULCs in a cross-border, African riverine, tributary, eco-epidemiological, *S. damnosum* s.l., immature habitat uncoalesced, spectral wavelength, signature frequency parameter(s) of a seasonal eco-georeferenced, breeding foci, may be comparable with the proposed value in the paradigm, with the assumption that the difference between the two will be approximately normally distributed. Typically the square of the difference is compared to a chi-squared distribution in such circumstances.

In probability theory and statistics, the chi-squared distribution (also chi-square or χ^2 distribution) with

degrees of freedom is the distribution of a sum of the squares of k independent standard normal random variables. It is a special case of the gamma distribution and is one of the most widely used probability distributions in inferential statistics, (e.g., in hypothesis testing or in construction of confidence intervals [10]). The chi-squared distribution is used in the common chi-squared tests for goodness of fit of an observed distribution to a theoretical one, the independence of two criteria of classification of qualitative data, and in confidence interval estimation for a population standard deviation of a normal distribution from a sample standard deviation. For a robust, uncoalesced, moderate resolution, spectral wavelength, forecast, vulnerability paradigm the more general noncentral chi-squared distribution may be more important for remotely targeting endmember, spectral, wavelength, frequency, cross-border, African riverine, tributary, eco-epidemiological, *S. damnosum* s.l., immature habitats. In probability theory and statistics, the noncentral chi-squared or noncentral distribution is a generalization of the chi-squared distribution [19]. This distribution often arises in the power analysis of statistical tests employed in endmember, moderate resolution, vector arthropod, iteratively interpolative, LULC, forecast, vulnerability eco-epidemiological, uncoalesced, endmember, spectral, wavelength, frequency models in which the null distribution is perhaps asymptotically a chi-squared distribution (e.g., likelihood ratio tests) [13, 27].



Emphasis may be predisposed towards the evolution of the deterministic differential equations in Geostatistical Analyst™ based on the probabilistic, compartmentizable, residual estimates from non-homogeneous, gamma distributions rendered from Negative, binomial equations or geo-spectrotemporal or geospatiotemporal, autocorrelation error, coefficients, from geospatially weighted matrices in SAS/GIS. These frequency model outputs may be employable for optimal remote identification of cross-border, African, riverine tributary, eco-georeferenceable, vector, arthropod, *Simuliid*, eco-epidemiological, capture point, seasonal, hyperproductive, breeding foci, models with their bio-ecological, geophysical, explanatorial, forecastable, LULC estimator employing moderate resolution, satellite data in SAS/GIS. In a comprehensive survey, the summarized modelling activity in a particular, cross-border, riverine, tributary, ecosystem in a vectored, African, conflict-ridden, LULC, geoclassified geolocation eco-cartographically illustrated in SAS/GIS may help reach a wider range of researchers working on epidemiology, transmission, and other aspects of onchocerciasis. This LULC data may facilitate onchocerciasis or epidemiologists to further develop suitable habitat identification models in the direction relevant to the present endemic scenario, in these politically unstable, riverine tributary, African, ecosystems whilst helping the biologists and local public health personnel to adopt better understanding of remotely sensed, modelling strategies to control the disease. Precisely iteratively interpolated, remotely sensed, geovisually identified, cross-border, eco-georeferenceable, seasonal, hyperproductive, *S. damnosum* s.l., eco-epidemiological, capture point, breeding foci signatures may reveal geolocations of unknown habitats in cross-border African, riverine tributary employing geoclassified moderate resolution LULC, grid-stratified data in ArcGIS. In so doing risk surveillance maps may be generated remotely targeting hyperproductive, seasonal, eco-georeferenceable, eco-epidemiological, black fly breeding foci in these unstable environments.

Methods for analyzing a general compartmental model in ArcGIS may be provided for a moderate resolution, eco-epidemiological, geoclassifiable, *S. damnosum* s.l., immature, habitat identification, wavelength, spectral, forecast, vulnerability, eco-georeferenceable, LULC model. In so doing, precise geovisual definitions of an eco-georeferenceable, cross-border, riverine tributary, seasonal, breeding foci, *S. damnosum* s.l., immature, hyperproductive, eco-epidemiological, capture point habitats in a weighted, autocorrelation endmember, spectral, wavelength, frequency matrix in AUTOREG may be presented via a general compartmental disease transmission, geoclassified, remotely sensed, model based on a system of ordinary differential equations (ODEs). A differential equation is a mathematical equation that relates some function with its derivatives whose functions usually represent physical quantities; the derivatives represent their rates of change [17].

An onchocerciasis researcher or epidemiologist may solve systems of first-order ordinary differential equations (ODEs) by employing the ODE subroutine in the SAS/IML language, which solves initial value problems. Equations of motion for the classic simple harmonic oscillator may illustrate how to solve differential equations in SAS employing uncoalesced, moderate resolution, cross-border, African, riverine, tributary, eco-georeferenceable, capture point, *S. damnosum* s.l., immature, habitat, eco-epidemiological, forecast, vulnerability model unbiased spectral wavelength estimators in a stochastic or deterministic interpolator. To estimate the endmember, spectral, wavelength, frequency parameters from sampled cross-border vector entomological, breeding foci explanatory LULC data an onchocerciasis researcher or epidemiologist may employ the techniques introduced by [34] and the examples in the documentation for the MODEL procedure in SAS/ETS software.

Any higher-order cross-border, African, riverine, tributary, *S. damnosum* s.l., capture point, eco-epidemiological, habitat identification model differential equation can be rewritten as a system first-order of differential equations. The following SAS/IML module may define the first-order system for the standardized simple harmonic oscillator:

```
proc iml;
/* Equations of motion for the simple harmonic oscillator. This function returns the vector
   field evaluated at time t and location z. */
start SHO(t, z);
  dxdt = z[2];      /* dx/dt = v */
  dvdt = -z[1];     /* dv/dt = -x */
  return( dxdt // dvdt ); /* return column vector */
finish;
```

Notice that because this differential equation is linear, an onchocerciasis researcher or epidemiologist may use matrix multiplication to define the module by using a single statement:



```
return( {0 1, -1 0}*z ); /* alternative approach */
```

The ODE subroutine would solve the moderate resolution *S. damnosum* s.l., geoclassifiable, eco-epidemiological, LULC immature habitat identification endmember, spectral wavelength, frequency unbiased, differential equations. In addition to specifying the function that evaluates the vector field, you an onchocerciasis researcher or epidemiologist may specify three moderate resolution LULC parameters to the ODE subroutine: For example, an onchocerciasis researcher or epidemiologist may use $x_0 = \{2, 0\}$, which corresponds to a cross-border, ecogeoreferenceable, immature, hyperproductive, seasonal foci that is displaced into two geoclassified, moderate resolution LULC units (presence of uncanopied, trailing vegetation, distance to Euclidean agro-village gris-stratified centroid).

The condition may be specified as a column vector. A time interval that specifies the length of integration, $[0, T]$ must be specified. A vector that specifies the minimum, maximum, and initial steps for the variable-step-size integrator in SAS/GIS can utilize ODE subroutine uses. Suppose an onchocerciasis researcher or epidemiologist uses the moderate resolution, parameters aggregated at a microtopographic geoclassified LULC = $\{1.e-6 \ 1 \ 1e-3\}$. For this example, an onchocerciasis researcher or epidemiologist may obtain and graph the solution at unevenly spaced grid-stratified points in time. If an onchocerciasis researcher or epidemiologist specifies a single time interval $[0, T]$, the immature habitat identification, remotely sensed paradigm will obtain the final solution $(x(T), v(T))$. However, he or she could obtain the solution at multiple time series habitat points by specifying an increasing sequence such as $t = \text{do}(0.2, 10, 0.2)$. In so doing, the ODE routine will return the solution at each of the specified back fly breeding foci, LULC. eco-georeferenceable, capture points.

The following statements in SAS/GIS, moderate resolution, geoclassifiable LULC parameters and call the ODE subroutine to compute the solution at a sequence of time points up to $T = 10$:

```
x0 = {2, 0}; /* initial values */  
t = do (0, 10, 0.2); /* compute solution at these time pts */  
h = {1.e-6 1 1e-3}; /* min, max, and initial step size */  
call ode (soln, "SHO", x0, t, h);
```

The solution would be returned in the solution weighted matrix, which will have two rows. Each column of the matrix will then contain the $(x(t), v(t))$ values for a specified forecasted immature habitat value of $t > 0$.

The following statements may write the ODE solution to a SAS data set and call the SGPLOT procedure to graph the endmember solution as a function of LULC in the immature habitat, endmember, spectral, wavelength, frequency unbiased, identification model:

```
traj = t || (x0` // soln`);  
create SHO from traj[c={"Time" "x" "v"}]; /* write to data set */  
append from traj;  
close SHO;  
quit;
```

The position of the habitat may be described by a cosine function and the velocity (the derivative of position) as described by the negative sine function. This may be expected because the simple linear system may be decomposable analytically.

A second way graph solution may also be rendered from SAS/GIS for quantiating geolocations of potential, cross-border, *S. damnosum* s.l., immature breeding foci, capture point in an African riverine tributary ecosystem. The following statements may display the solution as an endmember, moderate resolution, LULC parametric curve in the (x, v) plane.

```
title "One Trajectory for a Simple Harmonic Oscillator";  
proc sgplot data=SHO aspect=1; /* the ASPECT= option is a SAS 9.4 feature */  
series x=x y=v;  
x-axis grid label="Position";  
y-axis grid label="Velocity";  
run;
```




In so doing, the parametric curve would be a single trajectory of a "phase portrait," which can be used to analyze the qualitative dynamics of a cross-border ecosystem for identifying seasonal, eco-georeferenceable, hyper productive, *S. damnosum* s.l. immature habitat, capture points using differential equations and moderate resolution, geoclassified LULCs.

An onchocerciasis researcher or epidemiologist may do his or her differential equation work in MATLAB for constructing an eco-georeferenceable, cross-border breeding foci, *S. damnosum* s.l., immature, hyper productive, eco-epidemiological, capture point, moderate resolution, LULC habitat identification model. It would however necessitate converting the polygon table into a .csv (e.g. open the .dbf in a spreadsheet program and save as a .csv). Thereafter csvread in MATLAB can read the moderate resolution vector arthropod breeding foci LULC data as required. If the onchocerciasis researcher or epidemiologist desires to append the remotely identified or predicted cross-border, black fly, immature habitat, tabulated spectral wavelength, endmember values onto the original polygon data, he or she could employ csvwrite to write the cross-border, immature sampled habitat data back to .csv. The .csv in MATLAB only requires a simple table join with the original sampled *S. damnosum* s.l., cross-border remotely identified, immature habitat data.

Writing some code in ArcPy may be more efficient for constructing a robust, spectral wavelength, endmember cross-border, African, riverine, tributary, eco-epidemiological, forecast, vulnerability, moderate resolution, geoclassifiable, LULC, prognosticative, vulnerability model. The NumPy Python library, has been installed with ArcGIS since 9.2, which may help immensely, for constructing a cross-border, remotely sensed, moderate resolution, LULC, *S. damnosum* s.l. immature habitat, eco-epidemiological, capture point, identification model. Esri has some documentation on writing the model attributes into few Python Toolboxes (which are new in ArcGIS 10.1 and above), Python Script Tools in a standard toolbox (<https://www.python.org>). Specifying Python to write tools, for a remotely sensed black fly forecast vulnerability, habitat identification model may be advantageous since the scripting language can pragmatically write a "pure" Python LULC tool in a single Python script without having to link it up to a separately authored dialog. Further, an onchocerciasis researcher or epidemiologist could use code Python or any language capable of writing text files, to automate the writing of Python toolboxes for optimally constructing an eco-georeferenceable, cross-border, *S. damnosum* s.l., immature, eco-epidemiological, capture point, spectral wavelength, uncoalesced, immature habitat, identification model employing a dataset of, geoclassified moderate resolution African, riverine tributary, agro-village LULCs.

ArcPy is a site package that builds on (and is a successor to) the successful ArcGIS scripting module. Its goal is to create the cornerstone for a useful and productive way to perform geographic data analysis, data conversion, data management, and map automation with Python. ArcPy may provide access to geoprocessing tools as well as additional functions, classes, and modules that allow an onchocerciasis researcher or an epidemiologist to create simple or complex workflows quickly employing ArcGIS applications and scripts written for a remotely sensed, moderate resolution, cross-border, endmember, spectral wavelength, frequency unbiased, *S. damnosum* s.l. LULC, immature, habitat, capture point, breeding foci, identification model. Using ArcPy an onchocerciasis researcher or epidemiologist may benefit from being able to access and work with the entomological, eco-epidemiological, geoclassifiable LULC data within numerous Python modules developed by GIS professionals and programmers from many different disciplines. The additional power of employing ArcPy within Python is the fact that Python is a general purpose programming language that is easy to learn and use (www.python.org). It is interpretable and dynamically typed, which provides the ability to quickly prototype and test scripts in an interactive environment while still being powerful enough to support the writing of large applications such as for identifying immature, capture points, cross-border, *S. damnosum* s.l. capture point, hyper productive, seasonal, eco-georeferenceable, habitats in African, riverine, tributary ecosystems.

It may be shown that, if the coefficient values are < 1 in a black fly, vector arthropod, immature habitat, capture point, eco-epidemiological, eco-georeferenceable, identification differential equation model generated in ArcPy for quantitating the disease-free equilibrium which may be considered locally asymptotically stable.

Conversely, if the remotely quantitated, immature breeding foci, parameterized, covariate coefficient values were > 1 , then it would be classified unstable. Thus, the endmember LULC coefficient estimates would be a threshold parameter in an Arc, entomological, vulnerability, forecast, eco-epidemiological, remotely sensed, black fly, moderate resolution, capture point, immature habitat, identification model. An analysis of the local center manifold may yield a simple criterion for the existence and stability of super and sub-threshold endemic



equilibria for the breeding foci, eco-georeferenceable, LULC, capture point, regressed residuals in ArcPy near the value of 1. This criterion, together with the definition of the remotely sensed, eco-epidemiological, capture point, cross-border, African, riverine, tributary, eco-georeferenceable, *S. damnosum* s.l., hyper productive, seasonal, immature habitat, may be optimally illustratable in ArcPy employing unbiased, remotely sensed, moderate resolution, synthesized, vector–host, autoregressively parametrizable LULC model unbiased covariate, estimators. The black fly, optimized, eco-epidemiological model forecast residuals may be applied to more complex immature habitat identification models in ArcPy. The results may be significant for disease control in cross border, riverine, agro-village, tributaries ecosystems in Africa.

There may be variations in an hierarchical, compartmentalizable, eco-epidemiological, LULC, forecastable, endmember, spectral wavelength, frequency unbiased, breeding foci, seasonal, black fly, immature habitat, identification ArcPy model structure depending on the type of landscapes geoclassified [e.g. percentage of trailing vegetation, percentage of Precambrian rocks[35]. The incidence of onchocerciasis is not distributed uniformly across a region (e.g., cross border riverine tributary zone) but there is a clear correlation with basic geology[36], because the riverine conditions which create suitable breeding sites for the vector, *S. damnosum* s.l., are most common where the Precambrian basement rock is exposed to break the flow of the water and create rapids.

In pure mathematics, differential equations are studied from several different perspectives, mostly concerned with their solutions—the set of functions that satisfy the equation. Only the simplest differential equations are solvable by explicit formulas; however, some properties of solutions of a given differential equation may be optimally resolvable without finding their exact form in an LULC, *S. damnosum* s.l., moderate resolution, remotely sensed, cross-border, African, riverine tributary, immature, habitat identification, endmember, spectral, wavelength, frequency model. For example, if a self-contained formula for the solution is not available for an eco-epidemiological, time series, landscape, moderate resolution, iterative, interpolation, model for optimally geovisualizing a geosampled, eco-georeferenceable, blackfly, hyperproductive, breeding foci, capture point, in a cross-border African riverine tributary, the solution may be numerically approximated using the overhead derived covariates within ArcPy. A numerical solution may be parsimoniously obtainable for conducting a geomorphological, remote, geovisual, immature, habitat, endmember LULC analyses on moderate resolution, geoclassifiable, data geosampled at an eco-georeferenced, crossborder, riverine, tributary, *S. damnosum* s.l., hyper productive, breeding foci, capture point employing Python's NumPy module and the SciPy toolkit. Differential equations can be solved with different methods in Python. [e.g., (1) Euler's method, (2) the ODEINT function from Scipy.Integrate, and (3) APM].

The `scipy.integrate.odeint` function may be of particular interest for generating, immature habitat identification, moderate resolution, LULC, remote sensing models for optimizing geovisualization of an eco-epidemiological, hyper productive, seasonal, eco-georeferenceable *S. damnosum* s.l. breeding, foci, capture point, on moderate resolution, geoclassified LULCs. Unfortunately, the script would only work for first-order differential equations of the form $dy/dt = f(y, t, 0)$. Hence, an onchocerciasis researcher or an epidemiologist must log-transform geosampled immature, eco-epidemiological, uncoalesced datasets of time series, clinical, field or remotely sensed explanatory, geo-spectral or geospatial, uncoalesced, LULC variables prior to employing them for capture point, habitat identification purposes in ArcPy. For example, if an onchocerciasis researcher or epidemiologist is trying to solve $y'' + y' + 2y = 0$ using an uncoalesced, eco-epidemiological, moderate resolution dataset of *S. damnosum* s.l., habitat remotely sensed, parameterizable covariates, he or she may transform the geosampled, vector arthropod, breeding foci, LULC variables into a first-order ODE with some simple variable substitution in ArcPy initially before using the model estimators for iteratively interpolating a LULC signature for remotely identifying cross-border, black fly, immature, eco-georeferenceable habitats.

Furthermore, there would be a necessity to define $x_2(t) = y'(t)$ and $x_1(t) = y(t)$ for generating the capture point, black fly, immature habitat, predictive equation $y'' = Ay' + By$. In so doing, $x_1' = y' = x_2$ and $x_2' = y'' = Ax_1 - Bx_2$ would be optimally rendered by the analyses in ArcPy. This model estimation may be simplified employing the original equation into a system of equations in ArcPy where $x_1' = x_2$, $x_2' = Ax_1 - Bx_2$. which can then be subsequently plugged into `scipy.integrate.odeint` directly. To do this precisely for generating robust endmember LULC equations for optimally geovisualizing, *S. damnosum* s.l., cross-border, breeding foci on moderate resolution eco-georeferenceable geoclassified LULCs in civil torn, African, riverine tributaries, a function must be generated that takes a matrix Y and a time t and returns a new matrix with the values of x_1' , x_2' for that sample period. In so doing, the program could delineate a system of equations for optimally identifying cross-border, *S. damnosum* s.l., eco-epidemiological, capture points on geoclassified, LULCs along with their regressed



parameterizable African tributary, geoclassified, moderate resolution, habitat, eigen-decomposed, endmember, orthogonal, spectral, wavelength, frequency covariates. Thereafter to get the solution for the equations an onchocerciasis researcher or epidemiologist may write:

```
def main():  
    a_t = np.arange(0, 25.0, 0.01)  
    asol = integrate.odeint(solvr, [1, 0], a_t)  
    print(asol)  
  
if __name__ == '__main__':  
    main()
```

Running this program at the command line will render a moderate resolution, geoclassifiable, cross-border, *S. damnosum* s.l., breeding foci, capture point, remotely sensible, numeric value for y (and y' , t) at each time t (e.g., sample frame in the range $0 \leq t \leq 25$), employing moderate resolution geoclassifiable endmember LULC increments of 0.01. If an onchocerciasis researcher or epidemiologist wants a more exact solution, he or she could construct the immature habitat identification model in ArcPy employing smaller LULC increments and get more numbers (e.g., percentage of Precambrian rocks along a cross-border tributary). In so doing, the geosampled geoclassified, uncoalesced, black fly, endmember LULC, data would have to be stacked up a 3-column array in the `main()` function which may be written to a CSV as:

```
def main():  
    a_t = np.arange(0, 25.0, 0.01)  
    asol = integrate.odeint(solvr, [1, 0], a_t)  
    astack = np.c_[a_t, asol[:, 0], asol[:, 1]]  
    np.savetxt('approx.csv', astack, delimiter=',', header='t, y, yd', comments='')
```

A pseudo R^2 (i.e., coefficient of determination) could be then tabulated for the black fly habitat identification model using:

```
> approx <- read.csv('approx.csv')  
> plot(y ~ t, data=approx., type='l')
```

The Python solution is not just a mere plot of the analytic formulation but a method to aid in remote, optimal, LULC geovisualization of eco-georeferenceable, cross-border, eco-epidemiological, *S. damnosum* s.l. immature habitat, capture points, on geoclassified, moderate resolution, satellite data. As long as an onchocerciasis researcher or an epidemiologist is able to reduce the model to a first-order ODE system, SciPy can apply numeric solvers including the more generic `scipy.integrate.ode` for dealing with more complicated, seasonal, microtopographic, LULC types (e.g., partially shaded, cross border, African, riverine, tributary, trailing vegetation, uncoalesced, 5m, wavelength endmember variables). Python's numeric/mathematical capabilities may render more precision for remotely optimally targeting eco-georeferenceable, eco-epidemiological, black fly, capture point, hyper productive, capture point, breeding foci.

NumPy is the fundamental package for scientific computing with Python. It contains among other things: 1) a powerful N-dimensional array object 2) sophisticated (broadcasting) functions 3) tools for integrating C/C++ and Fortran code with linear algebra, Fourier transform, and random number capabilities



[http://\(www.numpy.org/\)](http://www.numpy.org/). NumPy can also be used as an efficient multi-dimensional container of generic data. Arbitrary lulc data-types can be defined such as those in cross-border, African, riverine, tributary ecosystems. NumPy may seamlessly and speedily integrate moderate resolution, endmember, cross-border, uncoalesced, LULC, African, riverine, tributary, ecosystem uncoalesced, endmember, spectral, wavelength, frequency data with a wide variety of ArcGIS databases. NumPy is the de facto standard for numerical computing in Python (www.esri.). It is highly optimizable and extremely useful for working with gridded LULC stratified matrices.

The standard matrix class in NumPy is called an array (http://matplotlib.org/users/pyplot_tutorial.html). Working with arrays, a number of useful functions may be generated that may aid in geovisualization of seasonal, hyper productive, eco-georeferenceable, capture point, breeding foci in a cross-border, riverine, tributary ecosystem in an African conflict-ridden zone. For example, the linear algebra capabilities of NumPy may allow vector space mappings between reference spaces at an eco-epidemiological, eco-georeferenceable, African, riverine tributary cross border ecosystem. These models may include lines (e.g., Euclidean distance measurements from an eco-georeferenceable, capture point to a agro-village gridded centroid), planes (e.g., meandering riverine seasonal pathway) and subspaces (e.g., trailing vegetation or Precambrian rock tributary habitat intervals) for remotely optimally identifying a target eco-georeferenceable, hyper productive, capture point, *S. damnosum* s.l. breeding foci.

There is no longer a secondary install of Python needed to run standalone scripts with Pro. In ArcGIS Pro 1.0, 1.1 and 1.2 a lightweight version of Python may be employed within the application, but to run standalone Python scripts you had to install a secondary "Python for ArcGIS Pro". At 1.3, ArcGIS Pro will install Python into the ArcGIS\Pro\bin\Python\envs\arcgispro-py3.

The theory of dynamical systems puts emphasis on qualitative analysis of systems described by differential equations [17]. While many numerical methods have been developed to determine solutions with a given degree of accuracy for predicting geolocations of eco-georeferenceable, hyperproductive, seasonal, entomological, vector arthropod, eco-epidemiological, capture points, ArcPy modeling techniques have not been utilized for identifying *S. damnosum* s.l. cross-border, African, riverine, tributary, ecosystem foci. This system may be non-linear, and may not admit generic analytic solutions. Nevertheless, significant moderate resolution, endmember, LULC results may be derived analytically for optimally remotely targeting seasonal, hyper productive, cross-border, eco-georeferenceable, *Simuliid*, breeding foci along African neighboring conflict-ridden tributaries in ArcGIS.

Further, remotely identified, *Simulium* breeding sites in ArcGIS may be optimally Integratable into the control of onchocerciasis. Remotely quantitated, moderate resolution, LULC endmember, spectral, wavelength, frequency changes in hyper productive, eco-epidemiological, geoclassifiable, black fly, breeding foci, seasonal patterns may be optimally operationally quantifiable within the eco-georeferenceable cross-border endemic regions of the vector resulting from transition remotely determinable in riverine tributaries [e.g., geospatial cluster ("hot spot")]. Utilizing ArcGIS technology may constitute a major step toward the establishment of reliable, eco-geographic and entomological, geoclassifiable LULC empirical databases on the biotic environment for onchocerciasis researchers and epidemiologists since political boundaries may be disregarded during *Simulium* field sampling. Describing biogeophysical explanatorily, endmember, geoclassifiable, LULC attributes in bioclimatic, riverine, cross border zones with their heterogeneous, geomorphological, eigen-decomposed, orthogonal, riverine, landscape parameterizable, regression covariates may reveal where, seasonal, hyperproductive, *S. damnosum* s.l., breeding foci exist employing eco-cartographic, illustrative databases in ArcGIS. These data may also provide an overview of the behavior of the vector and possible control strategy interventions as different strains of onchocerciasis (*Simulium nevi*) which may be geo-spatially and or geospectrotemporally localized in specific eco-georeferenceable, geoclassifiable LULC vicinities of un-shaded meandering cross-border tributaries, for example, within conflicting African, riverine, agro-village, zones without political ramifications.

Remotely sensed, moderate resolution, LULC data in ArcGIS can measure the intensity of radiation within one or more spectral bands, typically within the visible-infrared (VIR) portion of the spectrum, from which seasonal, hyper productive, *S. damnosum* s.l., breeding foci, eco-epidemiological, capture



point, mapping data products may be optimally geoclassifiable as riverine, uncanopied or partially uncanopied, agro-village, tributary, LULC classes, surface temperatures, or biophysical vegetation indices (VIs). In [11] an empirical dataset of regressively parameterizable, eco-geohydrological, partially canopied, landscape, eco-biological, semiparametric LULC estimators and various in-situ, plant fauna, uncoalesced variables associated with aneco-georeferenced, trailing vegetation, gri-stratified, *S. damnosums*.l., eco-epidemiological, hyper productive, breeding foci, capture point, in an agro-village, ecosystem complex in Northern Uganda. Water temperature and pH were obtained. DGPS, CSI Max receiver Global Positioning System (GPS) coordinates with a positional accuracy of 0.178m [37] was employed to measure the eco-epidemiological, breeding foci, capture point which was subsequently overlaid onto a dataset of moderate resolution sensor data (Rapid Eye™ 5m visible and NIR wavebands) in ArcMap. Regression models were constructed in SAS: PROC REG employing multiple geoclassified, dependent, LULC time series, eigen-decomposed, parameterizable, spectral wavelength covariate explanators. The results revealed the abundance of *Simulium* larvae from March to May and a decrease in population from June to September, with subsequent increase from October to November. The regressed plant fauna, LULC data revealed *Pterocarpussantalinoides* tree (28.5%) as the most predominant and *Tithonia diversifolia* (5.8%) as the least geoclassifiable uncanopied, vegetational LULC at the interventional, eco-epidemiological, study site agro-village complex study site. On choice of attachment, *Simulium* larvae preferred plant attachments (31.6%) which were of four plants species *Oryzabarthii*, *Pterocarpussantalinoides*, *Andropogongayanus* and *Lawsonia inermis* followed by rock crevices (44.8%) submerged twigs (21.4%), and decaying leaf matters (12.7%). The pH values ranged from 7.1 - 8.5, and mean temperature value was 26.4 C. No significant difference ($p > 0.05$) was observed between the abundance of *S. damnosums*.l habitats, pH and water temperature. The results provided information on the variation in landscape bioecology and attachment profile of capture point, *S. damnosums*.l., LULC, larval breeding sites along the West Nile tributary in northern Uganda.

Here we construct multiple landscape and vegetation, moderate resolution, LULC endmember signature models in ArcGIS using Rapid Eye, 5m satellite data (www.appollomapping.com) for determining immature habitat suitability of riverine tributary, *S. damnosums*.l., breeding foci in the Democratic Republic of Congo (DRC), 10 km from the Ugandan border. The RapidEye™ satellite was successfully launched on the DNEPR-1 Rocket on August 29th, 2008 at Baikonur Cosmodrome in Kazakhstan. Each of RapidEye™'s five satellites contain identical sensors that are equally calibrated and travel on the same orbital plane at an altitude of 630 km. Together, the 5 satellites can collect over 4 million km² of 5m resolution, 5-band, color imagery every day. Each sensor on the Rapid Eye™ imager is capable of collecting data in five distinct bands of the electromagnetic spectrum: Blue (440-510 nm), Green (520-590 nm), Red (630-690 nm), Red-Edge (690-730 nm) and NIR (760-880 nm). The nominal resolution on the ground is 6.5m, corresponding to National Imagery Interpretability Rating Scale (NIIRS). The NIIR is a subjective scale used for rating the quality of imagery acquired from various types of imaging system (<https://fas.org/irp/imint/niirs.htm>).

The Rapid Eye™ satellite is the first commercial satellite in the world to have a Red-Edge band which is mounted on the imager positioned between the Red band and the Infrared (IR) band. The satellite is able to acquire moderate resolution LULC data through a 12-bit dynamic range (4,096 gradations). The Red Edge band is geo-spectrally located between the Red band and the NIR band without overlap. In a typical response of green vegetation, the Red Edge band covers the portion of the electromagnetic spectrum where reflectance drastically increases from the red portion towards the NIR plateau.

Interestingly, the red portion is one of the spectral areas where chlorophyll (Chl) strongly absorbs light and the NIR is where the leaf cell structure produces a strong reflection. Chlorophyll is the molecule that absorbs sunlight and uses its energy to synthesize carbohydrates from CO₂ and water (i.e., photosynthesis). Chlorophyll is any of several closely related green pigments found in cyanobacteria and the chloroplasts of riverine algae and plants (www.chm.bris.ac.uk/motm/chlorophyll/chlorophyll_h.htm). Our assumption was that moderate resolution, geoclassified, LULC variations in both the Chl-a content and the leaf structure in aneco-georeferenceable, cross border, eco epidemiological *Simuliid*, capture point, hyper productive, 5m resolution, breeding foci on a heterogeneous, geoclassified, riverine, cross-border tributary, canopied or partially canopied, geo-classified, LULC in ArcGIS may be optimally reflected in the Red Edge band. All oxygenic photosynthetic organisms use chlorophyll *a*, but they differ in levels of accessory pigments ([38]). The use of spectral indicators for the determination of Chl content is based on the fact that Chl, as well as a number of other pigments, are strong absorbers of light in certain well-defined wavelengths, specifically in the blue and the red spectral region [8].



Many studies [39][40] have investigated the relationship between the eco-biological status of plants and their geo-spectral, moderate resolution, LULC radiance particularly in the Red Edge domain. These studies revealed that if Chl concentration increases, the typical slope in the Red Edge spectral region shifts towards the NIR. Very often the Red Edge inflection point wavelength (λ_i) is used as an indicator for this shift. However, both the detection of this inflection point and the assessment of the shift is only possible with very narrow spectral bands [41]. Accordingly, several breeding foci spectral indices employing narrow bands, both from 5m, Rapid Eye™ spectroradiometric LULC data may be successfully applied to determine green biomass, water content, and other plant fauna for optimal geoclassification, remotely sensed, geo—biophysical, microtopographic, feature attributes associated to an eco-georeferenceable, cross-border, African, riverine, tributary, *S. damnosums*.l., seasonal, hyper productive, eco-epidemiological, capture point, breeding foci.

We determined if RapidEye™ satellite data can detect geoclassifiable LULCs or vegetational or LULC changes in the Red Edge domain, (e.g., unmixed spectrally delineated discontinuous, unshaded canopy) for optimally identifying cross border, *S. damnosums*.l., eco-epidemiological, hyper productive, eco-georeferenceable, capture point, breeding foci in the DRC along the border of Uganda. By combining unmixed, waveband, LULC data capability in ArcGIS cyber environment with object-based classifiers, our assumption was that extensive, heterogeneous, riverine, geoclassifiable, LULC areas at a high temporal frequency in two eco-epidemiological, study site 5km² polygons would allow geovisualization of the cross-border, black fly, breeding foci. Since the constellation's Red Edge band is sensitive to Chl status in leaf and canopy structure, for example in [42], we also assumed that this band could contribute to the remote geo-characterization of different, 5m resolution, LULC reflectance waveband types associated to seasonal, capture point, hyperprotective, cross-border, *S. damnosums*.l. breeding foci. [43] tested the Red Edge band in a land use classification project. Sixteen LULCs were assessed. They found that with the Red Edge band, the overall classification accuracy was consistently higher than without it. In terms of individual classes, the most significant improvements were obtained with classes comprised of open landscape vegetation.

We also conducted a gris-stratified, remote LULC analyses employing Rapid Eye™ proxy, sub-pixel, endmember, signature, paradigms [e.g., Normalized Difference Vegetation Indices (NDVI) Soil Adjusted Vegetation Indices (SAVI)] signatures for identifying *Similiid* habitats in the cross-border, African, riverine tributaries. Endmembers are spectra that are chosen to represent pure surface materials in a spectral signal [8]. [44] developed remotely, sensed, geoclassified, vegetation, endmember, LULC models to predict, high and low, adult, West Nile virus, mosquito, abundance sites for determining arboviral activity in Fairfield county, Connecticut, USA. The best predictive models included non-forested areas for *Culex pipiens*, surface water and distance to estuaries for *Cx. salinarius*, surface water and grasslands/agriculture and seasonal difference in the NDVI. As a simple transformation of two spectral bands, NDVI are computed directly without any bias or assumptions regarding plant physiognomy, land cover class, soil type, or climatic conditions [45]. A combination of the widely-used NDVI and the Normalized Difference Red Edge Index (NDRE) was able to predict Chl concentration in wheatfield LULCs with a coefficient of determination of $R^2=0.77$ [46]. In [47], a set of uncertainty LULC geoclassified, propagation equations were designed in ArcGIS to model the calibration uncertainties employing the red channel (band 3: 0.63 to 0.69 μm) and the NIR channel (band 4: 0.76 to 0.90 μm) of a sub-meter, resolution, image sensor (i.e., Quick Bird visible and NIR) data to generate the Soil Adjusted Vegetation Index (SAVI) for forecasting a dataset of eco-georeferenceable, malaria, mosquito, vector immature habitat, LULC predictors of *Anopheles arabiensis*. In [47], the SAVI exhibited asymptotic (saturated) signals over areas of seasonal, hyperproductive, eco-georeferenceable, capture point, *An. arabiensis*, breeding foci suitability without decreasing atmospheric visibility for accurately identifying changing rice-cycle, LULCs (e.g., post-tillering to flooding) in a Riceland agro-village environment (Mwea Division) in central Kenya.

Here, the question, we were trying to resolve was “Is there an entomological contribution from immature, cross-border, *S. damnosum* s.l. immature, capture point habitats in the DRC on vectored breeding foci in Uganda? Our assumption was that by optimally determining entomological contributions from remotely identified *S. damnosums*.l. habitats on heterogeneous, riverine, tributary, cross-border, geoclassified uncoalesced, spectral, wavelength, frequency, endmember LULCs in the DRC employing Rapid Eye™ 5m resolution, satellite data, that we would be able to accurately quantitate prevalence for implementing larval control strategies. Transmission of the parasite *Onchocerca volvulus* is most intense in the river basins rendering many of these areas uninhabitable [11].

The approach of satellite targeted interventions for onchocerciasis to recognize the importance of the endmember LULC variation in vector production amongst geoclassifiable, eco-georeferenceable, *S. damnosum* s.l., breeding sites in design of control programs in ArcGIS which has been broadly accepted in suppressing



domestic, container-breeding, immature habitats of *Aedes aegypti*, a mosquito vector of Dengue and Yellow Fever [48, 49] and malaria mosquito vector of the *Anopheles gambiae* s.l. complex [50] and *An. funestus* [37]. However, this is not the case with *S. damnosus* s.l., the most efficient vector of onchocerciasis in tropical Africa, due to the complexity of breeding habitats and field geosampled uncertainties of larval bio-ecological and satellite landscape heterogeneous determinants in conflict ridden, riverine tributary, agro-village, endemic zones.

Therefore, our objectives here were 1) to construct multiple, biogeophysical, geoclassifiable, riverine, tributary, LULC, geospatial, explanatory models, 2) to iteratively interpolate multiple, uncoalesced proxy, vegetation, spectroscopic, bio signature extracted from a 5m, endmember, sub-pixel, wavelength radiance spectrum; and, 3) to field verify (“ground truth”) potential, hyper productive, eco-epidemiological, capture point, eco-georeferenceable, breeding foci of *S. damnosus* s.l. larval habitats in the DRC within a 10km range from the Ugandan border. Understanding and managing transmission potential in heterogeneous landscapes in ArcGIS Pro products may reveal seasonal, bio-ecological and geomorphological processes that regulate *Simulium*, population, LULC dynamics, feeding behavior, and vector-pathogen interactions in neighboring African countries and their riverine communities employing moderate resolution satellite data regardless of political boundaries or civil unrest.

2 Materials and Methodology

2.1 Study site: Democratic Republic of the Congo is located in central sub-Saharan Africa, bordered by (clockwise from the southwest) Angola, the South Atlantic Ocean, the Republic of Congo, the Central African Republic, South Sudan, Uganda, Rwanda, Burundi, Tanzania across Lake Tanganyika, and Zambia. The country lies between latitudes 6°N and 14°S, and longitudes 12° and 32°E. It straddles the Equator, with one-third to the North and two-thirds to the South. The size of Congo, 2,345,408 square kilometers (905,567 sq. mi).

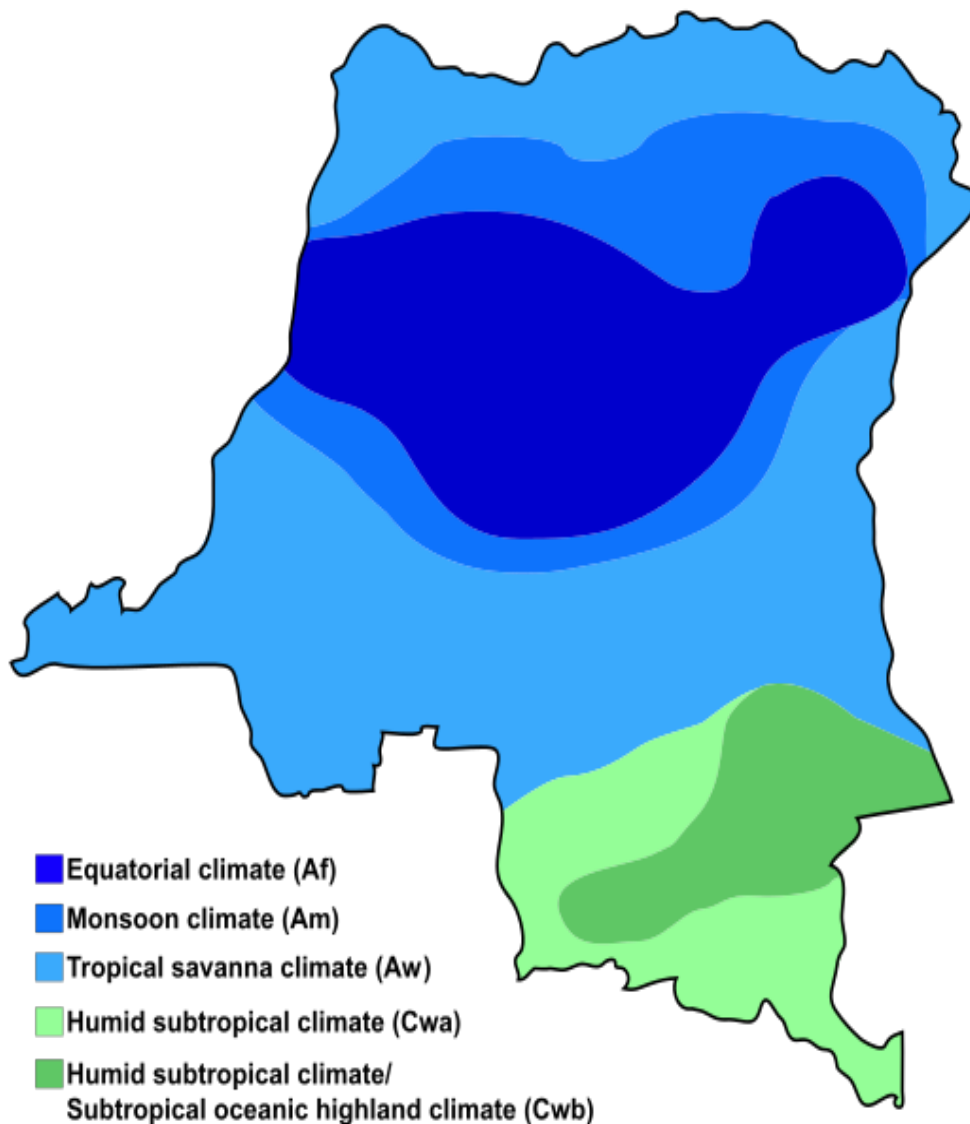
Figure 1: Study site map



Source: http://www.nationsonline.org/oneworld/map/dr_congo_map2.htm

Because of its equatorial geolocation, the DRC experiences high precipitation and has the highest frequency of thunderstorms in the world. The annual rainfall can total upwards of 2,000 millimeters (80 in) in some places, and the area sustains the Congo Rainforest, the second-largest rain forest in the world after the Amazon. This massive expanse of lush jungle covers most of the vast, low-lying central basin of the river, which slopes toward the Atlantic Ocean in the west. This area is surrounded by plateaus merging into savannas in the south and southwest, by mountainous terraces in the west, and dense grasslands extending beyond the Congo River in the north. High, glaciated mountains (Rwenzori Mountains) are found in the extreme eastern region

Figure 2: Democratic Republic of the Congo Climatic Classification Map



The name for the Congo state is derived in part from the river. The river basin (meaning the Congo River and all its myriad tributaries) occupies nearly the entire country and an area of nearly 1,000,000 km² (390,000 sq. mi). The river and its tributaries form the backbone of Congolese economics and transportation. Major tributaries include the Kasai, Sangha, Ubangi, Ruzizi, Aruwimi, and Lulonga.

The sources of the Congo are in the Albertine Rift Mountains that flank the western branch of the East African Rift, as well as Lake Tanganyika and Lake Mweru. The river flows generally west from Kisangani just below Boyoma Falls, then gradually bends southwest, passing by Mbandaka, joining with the Ubangi River, and running into the Pool Malebo (Stanley Pool). Kinshasa and Brazzaville are on opposite sides of the river at the Pool (see NASA image). Then the river narrows and falls through a number of cataracts in deep canyons, collectively known as the Livingstone Falls, and runs past Boma into the Atlantic Ocean. The river also has the second-largest flow and the second-largest watershed of any river in the world (trailing the Amazon in both respects). The river and a 37 kilometres (23 mi) wide strip of coastline on its north bank provide the country's only outlet to the Atlantic.

2.2 Preliminary data : Onchocerciasis control in the DRC)has hadmany challenges in the post-wareenvironment.Control measures entail larvicide spraying of blackfly breeding sites and treatment of endemic



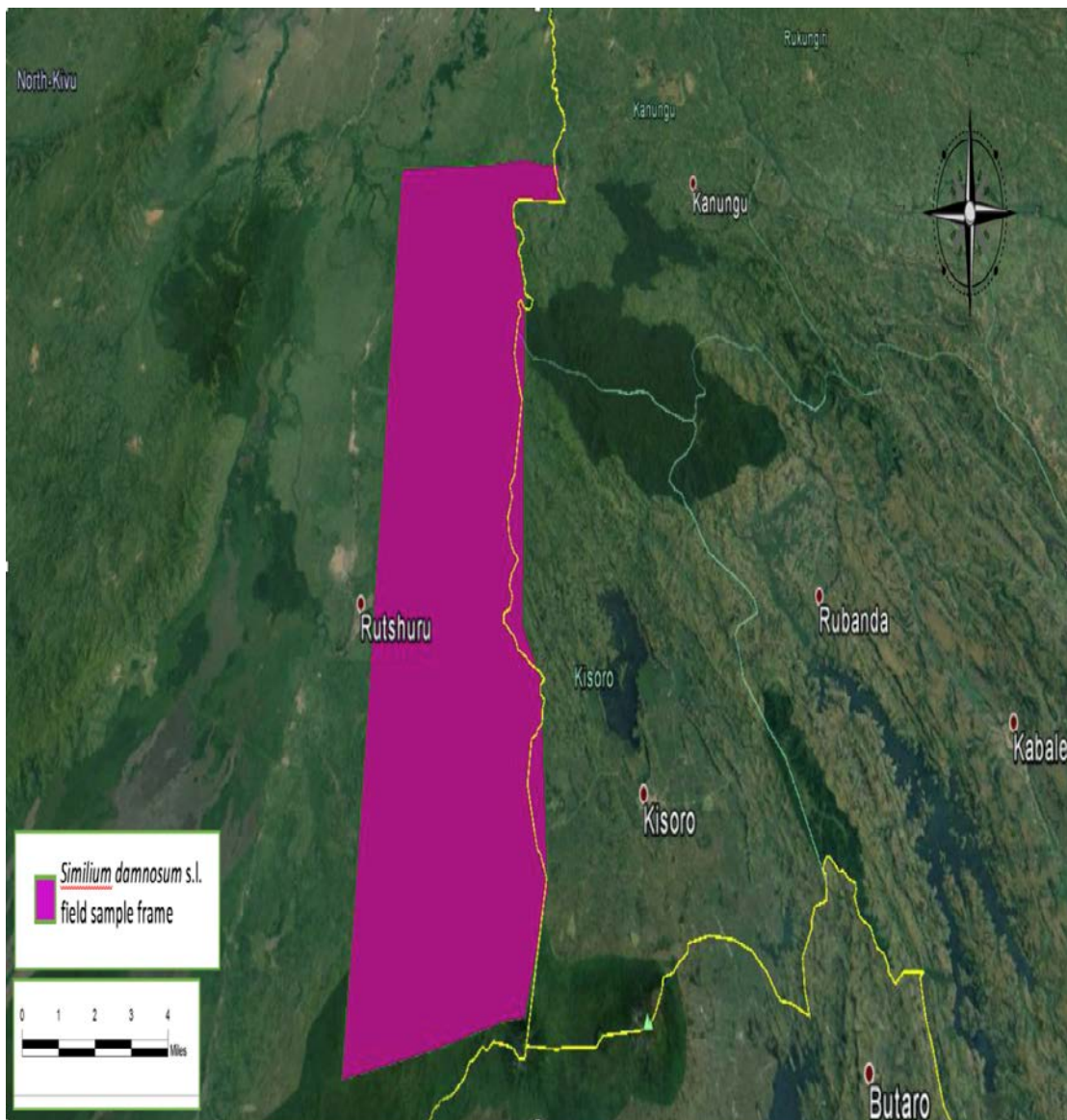
communities with the microfilaricide Mectizan® (ivermectin) (<http://www.iapb.org/vision-2020/what-is-avoidable-blindness/river-blindness>). In 1987 Merck announced the donation of Mectizan to all who needed it, for as long as needed and launched the Mectizan Donation Program (MDP) which is the longest-running, disease-specific, drug donation program and public/private partnership of its kind. In 1998, Merck expanded the mandate of the program to include lymphatic filariasis elimination through the co-administration of Mectizan and albendazole, donated by GlaxoSmithKline, in African countries and Yemen where lymphatic filariasis and onchocerciasis are co-endemic.

To evaluate onchocerciasis control activities in the DRC in the first 12 years of community-directed treatment with ivermectin (CDTI), Makenga et al. (2015) employed data from the National Programme for Onchocerciasis (NPO) provided by the National Onchocerciasis Task Force (NOTF) through the annual reports of the 21 CDTI projects for the years 2001-2012 in the DRC which were reviewed retrospectively. A hypothetical-inputs-process-outputs-outcomes table was constructed. Results revealed that Community-directed treatment with ivermectin expanded from 1968 communities in 2001 to 39,100 communities by 2012 while the number of community-directed distributors (CDD) and healthworkers (HW) multiplied. By 2012, there were ratios of 1 CDD per 262 persons and 1 HW per 2,318 persons at risk. More than 80% of the funding came from the fiduciary funds of the African Programme for Onchocerciasis Control. The cost of treatment per person treated fell from US\$ 1.1 in 2001 to US\$ 0.1 in 2012. The therapeutic coverage increased from 2.7% (2001) to 74.2% (2012); the eco-geographical coverage, from 4.7% (2001) to 93.9% (2012).

Eco-geographical coverage fell in 2005 due to deaths in loiasis co-endemic areas, and the therapeutic coverage fell in 2008 due to insecurity. *Loa loa* filariasis is a skin and eye disease caused by the nematode worm *Loa loa*. Humans contract this disease through the bite of a deer fly or mango fly (*Chrysops* spp), the vectors for *Loa loa*. (https://en.wikipedia.org/wiki/Loa_loa_filariasis). Knowing whether someone has a *Loa loa* infection has become more important in Africa because the presence of people with *Loa loa* infection has limited programs to control or eliminate onchocerciasis and lymphatic filariasis (elephantiasis).

We constructed multiple models in ArcGIS using Google Earth™ free imagery to determine precise geographic locations of flooded cross-border, vectored *S. damnosum* s.l. larval breeding sites for spatiotemporally quantifying endemic onchocerciasis transmission risk zones along multiple riverine tributaries at the study site. The advent of new mapping technologies such as Google Earth™ offers free satellite imagery and aerial photos of most of earth's land surface which has led to the increased uptake of mapping technology for use relevant to public health (www.esri.com)

Figure 3: Polygonised Google Earth™ LULC map revealing DRC study site



2.3 Remote sensing data: Two cloudless, ready-to-use, wide-area coverage mosaics, 5-m, natural color, Rapid Eye mosaics, 5kilometer (km)² polygons were ordered from Apollo mapping (<https://apollomapping.com/>). The Rapid Eye Basic product was radiometric and sensor corrected, providing imagery of two eco-epidemiological, study site polygons along the DRC border 10km from the Ugandan border as seen from the spacecraft without correction for any geometric distortions inherent in the imaging process. The imagery data was accompanied by all spacecraft telemetry necessary for processing of the DRC data which was geo-corrected and subsequently matched with a stereo pair for the generation of digital elevation LULC data. The images were resampled to a coordinate system defined by an ideal basic camera model for band alignment.

The radiometric corrections applied to the DRC polygons product included: 1) Correction of relative differences of the radiometric response between detectors and 2) Non-responsive detector filling which filled



nulls values from detectors that were no longer responding during the swath uptake. Conversion to absolute LULC radiometric values were based on calibration coefficients. The geometric sensor corrections applied to this product corrected for: 1) internal detector geometry which combined the two sensor chipsets into a virtual array, 2) optical distortions caused by sensor optics; and, 3) registration of all bands together to ensure all bands lined up with each other correctly.

The RapidEye™ Ortho product was radiometric, sensor and geometrically corrected and aligned to a cartographic map projection. The geometric correction used fine DEMs with a post spacing of between 30 and 90 meters. Ground Control Points (GCPs) were used in the creation of the DRC 5m resolution images. The file format was GeoTIFF with associated metadata files. The Bit Depth was 8-bit color balanced. The Projection/Datum was UTM WGS84. Table 1 shows the spectral bands, bandwidth and maximal resolution.

Table 1: Rapid Eye™ waveband data information for the DRC 5m polygons

Band name	Band with from [µm]	Band width to [µm]	Code	Maximal resolution [m]
1	0.44	0.51	BLUE	6.5
2	0.52	0.59	GREEN	6.5
3	0.63	0.685	RED	6.5
4	0.69	0.73	RED EDGE	6.5
5	0.76	0.85	NIR	6.5

2.4 Land use land cover analyses: We defined two 5km² polygons 10km from the Ugandan border. A LULC raster layer and parcel polygon layer for the DRC polygons was created using the GCPs. Three LULC geoclassifications were generated in ArcGIS including water, bare soil and noncanopied trailing vegetation which were defined as:

- 1) Water - Permanent bodies of water such as lakes, streams, rivers, storm water retention ponds and hydrophilic vegetation. Wetlands with a high-water table and areas which are often interspersed with channels or pools of open water, road side ditches, storm/rain and open channel tributaries were included in this class.
- 2) Bare Soil - Bare soil rock, sand, silt or gravel or other topographic aggregates of mineraloids. Examples of this endmember geoclassifiable, also LULC included exposed soil in riverine areas.
- 3) Non-canopied trailing vegetation: An ecosystem characterized by more or less dense and extensive cover. Typically, the cover is assessed as percent crown cover which may be remotely geovisually differentiated between open and closed-canopy forests (FAO, 1999). Other variants in this class included the use of basal area, wood volume, proportion of land with plant fauna above a minimum height, and proportion of land with biomass exceeding a minimum threshold, with no distinction made between single-stem or multi-stem forms.



We wanted to know the area and area percentage of each type of geoclassified LULC within each DRC polygon. We employed the Zonal Tools in Spatial Analyst™ in ArcGIS 10.3 for conducting the analysis. Specifically, **Tabulate Area** calculated and cross-tabulated the LULC areas in a output table for each DRC Rapid Eye™ polygon.

We employed data digitization on the Rapid Eye™ 5m polygons. Data layers were prepared in ArcMap™. A landcover suitability analyses was conducted employing the multi-criteria, geospatially, geospectrally weighted, LULC combinations in each polygon. Quantitation, standardization and scaling of the eco-epidemiological, LULC maps were then conducted in the eco-cartographic database. A raster map was generated. A vector and land suitability map was also generated. Each geoclassified LULC zone was delineated on the habitat maps.

2.4 Vegetation mapping: Raster modeling was performed in ArcGIS 10.2® which included performing image differencing on the NDVI layers, geo-classifying the layers into different classes and calculating a wetness index employing the Raster Calculator for each DRC study site 5m polygon.

It should be noted that NDVI is functionally, but not linearly, equivalent to the simple IR/red ratio (NIR/VIS) (<http://ntrs.nasa.gov/archive/nasa/casi.ntrs.nasa.gov>). The advantage of NDVI over a simple (IR)/red ratio would be therefore generally limited to any possible linearity of its functional relationship with quantitated vegetational LULC properties (e.g. biomass). But the most important concept in the understanding the NDVI algebraic formula is that, despite its name, it is a transformation of a spectral ratio (NIR/VIS), it has no functional relationship to a spectral difference (NIR-VIS) [51].

Here, the difference of the Rapid Eye™ visible and NIR bands for each DRC, 5m, resolution polygon was divided by their sum, which formed the functionally equivalent NDVI over the terrestrial surfaces of the DRC study sites. NDVI spectral variability (i.e., standard deviation of sub-grid-stratified, pixel estimates) could differentiate multiple LULCs. NDVI parameters, was computed directly within a range from -1.0 to 1.0 using visible and NIR reflectance, (p), utilizing and the expression:

$$1) \quad NDVI = \frac{\rho_{NIR} - \rho_{red}}{\rho_{NIR} + \rho_{red}}$$

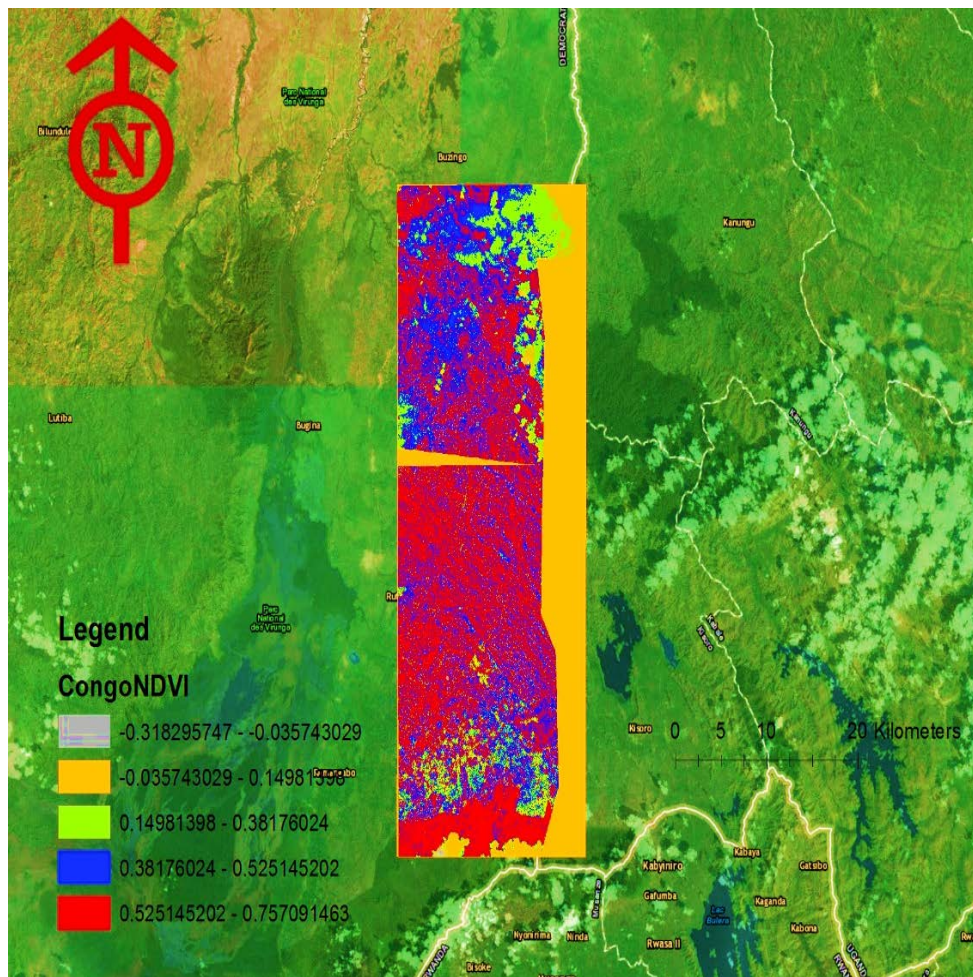
$$u_{total}^2(NDVI) = \left(\frac{\partial NDVI}{\partial \rho_{NIR}}\right)^2 u_{total}^2(\rho_{NIR}) + \left(\frac{\partial NDVI}{\partial \rho_{red}}\right)^2 u_{total}^2(\rho_{red}) + 2 \frac{\partial NDVI}{\partial \rho_{NIR}} \frac{\partial NDVI}{\partial \rho_{red}} u_{total}(\rho_{NIR} - \rho_{red})$$

$$\frac{\partial NDVI}{\partial \rho_{NIR}} = \frac{2 \rho_{red}}{(\rho_{NIR} + \rho_{red})^2}$$


$$\frac{\partial NDVI}{\partial \rho_{red}} = \frac{-2 \rho_{NIR}}{(\rho_{NIR} + \rho_{red})^2}$$

$$\frac{\partial NDVI}{\partial \rho_{NIR}} \frac{\partial NDVI}{\partial \rho_{red}} = \frac{-4 \rho_{NIR} \rho_{red}}{(\rho_{NIR} + \rho_{red})^4}$$

Figure 4: Rapid Eye red and NIR band combination of an NDVI using a 5m DRC map that highlights the LULC

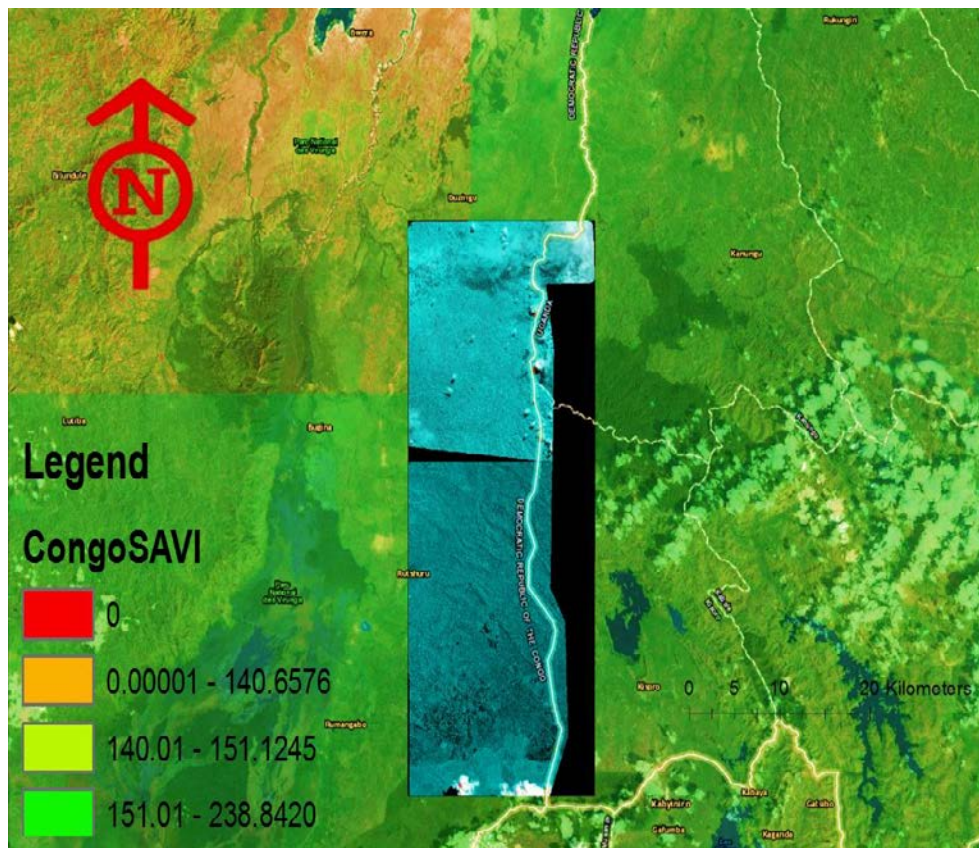


We then generated SAVI maps in ArcMap with the DRC Rapid Eye™ polygons(see Figure 4). The SAVI is structured similar to the NDVI but with the addition of a “soil brightness correction factor[52]. We

employed
$$SAVI = \frac{NIR - RED}{(NIR + RED + L)} * (1 + L)$$
 where NIR was the reflectance value of the NIR, RED was reflectance of the red band, and L was the soil brightness correction factor in the DRC study site, stratified polygons. We assumed that the value of L varied by the amount of the geoclassified endmember, LULC cover of uncanopied, trailing vegetation, within the eco-epidemiological, polygons. We employed eco-georeferenced high vegetation regions, L=0; and in areas with no trailing vegetation, L=1. Generally, an L=0.5 works well in most situations and is the default value used when L=0, then SAVI = NDVI[52]. The output of SAVI rendered from the DRC spectral wavelength LULC radiance was a new image layer in ArcGIS with values ranging from -1 to 1. which was gauged by the Band Arithmetic function . We employed the **Add Function** button  on the **Image Analysis** window to apply an SAVI, to each 5m resolution, DRC Rapid Eye™ polygon. We opened the **Image Analysis Options** dialog box, clicked the **SAVI** tab, then check **Scientific Output**. Also on this tab was the option **Use Wavelength**, which we utilized to identify the correct Rapid Eye™ wavelength bands information was part of the dataset. We assumed that lower the value of L, the lower the amount/cover of green vegetation in the DRC, study site, Rapid Eye™ polygons.

To assess the accuracy of the NDVI and SAVI thematic maps, a simple random sampling method was chosen to ensure sampled selection at an eco-georeferenceable, potential cross-border, African, riverine tributary, immature habitat eco-epidemiological, capture point, breeding foci, arbitrarily selected within the DRC, study site, grid-stratified polygon. To provide a statistically efficient assessment of accuracy, a conservative sampled size equation was then employed to calculate the remotesample sizes using an error matrix in Spatial Analyst™.

Figure 5: Rapid Eye red and NIR band combination of an SAVI using a 5m DRC map that highlights the LULC



2.5Kappa statistics: For each mapping region, stratified sampling formulas were applied to estimate spectral LULC error proportions in the ArcGIS-derived, trailing vegetation-related,canopied, LULC maps generated employing frequency radiance, wavelength estimates of overall and class-specific user's and producer's accuracy. The use of stratified formulas is important for validating field-sampling methods(www.esri.com).

Accuracy results were computed thereafter through weighting the cell proportions by the proportion of each Rapid EyeTM geoclassified 5m, LULC, spectral band within a given region in the DRC, Rapid EyeTM, 5m polygons. Specifically, the overall producer's accuracy was estimated employing post-stratified formulas.

We employed, post-stratified, Rapid EyeTM, geo-spectral, parameterizable, unbiased endmember, spectral radiance, wavelength LULC estimators for the known Red Green and Blue (RGB), Visible and IR and waveband totals for each land-cover class which was subsequently delineated by (Ni+). The data were treated as a stratified random sample of Red Edge (ni+) bands. The Ni+ and ni+) LULC waveband from the sampled 5m pixels were identified in each class in each polygon. User's accuracy (Ui) in ArcMapTM were based on the random sampling formulas:

$$\hat{P} = \frac{1}{N} \sum_{k=1}^q \frac{N_{k+} n_{kk}}{n_{k+}}$$

$$\hat{P}_{U_i} = n_{ii} / n_{i+}$$

$$\hat{P}_{A_j} = \frac{(N_{j+} / n_{j+}) n_{jj}}{\sum_{k=1}^q (N_{k+} / n_{k+}) n_{kj}}$$



The producer's accuracy was also calculated in ArcMapTM to determine the probability that a reference geosampled, Rapid EyeTM geoclassified, endmember, spectral radiance, LULC index for each polygon correctly mapped and measured the errors of omission (i.e., 1-producer's accuracy). In contrast, the user's accuracy indicated the probability that a sample from the Rapid EyeTM maps matched the reference, 5m, uncoalesced, LULC dataset and measured the error of commission (1-user's accuracy).

Kappa statistics were calculated employing SAS PROC FREQ. Kappa statistics (κ) are appropriate for testing whether agreement exceeds chance levels for binary and nominal ratings for remotely-sensed entomological, time series, vector arthropod, breeding foci, geoclassified LULC maps constructed from geo-spectral or geo-spatiotemporal dependent, eco-georeferenceable, uncoalesced parameterizable, moderate resolution, waveband, spectral, radiance estimators [37].

$$\kappa = \frac{\text{Pr}(a) - \text{Pr}(e)}{1 - \text{Pr}(e)}$$

The equation for κ was where Pr(a) was the relative observed agreement amongst the uncertainty based statistics and Pr(e) was the hypothetical probability of chance agreement between the, eco-georeferenceable, uncoalesced, geoclassified, observational, *S. damnosum*.l. breeding foci, endmember, spectral radiance, in each geoclassified LULC in the Rapid EyeTM imaged, 5m resolution, DRC polygons. The kappa coefficient had the value 0.3431, which indicated slight agreement between the Rapid EyeTM LULC, 5m, waveband data in the polygons. The hypothesis test confirmed that we could reject the null hypothesis of no agreement. This conclusion was further substantiated by the confidence interval of (0.2031, 0.4372), which suggested that the true kappa was greater than zero for the spectral endmember, radiance, LULC waveband datasets.

Table 2: FREQ Procedure Statistics for the grid-stratified, 5m, resolution DRC, polygons

Simple Kappa Coefficient	
Kappa	0.3449
ASE	0.0724
95% Lower Conf Limit	0.2131
95% Upper Conf Limit	0.4361

Test of H0: Kappa = 0	
ASE under H0	0.0632
Z	5.6366
One-sided Pr > Z	<.0001
Two-sided Pr > Z	<.0001

The AGREE option was employed to test for symmetry and the weighted kappa coefficient between the geoclassified, Rapid EyeTM endmember, LULC, spectral radiance, sensor indices in the DRC 5m polygons. We specified the AGREE option in the TABLES statement. In so doing, PROC FREQ computed tests and measures of agreement for square tables (that is, for 5m, tables where the number of rows equaled the number of columns) employing the geoclassified, uncoalesced, geo-spectral, 5m, resolution, LULC data in each polygon. Our tests and measures included McNemar's test for 2 x 2 tables, Bowker's test of symmetry, the simple kappa coefficient, and the weighted kappa coefficient. For quantitating multiple wavelength, geoclassified, LULC frequency strata, synthesized, explanatory, geoclassified, grid-stratified, 5m resolution LULCs for optimally identifying cross-border, riverine tributary *S. damnosum* s.l., eco-georeferenceable, breeding foci, capture points, n-way tables, where $n > 2$ were created. PROC FREQ also computed the overall simple kappa coefficient and the overall weighted kappa coefficient, and tested for equal kappa (i.e., simple and weighted, DRC, 5m, resolution LULC geospectral, wavelength, LULC variables) amongst the grid-stratified, 5m, polygon strata. Cochran's Q was also computed for multiway tables where each geosampled, 5m, Rapid EyeTM tabulated landscape sensor variable had been transformed into two levels, (e.g., $h \times 2 \times 2$ tables).



PROC FREQ computed the kappa coefficients for the weighted endmember, wavelength spectral radiance, LULC indices and their asymptotic standard errors which were subsequently optimally unbiasedly quantitated in each Rapid Eye™ DRC, 5m polygon. Their confidence limits were specified in the AGREE option employing the TABLES statement. The KAPPA option was specified in the TEST statement. In so doing, PROC FREQ computed the asymptotic test of the hypothesis that simple kappa equaled 0 in each geoclassified, polygonised 5m, LULC waveband. Similarly, the WTKAP option was specified in the TEST statement for each geosampled, LULC, wavelength, parameter estimator. PROC FREQ then computed the asymptotic test for the weighted kappa for each geoclassified LULC in the DRC polygon.

In addition to the asymptotic tests PROC FREQ provided exact p -values for McNemar's test, the simple kappa coefficient test, and the weighted kappa coefficient test for each polygon. We requested these exact tests by specifying the corresponding options in the EXACT statement. The EXACT statement requested the exact tests and determined the confidence limits for the specified decomposable, 5m, geoclassified, LULC, spectral, wavelength measurements in each polygon. PROC FREQ also computed the AGREE statistics. We employed the same methodologies as [53-55], for optimally deriving each LULC waveband for the invasive remote assessment of each DRC Rapid Eye™ polygon.

PROC FREQ then computed [56] for 2x2 tables for each endmember, spectral radiance, Rapid Eye™ geoclassified 5m, resolution, LULC waveband in the DRC polygons by specifying the AGREE option. McNemar's test is appropriate when analyzing uncoalesced, remotely sensed, *S. damnosum* s.l. endmember, LULC, wavelength, data from regressed matched subjects within an eco-georeferenceable, immature, habitat, capture point, spectral radiance eco-epidemiological, dichotomous response, risk model, [23]. By default, the null hypothesis for McNemar's test revealed marginal homogeneity within each LULC class, which was expressed as $P_{1.} = P_{.1}$; this was equivalent to a discordant proportion ratio (p_{12}/p_{21}) of 1. The corresponding test statistic was computed as $Q_M = (n_{12} - n_{21})^2 / (n_{12} + n_{21})$. Under the null hypothesis, Q_M had an asymptotic chi-square distribution with 1 degree of freedom within each grid-stratified, DRC, Rapid Eye™, 5m, gridded polygon.

We then specified the null ratio of discordant proportions (p_{12}/p_{21}) in the AGREE(MNULLRATIO=) option. McNemar's test was computed employing $Q_M(r) = (n_{12} - e_{12})^2 / e_{12} + (n_{21} - e_{21})^2 / e_{21}$ where $e_{12} = D/(1+r)$, $e_{21} = D/(1+r)$, and D was the number of discordant, endmember geoclassified, uncoalesced, LULC, 5m, spectral wavelength, data values, ($n_{12} + n_{21}$) as synthesized from the cross border LULC indices in each Rapid Eye™ DRC polygon. Under the null hypothesis, $Q_M(r)$ had an asymptotic chi-square distribution with 1 degree of freedom in each polygon aggregated score for each LULC geoclassification which was performed for remotely identifying cross-border, capture point, *S. damnosum* s.l. riverine tributary, immature habitat, breeding foci. PROC FREQ also computed an exact p -value for McNemar's test which was robustly specified employing the MCNEM option in the EXACT statement. In statistics, McNemar's test is a statistical test used on paired nominal data (<http://support.sas.com>). Here we applied the tabulated 2×2 contingency tables constructed from the uncoalesced, geoclassified, spectral, radiance, LULC wavelength, 5m sensor, waveband measurements in each Rapid Eye™ polygon with a dichotomous trait (e.g., matched pairs of LULC subjects), to determine whether the row and column marginal frequencies were equal just as in [57] for optimally identifying cross-border, *S. damnosum* s.l., immature habitats at the DRC study sites.

For Bowker's test of symmetry, the null hypothesis was that the cell proportions in each geoclassified, LULC waveband extracted from the Rapid Eye™ DRC polygon were symmetric, or that $P_{ij} = P_{ji}$ was quantifiable for all pairs of table cells. PROC FREQ provided the Bowker's test for each square table larger than 2×2 which was optimally synthesized from each DRC polygon, geoclassified, LULC parameter estimator dataset. The Bowker's test of symmetry was computed as $Q_B = \sum_{i < j} (n_{ij} - n_{ji})^2 / (n_{ij} + n_{ji})$. For large samples, Q_B has an asymptotic chi-square distribution with $R(R-1)/2$ degrees of freedom under the null hypothesis of symmetry [58].

The simple kappa coefficient, introduced by [59], was employed as measure of interrater between the uncoalesced wavelength datasets for each geoclassified LULC in each Rapid Eye™, DRC 5m, polygon. PROC FREQ computed the simple kappa coefficient for each extracted LULC from the Rapid Eye™ DRC polygon employing $\hat{\kappa} = (P_o - P_e) / (1 - P_e)$ where $P_o = \sum_i p_{ii}$ and $P_e = \sum_i p_{i.} p_{.i}$. It was assumed that the eco-



georeferenceable, wavelength LULC, frequencyresponse from each eco-epidemiological, cross-border, capture point, *S. damnosum* s.l. riverine, tributary, breeding foci, synthesized,from the grid-stratified, 5m spatial resolution, geoclassified, polygons,uncoalesced, spectral radiance were viewed with two independent ratings of the n subjects. In so doing, the kappa coefficient equaled 1 in each polygon based on acomplete agreement of the rater classification.

The asymptotic variance of the simple kappa coefficient forthe 5m polygon was computed as
$$\text{Var}(\hat{\kappa}) = (A + B - C) / (1 - P_e)^2 n$$
 where:
$$A = \sum_i p_{ii}(1 - (p_i + p_i)(1 - \hat{\kappa}))^2$$
,

$$B = (1 - \hat{\kappa})^2 \sum_{i \neq j} p_{ij}(p_i + p_j)^2$$
 and
$$C = (\hat{\kappa} - P_e(1 - \hat{\kappa}))^2$$
 as in[60]. PROC FREQ computedconfidence

limits for the simple kappa coefficient in each polygon as $\hat{\kappa} \pm (z_{\alpha/2} \times \sqrt{\text{Var}(\hat{\kappa})})$ where $z_{\alpha/2}$ was the $100(1 - \alpha/2)$ percentile of the standard normal distribution. The value of α was subsequently determined by the value of the ALPHA= option, which, by default, was 0.05 and produced 95% confidence limits for both grid-stratified polygons based on theuncoalesced frequency datasets of polygonized, DRC, geoclassifiable,5m,wavelength, LULC indicator, coefficient, radiance, estimator values.

To compute an asymptotic test for the kappa coefficient, we employed the standardized test statistic $\hat{\kappa}^*$, in PROC FREQ which had an asymptotic standard normal distribution under the null hypothesis that kappa equaled 0 for each regresseable, LULC wavelength coefficient value in each polygon. Here, the standardized test statistic for the Rapid Eye™ polygonLULC sensor data and their respected 5m,geoclassified,uncoalesced, spectral radiance indicator, coefficient estimate were optimally computed as $\hat{\kappa}^* = \hat{\kappa} / \sqrt{\text{Var}_0(\hat{\kappa})}$ where $\text{Var}_0(\hat{\kappa})$ was the variance of the kappa coefficient under the null hypothesis,

$$\text{Var}_0(\hat{\kappa}) = \left(P_e + P_e^2 - \sum_i p_i p_i (p_i + p_i) \right) / (1 - P_e)^2 n$$
 [55]. PROC FREQ also provided an exact test for the simple

kappa coefficient. The exact test was requested by specifying the KAPPA or AGREE option in the EXACT statement.

The weighted kappa coefficient is a generalization of the simple kappa coefficient that uses weights to quantify the relative difference between categories(<http://support.sas.com>). For each2x2 table constructed from the uncoalesced geoclassified, 5m, wavelength, LULC frequency data in each polygon, the weighted kappa coefficient equaled the simple kappa coefficient. PROC FREQ displayedthe weighted kappa coefficient for the tables.

PROC FREQ computed the kappa weights from the column scores of the uncoalesced, 5m,spectral wavelength, LULC data, by employing theCicchetti-Allison weights and Fleiss-Cohen weights, both of which were optimally described for the DRC polygons and their wavelength, indicator, radiance, coefficient values for identifying cross-border, riverine, tributary,*S. damnosum* s.l.,eco-georeferenceable, breeding foci, eco-epidemiological, hyper productive, immature, seasonal, capture points. The wavelength radiance covariates w_{ij} were constructed so that $0 \leq w_{ij} < 1$ for all $i \neq j$, $w_{ii} = 1$ for all i , and $w_{ij} = w_{ji}$. The weighted kappa coefficient for the geoclassified,DRC, decomposed, LULC values were computed as

$$\hat{\kappa}_w = \left(P_{o(w)} - P_{e(w)} \right) / \left(1 - P_{e(w)} \right)$$
 where
$$P_{o(w)} = \sum_i \sum_j w_{ij} p_{ij} P_{e(w)} = \sum_i \sum_j w_{ij} p_i p_j$$
 The tabulated asymptotic variance

of the weighted kappa coefficient in each 5m,DRC Rapid Eye™grid-stratified polygon was then
$$\text{Var}(\hat{\kappa}_w) = \left(\sum_i \sum_j p_{ij} (w_{ij} - (\bar{w}_i + \bar{w}_j)) (1 - \hat{\kappa}_w)^2 - (\hat{\kappa}_w - P_{e(w)} (1 - \hat{\kappa}_w))^2 \right) / (1 - P_{e(w)})^2 n$$
 where
$$\bar{w}_i = \sum_j p_j w_{ij}$$

$$\bar{w}_j = \sum_i p_i w_{ij}$$

PROC FREQ computed confidence limits for the weighted kappa coefficientconstructed from the geoclassified, DRC, Rapid Eye™,radiance, wavelength indicator coefficient, 5m, LULC estimates employing $\hat{\kappa}_w \pm (z_{\alpha/2} \times \sqrt{\text{Var}(\hat{\kappa}_w)})$ where $z_{\alpha/2}$ was the $100(1 - \alpha/2)$ percentile of the standard normal distribution. The value of α for the estimators were determined by the value of the ALPHA= option, which, by default, was 0.05 and produced 95% confidence limits.We assumed this value to be a strong statistical inference



signal for aiding in remotely identifying eco-georeferenceable, cross-border, riverine, tributary, *S. damnosum* s.l., breeding foci, eco-epidemiological, capture points at the DRC eco-epidemiological, study sites.

An asymptotic test was computed for the weighted kappa coefficient from the Rapid Eye™ 5m polygons and their grid-stratified, LULC, sensor wavelength estimators. PROC FREQ employed the standardized test statistic $\hat{\kappa}_w^*$, which had an asymptotic standard normal distribution under the null hypothesis that the weighted kappa equaled 0. The standardized test statistic was computed as $\hat{\kappa}_w^* = \hat{\kappa}_w / \sqrt{\text{Var}_0(\hat{\kappa}_w)}$ where $\text{Var}_0(\hat{\kappa}_w)$ was the variance of the weighted kappa coefficient under the null hypothesis, $\text{Var}_0(\hat{\kappa}_w) = \left(\sum_i \sum_j p_i p_j (w_{ij} - (\bar{w}_i + \bar{w}_j))^2 - P_{e(w)}^2 \right) / (1 - P_{e(w)})^2 n$. PROC FREQ provided an exact test for the weighted kappa coefficients synthetically derived from the DRC, Rapid Eye™, 5m, polygonized, LULC, frequency, radiance, indicator, parametrizable, covariate coefficient estimates for optimally geospectrally quantitating the cross-border, riverine, tributary, *S. damnosum* s.l., breeding foci, eco-georeferenceable, capture point, wavelength variables. Here the exact test was specified by the WTKAPPA in the EXACT statement.

PROC FREQ computed the kappa coefficient, wavelength, LULC weights in each DRC 5m, resolution, grid-stratified polygon by employing the column scores and one of the three available Rapid Eye™, geospectrally uncoalesced, LULC, endmember, wavelength, frequency covariate weightages. The column scores were determined by the SCORES= option in the TABLES statement. By default, PROC FREQ employed Cicchetti-Allison weights. (WT=FC) which was specified with the AGREE option for optimally quantitating the wavelength dissimilarities in each geosampled geoclassified, 5m, LULC variable in each, grid-stratified, eco-georeferenceable, geoclassifiable DRC, polygon. The most readily available types of kappa weights Cicchetti-Allison and Fleiss-Cohen weights (<http://support.sas.com>).

PROC FREQ computed Cicchetti-Allison, kappa coefficients for the polygonized, LULC 5m, geospectral, wavelength frequency radiance, weights employing $w_{ij} = 1 - \frac{|C_i - C_j|}{C_C - C_1}$ where C_i was the score for column i and C which was the number of categories or columns in [61]. In so doing, the SCORES= option in the TABLES statement determined the type of column scores employable to compute the kappa weight, DRC, 5m, resolution polygon, Rapid Eye™, geoclassifiable, LULC, uncoalesced, wavelength frequency weights and other score-based statistics. The default was analyzed employing the SCORES=TABLE for robustly quantitating the numeric LULC table scores and their endmembers synthesized in each polygon. Numeric values were assigned to the levels in a way that reflected the unmixed, wavelength, 5m, resolution, LULC indicators in the DRC polygons and their level of similarity. There were four levels and they were ordered according to similarity: 0, 2, 4, and 10. The Cicchetti-Allison kappa weights then quantitated the following values: $w_{12} = 0.8$, $w_{13} = 0.6$, $w_{14} = 0$, $w_{23} = 0.8$, $w_{24} = 0.2$, and $w_{34} = 0.4$. Note that when there were only two categories (that is, C = 2), the weighted kappa coefficient was identical to the simple kappa coefficient.

Since there were multiple 5m, frequency spectral, wavelength, reflectance, in the uncoalesced, LULC strata in each DRC, Rapid Eye™ polygon, PROC FREQ combined the stratum-level gridded estimates based on the kappa scores into an overall estimate of the supposed common value of kappa. It was assumed that there were q strata, LULC indexed in each polygon based upon $h = 1, 2, \dots, q$. Furthermore, $\text{Var}(\hat{\kappa}_h)$ denoted the variance of $\hat{\kappa}_h$ for the geoclassified, 5m, spectral radiance, endmember, LULC frequency wavelength indicators in the polygons. The estimate of the overall kappa coefficient was thereafter computed employing $\hat{\kappa}_T = \frac{\sum_{h=1}^q \hat{\kappa}_h}{\sum_{h=1}^q \frac{1}{\text{Var}(\hat{\kappa}_h)}}$ as in [55]. PROC FREQ computed an estimate of the overall weighted kappa in the same way for each wavelength LULC, frequency, indicator, coefficient estimate.

The grid-stratified, Rapid Eye™, DRC, polygonized, geoclassified, 5m, LULC variables were evaluated for equal wavelength, frequency spectral radiance, kappa coefficients. Since we had transformed the 5m wavelength data into multiple strata, a chi-square statistic test was subsequently employed to determine whether the stratum-level values of kappa were equal employing $Q_K = \sum_{h=1}^q (\hat{\kappa}_h - \hat{\kappa}_T)^2 / \text{Var}(\hat{\kappa}_h)$. Under the null hypothesis of equal kappa for the q strata, Q_K had an asymptotic chi-square distribution with q-1 degrees of freedom. PROC FREQ computed a test for each equal weighted, grid-stratified, wavelength, frequency, spectral



radiance, endmember, LULC kappa coefficients generated from the DRC,5m resolution, RapidEye™ polygons in the same way.

Cochran's Q was computed for multiway tables since each uncoalesced, DRC,Rapid Eye™,grid-stratified, wavelength radiance, endmember, LULC,geoclassified variable was organized into two levels, that is, for $2 \times 2 \cdots \times 2$ tables. Cochran's Q statistic was employed to test the homogeneity of the one-dimensional margins. We let m denote the number of 5m, spectral LULC variables in each polygon and N denote the total number of geoclassifiable, uncoalesced endmember, parameterizable, reflectance, covariate estimators.

Cochran's Q statistic was computed as
$$Q_C = m(m-1) \left(\sum_{j=1}^m T_j^2 - T^2 \right) / \left(mT - \sum_{k=1}^N S_k^2 \right)$$
 where T_j was the wavelength, frequency, spectral reflectance value for each LULC variable j, T was the total number of values overall for the polygonised variables, and S_k was the number of values for k. Under the null hypothesis, Cochran's Q had an asymptotic chi-square distribution with m-1 degrees of freedom. When there are only two binary response variables (m=2), Cochran's Q simplifies to McNemar's test(<http://support.sas.com>).

The CATMOD procedure performed categorical wavelength, forecast, vulnerability modeling of the remotely sensed, 5m, *S. damnosum* s.l., larval habitat, eco-epidemiological predictive model, uncoalesced, spectral radiance, endmember, LULC data that was represented by the contingency table. When there are more than two LULC response geoclassifiable categories in a remotely sensed, unbiased, *S. damnosum* s.l., larval habitat, eco-epidemiological predictive model, the marginal homogeneity may be tested by using the repeated measures capabilities of the CATMOD procedure[2].

We analyzed the relationship between the dependent variables r1, (overall 5m, LULC polygon, wavelength radiance and uncoalesced, geoclassified cross-border, LULC spectral values (r2) and the independent variables (a) eco-georeferenceable, riverine, tributary, uncanopied, trailing vegetation) and b (levels of turbidity). We analyzed the marginal probabilities of the dependent variables, and uses a main-effects model:

```
proc catmod;
LULCweight wt;
response marginals;
cross-border S. damnosum s.l.habitat id model r1*r2=a b;
quit;
```

In the capture point, *S. damnosum* s.l., breeding foci, African riverine tributary, uncoalesced, LULC endmember, wavelength, analyses the response functions were the default generalized logits. The keyword `_RESPONSE_` was employed for optimally quantitating the 5m, LULC frequency, wavelength radiance measurements in the MODEL statement which did fit a log-linear model. The keyword `_RESPONSE_` tells PROC CATMOD to model the variation among the dependent variables(<https://support.sas.com>). We specified the actual riverine tributary, cross-border, vector arthropod immature habitat, eco-epidemiological, identification model in the LOGLIN statement.

Next we analyzed the nominal dependent variables (r1, r2, and r3 (levels of, vegational, endmember, LULC signature interpolation) with a log-linear model. A maximum likelihood analysis was conducted in CATMOD which included the main effects and the r1*r2 interaction in the model. The predicted stratified grid-cell wavelength LULC frequency statement was written as:

```
proc catmod;
LULC weight wt;
cross-border S. damnosum s.l.habitat id model model r1*r2*r3=_response_ / pred=freq;
loglin r1|r2 r3;
quit;
```

We analyzed the relationship between the nominal dependent variable (r) and the independent variables (x1, x2) with a logistic regression analysis. The maximum likelihood estimation was performed by writing:

```
proc catmod;
LULC weight wt;
direct x1 x2;
```



cross-border *S. damnosum* s.l.habitat id model r=x1 x2;
 quit;

If x1 and x2 are continuous so that each observation has a unique value of these two variables, then it might be more appropriate to use the LOGISTIC or GENMOD procedure(www.sas.edu).

For performing the log-linear model analysis in PROC CATMOD, we requested the weighted least squares estimates and the maximum likelihood estimates. By default, PROC CATMOD calculated maximum likelihood estimates when the default response functions in the 5m Rapid Eye TM, LULC, geoclassified, *S. damnosum* s.l. eco-epidemiological, forecast, vulnerability, wavelength, risk model was employed.

Table 3: PROC CATMOD statements for the combinations of types of estimates in the 5m Rapid Eye, cross-border, *S. damnosums.l.*, LULC wavelength, endmember model

Estimation Method	MODEL Statement
Maximum likelihood(Newton-Raphson)	model a*b=_response_;
Maximum likelihood (Iterative Proportional Fitting)	model a*b=_response_ / ml=ipf;
Weighted least squares	model a*b=_response_ / wls;
Maximum likelihood and weighted least squares	model a*b=_response_ / wls ml;

The following statements yielded a maximum likelihood analysis of a saturated, cross-border, African riverine tributary *S. damnosum* s.l. 5m, resolution, log-linear, forecast, vulnerability, eco-epidemiological model for the dependent LULC variables *r1* and *r2*:

```
proc catmod;
LULC weight wt;
S. damnosum s.l.habitat id model r1*r2=_response_;
  loglin r1|r2;
run;
```

We then fit a reduced model with respect to the dependent variables (i.e., a capture point, breeding foci eco-georeferenceable 5m, resolution, immature habitat model of conditional independence), so as to specify the reduced model in a LOGLIN statement. For example, the following statements yielded a main-effects log-linear model, *S. damnosum* s.l., cross-border, riverine tributary, LULC, 5m,wavelength risk analysis of the factors *r1* and *r2*:

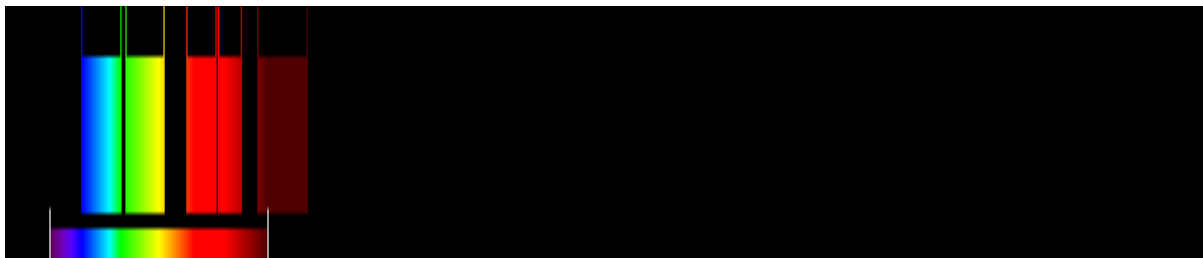
```
proc catmod;
LULC weight wt;
S. damnosum s.l. habitat model r1*r2=_response_ / pred;
  loglin r1 r2;
run;
```

The output included Wald statistics for the individual effects *r1* and *r2*, as well as predicted 5m, endmember LULC cell probabilities in each DRC polygon. Moreover, the goodness-of-fit statistic was the likelihood ratio test for the hypothesis of independence between *r1* and *r2* or, equivalently, a test of *r1*r2*.

2.6. Object-oriented classification Once a robust explanatory, dataset of the remotely-dependent, parameterizable, LULC predictor, covariate, 5m,estimator, wavelength, frequency, radiance coefficients was constructed, ENVI[®] spectral tools were used to analyze the quantitated data extracted from the Rapid Eye[™] image of the canopy, un-shaded vegetation, LULCgeoclassified within the DRCeco-epidemiological, study site polygons.Data was input into ENVI[®] technology using the GeoTIFF format. ENVI supports Input File Rapid Eye[™] functions including GeoTIFF, NITF and Tile Product (.til) (www.itvis.com/portals/0/pdfs/envi/). In ENVI 4.6[®], a spectrum plot, known as a z-profile, of the pixel under

the cursor was run through all 5m, wavebands of the RapidEye™DRC, grid-stratified, LULCpolygons. The basic workflow involved importing the geoclassified data collected rom the eco-epidemiological study sites into a spectral library. The library was employed in the endmember collection workflow to perform a supervised classification, based on the geosampled,geospatial,LULC geospectral, explanatory, LULC data,uncoalesced, feature attributes. Binary Encoding, Spectral Angular Mapping (SAM) and Spectral Feature Fitting were used to rank and match any unknown spectrum to the materials in the library.

Figure 6: Geovisualization of the Rapid Eye 5mspectrumsensor bands in ENVI



The endmembers of the eco-georeferenced,geoclassified, 5m, resolutionLULCs and its associated wavelength, frequency, microtopographic irradiance attributes were thenoptimally extracted them from ENVI®'s spectral library. Several spectra corresponding to the different backgrounds in the canopy, un-shaded and partially canopied, LULC structuralpixel components had to be included, since multiple scatterings between floating leaves, and a bright soil background increased the Rapid Eye™NIR reflectancein some vicinities on the geoclassified 5mpolygon data. Leaf cells have evolved to scatter (i.e., reflect and transmit) solar radiation in the NIR spectral region[8]. After the calibration estimates, had been determined the image was converted to match the library. Analogously, the Rapid Eye™reference LULC endmemberspectra in the library were transformed into 5m spectra of the image.

We employed a random selection of geoclassified LULC pixels to assess the satellite classification accuracy. Rapid Eye™class representative pixelswere selected and compared to a reference training dataset. During the segmentation procedure, image objects were generated based on several adjustable criteria of homogeneity such as color, shape, and texture. Data pre-processing involved converting the DN to radiance atmospheric correction employing FLAASH™, and co-registration techniques in the object-based classifier. Image classification was conducted employing the FLAASH™which generated a model (. gmd file) that converted the image's DN to at-sensor radiance and computed at-sensor reflectance while normalizing the solar elevation angle. The equation was as follows:

$$\rho_{BandN} = \frac{\pi(L_{BandN} * Gain_{BandN} + Bias_{BandN}) * D^2}{E_{BandN} * (COS((90 - \theta) * \pi / 180))}$$

where,

ρ_{BandN} = Reflectance for Band N

L_{bandN} = Digital Number for Band N

D = Normalized Earth-Sun Distance

E_{bandN} = Solar Irradiance for Band N

Selected uncoalesced, random,5m, LULC endmember frequency wavelength from the thematic,DRC, eco-epidemiological, grid-stratified study site polygons were then compared to the reference data. The estimated

$$P \left\{ -z_{\frac{\alpha}{2}} < \frac{x - m\theta}{\sqrt{m\theta(1-\theta)}} < z_{\frac{\alpha}{2}} \right\} = 1 - \alpha$$

accuracy for the spectrally extracted LULC data was calculated employing



where, x was the number of correctly identified LULC pixels, n =total number of LULC pixels in the sample, θ =the map accuracy and $(1-\alpha)$ was the confidence limit in each study site polygon. The Rapid Eye™ classifier identified the canopied/partially canopied, LULC and their associated ripple water LULC larger than 0.4 ha with generally satisfactory results (92.1%) with a lower detection limit of 0.1 ha in the cross border, riverine, tributary waterways in each polygon.

2.7 Endmember Analyses: We employed the Successive Projection Algorithm (SPA) to generate spectral endmembers from the 5m, Rapid Eye™ LULC spectra in each polygon. We let $P(i, j)$ denote the spectrum for the extracted, 5m, image pixel employing the image coordinates (i, j) , as the foundation of the unmixing algorithm which was optimally defined by employing $\vec{p}_{(i,j)} = \sum_{k=1}^m f_{(i,j)k} \vec{e}_k + \vec{\epsilon}_{(i,j)}$ and $f_{(i,j)k} \geq 0, k = 1, \dots, m, \sum_{k=1}^m f_{(i,j)k} = 1$ where m was the number of LULC endmembers, \vec{e}_k was the k th vegetational geoclassified partially-canopied associated endmember. Here $\vec{\epsilon}_{(i,j)}$ was the approximation error term (i.e., residual), and $f_{(i,j)k}$ was the fractional abundance for the k th bare soil endmember of a geoclassified, 5m, Rapid Eye™, LULC pixel (i, j) .

We omitted the error term in $\vec{p}_{(i,j)} = \sum_{k=1}^m f_{(i,j)k} \vec{e}_k + \vec{\epsilon}_{(i,j)}$ and computed the possible, linear, endmember, LULC mixtures from $\vec{p}_{(i,j)} = \sum_{k=1}^m f_{(i,j)k} \vec{e}_k$ and $f_{(i,j)k} \geq 0, k = 1, \dots, m, \sum_{k=1}^m f_{(i,j)k} = 1$ which formed a simplex C_m defined by m vertices that corresponded to the 5m endmembers, $\vec{e}_1, \vec{e}_2, \dots, \vec{e}_m$. According to [1] the volume of the simplex C_m can be calculated from the equation $V(C_m) = \frac{1}{(m-1)!} |\det(WW^T)|^{1/2}$ where $W = [\vec{e}_2 - \vec{e}_1, \vec{e}_3 - \vec{e}_1, \dots, \vec{e}_m - \vec{e}_1]$ in endmember geospace which may be interpreted as the volume of the simplex defined by m endmembers, when $\det(\cdot)$ denotes the determinant of a matrix representing the operation of an absolute geoclassified, microtopographic, LULC vegetation, value. Once the 5m LULC endmembers $\vec{e}_1, \vec{e}_2, \dots, \vec{e}_m$ were determined, their abundance was optimally estimated through the least squares method which was equivalent to a projection on the simplex.

Figure 7: ENV irradiance map of the riverine study site in the DRC



2.7 Geometric-optical LULC analyses: We employed the Li-Strahler model based on the assumption that the bidirectional reflectance distribution function (BRDF) would remotely retrieve vegetational and non-vegetational, canopied and partially-canopied, geoclassified, LULC, riverine tributary, structural variables in the DRC study site Rapid Eye™, 5m, resolution, polygons. The BRDF is a 4-dimensional function that defines how light is reflected at an opaque surface [8]. The BRDF for each explanatory, geoclassified spectral LULC wavelength was generated in ArcGIS. This function took incoming light directions, ω_i , and outgoing directions, ω_o , both defined with respect to an eco-georeferenced, geoclassified, LULCs surface, remotely geosampled site within the DRC, Rapid Eye™ polygons normalized n , and returned the ratio of the radiance exiting along ω_o to the irradiance incident on the riverine, ripple water, spectral components in the 5m, eco-epidemiological, study site polygons from direction ω_i . Note that each direction ω was itself parameterized by azimuth angle ϕ and zenith angle θ , therefore the BRDF for the Rapid Eye™ geoclassified LULCs in the DRC polygons was as a whole was 4-dimensional.

The BRDF we calculated had units sr^{-1} , with steradians (sr) being a unit of solid angle. The BRDF was defined by:
$$f_r(\omega_i, \omega_o) = \frac{dL_r(\omega_o)}{dE_i(\omega_i)} = \frac{dL_r(\omega_o)}{L_i(\omega_i) \cos \theta_i d\omega_i}$$
 where L was the radiance, E was the irradiance, and θ_i was the angle made between ω_i and the geoclassified LULCs and its associated ripple, water, riverine tributary, surface, reflectance, endmember emissivities. The BRDF defined how light was reflected and the function took an incoming light direction, ω_i , and outgoing direction, ω_o , which were both defined with respect to the geoclassified LULCs in the grid-stratified 5m polygons and its within canopy and ripple water surface n , geospectrally synthesized values and returned the ratio of reflected wavelength frequency LULC data exiting along ω_o to the irradiance incident from direction ω_i .

The inverted Li-Strahler geometric-optical model was then employed to retrieve specific spectral, moderate resolution, geoclassifiable, LULC, explanatory, eco-georeferenceable, parameterizable, endmember, predictor, covariate coefficients in the DRC polygons. Individual uncoalesced, sub-pixel, spectral, reflectance estimates from a QuickBird visible and NIR at 0.61m spatial resolution data of a semi-permanent *An. arabiensis*, floodwater immature habitat was extracted by using a Li-Strahler geometric-optical model in [62]. Individual pixel spectral reflectance estimates from the Quick Bird 0.61m spatial resolution data of an *An. arabiensis* aquatic, larval habitat were then geo-spectrotemporally extracted by employing a Li-Strahler geometric-optical model in ArcGIS. The model used three scene components: sunlit canopy (C), sunlit background (G) and shadow (T) generated from the Riceland image. The G, C, T components' classes were estimated using ENVI. In the object-based classifier, the Digital Number (DN) of the pixel in every QuickBird band was viewed using the z-profile from a spectral library. After making an atmospheric correction from the image for the study site, the DN was converted into ground reflectance. A convex eco-epidemiological, geometrical model was also employed for endmember LULC validation of the geospectrally decomposed aquatic larval habitat capture point. An ordinary kriged-based interpolation was performed in ArcGIS® Geostatistical Analyst using the reference signature generated from the unmixing models. Linear unbiased predictor dataset and variance estimates were derived for all hyper productive, seasonal, eco-georeferenceable, *An. arabiensis* breeding foci in the study site based on the extracted pixel endmember wavelength, frequency, LULC signature radiance estimates. The sub-pixel data along with other spatially continuous explanatory geoclassified, endmember, LULC variables sampled from productive habitats were then mapped and then treated as part of a larval control strategy.

Here the cross-border, *S. damnosum* s.l. eco-epidemiological, LULC, moderate resolution, immature habitat identification model used three scene components: (C), (G) and (T) generated from the Rapid Eye™, 5m resolution image data. The G, C, T components in the microtopographic LULC classes were estimated using Spectral Information Divergence (SID) in the ENVI, object-based classification software package.

SID is a spectral classification method that employs a divergence measure to match pixels to reference spectral. The smaller the divergence in a seasonal, hyper productive, cross-border, capture point, eco-georeferenceable, cross-border, vectored, *S. damnosum* s.l. hyperproductive, positively autocorrelated clustering, breeding foci, the more likely the pixels are similar [2]. LULC pixels representing the vector arthropod, 5m resolution, Rapid Eye™ image with a measurement greater than the specified maximum divergence threshold were not geoclassified. The endmember spectra used by SID came from the spectral libraries.

We selected one of the following: **Supervised Classification**. From the Endmember Collection dialog menu bar, we selected **Algorithm > Spectral Information Divergence**. The Classification Input File dialog



appeared. We selected an input file and performed optional spatial and spectral subsetting. We then clicked **OK**. The Endmember Collection: SID dialog appeared. From the Endmember Collection, SID dialog menu bar, we select **Import**>*spectra_source* and collected the Rapid Eye™ endmember LULC 5m spectra. In the Endmember Collection:SID dialog, we then clicked **Apply**. The Spectral Information Divergence Parameters dialog appeared. We selected the **Set Maximum Divergence Threshold** area with a **Maximum Divergence Threshold** field. This was the minimum allowable LULC variation between the endmember spectrum vector and the pixel vector. The default value was .05. A threshold that discriminates well for one pair of spectral vectors may be either too sensitive or not sensitive enough for another pair due to the similar/dissimilar nature of their probability distributions[63].

Multiple Values were entered and a different divergence to test each uncoalesced, endmember, wavelength, frequency, 5m, LULC class against its corresponding devised maximum spectral divergence. When selected, the Assign Maximum Divergence Threshold dialog appears (<http://www.harrisgeospatial.com>). We selected the LULC, cross-border, *S. damnosum* s.l., African, riverine, tributary, microtopographic, endmember, LULC class to assign a threshold value to and edit the value in the **Edit Selected Value** field. We clicked **Reset** to return to the default value. This process was repeated until the thresholds were edited. We then selected classification output.

ENVI added the resulting LULC output to the Layer Manager. The output from SID is a classified image and a set of rule images (one per endmember) (<http://www.harrisgeospatial.com>). The pixel values of the geoclassified LULCs now had a residual SID model value (i.e., the output of the equation that defined SID for a pair of spectral vectors). Lower spectral divergence measures represent better matches to decomposed, landscape, endmember spectra [8]. Areas in the DRC, endmember, grid-stratified, 5m, LULC polygon that satisfied the maximum divergence threshold criteria were carried over as classified areas in the Rapid Eye™ image.

In ENVI®, the DN of the pixel in every Rapid Eye™ waveband was viewed employing the z-profile from a spectral library. After making an atmospheric correction from the Rapid Eye™ image for the eco-epidemiological, study site DRC polygons the DN was converted into ground reflectance. A convex geometrical model was then used for endmember validation of the geo-spectrally decomposed in the polygons as in[2].

The quantitated wavelength reflectance associated with aneco-georeferenced LULCs in the DRC polygons was treated as an area-weighted sum of the fixed reflectance components (e.g., G Cand T). The sub-pixel, endmember, eco-epidemiological, geoclassifiable, endmember, LULC, spectral, wavelength, frequency components were optimally derived using the G, C, T components' classes which were initially estimated by the Rapid Eye™ image in ENVI®. For inverting the model, parts of the three spectral geoclassified LULC components were represented by (K_g) which was calculated using:

$$K_g = e^{-\pi \cdot M} [s(\theta_i) + s(\theta_v) \cdot O(\theta_i, \theta_v, \phi)] \quad (1.1)$$

$$O(\theta_i, \theta_v, \phi) = 1/\pi (s(\theta_i) + s(\theta_v)) (t - s \cdot c \cdot t \cdot c \cdot i \cdot t) \quad (1.2)$$

$$c = \frac{h |t \cdot a \theta_i - t \cdot a \theta_v \cdot \sin \phi|}{r (s(\theta_i) + s(\theta_v)) \cdot c} \quad (1.3)$$

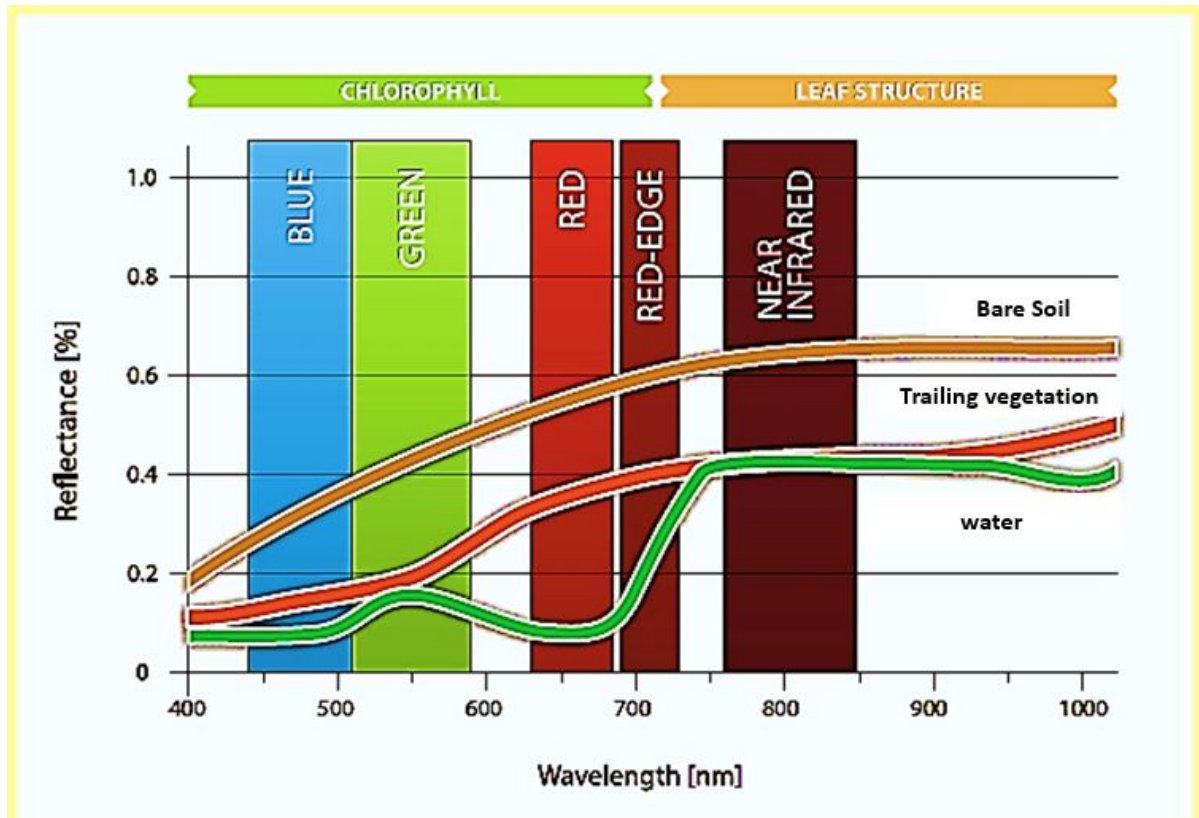
$$M = \frac{-1 (K_g)}{(s(\theta_i) + s(\theta_v)) (\pi - \epsilon t + c \cdot t \cdot s \cdot o \cdot t)} \quad (1.4)$$

$$C = 1 - e^{-\pi \cdot M} \quad (1.5)$$

where, I q u q were the zenith angles of illumination and viewing, O was the average of the overlap function between illumination and viewing shadows of the eco-georeferenceable, LULCs and its associated and

vegetational/non-vegetational orcanopied/non-canopied, 5m,endmember, eigen-decomposedLULC, components as projected onto the background. In the geometrical, optical probabilistic paradigm j was the difference in azimuth angle between illumination and viewing angles. Multiple signals were generated. An endmember signal was generated for each Rapid Eye™DRC polygon, simulated, LULC variable.

Figure 8: Spectral endmember signature of a Rapid Eye™canopied LULC signals sampled at the DRCstudy site



We used the **Options** menu in the Endmember Collection dialog to edit the LULC names, edit the endmember colors, and suppress backgrounds using BandMax in the object-based classifier. To edit endmember names, we selected **Options > Import spectrum names from ASCII**. We selected and opened the ASCII file that contained the spectrum names. The names of the Rapid Eye™ LULC 5m, spectra collected in the dialog were changed to the names from the ASCII file.

To reset the spectra to their initial names, we selected **Options > Reset spectrum names**. To assign default colors to all the geoclassified, 5m, DRC polygon uncoalesced, endmemberLULC spectra, we selected **Options > Assign default colors to all**. To assign default colors to all the undefined spectra colors (indicated by <none>), we selected **Options > Assign default colors to undefined**. To reset the geoclassified LULC spectra to their initial colors, we selected **Options > Reset colors**.

We then selected an optimal wavelength, frequency endmember, 5m, LULC subset from the input Rapid Eye™bands to differentiate the target spectra (i.e., capture point, eco-georeferenceable, cross-border, African riverine tributary ecosystem, immature, capture point, breeding foci)from the spectra of the LULC materials (backgrounds). The BandMax process isolated the 5m bands that best distinguishedthese potential selected LULC targets,this optimal spectral subset generated with BandMax increased the accuracy of the Rapid Eye™ LULC classification selected in the Endmember Collection dialog and speed processing.

We accessed BandMax in the SAM Target Finder with BandMax Wizard. We selected at least one spectrum to represent a target, eco-epidemiological, cross-border. African, riverine, eco-georeferencable, *S. damnosum* s.l., immature habitat, capture point, in the Endmember Spectra table of the Endmember Collection



dialog. From the Endmember Collection dialog menu bar, we selected **Options > BandMax Background Suppression** in the Endmember Collection dialog. The BandMax Background Suppression dialog appeared.

We employed the **Select Background** section of the dialog to collect any endmember LULC from the uncoalesced, 5m, DRC polygon spectra as backgrounds. The BandMax significance LULC values are calculated whenever a spectrum is added or deleted in the **Select Background** section (<http://www.harrisgeospatial.com/>)

We reviewed the **Significant Bands** list, which revealed the 5m, resolution, LULC bands that BandMax automatically determined were significant. We modified the **Band Significance Threshold** value as needed. The LULC threshold ranged from 0 to 1. ENVI uses only bands with a significance value greater than or equal to the significance threshold (<http://www.harrisgeospatial.com/>) in fewer selected bands in the subset. We clicked **Save Significant Bands to File**. We clicked **OK**. All the significant Rapid Eye™ 5m bands displayed in the **Significant Bands** section from the band subset was subsequently employed on the input LULC cross-border *S. damnum* s.l. African, riverine tributary, LULC capture point, breeding foci unbiased geoclassified wavelength uncoalesced estimators in the Endmember Collection dialog.

We employed the **Algorithm** menu in the Endmember Collection dialog to select a classification or advanced spectral processing method. The classification methods available are parallelepiped, minimum distance, Mahalanobis distance, maximum likelihood, SAM and binary encoding in ENVI (<http://www.harrisgeospatial.com/>). The advanced geospectral LULC processing methods we used on the eco-georeferenced, DRC, Rapid Eye™ geoclassified, LULC .polygon data included matched filtering, mixture tuned matched filtering, and spectral feature fitting.

For employing the Mahalanobis distance we imported the eigen-decomposed, Rapid Eye™ endmember, orthogonal, LULC spectra from statistic files as these classifications used endmember covariance statistics in entomological, eco-georeferencable, eco-epidemiological, unmixing, remote sensing, LULC, vector arthropod habitat, forecast, vulnerability models [2]. Henceforth, we employed a minimum of two 5m, LULC endmembers to confirm the wavelength frequency, uncoalesced, radiance measurements. From the Endmember Collection dialog menu bar, we selected **Algorithm > classification_method**. We downloaded the classification methods from the **Classification > Supervised** menu and then employed an advanced spectral processing method from the **Spectral Tools** menu. We clicked **Apply**. The Algorithm Parameters dialog appeared. We then entered the selected algorithm's required 5m LULC parameters.

2.8 Interpolation analyses: Geospectral, elucidative, linear predictors were generated from the eigen-decomposed, 5m, LULCs remotely geo

sampld within the DRC study site, eco-georeferenced polygon employing an Ordinary kriged-based interpolator. The dependent variable was the emissivity Rapid Eye™ band estimate ratio of the riverine, epidemiological, geoclassified LULC rendered from the Rapid Eye™ selected microtopographic extracted attribute pixels within each polygon. We transformed the emissivities to fulfill the diagnostic normality test prior to performing kriging. Interpolation algorithms can generate accurate autoregressive endmember endemic transmission-oriented geopredictive risk maps [7].

The unknown value $Z(x_0)$ was interpreted as a random explanatory microtopographic . geoclassified, LULC variable geolocated in (x_0) , as well as the values of neighbor's samples $(Z(x_i), i= 1, \dots, N)$ in each 5m resolution polygon. The estimator $Z(x_0)$ was also interpreted as a LULC random variable geolocated in the interpolator x_0 , as result of the linear combination of the tabulated spectral endmember LULC, predictor variables. In order to deduce the kriging system for the assumptions of the cross-border, riverine tributary, *S. damnosum* s.l. eco-epidemiological, forecast, vulnerability model, $Z(x)$ was estimated employing

$$Z(x_0) = \hat{Z}(x_0) - Z(x_0) - [W^T - 1][Z(x_1) \dots Z(x_N) Z(x_0)]^T - \sum_{i=1}^N w_i(x_0) \times Z(x_i) - Z(x_0)$$

The quality criteria was then expressed in terms of the mean and variance of the new random variable $\epsilon(x_0)$. In the crossborder, *S. damnosum* s.l. African, riverine tributary, forecast, vulnerability, immature habitat identification model. Since the random function was stationary, [i.e., $E(Z(x_i)) - E(Z(x_0)) - m$], the following constraint was observed:

$$E(\epsilon(x_0)) = 0 \Leftrightarrow \sum_{i=1}^N w_i(x_0) \times E(Z(x_i)) - E(Z(x_0)) - 0 \Leftrightarrow m \sum_{i=1}^N w_i(x_0) - m = 0 \Leftrightarrow \sum_{i=1}^N w_i(x_0) - 1 \Leftrightarrow 1^T W - 1$$



The variance of the *S. damnosums*.l. model was then minimized employing $2 \times 0 \text{ ()} \in Ex$. The 5m, explanatory endmember LULC estimators had $0 \text{ ()} \in x$, but the dispersion around their mean determined the difference between the quality of the Rapid Eye™ geoclassified estimators. The entomological, eco-georeferenceable, vector, arthropod, immature habitat, eco-epidemiological model rendered the following:

$$Var(\epsilon(x_0)) = Var([W^T - 1] \cdot [Z(x_1) \dots Z(x_N) Z(x_0)]^T) = [W^T - 1] \cdot Var([Z(x_1) \dots Z(x_N) Z(x_0)]^T) \cdot [W^T - 1] \quad \text{and}$$

$$Var(\epsilon(x_0)) = [W^T - 1] \cdot \begin{bmatrix} Var_{x_1} & Cov_{x_1, x_0} \\ Cov_{x_1, x_0}^T & Var_{x_0} \end{bmatrix} \cdot [W^T - 1] \quad \text{where the literals } \{Var_{x_1}, Var_{x_0}, Cov_{x_1, x_0}\} \text{ represented}$$

$$\{Var([Z(x_1) \dots Z(x_N)]^T), Var(Z(x_0)), Cov([Z(x_1) \dots Z(x_N)]^T, Z(x_0))\}$$

$\gamma(h)$ (i.e., variogram) was defined in the cross-border, *S. damnosums*.l. model during the analysis of $Z(x)$. An expression was written for quantiating the estimation variance of the uncoalesced, canopy, shaded, blue-green, algae, LULC estimator using the function of the covariance between the samples and the covariances to estimate:

$$\begin{cases} Var(\epsilon(x_0)) - W^T \cdot Var_{x_1} \cdot W - Cov_{x_1, x_0}^T \cdot W - W^T \cdot Cov_{x_1, x_0} + Var_{x_0} \\ Var(\epsilon(x_0)) - Cov(0) + \sum_i \sum_j w_i w_j Cov(x_i, x_j) - 2 \sum_i w_i C(x_i, x_0) \end{cases} \quad \text{which then iteratively minimized}$$

$$W^T \cdot Var_{x_1} \cdot W - Cov_{x_1, x_0}^T \cdot W - W^T \cdot Cov_{x_1, x_0} + Var_{x_0} \quad \text{into} \quad \begin{bmatrix} \mu \\ \mu \end{bmatrix} - \begin{bmatrix} Var_{x_1} & 1 \\ 1^T & 0 \end{bmatrix} \cdot \begin{bmatrix} Cov_{x_1, x_0} \\ 1 \end{bmatrix} - \begin{bmatrix} \gamma(x_1, x_1) & \dots & \gamma(x_1, x_n) & 1 \\ \vdots & \ddots & \vdots & \vdots \\ \gamma(x_n, x_1) & \dots & \gamma(x_n, x_n) & 1 \\ 1 & \dots & 1 & 0 \end{bmatrix}^{-1} \cdot \begin{bmatrix} \gamma(x_1, x^*) \\ \vdots \\ \gamma(x_n, x^*) \\ 1 \end{bmatrix} \quad \text{where the}$$

additional parameter μ was a Lagrange multiplier employed in the minimization of the kriging error $2 \text{ ()} \sigma$ to honor the unbiasedness condition. Finally, the estimation and error by Ordinary kriging was given by:

$$\hat{Z}(x_0) - W^T \cdot [Z(x_1) \dots Z(x_N)]^T : \gamma(\hat{Z}(x_0) - Z(x_0)) - W^T \cdot [\gamma(x_1, x_0) \dots \gamma(x_N, x_0)]^T$$

Additionally, we tested the cross border, riverine tributary, *S. damnosums*.l., eco-epidemiological, residual, LULC, signature model forecasts with that of current unmixing algorithms commonly applied for canopy-oriented, LULC, eigendecomposed, Chl-a endmember signature generation. This unmixing algorithm was based was on the following linear mixing model:

$$R_k = \sum_i^n a_i \cdot E_{i,k} + \epsilon_k \quad RMSE = \sqrt{\left(\sum_k^m \epsilon_k^2 \right)^{-m}}$$

R_k Reflectance of source at wavelength k
 $E_{i,k}$ Reflectance of endmember i at wavelength k
 a_i Abundance of endmember i
 ϵ_k Error at wavelength k
 $RMSE$ Root Mean square error of the ϵ_k
 n Number of endmembers
 m Number of wavelengths in the discrete spectrum

This model assumed that spectrum was a linear superposition of the geoclassified shaded canopy-related, LULC, 5m endmembers. The landscape abundances were computed using two standards the algorithm assumed that wavelengths were given in nanometers (i.e., BEAM's default wavelength unit). The spectral unmixing tool was invoked from VISAT's tool menu by selecting the Unmix command and by using the command line tool gpt (Graph Processing Tool) found in BEAM's bin directory in batch mode. The differential form of the equation for the standard spectral unmixing, forecast, vulnerability, sub-pixel, *S. damnosums*.l., crossborder, eco-georeferenceable, immature habitat, capture point, eco-epidemiological, iteratively qualitatively iteratively interpolated, LULC model was:



$$\frac{1}{c} \frac{\partial}{\partial t} I_v + \hat{\Omega} \cdot \nabla I_v + (k_{v,s} + k_{v,a}) I_v = j_v + \frac{1}{4\pi c} k_{v,s} \int_{\Omega} I_v d\Omega$$

where j_v was the canopy, shaded, emission coefficient, $k_{v,s}$ was the scattering cross section, and $k_{v,a}$ was the absorption cross section. We noticed that in the model the LULC differences were essentially due to the various forms for the canopy-related emission and absorption coefficients. The emission coefficient and absorption coefficient are functions of temperature and

density and are related by: $\frac{j_v}{\hat{\Omega}} = B_v(T)$ where is the black body spectral radiance at temperature T [8]. The

$$I_v(z) = I_v(z_0) e^{-\tau_v(z_0, z)} + \int_{z_0}^z B_v(T(z')) e^{-\tau_v(z', z)} dz'$$

solution to the equation of the predictive radiative transfer was then:

We employed the Eddington approximation for inserting the LULC endmembercovariates into the cross-border, *S. damnosum* s.l., riverine, tributary, Rapid EyeTM, LULC, immature, breeding foci, eco-georeferenceable, habitat model. The Eddington approximation is a special case of the two-stream approximation commonly applied in spectral unmixing algorithms [8]. The approximation assumed that the intensity in the eco-georefernced, canopied, riverine, LULC was a linear function of $\mu = \cos\theta$. (i.e. $I_v(\mu, z) = a(z) + \mu b(z)$) where z was the normal direction to the medium.

Geopatial, explanative, linear predictors were generated from the canopy, unshaded, LULCs and the riffled, eco-geohydrological components using an ordinary kriged-based, endmember interpolator and the eigen-orthogonal decomposed Rapid EyeTM data. The dependent variable was the spectral emissivity estimates generated from the decomposition of the Rapid EyeTM pixel(i.e., endmember target cross-border, *S. damnosum* s.l. LULC signature) which was transformed to fulfill the diagnostic normality test prior to performing kriging in Spatial AnalystTM the kriged-based algorithm was then employedto generate predictive, autoregressive, risk maps. Ordinary kriging was selected to interpolate the value $Z(x_0)$, the LULC and riffle water components, Z(x), at an unobserved geolocation x0 from the field and remote-sampled, endmember, RGB signature covariate coefficient estimates and $z_i = Z(x_i)$, i=1..., n at the riverintributarygeolocations at the DRC epidemiological study site polygons, x1, xn. Ordinary kriging was computed as a linear unbiased estimator, $\hat{Z}(x_0)$ of $Z(x_0)$, based on a stochastic model of the dependence quantitated by a variogram (x,y) and by the expectation (x)=E[Z(x)] and the covariance function c(x,y) of a random field. The kriging estimator was given by a linear combination of the algorithm in Spatial AnalystTM employing theuncoalesced, spectral LULC endmember, Rapid EyeTM dataset of $z_i = Z(x_i)$ with weights $w_i(x_0)$, i=1, n chosen such that the variance in the geospectral, autoregressive, predictive, risk, spectral wavelength 5m, uncoalesced, habitatidentification model was optimallycalculated. The interpolation in the model was spatially adjusted using multiple unmixing algorithms and the ENVI classifiers.

Most statistical tests rely upon certain assumptions about geoclassified, georeferenced, LULC variables used in an endmember analysis[8]. When these assumptionsare not met the results may not be trustworthy, resulting in a Type I or Type II error, or over- or under-estimation of significance or effect size(s) in a moderate resolution, endmember, LULC, *S. damnosum* s.l., immature habitat, eco-epidemiological, forecast, vulnerability model. In statistical hypothesis testing, a **type I error** is the incorrect rejection of a true null hypothesis (a "false positive"), while a **type II error** is incorrectly retaining a false null hypothesis (a "false negative")[64]. However, as[65] observe, few articles report having tested assumptions of entomological, endmember, vector, arthropod-related statistical tests they rely on for drawing their conclusions. Since several assumptions of multiple endmember regression are "robust" to violation (e.g., normal distribution of errors), and others arefulfilled in the proper design of a study (e.g., independence of observations), we focused on the assumptionsof multiple regression that were not robust to violation, and that onchocerciasis researchers or epidemiologists could deal with if violated in their remote, endmember, LUL, signature, interpolation experiments. Specifically, we checked the assumptions of linearity, reliability of measurement, homoscedasticity, and normality in the crossborder, *S. damnosum* s.l. riverine tributary, 5m habitat, capture point, eco-epidemiological, eco-georeferenceable, forecast, vulnerability model.

We accessed Spatial Analyst functionality, including tools, operators, functions, and classes, to import the Rapid EyeTM 5m, endmember, spectral wavelength frequency LULC data from the sa module. Using this import method, it was possible to access Spatial Analyst functionality in ArcGIS without providing a name space and imports overloaded operator, which allowed the DRC polygonised 5m raster's to beemployed with the operators in the scripting module. The sequence of imports to utilize Spatial Analyst functionality waswritten in ArcPy as:



```
Import arcpy
from arcpy import env
from arcpy.sa import *
```

This approach allowed us to

- 1) Set and get environment settings prefixed simply with **env using**.

```
env.workspace = "c:/base/DRC data.gdb"
```

We ran the geoprocessing tools and functionality directly from **arcpy** employing the statement:

```
arcpy.Buffer_DRC 5m polygon LULC analysis ("in features", "out buffer",
```

We employed Map Algebra without having to prefix every DRC polygon, geoclassified LULC, Rapid Eye™ class with **arcpy.sa** and then wrote

- 2) `outRas = Sin("inraster1") + Raster("inraster2") + 8`

Geoprocessing tools and functions (such as Sin, Slope, and Reclassify) were used in procuring the Map Algebra expressions to further extract vital endmember LULC statistics for each DRC grid-stratified, 5m polygon. Map Algebra within Python is composed of tools, operators, functions, and classes (www.esri.com). For example, to calculate the aspect for each cell in the 5m, raster dataset of orthogonal eigen-decomposed, polygonised, geoclassified, endmember LULC, Rapid Eye™ spectral wavelength, frequency, geoclassified data we employed the Aspect tool which was written as:

```
outRas = Aspect("C:/Datat/inraster")
```

Operators are symbols used to represent mathematical operations to be applied to the input (www.esri.com). The following statement was employed to add any two LULC rasters together derived from each Rapid Eye™ 5m, DRC polygon:

```
outRas = Raster("inraster1") + Raster("inraster2")
```

We could determine the total geoclassified, spectral wavelength, endmember LULC data in each polygon precisely. Casting the raster LULC data layers for each DRC polygon indicated that the operation could be applied to rasters, thus calling the Spatial Analyst implementation of the operator to optimally geospectrally quantitate the geoclassified LULCs resulting in an output raster object dataset. The input elements, such as the tabulated rasters, features, numbers, constants, objects, and regression variables in each DRC Rapid Eye™ polygon LULC components was optimally determined based on the statement written as:

```
outRas = Sin ("in raster")
```

We employed the statement to apply the sine calculation to each endmember LULC cell in the input raster. The output from a Map Algebra expression was a **Raster** object referencing temporary raster LULC data from each Rapid Eye™ 5m, grid-stratified polygon. We stored the results from the slope calculations from the DRC polygons as a **Raster** object named outRas:



```
outRas = Slope("inraster")
```

In Python we checked **out** a Spatial Analyst license before running the tool. We employed the statements:

```
# Check out the ArcGIS Spatial Analyst  
# extension license  
arcpy.CheckoutExtension("Spatial")
```

A dataset of ecogeoreferenceable, eco-epidemiological, cross-border, *S. damnosum* s.l. habitat LULCV signature covariates were constructed in ArcGIS using the python workflow which was written as:

Name: ThiessenPolygons.py

Description: Creates Thiessen based trade areas around selected riverine tributary LULCs

Author: Jacob

```
# Import system modules
```

```
import arcpy
```

```
arcpy.AddToolbox("C:\Program Files (x86)\ArcGIS\Desktop10.3\Business  
Analyst\ArcToolbox\Toolboxes\Business Analyst Tools.tbx")
```

```
# Acquire extension license
```

```
arcpy.CheckOutExtension("Business")
```

```
# input and output S. damnosum s.l. LULC parameters for the Thiessen Polygons tool
```

```
StorePath = "C:/temp/sf_stores.shp"
```

```
IdFld = "STORE_ID"
```

```
OutPath = "C:/temp/ThiessenPolygons.shp"
```

```
# Create Thiessen Polygon based trade areas
```

```
arcpy.ThiessenPolygons_ba(StorePath, IdFld, "ALL", OutPath)
```

```
# Release extension license
```

```
arcpy.CheckInExtension("Business")
```

```
except:
```

```
print arcpy.GetMessages(2)
```

The Boolean model for a random subset of the plane or higher dimensions, analogously is a common tractable model in stochastic geometry [8]. ArcMap performed a Boolean and operation on the eigendecomposed, endmember, geoclassified, endmember LULC 5m, uncoalesced cell values of two input rasters. If both input values are true (non-zero), the output value is 1. If one or both inputs are false (zero), the output is 0 [8].

We performed a Boolean and operation on two grid- stratified rasterized 5m, Rapid Eye TM LULC outputs in arcpy which was written as:

```
import arcpy
```

```
from arcpy import env
```

```
from arcpy.sa import *
```

```
env.workspace = "C:/cross-border S. damnosum s.l. id habitat model data"
```

```
outBooleanAnd = BooleanAnd("degs", "negs")
```

```
outBooleanAnd.save("C:/LULC /output/outbooland.img")
```



We then performed a Boolean And operation on two the geoclassified, geocalssified endmember microtopographic LULC signature grid rastersemploying :

```
# Name: BooleanAnd_Ex_02.py
# Description: Perform a Boolean operation on the 5m LULC cell values
#           of two input rasters

# Import system modules
import arcpy
from arcpy import env
from arcpy.sa import *

# Set environment settings
env.workspace = "C:/LULC /data"

# Set local variables
inRaster1 = "degs"
inRaster2 = "negs"

# Check out the ArcGIS Spatial Analyst extension license
arcpy.CheckOutExtension("Spatial")

# Execute BooleanAnd
outBooleanAnd = BooleanAnd(inRaster1, inRaster2)

# Save the output
outBooleanAnd.save("C:/cross-border, S. damnosum s.l. habitat id model /output/outbooland")
```

The Python window recognized the system environment variable **PYTHONSTARTUP**. If **PYTHONSTARTUP** has been previously set to a Python file, Python will automatically execute that file's code when the Python window is opened (<https://www.python.org>). The integrity of the endmember 5m, LULC geospatial analyses of the DRC Rapid Eye TM polygons was ensured since the Python window experience started with usage of the preloaded geoclassifieddata. Python utilities was written initially as # File: **pythonstartup.py**. This descriptive statement was employed to customize the state of the Python environment for optimally conducting theendmember 5m, endmember, LULC signature analyses on the DRC polygons. We specified module imports to a Spatial Analyst extension employing:

```
print "%s\n%s\n%s" %("import os, sys, string","importarcpy", "from arcpy.sa import *")

# Imports
importos, sys, string
importarcpy
fromarcpy import env
from arcpy.sa import *
```

In the **PYTHONSTARTUP** environment,initially we right-clicked**My Computer** and clicked**Properties**.We clicked the**Advanced tab**for quantitating the endmember 5m, African riverine tributary, cross border, *S. damnosum* s.l. microtopographic, spectral wavelength frequency, LULC variables. Under System variables, we clicked**New**. We added**PYTHONSTARTUP** to Variable name (i.e., Rapid Eye TM DRC geoclassified LULC signatures). We added the path of the Python file to **Variable value**and clicked**OK**.

We performed an invasive endmember, spectral wavelength frequency, LULC analyses on the Rapid Eye TM5mpolygon through a Tool dialog box in Python employing an interactive command line interface. Traditional operations and workflows for eco-georeferencable, geo-Spectro temporal, wavelength , frequency, LULC riskmapping with moderate resolution satellite data employMap Algebra in a Python



environment(www.python.org)Here we employed Map Algebra through the Spatial Analyst module; an extension of the ArcPy Python site package.

Like all languages, Map Algebra has specific rules for combining the language components. Here, the general structure of a Map Algebra statement was an assignment operator (=), which we employed to separate the action to its right from the name of the output (a raster DRC, geoclassified, Rapid Eye™ 5m, geospatial, polygonized, endmember, geoclassified, LULC object). A statement was generated employing algebraic form syntax of Map Algebra which was written as:

```
Output Name = Action
```

We also employed a Raster Calculator available for entering simple Map Algebra expressions that generated an output LULC raster layer for the 5m, DRC polygons.

Raster calculator builds and executes a single Map Algebra expression using Python syntax in a calculator-like interface (www.esri.com). The Raster Calculator tool allowed us to create and execute a Map Algebra expression that output a Rapid Eye™ 5m, raster layer with numerical, geoclassifiable, endmember LULC values. Mathematical operators were added to the expression by clicking the respective buttons in the tool dialog box. A list of commonly used conditional and mathematical tools was provided in the database, allowing us to easily add them to the eco-cartographic, cross border, African, riverine, tributary, *S. damnosum* s.l. capture point, eco-georeferenced, eco-epidemiological, uncoalesced, LULC datasets. Full paths to the LULC data in each polygon was specified thereafter in a workspace environment which was entered by quotes (""). Numbers and scalars were directly entered by the expression.

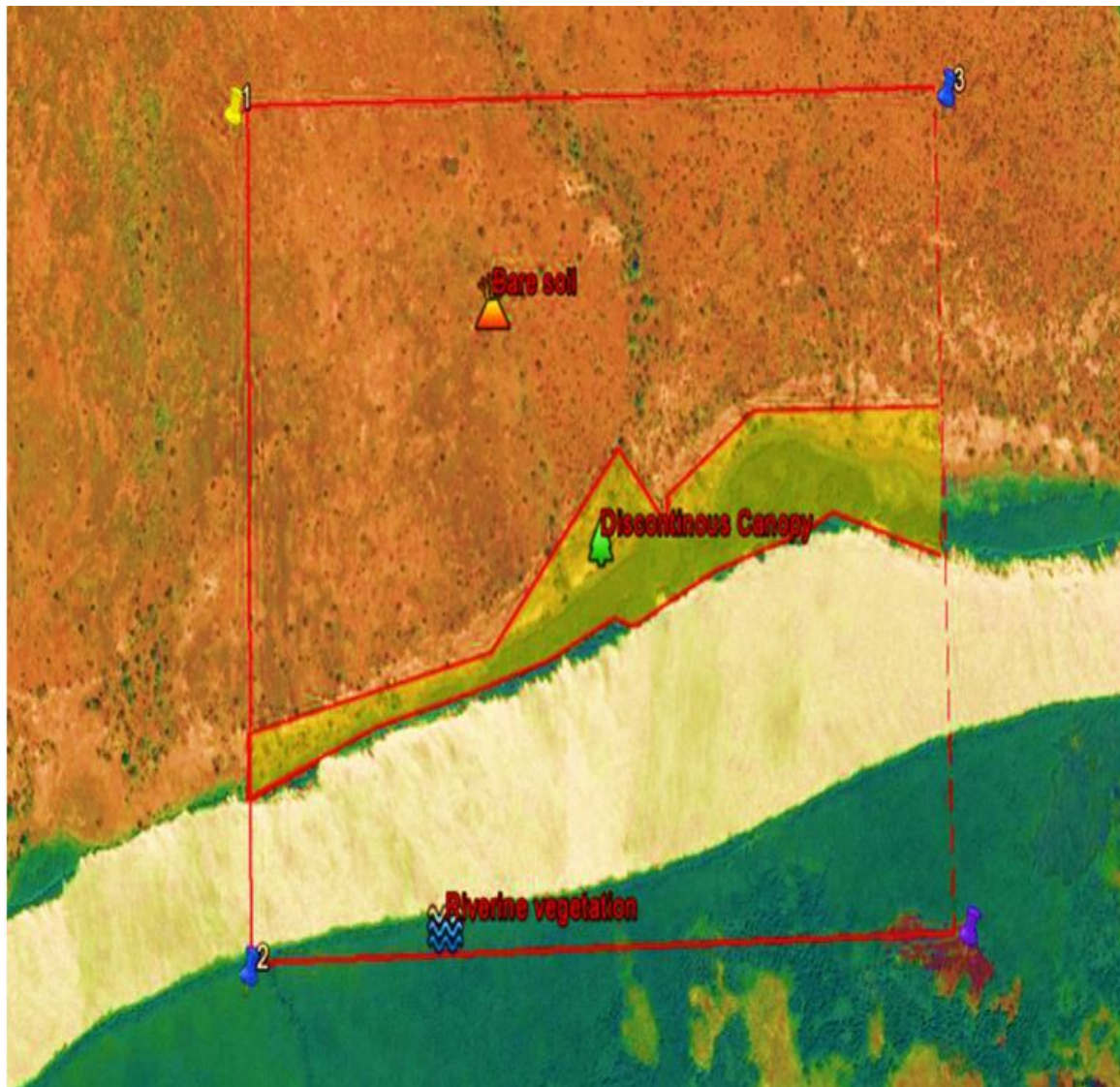
Spatial Analyst™ tools were accessed through an algebraic format. That is, an endmember explanatory LULC object whose name was identified to the left of an equal sign was created based on a tool or operator stated to the right of the equal sign. A statement calculated the slope for each cell in the indem dataset and created a raster object called outRas to store the LULC results

```
from arcpy.sa import *  
outRas = Slope("indem")
```

3. Results

The ArcGIS Spatial Analyst™ extension provided a rich set of spatial analysis and modeling tools for generating both raster (cell-based) and feature (vector), 5m, LULC data employing the Rapid Eye™ spectral bands in each geoclassified, DRC polygon. In the Spatial Analyst toolbox we could generate three LULC classes including: 1) bare soil, 2) water and 3) uncanopied trailing vegetation

Figure 9: Rapid Eye TM, LULC geoclassifications used for immature habitat identification in a DRC 5m polygon



We performed a PCA on a set of geoclassified LULC 5m raster bands and generated a single multiband raster as output. The value specified for the number of principal components determines the number of principal component LULC bands in the output multiband raster in Spatial Analyst™.

The raster bands did common intersection. If there is no intersection, in a regression decomposition exercise an error occurred and no output is created[8]. Within the output data file name specified, the correlation and covariance matrices, and the eigenvalues and eigenvectors, as well as the percent variance of each eigenvalue LULC was captured, and the accumulative variance described, was stored in an ASCII file.

The percent variance of each 5m geoclassified LULC identified the amount of the variance each eigenvalue captures. This was useful to help interpret the results of PCA in each DRC grid-stratified 5m polygon. If a few eigenvalues (each corresponding to bands in the output raster) capture the majority of the variance, then it may be adequate to use this subset of bands in a subsequent analysis since they may capture the majority of the interactions within the original multiband dataset[6].

When determining the percent variance each eigenvalue captures, the sum of eigenvalues as entered the following formula: $(\text{eigenvalue} * 100) / \text{Sum}$ in Spatial Analyst™. The first eigenvalue (and its associated band) captured the greatest variance, and the subsequent eigenvalues captured sequentially lesser variance. The



accumulative percent of variance was a sequential sum of the variance each, 5m LULC geoclassified *S. damnosum*.s.l., cross-border, African riverine, tributary, decomposed, eigenvalue captured. If the input is a layer created from a multiband raster with more than three bands, the operation will consider all the bands associated with the source dataset, not just the three bands that were loaded (symbolized) by the layer [6].

There are several ways to specify a subset of moderate resolution bands from a multiband raster to use as input into the tool (www.esri.com). We employed the tool dialog box and navigated to the multiband raster using the browse button next to **Input raster bands**. We opened the raster, and select the desired Rapid Eye bands.

Since the multiband raster was a layer in the Table of Contents, we used the **Make Raster Layer** tool to create a new multiband 5m layer containing only the desired bands. We created a new dataset that contained only the desired bands with Composite Bands and uses the resulting dataset as input to the tool. In Python, the desired LULC, cross-border *S. damnosum* s.l. capture point signature LULC 5m bands were directly specified in the tool parameter as a list. We performed the PCA on an input multiband 5m LULC raster and generates a multiband raster output employing

```
import arcpy
from arcpy import env
from arcpy.sa import *
env.workspace = "C:/sapy cross-border, S.damnsum s.l. 5m LULCdata"
outPrincipalComp = Principal Components(["African riverine tributary"], 4,"pcdata.txt")
outPrincipalComp.save
```

The image endmembers of the georeferenced *S. damnosum* s.l. habitat and its associated environmental attributes were extracted them from ENVI[®]'s spectral library. Several spectra corresponding to the different backgrounds in the sampled *S. damnosum* s.l. habitat (i.e., Precambrian rock and spectral rippled water pixel components) had to be included, since multiple diffuse scatterings between floating leaves in the habitat, for example, and a bright soil background increased the Quick Bird NIR reflectance. Leaf cells have evolved to scatter (i.e., reflect and transmit) solar radiation in the NIR spectral region[66]. After the calibration of the explanatory predictor covariate coefficient had been performed the image was converted to match the contents of the ENVI library. Analogously, the Quick Bird reference endmembers spectra in the library was transformed into the endmembers spectra of the image data. In this research, we used a random selection of pixels to assess the satellite classification accuracy. Quick Bird class representative pixels were selected and compared to a reference training dataset. During the segmentation procedure, image objects were generated based on several adjustable criteria of homogeneity such as colour, shape, and texture. Data pre-processing involved converting Digital Number(DN) values to radiance atmospheric correction using FLAASH[™], and co-registration techniques. Image classification was done using the object-oriented approach. FLAASH[™] generated a model (.gmd file) that converted the image's DN to at-sensor radiance and computed at-sensor reflectance while normalizing the solar elevation angle. The equation was as follows:

$$\rho_B = \frac{\pi(L_B - E_B) \cos \theta}{E_B (C_n - \cos \theta) \cos \theta} \frac{G_{n B d} \sin \theta}{(C_n - \cos \theta) \cos \theta} \frac{a_{B n B i d} \sin \theta}{(C_n - \cos \theta) \cos \theta} \frac{D_n^2}{(C_n - \cos \theta) \cos \theta}$$

where,

- ρ_{BandN} = Reflectance for Band N
- L_{bandN} = Digital Number for Band N
- D = Normalized Earth-Sun Distance
- E_{bandN} = Solar Irradiance for Band N

The reference data in this research was “ground truth” data of the spatiotemporal-sampled *S.damnsum* s.l. habitat predictor covariate coefficients. Selected random pixels from the thematic map were compared to the



reference data. The estimated accuracy for the spectrally extracted data was calculated:

$$P\left\{-z_{\frac{\alpha}{2}} < \frac{x-n\theta}{\sqrt{n\theta(1-\theta)}} < z_{\frac{\alpha}{2}}\right\} = 1-\alpha$$

where, x = number of correct identified pixels, n = total number of pixels in the sample, θ = the map accuracy, $(1-\alpha)$ = a confidence limit. The QuickBird classifier identified *S. damnosum s.l.* habitats and their associated Precambrian rock and ripple water larger than 0.4 ha with generally satisfactory results (92.1%) with a lower detection limit of 0.1 ha.

The NLP procedure (NonLinear Programming) offered a set of optimization techniques for minimizing or maximizing a continuous nonlinear function $f(x)$ of n (i.e., geoclassified microtopographic LULC variables), $x = (x_1, \dots, x_n)^T$ with lower and upper bound, linear and nonlinear, equality and inequality cross-border, *S. damnosum s.l.*, eco-epidemiological, capture point, breeding foci, uncoalesced, LULC 5m border constraints. This was expressed by solving

$$\begin{aligned} & \min_{x \in \mathbb{R}^n} f(x) \\ \text{subject to} & \quad c_i(x) = 0 \quad i = 1, \dots, m_e \\ & \quad c_i(x) \geq 0 \quad i = m_e + 1, \dots, m \\ & \quad u_i \geq x_i \geq l_i \quad i = 1, \dots, n \end{aligned}$$

where f was the objective function, c_i 's were the constraint functions, and u_i, l_i 's were the upper and lower bounds. The NLP procedure provides a number of algorithms for solving the special 5m, geoclassified bare soil, uncanopied, trailing vegetation and water, geoclassified, LULCs exact locations and number of pixels, based on the objective function. We solve the quadratic programming problem:

$$\begin{aligned} f(x) &= \frac{1}{2}x^T Gx + g^T x + b \\ \text{subject to} & \quad c_i(x) = 0 \quad i = 1, \dots, m_e \end{aligned}$$

where the $c_i(x)$'s were linear LULC, 5m, cross-border, *S. damnosum s.l.*, immature habitat, capture point LULC functions; $g = (g_1, \dots, g_n)^T$ and $b = (b_1, \dots, b_n)^T$ were vectors; and G was an $n \times n$ symmetric matrix. We assumed least-squares hence:

$$\begin{aligned} f(x) &= \frac{1}{2}\{f_1^2(x) + \dots + f_m^2(x)\} \\ \text{subject to} & \quad c_i(x) = 0 \quad i = 1, \dots, m_e \end{aligned}$$

where the $c_i(x)$'s were linear functions, and $f_1(x), \dots, f_m(x)$ were nonlinear 5m cross-border, African riverine tributary, Rapid Eye™ LULC geoclassified functions of x .

We then employed a first-order ODE $\frac{dy}{dx} = F(x, y)$, in ArcPy for optimally quantitating the microtopographic LULC spectral variables in each grid-stratified, Rapid Eye™, DRC polygon employing $F(x, y)$ which was expressed employing measurable wavelength separation of the 5m Rapid Eye™ spectral frequency data by $F(x, y) = X(x)Y(y)$. A ODE was written in the form $dy dt = f(t, y)$ where t was the field and remote, sampled, capture point breeding foci independent LULC variables and y was a



function of t . The solution to the cross-border, *S. damnosum* s.l., predictive risk model equation was a function $y = g(t)$ such that $dg/dt = f(t, g)$, and the solution contained one arbitrary constant.

Thereafter, the endmember 5m, LULC signature equation was expressed as $\frac{dy}{Y(y)} = X(x) dx$. The equation was solved by integrating both sides to obtain $\int \frac{dy}{Y(y)} = \int X(x) dx$. Any first-order ODE of the form $\frac{dy}{dx} + p(x)y = q(x)$ can be solved by finding an integrating factor $\mu = \mu(x)$ such that $\frac{d}{dx}(\mu y) = \mu \frac{dy}{dx} + y \frac{d\mu}{dx} = \mu q(x)$. [67].

$$\frac{1}{y} \frac{dy}{dx} + \frac{1}{\mu} \frac{d\mu}{dx} = \frac{q(x)}{y}$$

Dividing through by μy in ArcPy yielded [3.1] in each polygon. This condition enabled explicitly determining the appropriate μ for arbitrary P and Q in the, eco-epidemiological, eco-georeferencable, African, riverine, tributary, LULC, 5m, *S. damnosum* s.l. geoclassified, forecast, vulnerability cross-border, analyses. To accomplish this parsimoniously, we also employed $p(x) = \frac{1}{\mu} \frac{d\mu}{dx}$ in the equation [3.1], from which we recovered from the original equation (\diamond), which was then transformed into

the form $\frac{1}{y} \frac{dy}{dx} + p(x) = \frac{q(x)}{y}$ for the geoclassified, grid-stratified polygon, endmember LULC analyses. We integrated the Rapid EyeTM 5m, DRC forecast, vulnerability, immature habitat identification models with $\int p(x) dx = \int \frac{d\mu}{\mu} = \ln \mu + c$ $\mu = e^{\int p(x) dx}$. Now integrating both sides of (\diamond) in the LULC models rendered

$\mu y = \int \mu q(x) dx + c$ with μ as a known function, which we solved for y to obtain $y = \frac{\int \mu q(x) dx + c}{\mu} = \frac{\int e^{\int p(x') dx'} q(x) dx + c}{e^{\int p(x') dx'}}$, for each 5m grid-stratified polygon where c was an arbitrary constant of integration.

Given an n th-order linear ODE with constant geoclassified, Rapid EyeTM grid-stratified, endmember spectral wavelength frequency measurements, $\frac{d^n y}{dx^n} + a_{n-1} \frac{d^{n-1} y}{dx^{n-1}} + \dots + a_1 \frac{dy}{dx} + a_0 y = Q(x)$, was able to quantitate the microtopographic LULC, characteristics in each polygon by writing $y \equiv e^{rx}$ and setting $Q(x) = 0$ which subsequently rendered the n (i.e., complex roots of each LULC). Then $r^n e^{rx} + a_{n-1} r^{n-1} e^{rx} + \dots + a_1 r e^{rx} + a_0 e^{rx} = 0$ and $r^n + a_{n-1} r^{n-1} + \dots + a_1 r + a_0 = 0$. was determined in each polygon. Factoring of the LULC, 5m resolution, black fly, immature eco-epidemiological, forecast, vulnerability endmember, immature habitat identification differential equations revealed the roots r_i , $(r - r_1)(r - r_2) \dots (r - r_n) = 0$. For a non-repeated real root r , the corresponding solution was $y = e^{rx}$ in each 5m, DRC, grid-stratified polygon. If a real root r is repeated k times, the solutions are degenerate and the linearly independent solutions are $y = e^{rx}, y = x e^{rx}, \dots, y = x^{k-1} e^{rx}$ [17]. For non-repeated complex roots in the *S. damnosum* s.l. cross-border, LULC, eco-epidemiological, uncoalesced, spectral wavelength frequency, immature habitat identification 5m model the solutions were $y = e^{ax} \cos(bx), y = e^{ax} \sin(bx)$.

We employed Spatial Analyst(arcgpy.sa) which is a module of the ArcPy site package. ArcPy is a site package that builds on (and is a successor to) the successful arcgisscripting module (<http://help.arcgis.com/en/arcgisdesktop/10.0/help/index.html>). The goal was to perform an indepth, eco-geographic, remotely sensed, eco-epidemiological, immature, geoclassifiable, LULC, surface trend, data analysis



with map automation within Python for optimally quantitating the exactwavelength spectral, frequency values of each geoclassified microtopographic, LULC frequency in the 5m, DRC, grid-stratified, spatial, resolution polygons. The additional power of using ArcPy within Python is the fact that Python is a general-purpose programming language (<https://www.python.org>).

The ArcPypackage provided a rich and native Python experience and offered a code completion for optimally quantitating the geoclassified LULCs in the DRC, Rapid Eye™, 5m polygons. We typed a keyword (i.e., “polygon, 5m, DRC, stratified, gridded, LULC”) and a dot to get a pop-up list of properties and methods supported by that keywordwhich was subsequently revealed. Documentation for each function, module, and class was then generated for each DRC polygon.

Subsequently, multiple-layer, scattering models were constructed in Spatial Analyst™to mathematically, estimate the LULC canopy radiation penetration through discontinuous gaps in the DRC, riverine tributary, cross border, geoclassified, 5mgrid-stratified datasets. We mmeasured the Rapid Eye™endmember LULC composite spectra, representing various mixtures of trailing, discontinuous, canopy vegetation with different soil backgrounds which were compared with measures of greenness, including the NIR-red band ratios, the perpendicular vegetation index (PVI), and the greenness vegetation index (GVI), initially. Observed spectral wavelength, uncoalesced, African, riverine tributary, endmember LULC, patterns involving constant vegetation amounts with different soil backgrounds could not be explained nor predicted by either the ratio or the orthogonal greenness measures. All greenness measures were found to be strongly dependent on soil brightness. Furthermore, soil-induced greenness changes became greater with increasing amounts of vegetation up to 60% green cover in each polygon. The results suggest that soil and plant spectra interactively mixed in a nonadditive, partly correlated manner to produce composite LULC trailing vegetation, canopy spectra.

The Spatial Analyst™models could simulate multiple scattering, microtopographic reflectance LULC processes that occurred amongst different non-continuous, canopy geoclassified LULClayers along the riverine tributaries in the Rapid Eye™ polygons. The vertical distributions of upward, downward, and reflected, 5m radiation within the discontinuously canopied, riverine ecosystem, cross-border, endmember, LULC tributaries as well as the magnitude of sub-canopy radiation that penetrated to the soil surface was tabulated. Stoichiometricallyoptimally quantitated, endmember LULC 5m spectral wavelength, frequency estimatesbased on an uncoalesced, 5m wavelength dataset of shade-vegetated, geo-spectrally extracted riverine, tributary, canopy samples revealed no capture point, black-fly immature habitats in either LULC polygon.

Since soil-line vegetation indices employs the information of soil line in NIR-Red reflectance to reduce the effect of the soil on canopy reflectance[68], aSAVIand NDVI signatures was generated in ArcGIS from the Rapid Eye™ 5m LULC data for optimally targeting, intermittently vegetated, discontinuous, cross-border, capture point, eco-epidemiological, capture point, *S. damnosum* s.l., seasonal, uncanopied and partially canopied, trailing vegetation, eco-georeferenceable, larval habitats. An oviposition, endemic foci, capture point, endmember5m signalwas then iteratively qualitatively interpolated along multiple riverine tributaries in the DRC grid-stratified polygons. By developing new spectral indices in ArcGIS, the effect of differences in endmemberLULC reflectance did not identify any unknown, un-sampled, *S. damnosum* s.l., riverine, agro-village, tributary, endemic foci in the, grid-stratified polygons.

Using the ArcGIS cyberenvironment framework, all thepossible *S. damnosum* s.l. endmember, immature habitat, capturepoint, 5m, signature data LULC points based on Rapid Eye™grid-stratified, spectral wavelength, endmeber 5m,data encompassing LULC components were examined in n -dimensional space in ENVI. Endmembers present in the scene were found at the vertices of the simplex. The interior space of the simplex represented feasible mixtures. The task of finding orthogonal synthetic, endmembers associated to ahyper productive, seasonal, cross-border,African, riverine, tributary, *S. damnsoum* s.l. immature habitat, breeding foci (e.g., the Precambrian rock with ripple water reflectance) was then actually the identification of the simplex vertices in the object-based classifier which was the foundation for the interpretation of the eigen-decomposed, Rapid Eye™sub-pixel, spectral, wavelength,LULC wavelength frequencyinformation based on a convex geometrical endmember extraction algorithm in the object-based geoclassifier.

A meaningful endmember,geoclassified, 5m, spectral,wavelength, orthogonal, LULCspectral analyses was conducted for quantiating the vertex which we calculated employing the vector Euclidean norm to the subspace as defined by selected spectral endmembers in ENVI. To find these candidate microtopographic pixels, we constructed a Rapid Eye™endmember, geoclassified, LULCdataset employing P possible, black fly, vector arthropod, immature habitat breeding foci, capture point, consisting of r sub-pixel spectral emissivities that were closest to the vertex. We generated an endmember LULC subset using



$P_{candidate} = \{\vec{p}_{(x_1,y_1)}, \vec{p}_{(x_1,y_1)}, \dots, \vec{p}_{(x_c,y_c)}\}$ ($c \leq r, P_{candidate} \in P_{possible}$) which was selected from the r immature habitat, extracted LULC pixels ($P_{possible}$) which was subject to conditions based on: $x_i - x_j \leq t_{pixel}$ and $y_i - y_j \leq t_{pixel}$ ($i \neq j$). We employed the equation $s_angle(\vec{p}_{(x_i,y_i)}, \vec{p}_{(x_j,y_j)}) \leq t_\theta$ ($i \neq j$) as the spectral angle between the geo-spectrally extracted, 5m, spatial resolution, sub-pixel, LULC radiance in the grid-stratified, DRC polygons and optimally calculated $s_angle(\vec{p}_{(x_i,y_i)}, \vec{p}_{(x_j,y_j)}) = \cos^{-1}\left(\frac{\vec{p}_{(x_i,y_i)} \cdot \vec{p}_{(x_j,y_j)}}{|\vec{p}_{(x_i,y_i)}| |\vec{p}_{(x_j,y_j)}|}\right)$ where t_θ was the threshold value for the spectral angle beyond which the endmember LULC wavelength frequency spectra were not considered similar in each polygon. The value of t_θ was set at 2.5 degrees. The SPA identified $\vec{e}_1, \vec{e}_2, \dots, \vec{e}_m$ which represented the brightest, endmember, LULC data (i.e., ripple water pixel components) and the darkest data (i.e., shaded rock) in each polygon. The algorithm then iteratively found the remaining 5m endmembers employing orthogonal LULC projections until the number of endmembers defined was obtained

A number of ripple water, explanatorily, eco-georeferenceable, LULC components and other 5m immature habitat feature (e.g., open canopy) endmembers (m) were used to find the spectral angle threshold t_θ and the spatial threshold (i.e., t_θ Rapid EyeTM pixel). The next step in ENVI was to extract the first orthogonal endmember. The vector norms of the endmember 5m, LULC data determined the largest norm value. Endmember heterogeneity at the simplex vertices was then calculated which revealed the radiance spectral wavelength LULC frequency data in the image cube. The first geoclassified LULC 5m endmember was then estimated.

An orthogonal projection was employed for extraction of all the 5m, endmembers of the geoclassified, ripple water and rock, sub-pixel LULC components in the polygons. All the Rapid EyeTM eigen-decomposed, orthogonal, LULC, spectral, endmember data was fractionally calculated based on the visible and NIR spectrum. An endmember matrix was employed where $U = [\vec{e}_1, \vec{e}_2, \vec{e}_3]$ which optimally projected the LULC sub-pixel data into subspace S_{proj} orthogonal to the space spanned by U as $\vec{p}_{(i,j),proj} = O\vec{p}_{(i,j)}$, where $\vec{p}_{(i,j),proj}$ and $\vec{p}_{(i,j)}$ were the projected and original pixel vector at a possible geoclassified, LULC *S. damnosum* s.l. immature, breeding foci, capture point, immature habitat geolocation (i, j) respectively. O was the projection operator, $O = I - UU^+$ where I was the identity matrix and U^+ was the pseudo inverse of U which was denoted by $U^+ = (U^T U)^{-1} U^T$. We validated the endmember matrix (i.e., $U = [\vec{e}_1, \vec{e}_2, \vec{e}_3]$). The change of the simplex volume with each subspace projection in the DRC polygons was determined. The volume of the simplex was then calculated. The volume increase was summarized by the spectral LULC contrasts which was quantitated by the object classifier between the LULC endmembers, C_{l-1} and C_l , for example. These projections denoted the simplexes defined by the original endmember set, $\{\vec{e}_1, \vec{e}_2, \dots, \vec{e}_{l-1}, \vec{e}_l\}$ and the ratio of the volumes of C_{l-1} and C_l was calculated as $v_ratio_l = \frac{V(C_l)}{V(C_{l-1})}$. ($3 < l \leq m$). Each 5m, Rapid EyeTM, geoclassified, LULC, endmember proportion in each polygon was then calculated.

The BRDF of a geoclassified uncoalesced, pixel signature was modeled as the limit of its directional reflectance factor employing $R(i, v) = \frac{\iint_A R(s) \langle i, s \rangle \langle v, s \rangle I_i(s) I_v(s) ds}{A \cos \theta_i \theta_v}$ (3.1) where ds was a small Lambertian surface element over the 5m, LULC geoclassified area A from the Rapid EyeTM extracted, target pixel; $R(s)$ was the reflectance of ds ; i , v , and s represented the directions of illumination and viewing based on the LULC surface reflectance components, respectively. In the 5m, eco-epidemiological, cross-border, *S. damnosum* s.l. capture point, breeding foci, immature habitat, remote sensed, moderate resolution, identification model $\langle \dots \rangle$ was the cosine of the phase angle between two directions; θ was the zenith angle of a direction; $I_i(s)$ and $I_v(s)$ were indicator functions, equal to one when ds was illuminated (I_i) or viewed (I_v) or zero otherwise. If a surface exhibits Lambertian reflectance, light falling on it is scattered such that the apparent brightness of the surface to an observer is the same regardless of the observer's angle of view, thus, the surface luminance is isotropic [66]. Solving our double integral equation revealed that ds was integrated over the eigen-decomposed Rapid EyeTM pixel (i.e., the footprint of the sensor's Instantaneous Field of View (IFOV)). The IFOV is a measure of the spatial resolution of a remote sensing imaging system which may be



defined in an object-based classifier as the angle subtended by a single detector element on the axis of the optical system [8].

We noted that there were two kinds of prominent LULC microtopographic surfaces in the endmember explanatory uncoalesced spectra; A -background surface (i.e., partially canopied rock) and surface ripple water which were represented by Lambertian reflectance G and C , which was respectively also introduced into $R(i, v) = K_g G + \frac{C}{A} \iint_{A_c} \frac{\langle i, s \rangle \langle v, s \rangle}{\cos \theta_i \cos \theta_v} ds$, [Eqn 3.2] where $K_g = A_g / A$. The proportion of background 5m, imaged, spectral, wavelength, frequency LULC data members was illuminatable and hence viewable. In this equation, the union of A_g and A_c were the intersection of the dataset of surface elements which were quantifiable only when v and i coincided. The directional reflectance of the 5m scene depended also on the bare rock and ripple water LULC reflectance related to G and C in each polygon.

$$R(i, v) = K_g G + \frac{C}{A} \iint_{A_c} \frac{\langle i, s \rangle \langle v, s \rangle}{\cos \theta_i \cos \theta_v} ds$$

We focused on the two terms of $R(i, v)$. The first term described how the sunlit background, LULC wavelength proportion proceeded to a maximum point as viewing and illumination positions in the hemisphere coincided. The second term described how the sunlit, microtopographic, LULC surface, (e.g., partially canopied, trailing, immersed vegetation) composed of the Lambertian facets, became maximally exposed to view at the hotspot, while those facets became dominant at large viewing zenith angles. The hot spot correlation effect refers to the observed brightening which can occur when viewing a scene from the same direction as the solar illumination [69] which for predictive, entomological, vector arthropod immature habitat, forecast, vulnerability, eco-epidemiological, spectral wavelength modelling is commonly, noted in the visible and NIR spectral regions [2].

We analyzed how the first term $K_g G$ varied with illumination and viewing geometry. As in [70], we assumed that the spatial object of interest (i.e., cross-border, African, riverine, tributary, *S. damnosum* s.l., capture point, breeding foci) and its associated explanatory sub-pixel, orthogonally eigen-decomposed, explanatory, wavelength, frequency, uncoalesced, LULC, spectral predictor covariate coefficient estimates had the shape of a spheroid, with vertical half-axis equal to b , horizontal radius equal to R , and a height to the center of the spheroid h . To accommodate the spheroidal shape in the 5m, endmember LULC derivations of the

$$\theta' = \tan^{-1} \left(\frac{b}{R} \tan \theta \right)$$

shadowed areas, we used the transformation θ' . This equation was solved by replacing θ with the angle that would generate the same shadow area for a sphere. For simplicity, we assumed that the centers of the spheroids in the geoclassified LULCs in each polygon were randomly distributed in depth from h_1 to h_2 over A . The assumption was that G and C were constant as average endmember, wavelength LULC signatures over A_g and A_c for properly modelling K_g and $K_c = A_c / A$ for identifying a cross-border, eco-georeferenceable, capture, point, *S. damnosum* s.l., African, riverine, tributary, seasonal, eco-epidemiological, breeding foci.

$$R(i, v) = K_g G + \frac{C}{A} \iint_{A_c} \frac{\langle i, s \rangle \langle v, s \rangle}{\cos \theta_i \cos \theta_v} ds$$

Next, the equation was employed to further orthogonally eigen-

decompose the 5m geoclassified LULCs where K_g was expressed in a Boolean model and $K_g = e^{-\lambda \pi R^2 [\sec \theta'_i + \sec \theta'_v - \bar{O}(\theta_i, \theta_v, \phi)]}$ where $\bar{O}(\theta_i, \theta_v, \phi)$ was the average of the overlap function $O(\theta_i, \theta_v, \phi, h)$ between illumination and viewing shadows of the geoclassified LULCs and its associated ripple water features.

The Boolean model for a random subset of the plane or higher dimensions, analogously is a common tractable models in stochastic geometry. ArcMapTM performed a Boolean and operation on the eigen-decomposed, frequency endmember, geoclassified, LULC 5m, cell values of two input rasters. If both input values are true



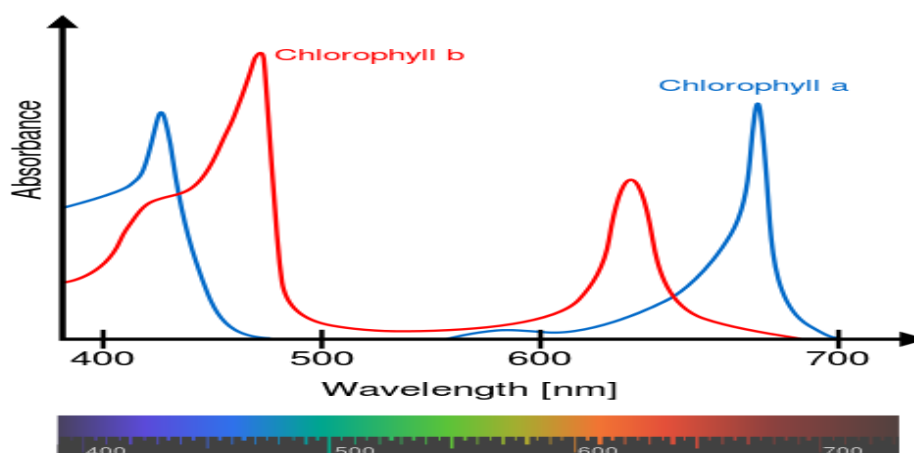
(non-zero), the output value is 1: if one or both inputs are false (zero), the output is 0 (www.esri.com).The spectral, wavelengthmember, LULCparameters eco-cartographically delineated by the model were λ and a probability distribution was defined onto compact sets for each sampled capture point ξ of the Poisson point process used as a set C_ξ from the distribution, and then definedas the union $\cup_\xi(\xi + C_\xi)$ of the translated sets. To illustrate tractability with one simple formula, the mean density of B as defined by a sub-pixel, endmember, Rapid Eye™ grid-stratified, endmember, LULC classification equaled $1 - \exp(-\lambda E\Gamma)$ where Γ denoted the sampled LULC area of C_ξ within each 5m polygon.

We assumed ϕ was the difference in azimuth angle between viewing and illumination positions of the partially canopied, 5m, resolution, geospatial, LULC objects associated to a possible cross-border, African, riverine, tributary, *S. damnsoum* s.l.,eco-epidemiological, capture point, breeding foci, eco-georeferenceable, immature habitat. To simplify the equation, we approximated the overlap function by the canopy LULC geoclassifiable, overlap area and center positions of the ellipses. This approximation is justified when solar zenith and viewing zenith angles are not too large [70]. In the case of long ellipsoidal shadows, however, this approximation could have overestimated the width of a potential, cross-border, riverine, tributary, *S. damnosum* s.l., eco-epidemiological, immature habitat hotspot(i.e., positively autocorrelated, microtopographic, partially canopied, LULC, shaded endmembers) in the azimuthal direction and underestimated the width of the hotspot in the azimuthal direction. To improve the accuracy and preserve the proper, black fly, immature, habitat hotspot width information, we developed another approximation as follows. We employed the equations $\phi = 0$ or $\phi = \pi$. First, we considered the overlap function in the principal plane. We used $\phi = 0$ and π as the elliptical illumination estimate of each partially canopied, geoclassified, microtopographic LULC in each DRC polygon where viewing shadows were aligned in the same direction. The overlap area was approximated by an ellipse with one axis equal to the overlap length and the other equal to the width encompassing the geoclassified discontinuous canopied, orthogonally decomposable, LULC feature attributes (e.g., unshaded, ripple water pixel

spectral components) in each polygon employing revealed multiple multiple canopy pigment irradiance

$$O(\theta_i, \theta_v, \phi) = \frac{1}{2} \left[\sec \theta'_i + \sec \theta'_v - \frac{h}{b} |\tan \theta'_i - \tan \theta'_v \cos \phi| \right]$$

Figure 10: An unmixed, canopy wavelength spectrum was displayed.



We then kriged the endmember pigment, spectral reflection of Chl-a 5m, LULC signature. Kriging of the pigment endmembers in Spatial Analyst™ generated an estimated surface from a scattered set of signature, 5m LULC points with z-values. Kriging is like inverse distance matrices in that it weights the surrounding measured values to derive a prediction for an unmeasured location [7]. Unlike other interpolation methods supported by ArcGIS Spatial Analyst™, employs the Kriging tool as an interactive investigation of the spatial



behavior of the phenomenon represented by the z-values before selecting the best estimation method for generating the output surface[66].

We assumed that the distance or direction between sampled discontinuous canopied endmember 5m, resolution LULC points reflected a spatial correlation that could be usable to explain variation in the surface spectral immature black fly, signature radiance for optimally identifying unknown, eco-georeferenceable, seasonal, cross-border, *S. damnosum* s.l., African, riverine tributary, breeding foci in the DRC grid-stratified, Rapid Eye™ polygons.

The Kriging tool in Spatial Analyst™ fit a mathematical function to a specified number of geoclassified, 5m endmember, LULC in the DRC polygon points within a specified radius, to determine the output value for each possible immature habitat eco-geographic sample location. Kriging is a multistep process; it includes exploratory endmember, geostatistical analysis of the LULC data, variogram modeling, for creating the surface, and optionally exploring a variance surface[7]. Kriging is most appropriate in iterative, vector entomological, eco-epidemiological, signature interpolation when there is a quantifiable spatially correlated distance or directional bias in the sample signature endmember unmixed LULC data[2].

The general formula for the interpolation in the 5m resolution, DRC geoclassified polygons was formed as a weighted sum of the geoclassified 5m, LULC endmembers which were quantitated in

$$\hat{Z}(s_0) = \sum_{i=1}^N \lambda_i Z(s_i)$$
 where: $Z(s_i)$ was the measured value at the i th LULC geolocation λ_i = an unknown signature weight for the measured value at the i th locations s_0 = the prediction breeding foci, cross-border, *S. damnosum* s.l. capture point, eco-georeferenced geolocation N = the number of measured, 5m, uncoalesced, spectral wavelength frequency values. In the interpolation the weight, λ_i , represented an eco-georeferenceable, potential cross-border, immature habitat, black fly capture point, which was depended solely on the distance to a prediction foci location.

An ordinary linear combination was also employed for the interpolation of the 5m NDVI and SAVI endmember LULC signatures. We assumed the cross-border *S. damnosum* s.l. immature habitat, breeding foci, was geo-spectrally associated with an eco-georeferenceable, eco-epidemiological, capture point, uncoalesced, 5m, endmember discontinuous canopy, spectral wavelength which was expressed with

$$Z^*(x) = \sum_{j=1}^n \lambda_j Z(x_j) \text{ with } \sum_{j=1}^n \lambda_j = 1$$
 [Eqn: 3.1] in Spatial Analyst™ where the constraint on the kriging weights $\sum_j \lambda_j = 1$ was imposed onto the LULC, 5m, parameterizable covariate estimator $Z^*(x)$ (i.e. the estimation errors) which was null on average, $E(\varepsilon) = 0$, with $\varepsilon = Z(x) - Z^*(x)$.

The ordinary kriging system was obtained by minimizing the sum of the square errors under the constraint in Equation [3.1] and by employing the least-square and Lagrange methods, which was expressed in

$$\begin{pmatrix} C_{zz} & \mathbf{u} \\ \mathbf{u}' & 0 \end{pmatrix} \begin{pmatrix} \Lambda_{ok} \\ \mu_{ok} \end{pmatrix} = \begin{pmatrix} \mathbf{c}_z \\ 1 \end{pmatrix}$$

the following block matrix equation: . In mathematical optimization, the method of Lagrange multipliers is a strategy for finding the local maxima and minima of a function subject

to equality constraints[7]. The error variance, σ_{ok}^2 , was equal to $\sigma_{ok}^2 = \sigma_z^2 - \mathbf{c}'_z \Lambda_{ok} - \mu_{ok}$ where C_{zz} represented the sample covariance matrix, Λ_{ok} was the vector of the ordinary kriging weights, \mathbf{u} was a unit vector with all the entries equal to 1, such as $\mathbf{u} = [1 \ 1 \ \dots \ 1]^t$, where superscript t was the vector transpose, μ_{ok} was the Lagrange multiplier due to the constraint on the kriging endmember, 5m, *S. damnosum* s.l. geoclassified, endmember, LULC weights which summed to 1, and \mathbf{c}_z was the vector of covariance between the estimation immature habitat capture point, x , and each of the sample discontinuous canopied points, \mathbf{x}_j

Lagrange multipliers were used to find the extrema of a multivariate LULC function $f(x_1, x_2, \dots, x_n)$ subject to the constraint $g(x_1, x_2, \dots, x_n) = 0$, where f and g were the functions with continuous first partial derivatives on the open set containing the curve $g(x_1, x_2, \dots, x_n) = 0$, and $\nabla g \neq 0$ at any estimated, cross-border, *S. damnosum* s.l., immature, eco-epidemiological, capture point on the curve where ∇ was the gradient in each polygon. For an extremum of f to exist on g , the gradient of f must line up with the gradient of g in an entomological, vector, arthropod-related, probabilistic paradigm[23] The gradient is a horizontal vector (i.e., it



has no z component) that shows the direction that the function increases; for \mathbf{g} it is perpendicular to the curve, which is a straight line in this case. If the two gradients are in the same direction, then one is a multiple ($-\lambda$) of the other, so $\nabla f = -\lambda \nabla g$. [67]. Here two vectors for any potential habitat on a geoclassified Rapid Eye™ 5m resolution polygon were equal, so all of their endmember LULC geoclassified components rendered $\frac{\partial f}{\partial x_k} + \lambda \frac{\partial g}{\partial x_k} = 0$ for all $k = 1, \dots, n$, where the constant λ was the Lagrange multiplier. The extremum was then found by solving the $n + 1$ equations in $n + 1$ unknowns, which was done without inverting \mathbf{g} ,

In order to maximize or minimize the function $f(x, y)$ which was subject to the constraint $g(x, y) = k$ in the cross-border, African riverine, tributary, *S. damnosum* s.l., capture point, immature habitat we followed the following procedure. We first create the LaGrange Function. This function was composed of the function to be optimized combined with the constraint function in the following way: $L(x, y) = f(x, y) - \lambda[g(x, y) - k]$ for obtaining optimal solution 0 constraints. We then found the partial derivative with respect to each 5m, Rapid Eye™ predictor, endmember LULC variable x, y and the Lagrange multiplier λ of the function shown: $L(x, y) = f(x, y) - \lambda[g(x, y) - k]$. We then set each of the partial derivatives equal to zero to get $L_x = 0, L_y = 0$ and $L_\lambda = 0$. Using $L_x = 0, L_y = 0$, we proceeded to solve for x and solve for y in terms of λ . We then substitute the solutions for x and y so that $L_\lambda = 0$ is in terms of λ only in the black fly immature habitat identification, forecast, vulnerability model. We then solved for λ and employed this value to find the optimal cross-border, *S. damnosum* s.l. immature habitat parameterizable 5m LULC endmember values x and y . Note: If M is the max or min value of $f(x, y)$ subject to the constraint $g(x, y) = k$, then the Lagrange multiplier λ is the rate of change in M with respect to k . (i.e. $\lambda = dM/dk$ and therefore λ approximates the change in M resulting in a one unit increase in k [6].

We selected the NOINT or NOSCALE in SAS/GIS option, where restrictions were replaced on the intercept or scale parameters. Lagrange multiplier statistics were computed for the Rapid Eye™, geoclassified African, riverine tributary, 5m, grid-stratified, DRC polygons. The statistics were assessed for the validity of the restrictions which were computed as $\chi^2 = \frac{s^2}{V}$ where s was the component of the score vector evaluated at the restricted maximum corresponding to the geoclassified LULC parameters employing $V = \mathbf{I}_{11} - \mathbf{I}_{12} \mathbf{I}_{22}^{-1} \mathbf{I}_{21}$, [3.2] the discontinuous canopy LULC parameters geospectrally retrieved from the iteratively interpolated 5m Chl-a target signature.

Under regularity conditions, this statistic has an asymptotic chi-square distribution with one degree of freedom, and P -values which here were computed based on a limiting distribution. [2], set $k = 0$ in a negative binomial model, s the score statistic of [71] for testing for overdispersion in a Poissonian cross-border, *S. damnosum* s.l. immature, habitat identification model against alternatives of the form $V(\mu) = \mu + k\mu^2$.

Equation [3.2] was an expanded matrix formulation from simple kriging taking into account the constraint on the uncoalesced, spectral wavelength LULC signature, ordinary kriging cross-border, African tributary, 5m weights. The block-matrix in Spatial Analyst™ inversion formula was used to rewrite the square matrix on the left side of Equation [3.2].

A block matrix or a partitioned matrix is a matrix that is interpreted as having been broken into sections called blocks or submatrices [8]. We assumed that, a cross-border, *S. damnosum* s.l., capture point, immature habitat matrix interpreted as a block matrix can be geovisualized as the original matrix with a collection of horizontal and vertical lines, partitioned into a collection of smaller matrices. In Spatial Analyst™ any matrix may be interpreted as a block matrix in one or more ways, with each interpretation defined by how its rows and columns are partitioned (www.esri.com).

This notion was made more precise by the matrix by partitioning the immature habitat black fly, identification model geoclassified Rapid Eye™, grid-stratified data, into a collection, and then partitioning them into a collection of microtopographic LULC categories (e.g., uncanopied, trailing vegetation). The original matrix was then considered as the "total" of these groups, in the sense that the entry of the original



matrix corresponded in Spatial Analyst™ to a 1-to-1 way with some offset entry. Block matrix algebra arises in general from byproducts in categories of matrices[8]. The solution was thus as follows:

$$\Lambda_{ok} = C_{zz}^{-1} c_z - C_{zz}^{-1} u (u^T C_{zz}^{-1} u)^{-1} u^T C_{zz}^{-1} c_z +$$

$$C_{zz}^{-1} u (u^T C_{zz}^{-1} u)^{-1} = \Lambda_{sk} - \Lambda_m u^T \Lambda_{sk} +$$

$$\Lambda_m = \Lambda_{sk} + (1 - u^T \Lambda_{sk}) \Lambda_m = \Lambda_{sk} + \lambda_m \Lambda_m$$

$$\Lambda_m = C_{zz}^{-1} u (u^T C_{zz}^{-1} u)^{-1} = -C_{zz}^{-1} u \mu_m$$

$$\lambda_m = 1 - u^T \Lambda_{sk}$$

$$\mu_m = - (u^T C_{zz}^{-1} u)^{-1}$$

$$\mu_{ok} = (u^T C_{zz}^{-1} u)^{-1} u^T C_{zz}^{-1} c_z - (u^T C_{zz}^{-1} u)^{-1} =$$

$$- \lambda_m (u^T C_{zz}^{-1} u)^{-1} = \lambda_m \mu_m$$

where Λ_{sk} was the vector of simple cross-border, forecasted, *S. damnosum* s.l. kriging weights defined, Λ_m was the vector of kriging weights for estimation of the LULC mean, and λ_m was the corresponding Lagrange multiplier. The latter was obtained by replacing the vector c_z with a zero vector of the same size in Equation [3.2], because of the nil correlation between a random 5m eco-georeferenceable, eco-epidemiological, geoclassifiable, endmember, LULC variable and its mean. λ_m was the weight of the mean in simple kriging, because Equation [3.1] was then expressed as

$$Z^*(x) = (1 - \sum_{j=1}^n \lambda_j) m + \sum_{j=1}^n \lambda_j Z(x_j) = \lambda_m m + \sum_{j=1}^n \lambda_j Z(x_j)$$

This equation was also used to deduce an additive relationship among the error variances of the Ordinary kriging, the local mean, and Simple kriging of the Chl-a and other LULC sub-pixel signatures. As the error variance $\sigma^2 m$ in estimating the mean is equal to λ_m [72], the Ordinary kriging variance σ_{ok}^2 (can be expressed as a function of the simple kriging error variance

$$\sigma_{ok}^2 = \sigma_{sk}^2 + \lambda_m^2 \sigma_m^2$$

and the estimation variance of the local mean employing in an entomological, vector arthropod-related, remote sensing, endmember, spectral wavelength, frequency, 5m, Rapid Eye™ geoclassified, eco-georeferenceable LULC forecast, vulnerability, eco-epidemiological, model[2][73].

The semivariogram was defined as $\gamma(s_i, s_j) = \frac{1}{2} \text{var}(Z(s_i) - Z(s_j))$ in Spatial Analyst™, where var was the variance. Our assumption was that if two seasonal, hyperproductive, cross-border, capture point, eco-georeferenceable, *S. damnosum* s.l., capture point locations, s_i and s_j , were close to each other in terms of the Euclidean distance eco-georeferenceable measure of $d(s_i, s_j)$, we would expect them to be similar, so the difference in their 5m, spectral, endmember, wavelength, frequency, immature black fly, eco-epidemiological, capture point LULC values, $Z(s_i) - Z(s_j)$, would be small. As s_i and s_j got farther apart, they become less similar (i.e., towards negative autocorrelation), so the difference in their values, $Z(s_i) - Z(s_j)$, will become larger [6].

We noted that the variance of the difference increased with the endmember, LULC interpolated signature distance, so the semi variogram in the cross-border, *S. damnosum* s.l., immature habitat remotely sensed, identification model was like a dissimilarity function. There are several terms that are often associated with this function, and they are also used in Geostatistical Analyst™ (www.esri.com) The height that the semivariogram reached when it levelled off (i.e., sill) was generated. It was composed of two parts: a discontinuity at the origin, called the nugget effect, and the partial sill; added together, these gave the black fly, immature habitat, identification, interpolation model sill value. The value that the semivariogram model attains at the range (the value on the y-axis) is called the sill. The partial sill is the sill minus the nugget.[7]. The nugget effect was further divided into measurement error and microscale variation. The nugget effect was simply the sum of measurement error and microscale variation and, since either LULC component could not have been zero, the



nugget effect was composed wholly of one or the other. The distance at which the semi variogram levels off to the sill is called the range [7].

The cross-border, *S. damnosum* s.l. immature habitat, eco-epidemiological, semivariogram was defined in Spatial AnalystTM as $\gamma(s_i, s_j) = \frac{1}{2} \text{var}(Z(s_i) - Z(s_j))$, where var was the variance. If two locations, s_i and s_j , are close to each other in terms of the distance measure of $d(s_i, s_j)$, they be expected to be similar, so the difference in their values, $Z(s_i) - Z(s_j)$, will be small in a stochastic or deterministic interpolator [7].

The nugget effect in the cross-border, *S. damnosum* s.l., immature habitat, capture point, eco-epidemiological, identification model was simply the sum of paradigm measurement error and microscale geoclassified, 5m quantitated, endmember, wavelength, LULC variation and, since either component could have been zero, the nugget effect was composed wholly of one or the other.

Criteria for covariance functions on the interpolated, 5m, cross-border, *S. damnosum* s.l., African, riverine, tributary, capture point, eco-georeferenceable, immature habitat, LULC signal intervals, was quantitated employing exponential models, and locally polynomial covariances in Spatial AnalystTM. We characterized the isotropic locally polynomial covariance functions of degree. The covariance of (X, Y) (X, Y) was defined by $\text{cov}(X, Y) = E[(X - E(X))[Y - E(Y)]]$ in the forecast, vulnerability, entomological, immature habitat identification, iterative stochastic interpolator. The variances were positive, where the correlation of (X, Y) (X, Y) was defined by $\text{cor}(X, Y) = \frac{\text{cov}(X, Y)}{\text{sd}(X)\text{sd}(Y)}$,

Besides plotting each microtopographic, LULC, discontinuous canopied, uncoalesced, feature attribute (e.g., partially canopied, trailing, immersed, vegetation) they were also grouped into lag bins in Spatial AnalystTM. This allowed for easier spatial quantitation of the surface elements for example, by computing the empirical semi variogram a graph was revealed of the averaged semi variogram with LULC values on the y-axis and the distance (or lag) on the x-axis of the uncoalesced, 5m LULC endmember spectral, wavelength, frequency, parametrizable covariates.

Residuals (response residuals from the model) were checked for normality. There were not problems reported by the default. Warning messages should be taken with care, since all departures from normality are problematic [6]. When the sample size is large, even the smallest deviation from normality might lead to a warning [7].

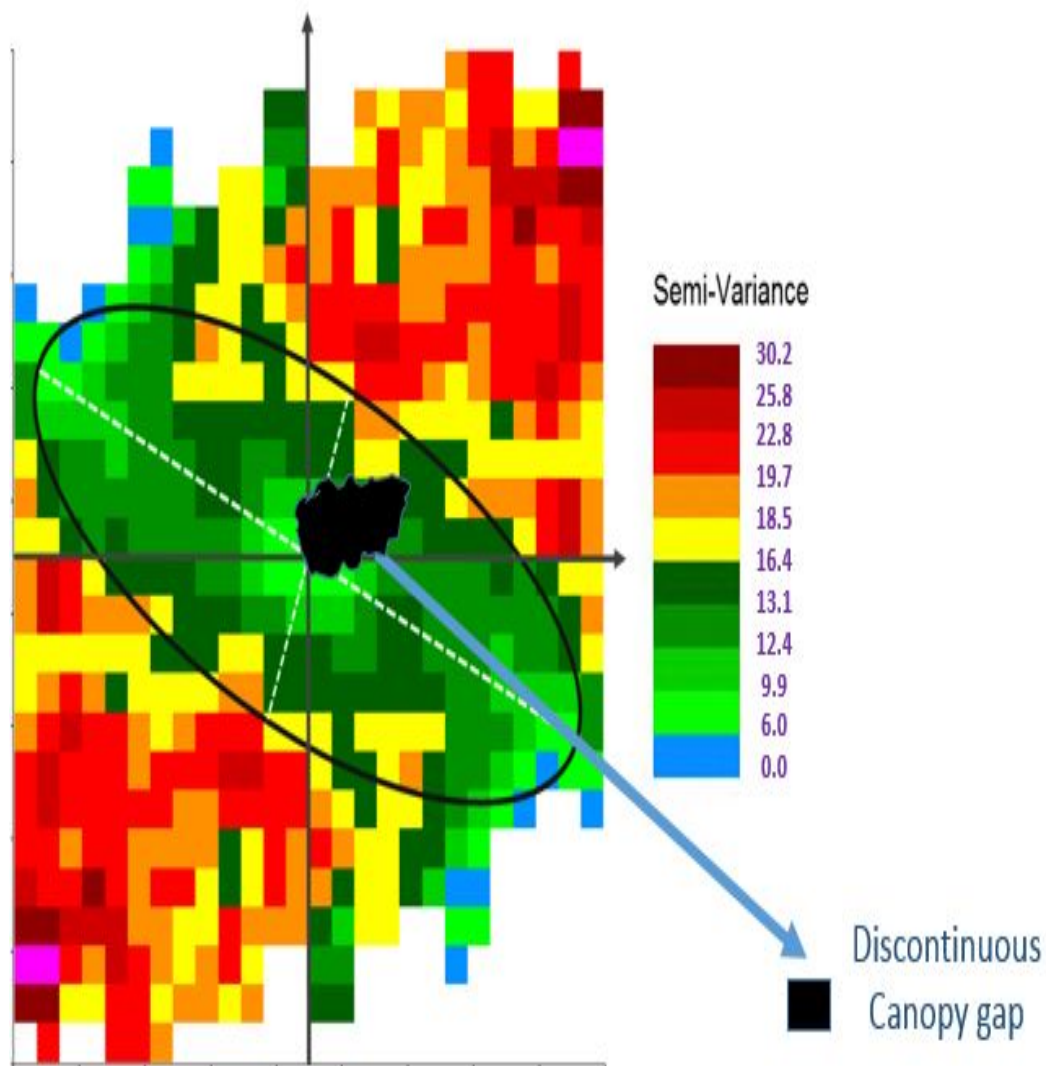
Spatial AnalystTM described the relationship between the Chol-a discontinuous signature and the other LULC endmember signals employing the kriging weights. The relationship between the corresponding geoclassified landscape covariate error variances was quantitated. The Ordinary kriging weights were expressed as the sum of the simple kriging weights which were quantitate whenst the local mean was multiplied by the weight for the mean. One obvious advantage of this formulation was the explicit expression of the impact of the constraint on the cross-border, *S. damnosum* s.l. immature habitat, capture point, kriging endmember weights. The error variance increases when using Ordinary kriging because it is necessary to estimate both the local mean and the residuals [7].

The kriging solution for the local mean was given by a summary statement. Furthermore, the estimation for the random function, $Z(x)$, was done with the kriging algorithms which yields the same solution. In other words, the estimation of the random function by Ordinary kriging was identical to the combination of the estimation of the mean employing Ordinary kriging and the estimation of the residual by Simple kriging rendered similar diagnostic outputs.

The kriging method and the weights based on the uncoalesced, interpolated, LULC, endmember, Rapid EyeTM microtopographic, LULC signature points were not able to identify or predict any cross-border, *S. damnosum* s.l. immature habitat, capture point, geolocations in either DRC 5m grid-stratified Rapid EyeTM polygon.

To employ the spatial arrangement and the 5mLULC weights, in a entomological, vector, arthropod-related, predictive geoclassifiable, eco-epidemiological, eco-georeferenceable risk model the spatial autocorrelation must be quantified[2, 27]. Hence, our kriging simulation exercise for optimally identifying, 5minterpolated LULC signature, cross-border, seasonal, eco-georeferenceable, *S. damnosum* s.l., was based on the the weight, λ_i , which was dependentalso on a fitted clustering model of the geoclassified spectral wayward points using the 5m signatures. We could identify clusters of microtopographic geoclassified LULCs based on Euclidean distance measurements(see Figure 8) However, once again noprediction immature *S. damnosum* s.l. habitat, capture point, breeding foci locations were remotely definable from the aggregated measuredmicrotopographic geospatially quantitated uncoalesced wavelength, LULCendmember 5m values.

Figure 11: Empirical semi variance for all pairs of microtopographic LULC points in the DRC polygonof uncanopied trailing vegetation spatial objects that were greater than 40 meters apart but less than 50 meters.



We converted a Rapid Eye TM DEM to a raster dataset. Using:

```
import arcpy
arcpy.DEMToRaster_conversion("c:/data/fixd.dem", "c:/output/fixeddem.tif",
```

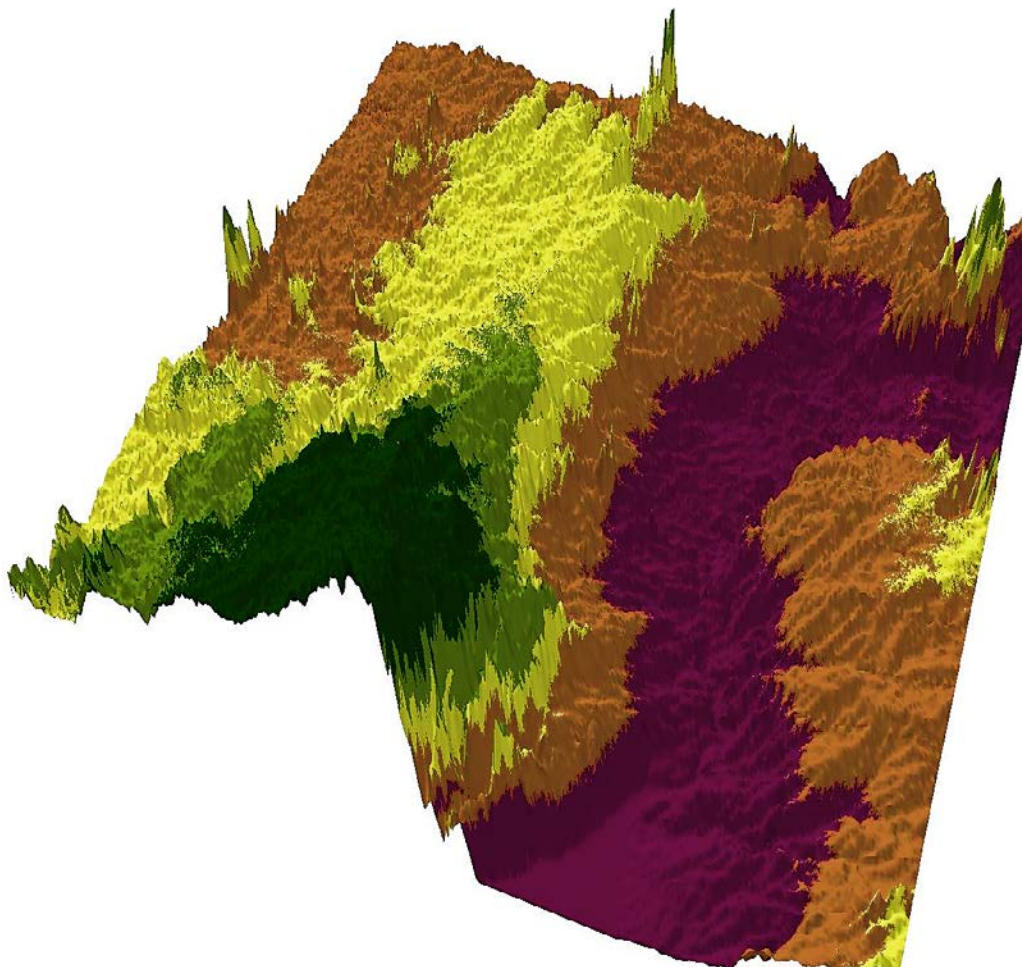
```
"FLOAT", 1)
```

In so doing the following output was realized:

```
zFactor = 0.30488  
# Execute DEMToRaster
```

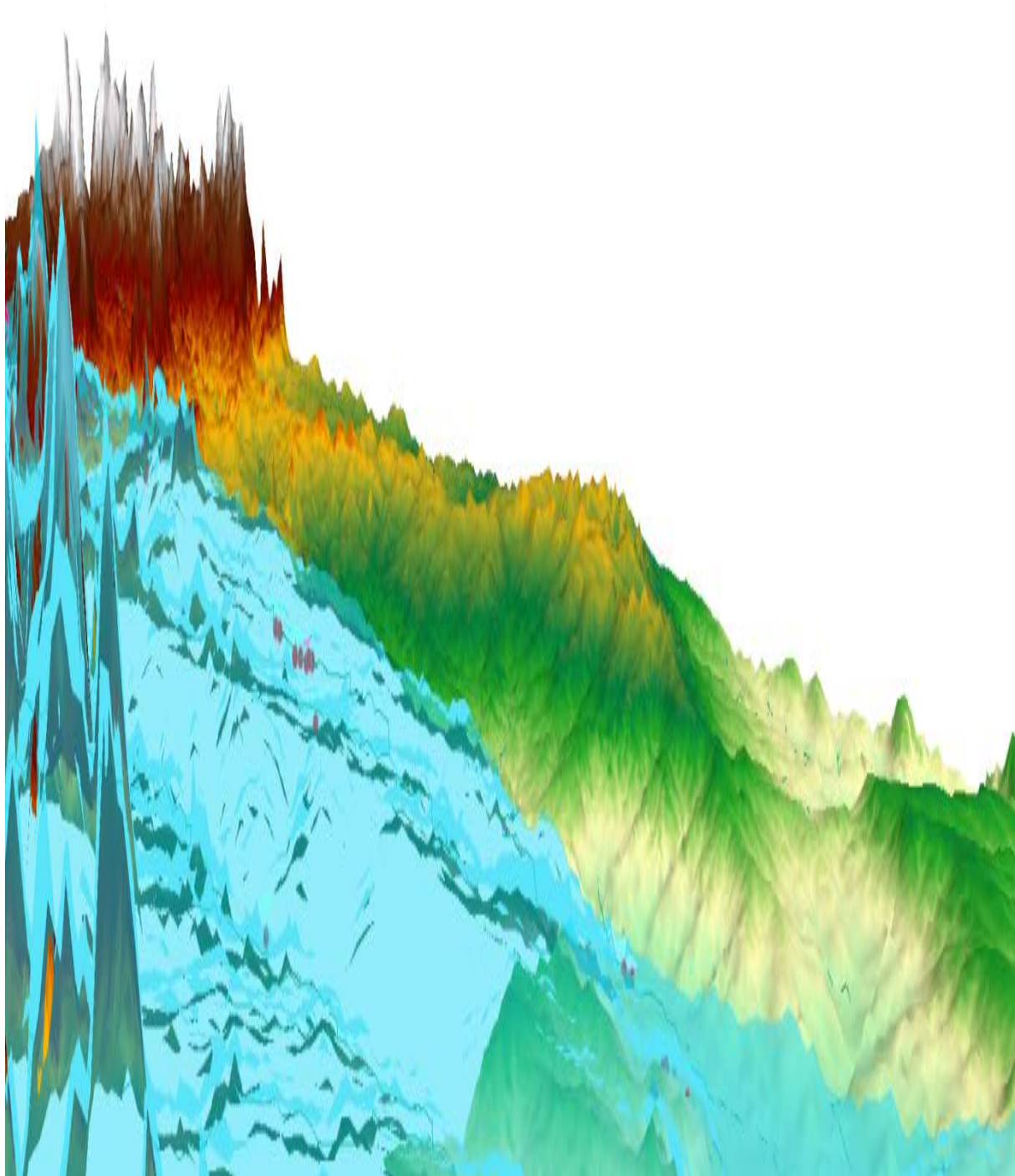
```
arcpy.DEMToRaster_conversion(inDEM, outRaster, rasterType, zFactor)
```

Figure 12: Three-Dimensional estimated model for the DRC eco-epidemiological, study site 5m polygon



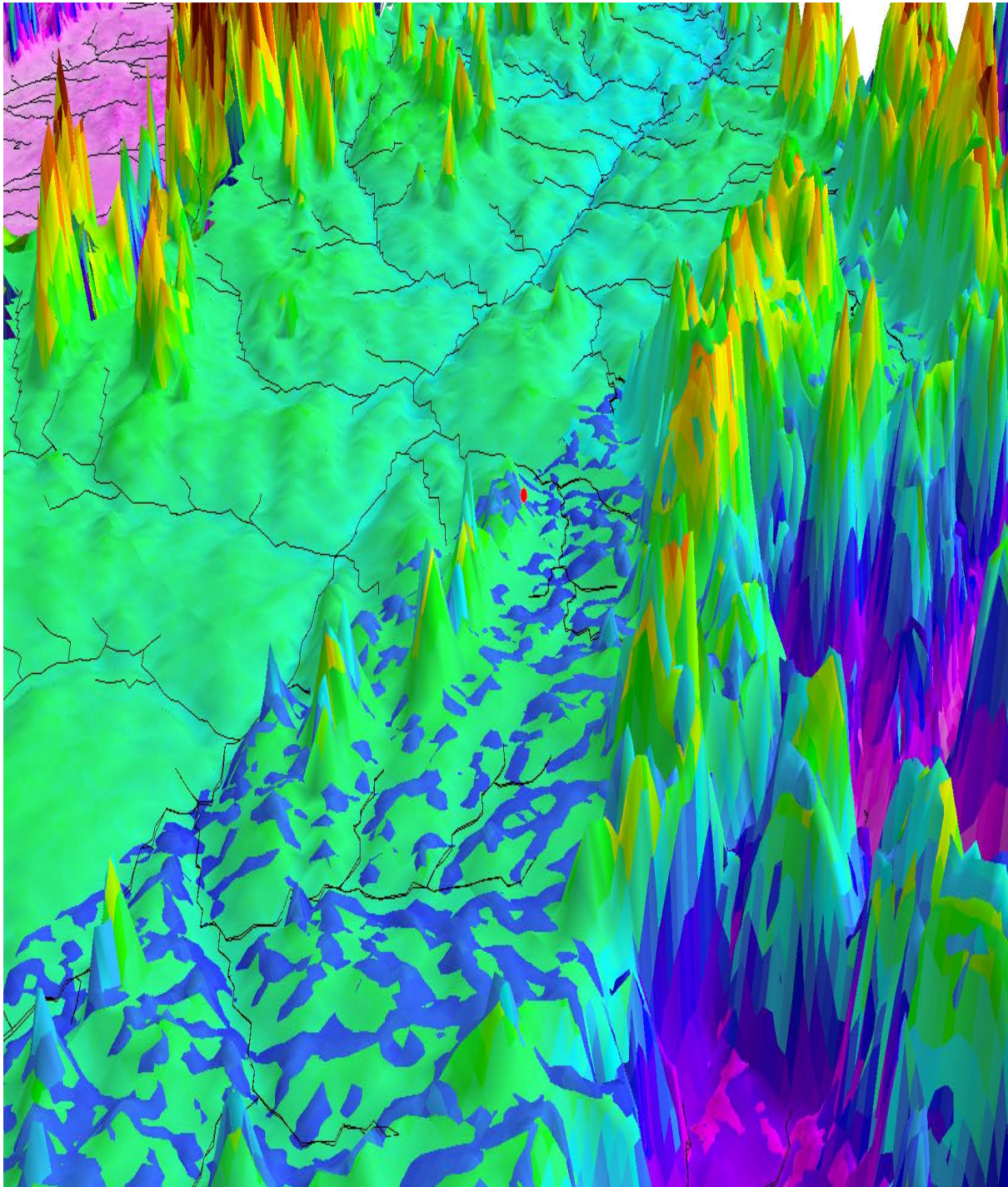
We interpolated the LULC endmember signatures in each Rapid Eye TM 5m spatial resolution polygon.

Figure 13: A riverine tributary habitatsignature 5m interpolated signal along the border of northern Uganda delineated in lightblue revealingno target cross-border, breeding foci *S. damnosum* s.l. forecasts



The overall spatial arrangement of the measured endmember points did locate a *S. nevi* habitat (see Figure 14).

Figure 14: A remotely identified, ground trothed *S. nevi* immature habitat breeding foci in the DRC polygon



The Rapid Eye™5m, LULC analyses of the canopied, trailing vegetation in the DRC geoclassified polygons was represented in NumPy, the fundamental package for scientific computing with Python. NumPy contains: 1) a powerful N-dimensional array object 2) sophisticated (broadcasting) functions 3) tools for integrating C/C++ and Fortran code; and 4) useful linear algebra, Fourier transform, and random number capabilities (<http://www.numpy.org/>). The most recent development versions of NumPy and SciPy were available through the official repositories hosted on Github. To check out the **NumPy** sources we used:

```
git clone https://github.com/numpy/numpy.git numpy
```

To check out the latest **SciPy** sources we used



```
git clone https://github.com/scipy/scipy.git scipy
```

NumPy ,an extension to the Python programming language, added support for the multi-dimensional 5m LULC arrays and grid-stratified matrices in the Rapid Eye™ polygons, along with a large library of high-level mathematical functions to operate on the DRC polygon which was written as:

```
>>> import numpy as np
>>> x = np.array([[1,2,3],[4,5,6],[7,8,9]])
>>> x
array([[1, 2, 3],
       [4, 5, 6],
       [7, 8, 9]])
>>> x.shape
(3, 3)
```

The cross-border, *S. damnosum* s.l. African, riverine, tributary habitat identification LULC array had 2 dimensions. In NumPy the number of dimensions is referred to as **rank** (www.numpy.org). The ndim was the same as the number of axes or the length of the output of x.shape which was written as:

```
>>> x.ndim
2

>>> x.size
9
```

The LULC arrays were conveniently displayed .

```
>>> x.sum(axis=0)
array([12, 15, 18])
>>> x.sum(axis=1)
array([ 6, 15, 24])

>>> x.mean(axis=0)
array([ 4.,  5.,  6.])
>>> x.mean(axis=1)
array([ 2.,  5.,  8.])
```

The arrays were useful as they interacted with other NumPy functions to make a sequence of LULC discrete integer values similar to *range* in the Python standard library. We employed the statements:

```
>>> np.arange(10)
array([0, 1, 2, 3, 4, 5, 6, 7, 8, 9])
>>> np.arange(5,10)
array([5, 6, 7, 8, 9])
>>> np.arange(5,10,0.5)
array([ 5. ,  5.5,  6. ,  6.5,  7. ,  7.5,  8. ,  8.5,  9. ,  9.5])
```

Also, we recreated the first black fly, vector habitat id matrix by **reshaping** the output of the 5m geoclassified LULC arrangements in the DRC Rapid Eye polygons.

```
>>> x = phalange(1,10).reshape(3,3)
>>> x
array([[1, 2, 3],
       [4, 5, 6],
       [7, 8, 9]])
```

We employed similar function to *arange* for investigating each line space which filled a vector within the evenly spaced, gridded, Rapid Eye™ 5m, LULC data whose interval was specified using.

```
>>> x = np.linspace(0,5,5)
>>> x
array([ 0. ,  1.25,  2.5 ,  3.75,  5.  ])
```



We accessed the documentation for conducting the remote endmember, LULC quantitation of the moderate resolution geoclassified capture point variables for remotely identifying the cross-border, African riverine tributary, black fly immature habitat, breeding foci, eco-epidemiological, capture points in the DRC polygons at anytime using

```
~$ pydoc numpy.linspace
```

which was geo-visualizable in space employing:

```
import numpy as np  
import matplotlib.pyplot as plt  
fig = plt.figure()  
ax = fig.add_subplot(111)  
N = 8  
y = np.zeros(N)  
x1 = np.linspace(0, 10, N, endpoint=True)  
p1 = plt.plot(x1, y, 'o')  
ax.set_xlim([-0.5, 10.5])  
plt.show()
```

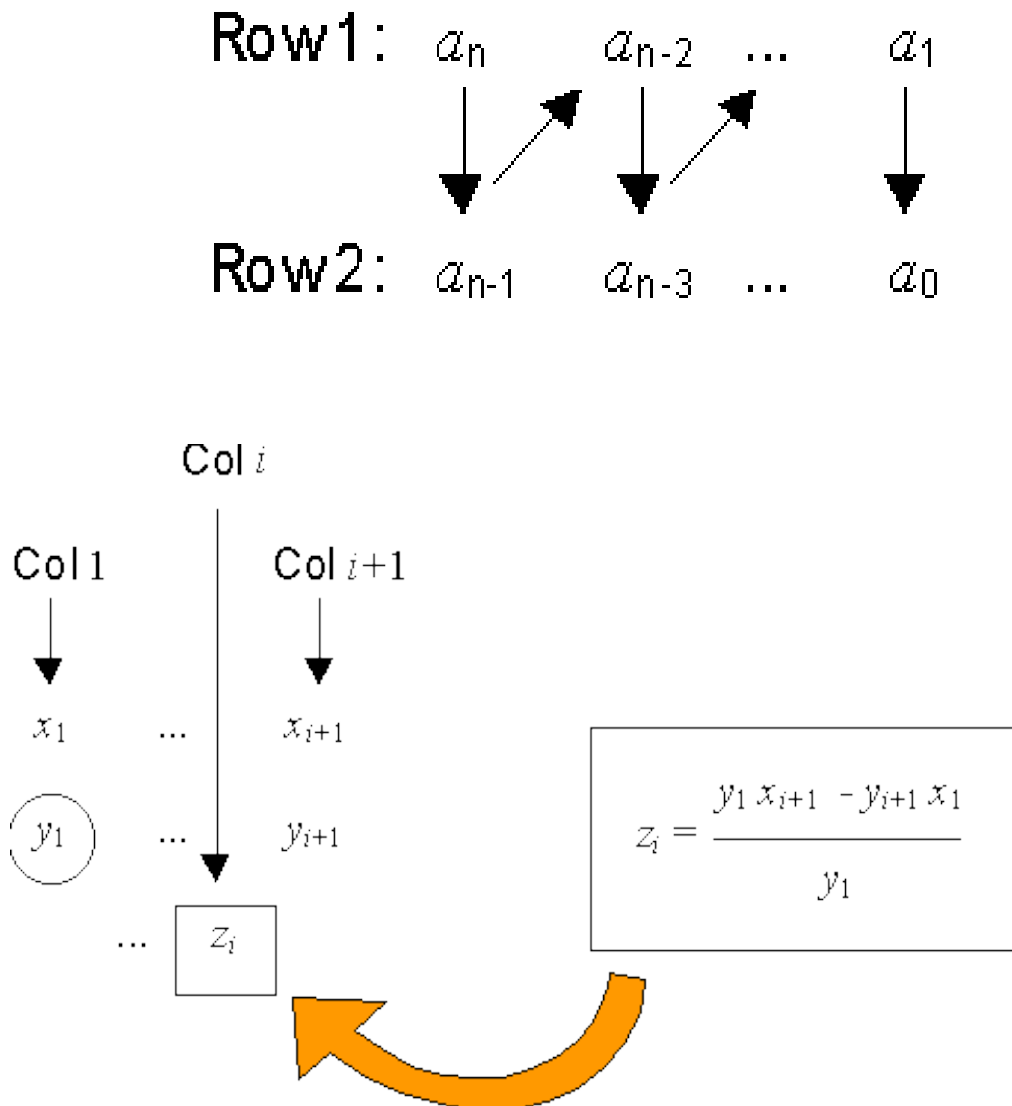
Arrays were made for each type of geoclassified LULC data type in each 5m polygon employing:

```
>>>x = np.array([1,2,3])  
>>>x.dtype  
dtype('int64')  
>>>x = np.array([0.1,0.2,0.3])  
>>>x  
array([ 0.1,  0.2,  0.3])  
>>>x.dtype  
dtype('float64')  
>>>x = np.array([1,2,3],dtype='float64')  
>>>x.dtype  
dtype('float64')
```

There were several convenience functions for making arrays including 0=no habitats/ 1 = habitat in a binomialized, logistic interpolation with az value generated per grid-cell and neighboring grid cell quantitated interaction which was written for each polygon as:

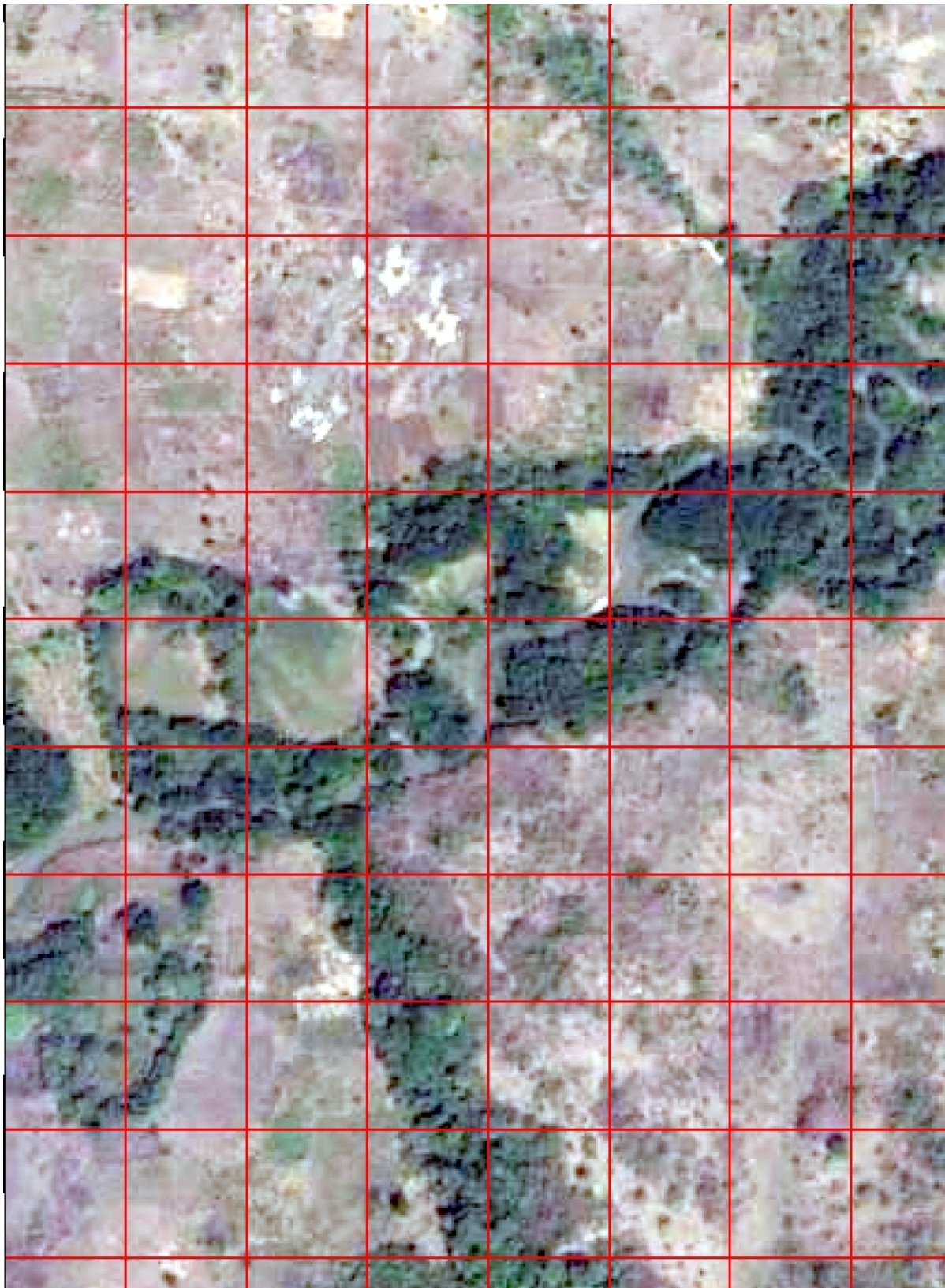
```
>>>x  
array([[ 0.,  0.,  0.,  0.],  
       [ 0.,  0.,  0.,  0.],  
       [ 0.,  0.,  0.,  0.]])  
>>>x  
array([[ 1.,  1.,  1.,  1.],  
       [ 1.,  1.,  1.,  1.],  
       [ 1.,  1.,  1.,  1.]])
```


Figure 15: Interpolation simulations of endmember LULC signatures using arrays run through each row and column of the grid matrix overlaid onto the 5m Rapid Eye TM DRC polygons with Z scores for positively autocorrelated non-habitat signature feature attributes



Based on the LULC signature iterative interpolation of the 5m endmember signatures, no cross-border, *S. damnosum* s.l. immature habitat, breeding foci were remotely identifiable within each grid-stratified DRC geoclassifiable polygon. The forecast vulnerability, remotely sensed, eco-epidemiological, capture point model revealed a moonscape land cover in both DRC polygo

Figure 16: Moonscape land cover in the 5m resolution 5m DRC study site





Discussion

The CATMOD procedure provided a wide variety of categorical and binary explanatory, endmember, LULC, data analyses, many of which were generalizations of the continuous data in the *S. damnosum* s.l. immature, habitat identification, exploratory analysis methods. In the analysis of variance, for example, the partitioning of the LULC variation in each Rapid Eye™, DRC, geoclassified polygon was optimally tabulated amongst the means into various sources. Here, the term analysis of variance was used to denote the analysis of response in the remotely specified, microtopographic LULC diagnostic, wavelength 5m, resolution, radiance functions in each polygon and the partitioning of the variation amongst the functions into various unbiased sources. The response functions were then interpreted as mean scores since the dependent variables in the multivariate LULC analyses were ordinally scaled. Marginal probabilities and cumulative logits were also optimally tabulated for each stratified, gridded, DRC polygon. We incorporated the essential remote microtopographic information (e.g., percent of uncanopied, trailing vegetation) from the wavelength, spectral, frequency variables in each geoclassified LULC in each eco-georeferenced DRC polygon.

PROC CATMOD fits a linear LULC model to functions of the response spectral wavelength frequencies employing the 5m sensor geo-spectrally quantitated data LULC in each DRC polygon. Log-linear modelling, and a formal repeated measurement analysis was also conducted employing the wavelength response data as the dependent variable in the immature habitat identification model. Log-linear analysis examines the relationship between more than two categorical variables [10]. Both models were tested to find the most parsimonious (i.e., least complex) model that best accounted for the variance in the observed, wavelength, LULC frequencies. For example, the log-linear model analysis in PROC CATMOD quantitated multiple, resampled, cross-border, eco-georeferenceable, capture point, *S. damnosum* s.l., African, immature, riverine tributary, breeding foci, LULC population variables by employing the POPULATION statement. By including the immature habitat, identification, vulnerability, endemic model effects on the right side of the MODEL statement that contained the independent variables, the rendered forecasts (covariates of statistical significance level with a 95% confidence interval) revealed LULC wavelength predictors.

Backward elimination was employed to determine which of the immature habitat model components were necessary to be retained in order to best account for the 5m geoclassified LULC data in each polygon. Backward elimination, involves starting with all candidate variables, testing the deletion of each variable using a chosen model fit criterion, deleting the variable (if any) whose loss renders the most statistically insignificant deterioration of the model fit, and repeating this process until no further variables can be deleted without a statistically significant loss of fit [74]. [11] employed a backward stepwise regression model process to tease out multicollinearity in an empirical dataset of African, riverine, tributary ecosystem, immature habitat. [75] computed percentage points of the multiple correlation coefficient by simulation and showed that a final regression obtained by selection methodology, said by the F-procedure to be significant at 0.1%, was in fact only significant at 5%. When estimating the degrees of freedom, the number of the candidate independent explanatory variables in a cross-border, *S. damnosum* s.l., African, riverine, tributary, moderate resolution, immature habitat, eco-epidemiological, capture point, the best fit selected may be smaller than the total number of final model spectral wavelength, frequency uncoalesced, geoclassifiable LULC variables, causing the fit to appear better than it is when adjusting the r^2 value. It is important to consider how many degrees of freedom have been used in the entire immature habitat, identification, forecast, vulnerability model, not just count the number of immature capture point, geosampled independent variables in the resulting fit. Models that are created may be over-simplifications of the real models of the data. Such criticisms, based upon limitations of the relationship between a model and procedure and data set used to fit it, may be addressed by verifying the model on an independent remotely sampled cross-border, African riverine, tributary, moderate resolution, LULC dataset, as in the PRESS procedure. In statistics, the predicted, residual, error, sum of squares (PRESS) statistic is a form of cross-validation used in regression analysis to provide a summary measure of the fit of a model to a sample of LULC observations that were not themselves used to estimate the model calculated as the sums of squares of the prediction residuals for those observations [10]. Here a fitted, eco-georeferenced, cross-border, *S. damnosum* s.l. eco-epidemiological, immature habitat, identification model having been produced, each erroneous covariate term was removed and the model was refitted using the remaining LULC observations.

In PROC CATMOD the following estimation methods may be employable for constructing a wide range of general, linear, eco-georeferenceable, cross-border, *S. damnosum* s.l. African, riverine, tributary, breeding foci, eco-endemic, moderate resolution, immature habitat, identification models including weighted



least squares (WLS) estimation of LULC eco-epidemiological, parameters and maximum likelihood estimation employing 5m wavelength frequency parameters for log-linear models and the analysis of generalized logits. There would be stipulations, however (e.g., each quantized 5m geoclassifiable, microtopographic LULC effect must include the `_RESPONSE_` keyword). For example, suppose the dependent variables $r1$ and $r2$ in a cross-border, African, riverine, tributary, seasonal, hyper productive, *S. damnosum* s.l. breeding foci, 5m, grid-stratified, endmember polygon dichotomous, and the independent variable group has three levels in an immature habitat, identification, forecast, vulnerability model. Then the following statements may specify a saturated sub-model (e.g., three degrees of freedom for `_RESPONSE_` and six degrees of freedom for optimally quantitating the interaction between `_RESPONSE_` and LULC group) employing the following statement:

```
proc cat mod;
  LULC weight wt.;
  S. damnosum s.l. habitat id model r1*r2=_response_group*_response_;
  loglin r1|r2;
run;
```

From another point of view, `_RESPONSE_*group` can be regarded as a main effect in a geoclassified, moderate resolution group, in a black fly, cross-border, forecast, vulnerability, moderate resolution, eco-epidemiological, forecast, vulnerability, geoclassified, LULC model employing response, 5m functions. Whilst `_RESPONSE_` can be regarded as an intercept effect with respect to the functions in a robust, eco-georeferenceable, seasonal, hyperproductive, eco-epidemiological, *S. damnosum* s.l. African, riverine tributary, moderate resolution, eco-epidemiological, eco-georeferenceable, capture point the statements would render essentially the same results as a logistic analysis which could be written as:

```
proc catmod;
  LULC weight wt.;
  S. damnosum s.l., habitat id model r1*r2=group;
run;
```

The ability to model the covariate interaction terms between the independent and the dependent variables in an eco-epidemiological, capture point, cross-border, oviposition, entomological, forecast, vulnerability, black fly, eco-epidemiological, eco-georeferenceable, moderate resolution, LULC, regression model becomes particularly useful when a reduced model is specified for the immature habitat explanatory dependent variables. For example, the following statements can specify an immature, cross-border, *S. damnosum* s.l., capture point, habitat identification model with two degrees of freedom for `_RESPONSE_` (one for $r1$ and one for $r2$) and four degrees of freedom for the interaction of `_RESPONSE_*LULC group`:

```
proc catmod;
  LULC weight wt.;
  S. damnosum s.l., habitat id model r1*r2=_response_group*_response_;
  loglin r1 r2;
run;
```

The likelihood ratio goodness-of-fit statistic (three degrees of freedom) would then test the hypothesis that $r1$ and $r2$ are independent in each of the three groups in the cross-border, African riverine tributary, geoclassified, moderate resolution, Rapid Eye™ 5m, LULC, *S. damnosum* s.l., immature, breeding, foci, probabilistic paradigm.

An iterative proportional fitting (IPF) algorithm may fit a diagnostic, hierarchical, log-linear, geoclassifiable, moderate resolution, Rapid Eye™ 5m, geoclassifiable, LULC, *S. damnosum* s.l., cross-border, African, riverine tributary, forecast, vulnerability, eco-epidemiological, model with no independent variables and no immature population variables in Geostatistical Analyst™. The advantage of IPF over the Newton-Raphson (NR) algorithm and over the WLS method for optimally regressively quantitating cross-border, 5m, LULC spectral, uncoalesced, wavelength frequencies is that when the contingency table for the remotely sensed, entomological, capture point, vector arthropod, breeding foci, is quantifiable geovisually, the vulnerability eco-epidemiological, forecasts (e.g., targeted hyperproductive eco-georeferenceable, seasonal foci) would have several dimensions that vary over time. In statistics, a contingency table is a type of table in a matrix format that displays the (multivariate) frequency distribution of the variables. [10]. Obtaining the log likelihood, the goodness-of-fit G^2 , and the predicted frequencies or probabilities without performing potential spectral,



wavelength, frequency, uncertainty-oriented, parameter estimation and covariance matrix calculations could lead to misspecifications in cross-border, African riverine, tributary, LULC, *S. damnosum* s.l., vulnerability wavelength, eco-epidemiological forecasts.

Optimally comparing two seasonal, cross-border, African riverine tributary, eco-georeferenceable, capture point, eco-epidemiological, breeding foci in forecast, vulnerability, ArcGIS models would require computing the likelihood ratio statistics which would test the significance of the contribution of remotely sensed, geoclassified, 5m, resolution, uncoalesced, LULC immature habitat, breeding foci, predictor variables in one model that may not occur in the regression of the other model variables. Alternatively computing predicted values of the uncoalesced LULC cell probabilities or frequencies for the eco-epidemiological, black fly, immature habitat, identification, eco-epidemiological model would lead to more robust forecasts (e.g., targeted, hyperproductive, uncanopied, targeted cross-border, *S. damnosum* s.l., trailing vegetation, eco-georeferenceable, immature, capture points).

In the PHREG Procedure, an onchocerciasis researcher or epidemiologist could let $L(\beta)$ be one of the explanatory, likelihood functions for remotely, robustly, identifying a spectral wavelength, frequency, Rapid Eye™ cross-border, eco-georeferenceable, seasonal, hyperproductive, eco-epidemiological, African, riverine tributary, breeding foci on an imaged, 5m geoclassified LULC. If he or she could let $l(\beta) = \log L(\beta)$ in the cross-border, immature, habitat paradigm, quantitate β such that $L(\beta)$ could be maximized, the process would optimally

finding the solution $\hat{\beta}$ to the likelihood forecast, vulnerability equations $\frac{\partial l(\beta)}{\partial \beta} = 0$. With $\beta^0 = \mathbf{0}$ as the initial solution, the iterative scheme in the entomological, black fly, vector, arthropod, Rapid Eye™, 5m, resolution, forecast, vulnerability, SAS/GIS, LULC model could then be expressed as

$$\hat{\beta}^{j+1} = \hat{\beta}^j - \left[\frac{\partial^2 l(\hat{\beta}^j)}{\partial \beta^2} \right]^{-1} \frac{\partial l(\hat{\beta}^j)}{\partial \beta}$$
 The term after the minus sign would be the Newton-Raphson step. If the likelihood function evaluated at $\hat{\beta}^{j+1}$ is less than that evaluated at $\hat{\beta}^j$, then $\hat{\beta}^{j+1}$ should be recomputed using half the step size in the immature, eco-epidemiological, habitat, black fly, capture point, eco-epidemiological, forecast, vulnerability, model, construction process. Regardless, the iterative scheme would continue until optimal convergence is obtained—that is, until $\hat{\beta}^{j+1}$ is sufficiently close to $\hat{\beta}^j$. Thereafter, the maximum likelihood estimate of β would be $\hat{\beta} = \hat{\beta}_{j+1}$. As such, a seasonal, hyper productive, cross-border, *S. damnosum* s.l., immature habitat, African riverine, tributary, model-based, variance estimate of $\hat{\beta}$ would be obtainable by

inverting the information matrix [i.e., $\mathcal{I}(\hat{\beta}) \hat{V}_m(\hat{\beta}) = \mathcal{I}^{-1}(\hat{\beta}) = - \left[\frac{\partial^2 l(\hat{\beta})}{\partial \beta^2} \right]^{-1}$] in ArcGIS.

We employed an endmember, stochastic, signature, interpolator to krige the eigen-decomposed, 3-D DEM parameters and the trailing vegetation reference LULC, signatures in Geospatial Analyst™ for identifying any cross-border, eco-georeferenceable, riverine tributary, immature, capture point, *S. damnosum* s.l., breeding foci in the DRC, 5m, geoclassified, LULC polygons. Under suitable assumptions on the priors, Ordinary kriging renders unbiased, optimal, linear, endmember predictors and intermediate values from a stochastic iteration of a moderate resolution, partially canopied, orthogonally eigen-decomposed, *S. damnosum* s.l., capture point, immature habitat, target signal in ArcGIS [11]. Here the interpolation method did not forecast any cross-border, *S. damnosum* s.l., riverine, tributary habitats. Although the value of the uncoalesced, Rapid Eye™, immature habitat, interpolative, endmember LULC signature was robustly tabulated employing a weighted spectral average of the spatial filtered, orthogonal eigen-decomposed, vector, arthropod habitat, immature, moderate resolution, habitat, wavelength, spectral radiance, the interpolator did not eco-geographically iteratively geolocate any unknown, unsampled, immature habitats based on the signature function in the geoclassified neighborhood.

Although the constructed, eco-epidemiological, forecast, vulnerability, eco-georeferenceable, *S. damnosum* s.l., moderate resolution, capture point, immature habitat, identification model did not find any cross-border, breeding foci in the moderate resolution, 5m, DRC polygons, many tools and insights developed here may be applicable for future research for optimally remotely identifying this important vector arthropod species in these unstable ecosystems. For example, the Zonal tools in ArcGIS allowed performing the moderate resolution, eco-cartographic endmember, vegetation LULC classification signature interpolation where the



output was a result of computations performed on all 5m, resolution cells that belonged to each input zone in each geoclassified parcel within each Rapid Eye™ polygon. A zone was defined as being one single, geo-specified, eco-georeferenceable, DRC area of a particular geoclassified 5m, LULC value in each polygon. The three, Rapid Eye™, geoclassified LULC zones defined by raster feature datasets (bare soil, water, uncultivated vegetation) were well displayed. Rasters must be of integer type, and features must have an integer or string attribute field (www.esri.com).

The Zonal tools parsimoniously quantitated the geoclassified, Rapid Eye™, 5m, LULC properties based on geometry and shape, of the zone input which did not require any other inputs. The zonal tools employed the zone input to robustly define the geolocations for which the grid-stratified, landscape parameterizable covariates in the DRC polygons may have been geo-spatially associated with a seasonal, hyperproductive, cross-border, African, riverine tributary, habitats of immature *S. damnosum*. These tools calculated statistics employing LULC data and decomposed, spectral, wavelength frequencies. A Zonal tool filled the specified zones with the minimum value found all LULC zone boundaries.

Python scripts were employed for optimal remote revisualization of cross-border, *S. damnosum* habitats on geoclassified, moderate resolution, riverine, tributary LULCs which was written also in Numpy and matplotlib as well. Python is intended to be a highly readable language and is designed to have an uncluttered visual layout with fewer syntactic exceptions and special cases than C or Pascal (<https://www.python.org>). The most frequently employed plotting package in Python, matplotlib, is written in pure Python and is heavily dependent on NumPy (www.scipy.org)

Python to NumPy and SciPy (Scientific Python) are open-source add-on modules to Python that provide common mathematical and numerical routines in pre-compiled, fast functions which we employed to optimally spectrally quantitate the Rapid Eye™, 5m, geoclassifiable, wavelength, uncoalesced, LULC, radiance for remotely defining an eco-georeferenceable, *S. damnosum* s.l., African riverine, tributary, eco-epidemiological, capture point, breeding foci at the DRC study site. These data may grow into highly mature packages that provide functionality that meets, or perhaps exceeds, that associated with common commercial scripting languages. The NumPy (Numeric Python) package provided basic routines for manipulating large arrays and matrices of numeric, moderate resolution, oviposition, geoclassified, black fly, seasonal, 5m, LULC data.

The SciPy package extends the functionality of NumPy with a substantial collection of useful algorithms, like minimization, Fourier transformation, regression, and other applied mathematical techniques which may also aid in remotely identifying cross border, moderate resolution, imaged, *S. damnosum* s.l. immature habitats in African riverine tributary, ecosystems.

Here, NumPy targeted the CPython reference implementation of Python, which is a non-optimizing bytecode interpreter. Mathematical algorithms were written for this version of Python employing the compiled cross-border, geoclassified, *S. damnosum* s.l. decomposed, immature, capture point, eco-georeferenceable, LULC data. By providing multidimensional arrays and functions and operators that were implementable efficiently on arrays, we could conduct a robust microtopographic landscape, investigation which revealed there were no cross-border, *S. damnosum* s.l., immature habitat, capture points, at the eco-epidemiological, study site. The only requirement was rewriting some LULC codes, mostly inner loops using NumPy.

Using NumPy in Python may render functionality comparable to MATLAB for an onchocerciasis researcher or epidemiologist to perform a robust, forecast, eco-epidemiological, vulnerability, moderate resolution, microtopographic, geoclassifiable, endmember, LULC analyses for optimally identifying, seasonal, hyperproductive, breeding foci, cross-border, African, riverine, tributary, *S. damnosum* s.l., immature habitats. Since both systems are both easily interpretable and they both allow the user (onchocerciasis researcher or epidemiologist) to write fast programs, they may be employable in tandem for optimally identifying landscapes where these capture point, immature habitats reside. However one of the stipulations in the vector arthropod, African, riverine, cross-border, tributary, forecast, vulnerability, eco-epidemiological, uncoalesced, spectral wavelength, moderate resolution, immature habitat, identification model generation process in NumPy is that the operations must work on arrays or matrices instead of scalars. In comparison, MATLAB can employ a large number of additional toolboxes, notably Simulink, for remotely identifying cross-border, black fly, breeding foci on geoclassifiable, 5m, resolution, African riverine, cross-border, moderate resolution, geoclassifiable LULCs. Moreover, complementary Python packages are available; SciPy is a library that adds more MATLAB-like



functionality. Matplotlib is a plotting package that provides MATLAB-like plotting functionality. Internally, both MATLAB and NumPy rely on BLAS and LAPACK for efficient linear algebra computations

Linear Algebra, vector spaces and linear mapping may be robustly employable for optimally remotely detecting eco-epidemiological, seasonal, hyperproductive, cross-border, *S. damnosum* s.l. immature habitat, breeding foci in African politically unstable ecosystems. In so doing, set of sampled eco-epidemiological, eco-georeferenceable, geoclassified, breeding foci, immature habitats may satisfy a predictive, linear equation that may include forming a hyperplane of the sampled, cross-border *S. damnosum* s.l., in n -dimensional space. In geometry, a hyperplane is a subspace of one dimension less than its ambient space [7]. If a space in a cross-border black fly, capture point, eco-epidemiological, forecast, vulnerability, immature habitat identification model is 3-D then its hyperplanes may be the 2-dimensional LULC planes, while if the space is 2-dimensional, its hyperplanes may be the 1-dimensional habitat boundary lines (e.g. Spatially continuous unshaded canopy to discontinuous canopy) as eco-cartographically revealed.

Such an investigation may be initially motivated by a system of linear equations containing several unknowns for determining eco-geographic, geolocations of immature breeding foci, capture point, eco-georeferenceable, seasonal, hyperproductive, eco-epidemiological habitats in a cross-border African riverine tributary. Such equations may be naturally represented employing the formalism of matrices and vectors from linear algebra.

Linear algebra is central to both pure and applied mathematics. For instance, abstract algebra arises by relaxing the axioms of a vector space, leading to several generalizations. Functional analysis studies the infinite-dimensional version of the theory of vector spaces. Combined with calculus, linear algebra facilitates the solution of linear systems of differential equations which may then be usable for robustly remotely identifying seasonal, eco-georeferenceable, cross-border, *S. damnosum* s.l. breeding foci

The core functionality of NumPy for remote identification of an eco-epidemiological, eco-georeferenceable, seasonal, hyperproductive, cross-border, *S. damnosum* s.l., immature, seasonal, hyperproductive, capture point, breeding foci, in an African, riverine, tributary ecosystem is its "ndarray", for optimally quantitating n -dimensional array, immature, habitat, data structures (e.g., uncanopied, trailing vegetation, geoclassified Rapid Eye™ LULCs). These arrays are strided views on memory; thus, any time series, explanatory, immature habitat, identification model constructed in ArcGIS may be optimized. In contrast to Python's built-in list data structure (which, despite the name, is a dynamic array), these arrays are homogeneously typed. Unfortunately for constructing a robust, cross-border, African, riverine tributary, *S. damnosum* s.l. immature habitat, signature identification, model all elements of a single array must be of the same type. Such arrays can also be views in memory buffers allocated by C/C++, Cython, and Fortran extensions to the CPython interpreter without the need to copy the geoclassified, 5m resolution, wavelength, endmember, LULC data for rendering a degree of compatibility with existing numerical libraries in ArcGIS. This functionality is further exploitable by the SciPy package, which may wrap a number of such libraries (notably BLAS and LAPACK) for aiding in cross-border, *S. damnosum* s.l., Rapid Eye™, immature habitat, capture point, seasonal, eco-georeferenceable, eco-epidemiological, breeding foci, immature, habitat identification. NumPy has built-in support for memory-mapped ndarrays (www.numpy.org)

Importantly NumPy's arrays for compiling moderate resolution, geoclassifiable LULCs for identifying cross-border, *S. damnosum* s.l., seasonal, hyperproductive, breeding foci must be views on contiguous memory buffers. A replacement package called Blaze attempts can overcome this limitation. Algorithms that are not expressible as a vectorized operation will typically run slowly because they must be implemented in "pure Python", (<https://www.python.org>) while vectorization may increase memory complexity of some operations for constructing, robust, cross-border, African, riverine tributary, *S. damnosum* s.l. habitat identification from constant to linear, because temporary arrays must be created that are as large as the inputs. Runtime compilation of numerical code has been implemented to avoid these problems; open source solutions that interoperate with NumPy include `scipy.weave`, `numexpr` and `Numba`. Cython is a static-compiling alternative to these.

As Map Algebra has been integrated in Python, all the functionality of Python and ArcPy and its extensions (modules, classes, functions, and properties) are parsimoniously employable for conducting a robust, 5m, LULC analyses on the Rapid Eye™, DRC polygons. Map Algebra is a simple and powerful algebra with which an onchocerciasis researcher or epidemiologist can execute all Spatial Analyst™ tools, operators, and functions to perform geographic analysis (www.esri.com). Map Algebra is available through the Spatial Analyst



TM module; an extension of the ArcPy Python site package. As Map Algebra, has been integrated in Python, all the functionality of Python and ArcPy and its extensions (modules, classes, functions, and properties) is available for constructing, an optimal, capture point, cross-border, *S. damnosum* s.l., paradigm or any vector arthropod, forecast, vulnerability, eco-georeferenceable, eco-epidemiological, moderate, resolution, LULC model for remote immature habitat identification.

Here, Spatial Analyst tools were accessed through an algebraic format. That is, across-border, *S. damnosum* s.l. habitat object whose name was identified to the left of an equal sign was created based on a tool or operator stated to the right of the equal sign as in:

```
from arcpy.sa import *  
outRas = Slope("indem")
```

The above statement calculated the slope for each cell in a 5m, resolution, DEM dataset and created a raster object called outRas to store the entomological, forecast, vulnerability, eco-epidemiological, remotely sensed, LULC model, residual results. By so doing, the 3-D, parameter was infused into a remotely sensed, LULC, regression equation to determine the level of statistical significance of the estimator.

Fractional vegetation cover (FVC) one of the most critical signature LULC parameters in monitoring vegetation status was estimated in the DRC polygons employing two unmixed, spectral endmembers in the 5m, Rapid Eye TM, LULC image. The endmembers were based on the geoclassified bare soil, water and uncanopied trailing green vegetation LULCs. The spectral properties of the two endmembers were determined based on remote measurements, estimated using additional data sources (e.g., soil databases and land cover maps), or extracted directly from the imagery (e.g., slope coefficients). Most FVC estimation approaches do not consider that the spectral properties of LULC endmembers may vary across geospacer [8]. However, due to local differences in climate, soil type, vegetation species, etc., the spectral characteristics of the uncanopied trailing green vegetation LULCs at the DRC cross-border, eco-epidemiological, study site exhibited positive spatial autocorrelation. We took these local variations into account for estimating FVC in the DRC polygon LULCs for optimally remotely identifying geospatial, eco-georeferenceable clusters of cross-border black fly habitats.

DEMs are usually classified as either sinks or peaks. A sink is an area surrounded by higher elevation values and is also referred to as a depression or pit. This is an area of internal drainage. Many sinks are imperfections in the DEM (www.esri.com). Likewise, a spike or peak is an area surrounded by cells of lower value. These are more commonly natural features and are less detrimental to the calculation of flow direction.

Errors such as these, especially sinks, should be removed before attempting to derive any surface information. Sinks, being areas of internal drainage, prevent downslope flow routing of water. Learn more about removing or filling sinks

The number of sinks in each DEM is normally higher for coarser resolution DEMs. Another common cause of sinks results from storing the elevation data as an integer number. This can be particularly troublesome in areas of low vertical relief. It is not uncommon to find 1 percent of the cells in a 30-meter-resolution DEM to be sinks. This can increase as much as 5 percent for a 3 arc-second DEM.

DEMs may also contain noticeable horizontal striping, a result of systematic sampling errors when creating the DEM. Again, this is most noticeable on integer data in flat areas. The hydrologic analysis functions described here are designed to model the convergence of flow across a natural terrain surface for eco-cartographically interpolating a uncoalesced LULC 5m signature. There is an assumption that the surface contains sufficient vertical relief that a flow path can be determined. The functions assume that water can flow in from many cells but out through only one cell.

The FVC extraction method in ArcGIS was also employed an invariant $NDVI_{soil}$ for determining if there existed any riverine, tributary, *S. damnosum* s.l., immature habitats based on the 5m signal in the DRC study site polygons. The NDVI is a simple graphical indicator that can be employed to analyze remote sensing LULC measurements, typically but not necessarily from a space platform, and assess whether the target being observed



contains live green vegetation or not [68]. NDVI_{soil} mapping methods estimated FVC in the DRC study site Rapid Eye™ polygons. The method employed the 5m, NDVI model along with information on LULC to estimate NDVI_{soil} for optimally identifying immature, capture point, habitat, LULC structures associated with black flies (e.g., un-shaded, riffle water, partially canopied, Precambrian rock, hanging, trailing vegetation). The influence of variations of NDVI_{soil} derived from the ArcGIS land surface model based on FVC estimation was employed for categorical mapping discontinuously canopied, vegetation and bare soil LULC signatures types at the DRC eco-epidemiological, study site. These LULC types have been used for identification of multiple, oviposition, *S. damnosum* s.l., endemic, breeding foci, throughout northern Uganda [11]. The signal was based on 5m Red, Blue and Green (RGB) spectral values.

The 5m, cross-border, eco-epidemiological, LULC, forecast, vulnerability analysis revealed that there was no *S. damnosum* s.l., immature habitats based on the NDVI_{soil} signal. The FVC estimation introduced by NDVI_{soil} variability analyses revealed -0.71 using a spatial scale where bare soil LULC was delineated closer to -1.0 and partially canopied, trailing vegetation LULC was between .7 to 1.0. Based on the NDVI_{soil} signal there was no reflectance occurring in any geoclassified, 5m resolution, LULC vegetation, types for identifying eco-epidemiological, hyperproductive, seasonal, eco-georeferenceable, *S. damnosum* s.l. habitats. There was little to none discontinuous, trailing, hanging vegetation, turbid water or partially canopied, Precambrian rocks along the riverine tributaries. Although canopy gaps were eco-cartographically identifiable along the meandering riverine banks, in the DRC polygon employing a FVC, signal proxy, the 5m, RGB signature extracted from a capture point, *S. damnosum* s.l., immature, endemic foci geosampled in northern Uganda revealed no habitats along the Congolese tributaries.

Values of SAVI, calculated from the Rapid Eye™ satellite information were successfully overlaid onto the eco-georeferenced LULC data in the DRC polygons. The VI revealed the geoclassified LULC with low, intermediate and heavy vegetated values. An eco-cartographic, illustrative database was then generated for the cross-border, study site, 5m polygons with the mean, minimum, maximum, and standard deviations for the Rapid Eye™ SAVI. The VI datasets for the DRC study site were then merged with the geoclassified, eco-epidemiological, 5m LULC datasets. Although the VI was sensitive to the presence of uncanopied vegetation, bare soil and water classes, no *S. damnosum* s.l., breeding foci was identified employing the vegetation signal. The change in the soil background caused by the transition in LULC throughout did not alter the red and NIR reflectance and calculated SAVI. Visually the data suggested that there was no higher soil influences in the SAVI as compared with the NDVI

It was of interest to determine how the Red Edge band inclusion into the VI would identify the 5m resolution LULC's for making inferences of immature *Simulium* immature habitat abundance. Red Edge refers to the region of rapid change in reflectance of vegetation LULC in the NIR range of electromagnetic spectrum. Chlorophyll contained in vegetation absorbs most of the light in the visible part of the spectrum but becomes almost transparent at wavelengths greater than 700 nm [8]. This way, vegetation cellular structure takes its major part in the reflectance because each cell acts like an elementary corner reflector [76]. This LULC reflectance change in Chl-a reflectance was captured between 680 nm to 730 nm for the uncanopied, LULC, *S. damnosum* s.l., eco-georeferenced, capture point. Typically, ~1% of the solar energy captured by plants is re-emitted by chlorophyll as fluorescence which provides a distinct 'glow' at wavelengths of ~690–800 nm that is quite specific to green plants. [77].

A graph of the photosynthetically active radiation (PAR) spectral LULC region in the Rapid Eye™ DRC polygons was then determined for identifying the cross-border, eco-georeferenceable, eco-epidemiological, *S. damnosum* s.l., immature habitats at the eco-epidemiological study site. Photosynthetically active radiation, often abbreviated PAR, designates the spectral range (wave band) of solar radiation from 400 to 700 nanometers that photosynthetic organisms are able to use in the process of photosynthesis [8]. There are two common measures of PAR, photosynthetic photon flux (PPF) and yield photon flux (YPF). PPF values all LULCs mapped from the from 400 to 700 nm equally, while YPF weights are in the range from 360 to 760 nm based on the geoclassified endmember signature datasets of the plant's LULC photosynthetic response [8]. PAR may aid in biophysically describing PPF in an endmember, LULC, Rapid Eye, iteratively interpolated, 5m, spectral endmember signature.

ENVI distinguishes between different LULC wavelengths between 400 and 700 nm, and will assume that wavelengths outside this range have zero photosynthetic action. If the exact spectrum of the light is known, the photosynthetic photon flux density (PPFD) values in $\mu\text{mol/s}$ can be modified by applying different



weighting factor to different wavelengths in a Rapid Eye™, cross-border, *S. damnosum* s.l., trailing vegetation, partially uncanopied, forecast, vulnerability probabilistic paradigm In the graph the eco-epidemiological, immature habitat identification model may reveal that photons around 610 nm (orange-red) have the highest amount of photosynthesis per photon. However, because short-wavelength photons carry more energy per photon, the maximum amount of photosynthesis per incident unit of energy at an uncoalesced, Rapid Eye™ wavelength may be around 650 nm (deep red).

In terrestrial plants in the ecogeoreferenceable, 5m resolution DRC polygons reflection flux, canopy leaves absorbed mostly red and blue light in the first layer of photosynthetic cells probably due to Chl-*a* absorbance. Green light, however, penetrates deeper into the leaf interior and can drive photosynthesis more efficiently than red light [76]. Because green and yellow wavelengths can transmit through chlorophyll and the entire leaf itself, they may play a crucial role in quantitating growth beneath an eco-georeferenceable, capture point, eco-epidemiological, hyperproductive, cross-border, *S. damnosum* s.l., habitat capture point, plant canopy. These 5m, LULC wavelength indicators may aid in identification of breeding foci of cross border, riverine, tributary, agro-village, *S. damnosum* s.l. in African riverine tributaries.

Exact statistics were useful for determining if spectral similarities between the asymptotic assumptions in the 5m wavelength radiance was met in each grid-stratified, eco-georeferenced, DRC, polygon, geo-specified LULC. The asymptotic *p*-values were close approximations for the true *p*-values in the kappa coefficients. Standard asymptotic methods involve the assumption that the test statistic follows a distribution when the sample size is sufficiently large [6]. Even though there was a level of similarity between the uncoalesced, 5m, spectral, wavelength, geoclassified, LULC, endmember signature, dataset the asymptotic results were not valid, for identifying any *S. damnosum* s.l., immature habitats in the DRC 5m, grid-stratified polygons. Asymptotic results might be unreliable when the distribution of the data is sparse, skewed, or heavily tied [54, 78].

The Exact computations generated for each 5m, LULC, geo-classification in the DRC polygons was based on the statistical theory of exact conditional inference for contingency tables as reviewed by [79]. Exact statistics were rendered via PROC FREQ tests. For one-way tables, PROC FREQ provided exact *p*-values for the binomial proportion tests and the chi-square goodness-of-fit test between the 5m, geoclassified, Rapid Eye™ geoclassified LULCs. Exact (Clopper-Pearson) confidence limits were available for parsimoniously conducting a binomial proportion LULC analyses. For two-way tables, PROC FREQ provides exact *p*-values for the following tests: Pearson chi-square test, likelihood ratio chi-square test, Mantel-Haenszel chi-square test, Fisher's exact test, Jonckheere-Terpstra test, and Cochran-Armitage test for optimally quantitating spectral frequency trends between the geoclassified LULCs associated to an ecogeoreferenceable, eco-epidemiological, seasonal, hyperproductive, cross-border, capture point, *S. damnosum* s.l., immature, breeding foci. However, the primary simple kappa coefficient, and weighted kappa coefficients revealed that there was a significant level of spectral similarities between the geoclassified LULC indices in the DRC, 5m, Rapid Eye™ polygons.

PROC FREQ may compute exact *p*-values for tests of the following statistics: Kendall's tau-b, Stuart's tau-c, Somers' $D(C|R)$, Somers' $D(R|C)$, Pearson correlation coefficient, Spearman correlation coefficient which may be usable for optimally determining LULCs wavelength radiance similarities in moderate resolution, geoclassifiable, uncoalesced, *S. damnosum* s.l., immature habitat, remotely sensed, cross-border, African, riverine, ecosystem model, parameter estimator, eco-epidemiological datasets. For 2×2 tables, PROC FREQ provides McNemar's exact test and exact confidence limits for the odds ratio. PROC FREQ also provides exact unconditional confidence limits for optimally quantitating the proportion (risk) difference for computing the relative risk for identifying geoclassifiable LULCs associated to a capture point, eco-georeferenceable, cross-border, African, riverine, tributary, black fly, seasonal, breeding foci. For stratified 2×2 tables, PROC FREQ can provide Zelen's exact test for equal odds ratios, exact confidence limits for the common odds ratio, and an exact test may be also incorporated into a cross-border, moderate resolution, geoclassifiable, eco-epidemiological, LULC, *S. damnosum* s.l., immature habitat, forecast, vulnerability, identification, model for determining seasonal geolocations of eco-georeferenceable, hyperproductive, eco-georeferenceable, African, riverine tributary, capture points.

We generated Agree statistics to quantitate the level of dissimilarities between the 5m, resolution, wavelength, LULC classes in the DRC, Rapid Eye™, grid-stratified, 5m polygons. The AGREE statistics were defined only for square tables, where the number of rows equaled the number of columns. If a table is not



square, PROC FREQ does not compute AGREE statistics for the table(<http://support.sas.com>). If the corresponding table contains r rows but only $r-1$ columns, the table is not square and PROC FREQ does not compute AGREE statistics (www.sas.edu). To create a square table in the explanatorial, cross-border, Rapid Eye™, capture point, *S. damnosum* s.l., immature habitat, identification model we employed the ZEROS option in the WEIGHT statement, which included zero-weight, 5m, resolution, orthogonally decomposed, LULC observations. The input data specified the ZEROS option; the analysis included all rating levels.

By default, PROC FREQ ignored the remotely sensed, Rapid Eye™, explanatorial, LULC, eco-georeferenceable, cross-border, *S. damnosum* s.l. immature habitat, eco-epidemiological, eco-georeferenceable observations with zero weights. If the ZEROS option is specified, frequency and cross-tabulation tables may display any level corresponding to observations with zero weights (www.sas.edu). Without the ZEROS option, PROC FREQ will not process moderate resolution, eco-dereferenceable, cross-border, or non-cross-border, African, riverine, tributary, *S. damnosum* s.l., immature, eco-epidemiological, immature habitat, capture point, LULC 5m observations with zero weights. With the ZEROS option, PROC FREQ includes levels with zero weights in the chi-square goodness-of-fit test for one-way tables. Also, PROC FREQ includes any levels with zero weights in binomial computations for one-way tables (www.sas.edu). This makes it possible to compute binomial tests and render estimates when the specified level contains no LULC, hyperproductive, observations with positive weights in a cross-border, African, riverine, tributary, hyperproductive, seasonal, *S. damnosum* s.l., eco-epidemiological, forecast, vulnerability, immature, habitat, identification model.

For two-way tables, the ZEROS option can enable computation of kappa statistics when there are levels that contain no capture point, oviposition, eco-epidemiological, *S. damnosum* s.l., forecast, vulnerability, seasonal, hyperproductive, breeding foci, moderate resolution, eco-georeferenceable, LULC observations with positive weight. Note that even with the ZEROS option, PROC FREQ will not compute the CHISQ or MEASURES statistics for two-way tables when constructing a moderate resolution, cross-border, *S. damnosum* s.l., remotely sensed, forecast, vulnerability, immature, habitat, identification, LULC model when the table has a zero row or zero column because most of these statistics are undefined in this case. The ZEROS option will invoke the SPARSE option in the TABLES statement, which may include table cells with a zero frequency count in the LIST output and in the OUT= dataset. By default, without the SPARSE option, PROC FREQ will not include zero frequency cells in the LIST output or in the OUT= dataset in the cross-border, immature habitat, *S. damnosum* s.l., identification, eco-epidemiological, forecast, vulnerability model. If an onchocerciasis researcher or epidemiologist specifies the ZEROS option in the WEIGHT statement but does not want the SPARSE option, he or she can specify the NOSPARSE option in the TABLES statement.

By default, PROC FREQ will not process capture point, explanative, eco-georeferenceable, uncoalesced, eco-epidemiological, cross-border, *S. damnosum* s.l., moderate resolution, geoclassified, LULC observations that have weights of 0 because these observations do not contribute to the total frequency count, and because many of the tests and measures of association are commonly undefined for tables that contain zero-weight rows or columns. However, kappa statistics are defined for tables that contain zero-weight rows or columns, and the ZEROS option enables onchocerciasis researchers and epidemiologists to input zero-weight, moderate resolution, grid-stratified, 5m, LULC cross-border, *S. damnosum* s.l., African, riverine, tributary, capture point, breeding foci, eco-georeferenceable, observations and construct the tables needed to compute kappa statistics.

Thereafter we employed spatial interpolation (Ordinary kriging) to predict variations (canopy discontinuity) in the spectral characteristics of bare soil, water and uncanopied trailing green vegetation, geoclassified LULCs. When the spatially-interpolated values were used in place of scene-invariant endmember values to estimate FVC in the Rapid Eye™ 5m image, the accuracy of FVC estimates increased, providing evidence that the photosynthetic product may be useful to consider the effects of spatial autocorrelation for spectral mixture analysis for an eco-georeferenceable, cross-border, African, riverine tributary, *S. damnosum* s.l. immature, eco-epidemiological, capture point., breeding foci.

In remotely sensed, eco-epidemiological, forecast, compartmentalizable, eco-georeferenceable, moderate resolution, LULC models of capture point, *S. damnosum* s.l., hyper productive, breeding foci and their transmission potentiality based on larval abundance and eco-georeferenceable, grid-, stratified, distance to village centroid covariates, the fundamental process to be described may be time. This is because when a



pathogen appears in a host community, it partitions individuals in the community into categories depending on parasite density inside them and the type of infection [5]. These categories or compartments in a black-fly, vector, arthropod, entomological, forecast, vulnerability, probabilistic time series, eco-epidemiological, LULC risk model may be thus represented by standard notation of a pseudo susceptible-exposed-infectious-removed (S-E-I-R) model after the pioneering work of [80] in ArcGIS.

ArcGISModel Builder. LULCtools may be employable for implementing targeted larval control strategies (e.g., prioritization of stratified eco-georeferenceable, geospatial clusters of seasonal, hyper productive, LULC capture points) employing a regressively forecasted dataset of geo-visualizable, *S. damnosum* s.l. breeding foci, cross-border, seasonal, hyperproductive, immature habitats in a moderate resolution, endemic transmission, vulnerability model. A compartmental mathematical, moderate resolution, LULC, immature habitat identification model, may simulate eco-georeferenceable, agro-village complexes and black fly habitats along a cross-border, African, riverine environment using a SEIR framework in Geospatial Analyst™. A regression model may be also created in Geostatistical Analyst™ with the monthly larval abundance counts from these remotely identified LULC foci employing SEIR proportions and moderate resolution, uncoalesced, parameterizable, eco-cartographic, endmember, geoclassifiable covariates as input factors (i.e., independent variables). The results may be field-validated (“ground-trothed”) to assess the accuracy of the epidemic model before application to determine infection estimation in an African riverine, tributary ecosystem cross border landscape based on remotely identified breeding foci.

An ArcGIS spatial SEIR model for onchocerciasis infection estimation based on remotely stratified, grid-based, *S. damnosum* s.l., cross-border, breeding foci may also quantitate human-black fly contact probability which may be accounted for in a Poissonian regression count-variable network. The Poisson model employs a dependent variable that is an actual count rather than a log-transformed variable (e.g., logistic, binomialized, dichotomous, dependent variable where 0=0 and 1 = regressed values >0). Unfortunately violations of the Poissonian assumptions that the variance is equal to the mean[81] are common in eco-epidemiological, regression forecast, vulnerability, vector arthropod –related, remotely sensed, LULC paradigms. In such circumstances a negative binomial with a non-gamma distributed, non-homogenous mean can compensate for the over Poissonian variation (e.g., outliers) in the model biased estimators. In so doing, the regressed model, eco-georeferenceable, foci predictors may be exported into a SAS/GIS module where a robust eigenfunction algorithm may orthogonally decompose the model linearly adjusted variables into a weighted autocorrelation model spatial filters. In so doing, all clustering tendencies in the immature habitat datasets will be determined based on a product moment correlation coefficient [31, 82, 83]. Temporal-spatial abundance and distributions of cross-border, *S. damnosum* s.l., breeding foci, capture points may reveal substantial risk in specific moderate resolution geoclassified, African, cross-border, riverine, eco-georeferenceable, LULC geoclassifications (e.g. Unshaded trailing vegetation along tributary corners where high turbidity exists).

An eco-epidemiological, SEIRsforecast, vulnerability, ArcGIS model may remotely identify *S. damnosum*s.l., capturepoint, breeding foci, habitats on seasonal, moderateresolution, geoclassified LULCs employing a fraction of the susceptible (*S*) population in a riverine, agro-village, community in a cross-border, eco-georeferenceable, conflict-ridden, tributary zone may be labeled as exposed (*E*) to infection, (*I*). Some from the *I* class may recover from the disease, and become part of the *R* class. The Arcpy, black fly, eco-epidemiological, eco-georeferenceable, immature, habitat identification SEIR model framework could include

$$\begin{aligned}\frac{dS}{dt} &= B - \beta SI - \mu S \\ \frac{dE}{dt} &= \beta SI - (\nu + \mu) E \\ \frac{dI}{dt} &= \nu E - (\gamma + \mu + \delta) I \\ \frac{dR}{dt} &= \gamma I - \mu R\end{aligned}$$

with $S > 0, E \geq 0, I > 0, R \geq 0$. Here, B would be new recruitment by birth etc. Since an onchocerciasis epidemic occurs in a long-time, an researcher or epidemiologist could ignore loss of temporary immunity. Therefore, there would be no transfer from the recovered compartment back to the susceptible compartment in the model.



Henceforth, this is the reason SEIR does not appear in any of the first three black fly, immature habitat identification, predictive equations above. By analyzing the first three equations a new reduced ArcGIS, eco-epidemiological, forecast remote sensing, modeling system for immature habitat identification of an eco-georeferenceable, cross border, African, riverine, tributary, *S. damnosum* s.l., capture point may be specifiable employing:

$$\begin{aligned}\frac{dS}{dt} &= B - \beta SI - \mu S \\ \frac{dE}{dt} &= \beta SI - \nu E - \mu E \\ \frac{dI}{dt} &= \nu E - (\gamma + \mu + \delta) I\end{aligned}\quad (1.3)$$

Adding these three equations of system (1.3), an onchocerciasis researchist or epidemiologist would have as residual explanatory forecast $B - \mu(S + E + I) - \delta I - \gamma I \frac{d}{dt}(S + E + I) = (S + E + I)' \leq B - \mu(S + E + I)$. Then $\limsup_{t \rightarrow \infty} (S + E + I) \leq \frac{B}{\mu}$. So, the feasible region for (1.3) for unbiasedly identifying an eco-georeferenceable, black fly, endemic, capture point, breeding foci may be $\Lambda = \left\{ (S, E, I) : S + E + I \leq \frac{B}{\mu}, S > 0, E \geq 0, I > 0 \right\}$ (1.4).

An African, cross border, riverine tributary, *S. damnosum* s.l., hyper productive, eco-georeferenceable, breeding foci may be found by using the next generation matrix as found in [84]. In this contribution, the authors conclude that the disease-free equilibrium (DFE) is locally asymptotically stable when reproduction number is less than one. Some conditions on the model LULC parameter estimators may be obtainable to show the existence as well as nonexistence of limit cycle. Some sufficient conditions for global stability of the endemic equilibrium may be quantitated in a cross-border, *S. damnosum* s.l., breeding foci, moderate resolution, identification model using Lyapunov function.

Lyapunov functions are scalar functions that may be used to prove the stability of an equilibrium of an ODE. Named after the Russian mathematician Aleksandr Mikhailovich Lyapunov, Lyapunov functions (also called the Lyapunov's second method for stability) are important to stability theory of dynamical systems and control theory. A similar concept appears in the theory of general state space Markov chains, under the name functions. For certain classes of ODEs, the existence of Lyapunov functions is a necessary and sufficient condition for stability. Whereas there is no general technique for constructing Lyapunov functions for ODEs in ArcPy, in many specific cases, the construction of Lyapunov functions in SAS® 9.3 Functions and CALL Routines is known. For instance, quadratic functions suffice for systems with one state; the solution of a particular linear matrix inequality provides Lyapunov functions for linear systems; and conservation laws can often be used to construct Lyapunov functions in SAS for physical modelling systems (e.g., eco-epidemiological, moderate resolution, LULC, forecast, vulnerability, immature habitat, endmember mapping of cross-border, African, riverine tributary, eco-georeferenceable foci of *S. damnosum* s.l.)

Development of artificial neural networks (ANN's) and complex, probabilistic, estimation networks, called Bayesian networks (BN) can enable onchocerciasis researchers or epidemiologists to incorporate many kinds of prior knowledge into ArcGIS that can be used for pre-field, operative, sampling and 5m, LULC characterization of complex, cross-border, African, riverine tributary, eco-georeferenceable, capture point, *S. damnosum* s.l., breeding foci, (partially canopied, shaded foci) in a moderate resolution, remotely sensed, eco-epidemiological, immature habitat, eco-georeferenceable, LULC identification model. Because a Bayesian network may create a complete model for optimally regressing an empirical optimizable dataset of moderate resolution, African, riverine tributary, LULC endmember, signature, ecosystem variables and their relationships, it may be useable to answer probabilistic queries about these eco-georeferenceable, capture point, immature habitats. Bayesian network, Bayes network, belief network, Bayes model or probabilistic directed acyclic graphical model is a probabilistic graphical model (a type of statistical model) in ArcGIS of in SAS (PROC MCMC) that represents a set of random variables and their conditional dependencies via a directed acyclic



graph (DAG). For example, the network can be used to find out updated knowledge of the state of a moderate resolution, uncoalesced, geo-specified subset of orthogonally eigen-decomposed, eco-georeferenceable, *S. damnosum* s.l., breeding foci, regressible, timeseries, moderate resolution, geoclassifiable, capture point LULC variables when other observed, evidence variables (e.g., time series, water temperature covariates) are available as input parameterizable covariates.

Empirical Bayesian kriging differs from other kriging methods in Geostatistical Analyst™ by using an intrinsic random function as the kriging model. Other kriging models assume that the process follows an overall mean (or specified trend) with individual variations around this mean. Large deviations are pulled back toward the mean, so values never deviate too far. However, EBK does not assume a tendency toward an overall mean, so large deviations in a cross-border, African, riverine tributary ecosystem, immature, habitat eco-epidemiological model are just as likely to get larger as they are to get smaller. Hence, intrinsic random functions inherently correct for trends in the data. Semi variogram model for a given distance h , empirical Bayesian kriging supports the following semi variograms:

- Power
 - $\gamma(h) = \text{Nugget} + b/h^\alpha$
- Linear
 - $\gamma(h) = \text{Nugget} + b/h$
- Thin Plate Spline
 - $\gamma(h) = \text{Nugget} + b/h^2 * \ln(|h|)$

The Nugget and b (slope) must be positive, and α (power) must be between 0.25 and 1.75. Under these restrictions, the parameters are estimated using REML. These semivariogram models do not have a range or sill parameter because the functions have no upper bound.

In EBK, it's possible to analyze the empirical distribution of uncoalesced, *S. damnosum* s.l., immature parameter estimates because many semivariograms are estimated at each location. Clicking the Nugget, Slope, or Power tab displays the distributions of the associated, moderate resolution, LULC parameters. The following graphic shows the distributions of the semivariogram parameters for the simulated semivariograms shown in the previous graphic: Empirical Bayesian kriging offers the multiplicative skewing normal score transformation with the choice of two base distributions: Empirical and Log Empirical. The Log Empirical transformation requires all data values to be positive, and it will guarantee that all predictions will be positive. This is appropriate for cross-border, *S. damnosum* s.l. immature habitat, capture point LULC data such as temperature variables associated with a moderate resolution, geo-classified, seasonal, capture point, black fly, epidemiological, immature habitat, identification model.

[85] determined the minimum water temperature for development ($t(0)$) and the thermal constant (K) for the development of immature stages of *S. damnosum* s.l. in West Africa was estimated as 20.1 °C and 93 day-degrees, respectively, based on analyses of published data on development rates of eggs, larvae and pupae at different water temperatures (24.0 °C and 31.5 °C). Thus, at a constant water temperature of 30.0 °C (approximately 10 °C above $t(0)$), adult flies would emerge about 9 days after oviposition. This process of computing the posterior distribution of LULC variables given evidence may be assumed to be probabilistic inference in an eco-epidemiological, moderate resolution, African, riverine tributary, eco-georeferenceable, LULC, cross-border, *S. damnosum* s.l., immature, habitat, forecast, forecast, vulnerability model [11]. Thus, the posterior in an *S. damnosum* s.l., eco-epidemiological, hyper productive, seasonal, capture point, breeding foci, forecast, vulnerability, cross-border, ecosystem, identification model could render a universal sufficient statistic for remote, geoclassified, LULC, habitat, detection applications in African riverine tributary ecosystems

Other eco-epidemiological sampling methods for cross-border, *S. damnosum* s.l., capture point, immature habitat, identification, in African riverine tributary environments in ArcGIS Pro may include stochastic simulation, mini-bucket elimination, loopy belief propagation, and generalized belief propagation, variationally methods. In so doing, a hierarchical structure of a range of deterministic risk models encompassing different levels of linear and non-linear complexities may be constructed for remotely distinguishing, seasonal, breeding, capture point, endemic foci of resampled cross-border *S. damnosum* s.l. habitats. Amongst the



objectives for model construction may be to elaborate parameterizable covariate, estimator unbiasedness employing some of the representative mathematical LULC models, in ArcGIS Pro may be to precisely statistically describe onchocerciasis incidence in African, cross-border, riverine, agro-village, tributary zones precisely by including the critical attributes and other features of black fly, host-vector-parasite interactions in these zones.

Both the Multiple R-Squared and Adjusted R-Squared values are measures of model performance that may be usable in an ArcGIS Pro-derived, endmember, moderate resolution, cross-border, African, riverine, tributary, seasonal, hyper productive, eco-georeferenceable, *S. damnosum* s.l. eco-epidemiological, seasonal, immature, capture point, parameterizable LULC estimator dataset. Possible values range from 0.0 to 1.0. The Adjusted R-Squared value is always a bit lower than the Multiple R-Squared value, because it reflects model complexity (the number of variables) as it relates to the data and is consequently a more accurate measure of model performance [10]. Adding an additional, black fly-related, breeding foci, explanatory variable to the moderate resolution, LULC habitat identification model will likely increase the Multiple R-Squared value but may decrease the Adjusted R-Squared value. Suppose an onchocerciasis researcher or epidemiologist is constructing a regression model of a cross-border, agro-village, grid-stratified, vulnerability, *S. damnosum* s.l., African, riverine, tributary, eco-epidemiological, breeding foci, forecast model in ArcGIS Pro where the number of remotely identified habitats is associated with each geoclassified moderate resolution, LULC is the dependent/response variable. An Adjusted R-squared value of 0.37 would indicate that the immature vector arthropod, habitat identification, model oviposition, explanatory variables modeled using linear regression) explains approximately 37 percent of the variation in the dependent variable. Said another way, the model explains approximately 37 percent of the variation in the immature, eco-epidemiological, LULC habitat model, explanatory, eco-georeferenceable regressors.

In Geostatistical Analyst™ Coefficient, Probability or Robust Probability, and Variance Inflation Factor (VIF) may be employed to assess each explanatory, moderate resolution, endmember, LULC, variable in a remotely sensed, regression, *S. damnosum* s.l., immature habitat, identification model. The coefficient for each seasonal, African riverine, moderate resolution, LULC, specified, vulnerability, optimizable, endmember, geoclassifiable, predictor variable should optimally reflect both the strength and type of relationship when the explanatory variable has to the dependent variable (e.g., number of remotely identified black fly breeding foci in a cross-border, tributary ecosystem). When the sign associated with the coefficient is negative, the relationship would be negative (e.g., the larger the Euclidean distance from the riverine, tributary, grid-stratified cross-border, agro-village, eco-georeferenced, centroid, the smaller the number of adult black fly oviposition traps). When the sign is positive, the relationship is positive (e.g., the larger the black population, the larger the prevalence of onchocerciasis).

Coefficients are given in the same units as their associated explanatory variables (e.g., a coefficient of 0.005 associated with an eco-epidemiological, remotely sensed, moderate resolution, LULC variable representing black fly population counts may be interpreted as 0.005). Optimally, the remotely sensed black fly, habitat coefficient should reflect the expected change in the dependent variable for every 1 unit LULC change in the associated moderate resolution, endmember, microtopographic attribute quantitated (e.g., partially discontinuous, canopied, explanatory variable), holding all other variables constant (e.g., a 0.005 increase in percent of uncanopied, rock at a capture point) is expected for each habitat in a moderate geoclassified resolution LULC block, holding all other breeding foci, explanatory variables constant). The t test may be used to assess whether an immature habitat cross-border, *S. damnosum* s.l. explanatory LULC variable is statistically significant (e.g., remotely positive for breeding foci). The null hypothesis could be that the LULC coefficient is, for all intents and purposes, equal to zero (and consequently is not helping the black fly habitat identification model). When the probability or robust probability (p-value) is very small in a cross-border, moderate resolution, geoclassified, LULC, immature *S. damnosum* s.l., capture point, habitat, identification model, the chance of the coefficient being essentially zero is also small.

Means and other measures of central tendency rightfully may occupy a distinguished place in the theory and practice of statistical data analysis for remotely sensed, moderate resolution LULC, *S. damnosum* s.l., cross-border, immature habitat identification in ArcGIS but an onchocerciasis researcher or epidemiologist may be entitled to ask, "Does the conditional expectation or any other measure of conditional central tendency adequately characterize a statistical relationship amongst the cross-border, African, riverine tributary, eco-georeferenced, vector arthropod LULC variables?" An affirmative answer seems possible only within the



confines of extremely restrictive parametric models. In principle, an onchocerciasis researcher or epidemiologist would like to know the entire conditional distribution function, or equivalently, but perhaps preferably the conditional quantile function [2]. In probability and statistics, the quantile function specifies, for a given probability in the probability distribution of a random variable, the value at which the probability of the random variable being less than or equal to this value is equal to the given probability. It is also called the percent point function or inverse cumulative distribution function [86]. (Statistical Modelling with Quantile Functions.) Hence, it may be suggested that a natural approach to robust, moderate resolution, LULC estimation of the conditional quantile function for linear, oviposition, cross-border, remotely sensed, moderate resolution, LULC, *S. damnosum* s.l., immature habitats eco-epidemiological models may be based on the analogues of the sample quantiles as introduced in [87]. The asymptotic theory of these black fly-related endmember LULC regression quantiles may be extended to linear models with a family of linear scale processes in ArcGIS. The problem of estimating the precision of these "regression quantile" estimates may be addressed in ArcGIS where a robust approach to problems of testing homoscedasticity may be developed.

With onchocerciasis still thriving and threatening to be a major source of disability due to changing political scenarios, and LULC conditions (e.g., droughts, riverine flooding, deforestation), throughout cross-border, African, tributary, agro-village, riverine environments, it may be necessary to make a critical assessment of the existing models, and study their evolution and efficacy in describing the black-fly host-parasite biology in these ecosystems using geoprocessing tools in Geostatistical Analyst™. Starting from the basic, logistic, dichotomized, mathematical models and their underlying features (e.g., binary, dependent variable) for optimally, regressing, hyper productive, eco-georeferenceable, *S. damnosum* s.l. eco-epidemiological, breeding foci LULC signatures with their respective parameterizable, optimally geoclassifiable, uncoalesced, wavelength, hyper productive, capture point, moderate resolution, eco-epidemiological, predictors to advanced Bayesian neural networks, the spread and transmission of the riverine disease may be eco-geographically geolocalized by remotely identifying and mapping cross-border, African, riverine tributary, *S. damnosum* s.l., breeding foci, immature habitats in ArcGIS.

A compartmental, generalizable, epidemic, heterogeneous, moderate resolution, LULC, time series ArcGIS, explanatorial model may be employable for identification of cross border, riverine tributary, African, breeding foci of *S. damnosum* s.l. however, in the ArcGIS spatial, SEIR model example, the *I* class of individuals may not recover at all and may eventually be blinded; *R* can consist of individuals, who recover with temporary or permanent immunity, thereby further subdividing the compartments in the forecast, eco-epidemiological, onchocerciasis, vulnerability model.

Using these notations, eight classes of compartmental, LULC, *S. damnosum* s.l., eco-epidemiological, capture point, habitat, identification models may be optimally constructed in ArcGIS and used for remotely, precisely, geovisually identifying, eco-georeferenceable, hyper productive, breeding foci, capture points in a conflict-ridden cross-border, African, riverine tributary, agro-village zone including -SI, SIS, SEI, SEIS, SIR, SIRS, SEIR and SEIRS. The way that these compartments interact may be based upon phenomenological assumptions. When immunity is lost, a riverine, tributary, African, cross-border, ecosystem, eco-epidemiological, eco-dereferenceable, study site may become susceptible to pathogen attack again, and enter the *S* class.

The ArcGIS- SEIR modeling system may reveal vital moderate resolution, LULC dynamics for optimal geovisualization of eco-georeferenceable, *S. damnosum* s.l. seasonal, hyperproductive, breeding foci on geoclassifiable LULCs. The first step in the eco-epidemiological, forecast, vulnerability, eco-georeferenceable, moderate resolution model simulation in Geostatistical Analyst™ would be to identify the independent and dependent, explanatorily, entomological, vector, arthropod, breeding foci, regression variables associated to a hyperproductive, eco-georeferenced, cross border, African, riverine, tributary, capture point, in a regression model. After so doing, the immature habitat environmental and LULC covariates may be extracted and expressed by a set of ordinary differential equations. Thus, a geo-Spectro temporal or geo-spatiotemporal, eco-epidemiological, forecast-oriented, moderate resolution, LULC vulnerability model constructed in ArcGIS may define a relationship between any two Eco georeferenced, *S. damnosum* s.l., remotely sensed, parameterizable, moderate resolution, endogenous estimators, (e.g., percentage of partially canopied, trailing vegetation at a breeding foci and, number of Precambrian rocks at the foci) geosampled in crossborder riverine tributaries along conflict-ridden geolocations in Africa.

The estimate to be calculated, (i.e. an output cross-border, immature *S. damnosum* s.l. habitat pixel value) \hat{Z} , would be a linear combination of endmember LULC weight factors (w_i) and known input point



values (Z_i): $\hat{Z} = \sum (w_i * Z_i)$ In case the value of an output black fly seasonal, hyperproductive foci pixel would only depend on 3 input points, this would read:
 $\hat{Z} = w_1 * Z_1 + w_2 * Z_2 + w_3 * Z_3$ in Geospatial Analyst™ Thus, to calculate one output pixel value \hat{Z} , first, three weight factors w_1, w_2, w_3 would have to be found (one for each input point value Z_1, Z_2, Z_3), then, these weight factors can be multiplied with the corresponding input point values, and summed. In Kriging, the weight factors are calculated by finding the semi-variogram values for all distances between input points and by finding semi-variogram values for all distances between an output pixel and all input points; then a set of simultaneous equations has to be solved [7]. When the spherical distance option is used, distances are calculated over the sphere using the projection of the coordinate system that is used by the georeference of the output raster map.

A sufficient condition for the Ker+(B)-sign-stability of Metzler sign-matrices may be also obtainable for a moderate resolution, geoclassifiable, cross-border, LULC, *S. damnosum* s.l., African, riverine tributary, immature habitat, identification model formulated using inverses of sign-matrices and the concept of L+-matrices. Several applications of the results may be configured in ArcGIS for remotely targeting seasonal, hyperproductive, eco-georeferenceable, moderate resolution, imaged, geoclassifiable, LULC, black fly, cross-border habitats in these environments. In mathematics, the class of Z-matrices are those matrices whose off-diagonal entries are less than or equal to zero; that is, a Z-matrix Z satisfies [88]. Note that this definition coincides precisely with that of a negated Metzler matrix or quasipositive matrix for optimally regressively quantitating cross-border, *S. damnosum* s.l., immature habitat, capture points. The term quasinegative matrix appears from time to time in GIS literature, though this is rare and usually only in contexts where references to quasipositive matrices are made.

Let positive and non-negative, discrete integers respectively describe matrices in a moderate resolution, cross-border, *S. damnosum* s.l., eco-epidemiological, ArcGIS, immature habitat identification, forecast, vulnerability eco-georeferenceable model within an exclusive field-operationizable, explanatorily dataset of uncoalesced, geoclassified, orthogonally decomposable, moderate resolution, wavelength classes and matrices with exclusively non-negative real, geosampled, African, riverine tributary, eco-georeferenceable, capture point, LULC components. The eco-georeferenceable, eigenvalues of the vector, arthropod, eco-epidemiological, forecast, vulnerability model would then have a real square matrix A which would then be revealed as a series of complex numbers that make up the spectrum of the matrix.

The exponential growth rate of the matrix powers A^k as $k \rightarrow \infty$ would be controlled by the eigenvalue of A with the largest absolute value in the cross-border, vector habitat, identification model. The Perron–Frobenius theorem could describe the properties of the leading eigenvalue and of the corresponding orthogonal eigenvectors for identifying a geospatial LULC object in geospace [e.g., georeferenced, hyper productive, capture point cross border, African, riverine tributary, *S. damnosum* s.l. habitat) when A is a non-negative real square matrix. In linear algebra, the Perron–Frobenius theorem, proved by [89, 90] asserts that a real square matrix with positive entries has a unique largest real eigenvalue and that the corresponding eigenvector can be chosen to have strictly positive components, and also asserts a similar statement for certain LULC classes of nonnegative matrices.

Many statements that are equivalent to this definition of non-singular M-matrices are known in ArcGIS, and any one of these statements can serve as a starting definition of a non-singular M-matrix in a moderate resolution, eco-georeferenceable, LULC cross border, African, riverine tributary, *S. damnosum* s.l., cross-border, breeding foci, 5m resolution, capture point, forecast, vulnerability model for example, Plemmons lists 40 such equivalences. These characterizations have been categorized by Plemmons in terms of their relations to the properties of: (1) positivity of principal minors, (2) inverse-positivity and splitting, (3) stability, and (4) semi positivity and diagonal dominance. Thus, it would make sense to categorize endmember, moderate resolution, uncoalesced, microtopographic, LULC properties when identifying seasonal, hyper productive, African, cross-border, riverine tributary, *S. damnosum* s.l., immature habitat, capture points using a stochastic or deterministic interpolator in Geospatial Analyst™. This way as the statements within a particular group (i.e., positively autocorrelated geospatial black fly, eco-georeferenceable cluster) would be related to each other even when matrix A is an arbitrary matrix, and not necessarily a Z-matrix.

The Hosmer-Lemeshow goodness-of-fit statistic is obtainable by calculating the Pearson chi-square statistic from the $2 \times g$ table of observed and expected wavelength frequencies in ArcGIS where g is the number



of moderate resolution, geoclassified, LULC groups quantitated for identifying, seasonal, hyper productive, eco-referenceable cross-border, *S. damnosum* s.l., breeding foci. the statistic may be written

$$\chi_{HL}^2 = \sum_{i=1}^g \frac{(O_i - N_i \bar{\pi}_i)^2}{N_i \bar{\pi}_i (1 - \bar{\pi}_i)}$$
 where N_i could be the total frequency of subjects (e.g., black fly, seasonal geosampled, habitat covariates) in the i th group, O_i could be the total LULC uncoalesced, waveband frequencies for generating a hyperproductive black fly, eco-epidemiological, capture point. In the i th group, when $\bar{\pi}_i$ is the average estimated predicted probability of an immature, cross-border, African, riverine tributary, black fly, habitat identification outcome for the i th group. the predicted probabilities may be computed as linear predictor, predicted probability, with confidence limits The Hosmer-Lemeshow statistic is then comparable to a chi-square distribution with $(g - n)$ degrees of freedom, where the value of n can be specified in the LACKFIT option in the MODEL statement. The default is $n = 2$. Large values of χ_{HL}^2 (and small p -values) would then indicate a lack of fit of the eco-georeferenceable, eco-epidemiological, *S. damnosum* s.l. cross-border, African, riverine tributary, forecast, vulnerability model.

Python features a dynamic type system and automatic memory management and supports multiple programming LULC paradigms, including object-oriented, imperative, functional programming, and procedural styles. It has a large and comprehensive library. Python has a large standard library, commonly cited as one of Python's greatest strengths[91]. This library can provide tools suited to many tasks associated with geospatiotemporally or geospectrotemporally orthogonally and remotely identifying, eco-epidemiological, cross-border, African, riverine tributary, *S. damnosum* s.l., immature, capture point, seasonal, hyperproductive, breeding foci on 5m eco-georeferenced LULCs. Modules for creating graphical user interfaces, connecting to relational databases, generating pseudorandom numbers, arithmetic with arbitrary precision decimals, manipulating regular expressions, and doing unit testing may be included in future research also for black fly capture point, habitat identification on 5m, geoclassified, imaged, LULC data.

Some parts of the Python standard library are covered by specifications (e.g., the Web Server Gateway Interface (WSGI) implementation follows PEP 333[92]) They are specified by their code, internal documentation, and test suites (if supplied). However, because most of the standard library is cross-platform Python code, only a few modules need altering or rewriting for variant implementations such as those employed in cross-border, African riverine, tributary *S. damnosum* s.l. eco-epidemiological, capture point, immature habitat identification model.

As of November, 2016, the Python Package Index, the official repository containing third-party software for Python, contains over 92,000 packages offering a wide range of functionality for cross-border *S. damnosum* s.l. capture point, geoclassifiable, LULC, moderate resolution, immature habitat identification. including: graphical user interfaces, web frameworks, multimedia, databases, networking and communications test frameworks, automation and web scraping, documentation tools, system administration scientific computing, text processing and image processing. Most Python implementations (including CPython) include a read-eval-print loop (REPL), meaning they can function as a command line interpreter, for which the onchocerciasis researcher or epidemiologist only need to enter statements for geoclassifying, microtopographic, partially, canopy-shaded, Precambrian rock, LULC, for example, sequentially, for which results will be received immediately. Other shells add abilities beyond those in the basic interpreter, including IDLE and IPython. While generally following the visual style of the Python shell, they can implement LULC features like auto-completion, and syntax highlighting. In addition to standard desktop integrated development environments (Python IDEs), there are also web browser-based IDEs, SageMath (intended for developing math-related Python programs), and a browser-based IDE and hosting environment, PythonAnywhere. Additionally, the Canopy IDE is also an option for writing Python programs for identifying cross-border, African riverine, tributary, capture point, *S. damnosum* s.l., breeding foci employing an iteratively interpolatable, Chl-a, Rapid Eye™ 5m, LULC signature.

PyPy is a fast, compliant interpreter of Python 2.7 and 3.2. Its just-in-time compiler brings a significant speed improvement over CPython. A version taking advantage of multi-core processors using software transactional memory is being created. Stackless Python is a significant fork of CPython that implements microthreads; it does not use the C memory stack, thus allowing massively concurrent programs. PyPy also has a stackless version.^[92]



MicroPython is a lean, fast Python 3 variant that is optimized to run on microcontrollers. Other just-in-time compilers have been developed in the past, but are now unsupported: Google began a project named Unladen Swallow in 2009 with the aim of speeding up the Python interpreter fivefold by using the LLVM, and of improving its multithreading ability to scale to thousands of cores. Psyco is a just-in-timespecializing compiler that integrates with CPython and transforms bytecode to machine code at runtime. The emitted code is specialized for certain iterative, interpolative, signaturedata types for geoclassifiable 5m, spatial resolution, LULCs for immature *S. damnosum* s.l. immature habitat, identification and is faster than standard Python code.

In 2005, Nokia released a Python interpreter for the Series 60 mobile phones named PyS60. It includes many of the modules from the CPython implementations and some additional modules to integrate with the Symbian operating system. This project has been kept up to date to run on all variants of the S60 platform and there are several third-party modules available. The Nokia N900 also supports Python with GTK widget libraries, with the feature that programs can be both written and run on the target device. There are several compilers to high-level object languages, with either unrestricted Python, a restricted subset of Python, or a language similar to Python as the source language: Jython compiles into Java byte code, which can then be executed by every Java virtual machine implementation. This also enables the use of Java class library functions from the Python program. IronPython follows a similar approach to run Python programs on the .NET Runtime. The Python language can be compiled to C, Java bytecode, or Common Intermediate Language, and may be to build the PyPy interpreter of Python for immature, capture point, eco-georeferenceable, immature habitat identification of cross-border, *S. damnosum* s.l., African riverine tributary, breeding foci.

Pyjamas compiles Python to JavaScript. Shed compiles Python to C++. Cython and Pyrex compile to C. Google's Grumpy compiles Python to Go. A performance comparison of various Python implementations on a non-numerical (combinatorial) workload was presented at EuroSciPy '13. [93].

ffpack is a comprehensive software library for solving partial differential equations. For the experienced user and C++ programmer, Diffpack offers lots of functionality which simplify the development of new simulators for optimally remotely identifying an eco-georeferenceable, eco-epidemiological, hyper productive, *S. damnosum* s.l. breeding foci along a crossborder, African riverine, tributary. However, the nature of Diffpack/C++ programming is more detailed and cumbersome than programming in environments like Matlab and Maple. Coupling of Diffpack with other packages at the C++ level may make it possible to optimally remotely quantitate an empirical uncoalesced dataset of moderate resolution geoclassifiable, LULCs for optimally generating an endmember signature which may be subsequently iteratively qualitatively interpolated to geolocate a cluster of eco-georeferenceable, cross border, African, riverine tributary, black fly, immature habitats. Stochastically or deterministically interpolated, immature habitat, endmember signatures may reveal geolocations of unknown, unsampled, capture point, eco-georeferenceable, *S. damnosum* s.l. immature habitats in an African, riverine tributary (Jacob et al. 2013). Operating Diffpack through high-level Python scripts for eco-epidemiological, *S. damnosum* s.l. breeding foci, vulnerability, endemic forecasting based on identification of eco-georeferenceable capture points may meet these shortcomings.

Coupling Diffpack/C++ and Python is a non-trivial task. However, there is a tool, SWIG, which provides the possibility to automate the coupling of C/C++ and Python such that Python scripts can call C/C++ functions and operate directly on the C/C++ data structures. Applying SWIG to a large unit of software such as Diffpack faces many technical challenges for optimally identifying cross-border, African, riverine, tributary, seasonal, hyperproductive, cross-border, *S. damnosum* s.l. immature habitats. Introducing new tools in Diffpack may enable application of SWIG to generate Python interfaces to Diffpack simulators in an almost automatic way for optimally identifying these, capture point, breeding foci.

An onchocerciasis researchist or epidemiologist may utilize some step-by-step examples on equipping Diffpack simulators with Python interfaces for remotely identifying cross-border, *S. damnosum* s.l., immature habitats on moderate resolution, geoclassifiable LULCs. A complete application employing a Python script would enable running a Diffpack LULC simulator interactively through ArcGIS whilst modifying any iterative interpolation simulation exercise. The python script may reveal parameterizable habitat covariates associated to an eco-georeferenceable, eco-epidemiological, seasonal hyperproductive, capture point, cross-border, African riverine tributary, *Simuliid*, breeding foci which may be also geovisualized using a Diffpack LULC simulation kit with the aid of the Visualization Toolkit VTK package.

The VTK is an open-source, freely available software system for 3D computer graphics, image processing, and visualization. It consists of a C++ class library and several interpreted interface layers including



Tcl/Tk, Java, and Python. VTK supports a wide variety of geo-visualization LULC algorithms including scalar, vector, tensor, texture, and volumetric methods, as well as advanced modeling techniques such as implicit polygon reduction, mesh smoothing, cutting, contouring, and Delaunay triangulation. In mathematics and computational geometry, a Delaunay triangulation for a set P of points in a plane is a triangulation DT(P) such that no point in P is inside the circumcircle of any triangle in DT(P). (www.esri.com). VTK has an extensive information geo-visualization framework and a suite of 3D interaction widgets. The toolkit supports parallel processing and integrates with various databases on GUI toolkits such as Qt and Tk. VTK is cross-platform and runs on Linux, Windows, Mac, and Unix platforms. VTK is part of Kitware's collection of commercially supported open-source platforms for software development (www.vtk.org). If an ochocerciasis researchist or epidemiologist demonstrates how Python scripts may act as a bridge between Diffpack and other software packages when identifying eco-georeferenceable, capture point, hyperproductive, seasonal, cross-border, *S. damnosum* s.l. breeding foci in an African riverine tributary ecosystem on moderate resolution geoclassifiable, this LULC information may be exported into other statistical databases (SAS, R) In so doing, near-real-time, linear and non-linear exploratory,time series, regression paradigms may be constructed. The model residual eco-epidemiological, forecasts may optimally target seasonal, hypeproductive, *S. damnosum* s.l. breeding foci in cross-border, African, riverine tributaries employing moderate resolution geoclassified LULCs. These biophysical, geo-ecological, black fly, immature habitat, explanatory, eco-georeferenecable, eco-epidemiolgoical predictors may be prioritized by seasonal sampled, feature attributes (e.g., percentage of unshaded trailing vegetation at a focus, number of Precambrian rocks, larval count data, etc). vegetation canopy can maximally absorb 90-94% of incident photosynthetically active radiation vegetation canopy can maximally absorb 90-94% of incident photosynthetically active radiation(PAR)

Remote sensing discontinuous canopy photosynthetic and stomatal conductance efficiencies may be investigated with the aid of 1 and 3D -dimensional radiative transfer methods coupled to a semi empirical mechanistic cross-border, *S. damnosum* s.l., immature habitat, eco-epidemiological, capture point, eco-georeferenceable forecast, vulnerability model of leaf photosynthesis and stomatal conductance. Desert likevegetation may be modeled as clumps of leaves randomly distributed on a bright dry soil with partial ground cover. Normalized difference vegetation index canopy photosynthetic (E_p), and stomatal efficiencies (E_s) may be calculatable for various geometrical, optical, and illumination conditions for determining geolocations of seasonal, hyper productive, *S. damnum*sale breeding foci in cross-border, African riverine tributary ecosystem. A base case may be defined to investigate the dynamics of E_p and E_s with respect to ground cover, clump leaf area index, soil reflectance, and atmospheric conditions in a potential endemic location. The contribution of various radiative fluxes to estimates of E_p may be evaluated in an ArcGIS cyberenvironment and the magnitude of errors in bulk canopy formulation of problem parameters may be quantitated. The nature and sensitivity of the relationship between E_p and E_s to NDVI may be investigated for determining geolocations of a cross-border, *S. damnosum* s.l. immature habitat and an algorithm may be proposed for use in operational remote sensing.

In summary, 5m, spatial resolution, reference maps revealed no cross-border,*S. damnosum* s.l., immature habitats in the DRC study site polygons based on FVC yields and invariant NDVI_{soil} values. The NDVI of bare soil was the predominant LULC. There was marginal spatial variability (e.g., homogeneous, non-canopied, non-vegetated LULCs) at the riverine tributary study site. Based on these model outputs, *S. damnosum* s.l., seasonal, immature habitat in Ugandan, agro-village, riverine, tributaries are not influenced by abundance and distribution of black-flies from the DRC. The vegetation signature LULC interpolation accounted for the brightness of foliage in the IR spectrum which was extensively utilized in the NDVI. Regardless no *S. damnosum*, s.l., breeding foci was geovisually identifiable. An n^{th} -order linear ODE with

constant 5m, decomposed, Rapid Eye™ geoclassified LULCs $\frac{d^n y}{dx^n} + a_{n-1} \frac{d^{n-1} y}{dx^{n-1}} + \dots + a_1 \frac{dy}{dx} + a_0 y = Q(x)$, was able to solve the microtopographic characteristics in each polygon by writing $y \equiv e^{r \cdot x}$ and setting $Q(x) = 0$ which subsequently rendered the n complex roots. Then $r^n e^{r \cdot x} + a_{n-1} r^{n-1} e^{r \cdot x} + \dots + a_1 r e^{r \cdot x} + a_0 e^{r \cdot x} = 0$ and $r^n + a_{n-1} r^{n-1} + \dots + a_1 r + a_0 = 0$. was determined in each polygon . Factoring of the LULC, 5m resolution, differential equations revealed the roots r_i , $(r - r_1)(r - r_2) \dots (r - r_n) = 0$. For a non-repeated real root r , the corresponding solution was $y = e^{r \cdot x}$ in each polygon Although. ArcPy functions resolved multiple differential diagnostic equations and provided functions for the vegetation, proxy, 5m, endmember, LULC signatures for optimally displaying vegetational and non-vegetational, partially shaded, geoclassified regressors. the functions and classes did provide additional functionality to support Python-based workflows in the gridded datasets for identifying a single breeding foci of



S. neivi, no cross-border *S. damnosum* s.l. habitats were found at the cross-border study site. Regardless, the modeling approach and the ArcGIS scripting module presented here is potentially useful for identifying eco-georeferenceable geoclassifiable landscapes in cross-border, riverine tributaries in politically unstable regions in Africa where the vector foci could exist (North and South Sudan). Continued compiling of moderate resolution, geoclassifiable, LULCs, employing *S. damnosum* s.l., breeding foci, endmember signatures in conflict-ridden, African, riverine environments using Rapid Eye™ data and ArcGIS scripting languages (Java, PowerShell, Ruby, Scala, Perl,) may reveal specific landscape features such as meandering, seasonal, water, body reformations or specific plant fauna for implementing, targeted, larval, control strategies in these cross-border ecosystem

References

1. Jacob B.G., et al., *Quasi-likelihood techniques in a logistic regression equation for identifying Simulium damnosum sl. larval habitats intra-cluster covariates in Togo*. Geo-spatial Information Science, 2012. 15(2): p. 117-133.
2. Novak, R.J., - *Unbiasing a Stochastic Endmember Interpolator Using ENVI Object-Based Classifiers, a Farquhar's Single Voxel Leaf Photosynthetic Response Explanatory Model and Boolean Time Series Statistics for Forecasting Shade-Canopied Simulium damnosum s.l. Larval Habitats in Burkina Faso*. - Journal of Geophysics & Remote Sensing, (- 1): p. - 1.
3. Sam-Wobo, S., et al., *Ecological and attachment profile of Simulium damnosum sl larvae in breeding sites along Ogun River, Ogun State, Nigeria*. Journal of Entomology and Zoology Studies, 2014. 2(4): p. 197-200.
4. Adeleke, M., et al., *Molecular characterisation of the Simulium damnosum complex (Diptera: Simuliidae) found along the Osun River system, in south-western Nigeria*. Annals of Tropical Medicine & Parasitology, 2010. 104(8): p. 679-683.
5. Patz, J.A., et al., *Effects of environmental change on emerging parasitic diseases*. International journal for parasitology, 2000. 30(12): p. 1395-1405.
6. Griffith, D.A., *Spatial autocorrelation on spatial filtering*, in Springer 2003.
7. Noel, C., *Statistics for spatial data*. Probability and Mathematical Statistics, 1993.
8. Hodgson, M.E., et al., *An evaluation of lidar-derived elevation and terrain slope in leaf-off conditions*. Photogrammetric Engineering & Remote Sensing, 2005. 71(7): p. 817-823.
9. Green, A.A., et al., *A transformation for ordering multispectral data in terms of image quality with implications for noise removal*. IEEE Transactions on geoscience and remote sensing, 1988. 26(1): p. 65-74.
10. Hosmer, D.W. and N.L. Hjort, *Goodness-of-fit processes for logistic regression: simulation results*. Statistics in Medicine, 2002. 21(18): p. 2723-2738.
11. J. Novak, R., - *Ecogeographically and Non-Ecogeographically Forecasting Discontinuous Canopied Simulium damnosum s.l. Habitats by Interpolating Metrizable Sub-Mixel Mean Solar Exoatmospheric Quantum Scalar Irradiance*. - Journal of Remote Sensing & GIS, (- 1): p. - 1.
12. Jacob, B.G., et al., *Validation of a remote sensing model to identify simulium damnosum sl Breeding sites in Sub-Saharan Africa*. PLoS Negl Trop Dis, 2013. 7(7): p. e2342.
13. Jacob, B.G., et al., *A heteroskedastic error covariance matrix estimator using a first-order conditional autoregressive Markov simulation for deriving asymptotical efficient estimates from ecological sampled Anopheles arabiensis aquatic habitat covariates*. Malaria Journal, 2009. 8(1): p. 216.
14. Griffith, D.A., *A linear regression solution to the spatial autocorrelation problem*. Journal of Geographical Systems, 2000. 2.
15. Draper, N.R. and H. Smith, *Fitting a straight line by least squares*. Applied Regression Analysis, Third Edition, 1998: p. 15-46.
16. Komi, M. and J. Benjamin, - *Differentiating Non-Homoscedasticity and Geospatially Extreme Outliers for Urban and Rural Landscape Dataset Using Pearson's Product Moment Correlation Coefficients for Quantitating Clustering Tendencies in Non- Vaccinated Measles Populations in Nigeria*. - Journal of Remote Sensing & GIS, (- 4): p. - 1.
17. Hazewinkel, M., *Kolmogorov-smirnov test*. Encyclopedia of Mathematics, Springer, ISBN, 2001: p. 978-1.
18. Jacob, B., et al., *Definiability of combinatorial functions and their linear recurrence relationships within a polylogarithmic triangularizable matrix employing surjective bilipschitz functions and other isomorphisms of metric spaces for forecasting seasonal endemic onchoc*. Scientific Journal of Pure and Applied Sciences, 2013. 2(12): p. 401-460.



19. Stewart, G.W., *Matrix Algorithms: Volume II: Eigensystems* 2001: SIAM.
20. Venables, W.N. and B.D. Ripley, *Random and mixed effects*, in *Modern applied statistics with S* 2002, Springer. p. 271-300.
21. Anderson, D.R. and K.P. Burnham, *Avoiding pitfalls when using information-theoretic methods*. The Journal of Wildlife Management, 2002: p. 912-918.
22. Dodge, Y., *The Oxford dictionary of statistical terms* 2006: Oxford University Press on Demand.
23. Jacob, B.G., et al., *Denoising a model employing automated bandwidth selection procedures and pre-whitened Euclidean-based quadratic surrogates in PROC ARIMA for optimizing asymptotic expansions and simulations of onchocerciasis endemic transmission zones in Burkina Faso*. Journal of Public Health and Epidemiology, 2014. 6(11): p. 347-389.
24. Altman, N.S., *An introduction to kernel and nearest-neighbor nonparametric regression*. The American Statistician, 1992. 46(3): p. 175-185.
25. Raven, P.H., R.F. Evert, and S.E. Eichhorn, *Biology of plants* 2005: Macmillan.
26. Jacob, B.G., et al., *Remote and field level quantification of vegetation covariates for malaria mapping in three rice agro-village complexes in Central Kenya*. International Journal of Health Geographics, 2007. 6.
27. Griffith, D.A., *A comparison of six analytical disease mapping techniques as applied to West Nile Virus in the coterminous United States*. International Journal of Health Geographics, 2005. 4(1): p. 18.
28. Jaynes, E.T., *Bayesian methods: General background*. 1986.
29. Jacob, B.G. Shafer S. Alinda P. Loun D, McKinnon A. Munu D. Katarwa M. N., Lakwo T. Habomugish P., Unnasch T. R. Lexicographically, cartesian-ordered, differential calculi in canonically extractable in-situ near infra-red fluorescence quantum spectroscopic sub-surface continuous geodesic fluxions for metaheuristic chorophyll-atranslucent emissivity mapping intermittently canopied immature narrow riverine tributary *Simulium damnosum* s.l. oviposition sites for bio-optically delineating multivariate normalized Gaussian processes elucidatively administered by prior covariances and a spline within a reproducing non-frequentist simultaneous diagonalization of amalgamized positive definite kernels in Hilbert space: Implementation of a 'Slash and Clear' control intervention in two eco-georeferenceable agro-village complexes in northern Uganda Uganda *Journal of Geophysics and Remote sensing* (in press 2016)
30. Diuk-Wasser, M.A., et al., *Effect of rice cultivation patterns on malaria vector abundance in rice-growing villages in Mali*. The American journal of tropical medicine and hygiene, 2007. 76(5): p. 869-874.
31. Jacob, B.G., et al., *Evaluation of Environmental Data for Identification of Anopheles (Diptera: Culicidae) Aquatic Larval Habitats in Kisumu and Malindi, Kenya*. Journal of medical entomology, 2005. 42(5): p. 751-755.
32. Fisher, R.A., *On the interpretation of χ^2 from contingency tables, and the calculation of P*. Journal of the Royal Statistical Society, 1922. 85(1): p. 87-94.
33. Freedman, D.A., *Linear Statistical Models for Causation: A Critical Review*, in *Encyclopedia of Statistics in Behavioral Science* 2005, John Wiley & Sons, Ltd.
34. Erdman, D. and M. Morelock. *A study of kinetics: The estimation and simulation of systems of first-order differential equations*. in *Proceedings of the twenty-first annual SAS® users group international conference*. 1996.
35. Crosskey, R.W., *Taxonomic Study of the Larvae of West African Simuliidae (Diptera: Nematocera) with Comments on the Morphology of the Larval Black-Fly Head*. Bulletin of the British Museum (Natural History), 1960. 10(1): p. 1-74.
36. Crosskey, R., *A review of Simulium damnosum sl and human onchocerciasis in Nigeria, with special reference to geographical distribution and the development of a Nigerian national control campaign*. Tropenmedizin und Parasitologie, 1981. 32(1): p. 2-16.
37. Jacob, B., et al., *Land use land cover change on Anopheles arabiensis (Diptera: Culicidae) aquatic habitats in Karima village, Mwea Rice Scheme, Kenya*. American Journal of Tropical Medicine Hygiene, 2007. 76: p. 73-80.
38. Papageorgiou, G.C., *Chlorophyll a fluorescence: a signature of photosynthesis*. Vol. 19. 2007: Springer Science & Business Media.
39. Pinar, A. and P. Curran, *Technical note grass chlorophyll and the reflectance red edge*. International Journal of Remote Sensing, 1996. 17(2): p. 351-357.
40. Filella, I. and J. Penuelas, *The red edge position and shape as indicators of plant chlorophyll content, biomass and hydric status*. International Journal of Remote Sensing, 1994. 15(7): p. 1459-1470.



41. Baranoski, G. and J. Rokne, *A practical approach for estimating the red edge position of plant leaf reflectance*. International Journal of Remote Sensing, 2005. 26(3): p. 503-521.
42. Rodriguez, D., et al., *Detection of nitrogen deficiency in wheat from spectral reflectance indices and basic crop eco-physiological concepts*. Crop and Pasture Science, 2006. 57(7): p. 781-789.
43. Schuster, C., M. Förster, and B. Kleinschmit, *Testing the red edge channel for improving land-use classifications based on high-resolution multi-spectral satellite data*. International Journal of Remote Sensing, 2012. 33(17): p. 5583-5599.
44. Diuk-Wasser, M.A., et al., *Modeling the spatial distribution of mosquito vectors for West Nile virus in Connecticut, USA*. Vector-Borne & Zoonotic Diseases, 2006. 6(3): p. 283-295.
45. Tucker, C. and P. Sellers, *Satellite remote sensing of primary production*. International journal of remote sensing, 1986. 7(11): p. 1395-1416.
46. Schelling, K. *Approaches to Characterize Chlorophyll/Nitrogen Status of Crop Canopies*. in *DPGF Workshop Analysis of Remote Sensing Data, Hannover*. 2010.
47. Muturi, E.J., et al., *Mosquito species diversity and abundance in relation to land use in a riceland agroecosystem in Mwea, Kenya*. Journal of Vector Ecology, 2006. 31(1): p. 129-137.
48. Chadee, D., *Key premises, a guide to Aedes aegypti (Diptera: Culicidae) surveillance and control*. Bulletin of entomological research, 2004. 94(03): p. 201-207.
49. Focks, D.A., et al., *Transmission thresholds for dengue in terms of Aedes aegypti pupae per person with discussion of their utility in source reduction efforts*. The American journal of tropical medicine and hygiene, 2000. 62(1): p. 11-18.
50. Jacob, B.G., et al., *Quantifying stochastic error propagation in Bayesian parametric estimates using non-linear parameters of Anopheles gambiae s.l. habitats*", in *International Journal of Remote Sensing* 2009.
51. Rouse Jr, J.W., et al., *Monitoring vegetation systems in the Great Plains with ERTS*. 1974.
52. Huete, A.R., *A soil-adjusted vegetation index (SAVI)*. Remote sensing of environment, 1988. 25(3): p. 295-309.
53. Agresti, A., *Wiley series in probability and statistics. Analysis of Ordinal Categorical Data*, Second Edition, 2002: p. 397-405.
54. Agresti, A., *An introduction to categorical data analysis, 2nd edn*. Hoboken, 2007, NJ: John Wiley & Sons, Inc.
55. Fleiss, J.L., B. Levin, and M.C. Paik, *Poisson regression*. Statistical Methods for Rates and Proportions, Third Edition, 2003: p. 340-372.
56. McNemar, Q., *Note on the sampling error of the difference between correlated proportions or percentages*. Psychometrika, 1947. 12(2): p. 153-157.
57. Lancaster, H., *Significance tests in discrete distributions*. Journal of the American Statistical Association, 1961. 56(294): p. 223-234.
58. Bowker, A.H., *A test for symmetry in contingency tables*. Journal of the american statistical association, 1948. 43(244): p. 572-574.
59. Cohen, J., *A coefficient of agreement for nominal scales*. Educational and psychological measurement, 1960. 20(1): p. 37-46.
60. Fleiss, J.L., J. Cohen, and B. Everitt, *Large sample standard errors of kappa and weighted kappa*. Psychological Bulletin, 1969. 72(5): p. 323.
61. Cicchetti, D.V. and T. Allison, *A new procedure for assessing reliability of scoring EEG sleep recordings*. American Journal of EEG Technology, 1971. 11(3): p. 101-110.
62. Jacob, B.G., et al., *A Taxonomy of Unmixing Algorithms Using Li-Strahler Geometric-Optical Model and other Spectral Endmember Extraction Techniques for Decomposing a QuickBird Visible and Near Infra-Red Pixel of an Anopheles arabiensis Habitat*. The Open Remote Sensing Journal, 2011. 4(1).
63. Du, Y., et al., *New hyperspectral discrimination measure for spectral characterization*. Optical Engineering, 2004. 43(8): p. 1777-1786.
64. Sheskin, D., *Handbook of parametric and nonparametric statistical procedures*, CRC Press. Boca Raton, FL, 2004.
65. Osborne, J., W. Christensen, and J. Gunter. *Educational psychology from a statistician's perspective: A review of the power and goodness of educational psychology research*. in *national meeting of the American Education Research Association (AERA)*, Seattle, WA. 2001.
66. Paola, J.D. and R.A. Schowengerdt, *The effect of neural-network structure on a multispectral land-use/land-cover classification*. Photogrammetric Engineering and Remote Sensing, 1997. 63(5): p. 535-544.
67. Arfken, G., *The method of steepest descents*. Mathematical methods for physicists, 1985. 3: p. 428-436.



68. Tucker, C., et al., *Mean and inter-year variation of growing-season normalized difference vegetation index for the Sahel 1981-1989*. International Journal of Remote Sensing, 1991. 12(6): p. 1133-1135.
69. Burrough, P.A. *Dynamic modelling and geocomputation*. in *Geocomputation: a primer*. 1998. Chichester, UK: John Wiley & Sons.
70. Strahler, A.H. and D.L.B. Jupp, *Modeling bidirectional reflectance of forests and woodlands using Boolean models and geometric optics*. Remote Sensing of Environment, 1990. 34: p. 153-166.
71. Colin Cameron, A. and P.K. Trivedi, *Regression analysis of count data*. ECONOMETRIC SOCIETY MONOGRAPHS, 1998. 30.
72. Ma, Y. and D. Myers. *Simple and ordinary factorial cokriging*. in *3rd CODATA Geomathematics and Geostatistics Conference: Science de la Terre, Ser. Inf., Nancy*. 1994.
73. Jacob, B.G., et al., *Developing GIS-based eastern equine encephalitis vector-host models in Tuskegee, Alabama*. International journal of health geographics, 2010. 9(1): p. 12.
74. Draper, N. and H. Smith, *Applied regression analysis. Series in probability and mathematical statistics*. Wiley, 1981.
75. Wilkinson, L. and G.E. Dallal, *Tests of significance in forward selection regression with an F-to-enter stopping rule*. Technometrics, 1981. 23(4): p. 377-380.
76. Huete, A., C. Justice, and H. Liu, *Development of vegetation and soil indices for MODIS-EOS*. Remote Sensing of Environment, 1994. 49(3): p. 224-234.
77. Joiner, J., et al., *First observations of global and seasonal terrestrial chlorophyll fluorescence from space*. Biogeosciences, 2011. 8(3): p. 637-651.
78. Bishop, Y.M., S.E. Fienberg, and W. Paul, *Holland. 1975*. Discrete Multivariate Analysis: Theory and Practice, 1995: p. 57-122.
79. Agresti, A., *A survey of exact inference for contingency tables*. Statistical science, 1992: p. 131-153.
80. Kermack, W.O. and A.G. McKendrick. *A contribution to the mathematical theory of epidemics*. in *Proceedings of the Royal Society of London A: mathematical, physical and engineering sciences*. 1927. The Royal Society.
81. Haight, F.A., *Handbook of the Poisson distribution*. 1967.
82. Moran, P.A., *Notes on continuous stochastic phenomena*. Biometrika, 1950. 37(1/2): p. 17-23.
83. Griffith, D.A., *Spatial Autocorrelation and Spatial Filtering: Gaining Understanding Through Theory and Scientific Visualization*2003: Springer.
84. Van den Driessche, P. and J. Watmough, *Reproduction numbers and sub-threshold endemic equilibria for compartmental models of disease transmission*. Mathematical biosciences, 2002. 180(1): p. 29-48.
85. Lamberton, P.H., et al., *Onchocerciasis transmission in Ghana: biting and parous rates of host-seeking sibling species of the Simulium damnosum complex*. Parasites & vectors, 2014. 7(1): p. 511.
86. Gilchrist, W., *Statistical modelling with quantile functions*2000: CRC Press.
87. Koenker, R. and G. Bassett Jr, *Regression quantiles*. Econometrica: journal of the Econometric Society, 1978: p. 33-50.
88. Huang, T.-Z., G.-H. Cheng, and X.-Y. Cheng, *Modified SOR-type iterative method for Z-matrices*. Applied mathematics and computation, 2006. 175(1): p. 258-268.
89. Perron, O., *Zur theorie der matrices*. Mathematische Annalen, 1907. 64(2): p. 248-263.
90. Frobenius, F.G., *Über Matrizen aus nicht negativen Elementen*. 1912.
91. Van Rossum, G. *Python Programming Language*. in *USENIX Annual Technical Conference*. 2007.
92. Eby, P.J., *PEP 333—Python Web Server Gateway Interface v1. 0*, 2006.
93. Murri, R., *Performance of Python runtimes on a non-numeric scientific code*. arXiv preprint arXiv:1404.6388, 2014.